Nonequilibrium Processes in the Early Universe and Their Cosmological Effects and Constraints

Daniela Petrova Kirilova

A dissertation submitted in partial fulfillment
of the requirements for the degree of
Doctor of Physical Sciences

in The Institute of Astronomy and NAO
Bulgarian Academy of Sciences

2015

To Mihail, Rosanna, Vassillen and Emanuil

ACKNOWLEDGEMENTS

I am grateful to Alexander D. Dolgov for the scientific supervision, advice and care. I am thankful to Yakov B. Zeljdovich, and Matey D. Mateev for supporting my desire to work in Cosmology and Astroparticle Physics in the beginning of my studies. I am obliged to my coauthors: A. D. Dolgov, M. V. Chizhov, J.-M. Frere for the honor and the pleasure to work together. I appreciate the fruitful discussions with A. Smirnov, D. Sciama, I. Tkachev, V. Kadyshevsky, A. Starobinsky, V. Semikoz, I. Novikov,M. Shaposhnikov, M. Sazhin, G. Senjanovic, M. Tytgat, J. Lesgourgues, A. Zakharov, O. Atanckovic-Vukmanovic, R. Daemi, V. Genchev, R. Tsenov, L. Litov, E. Christova, D. Mladenov, S. Petcov, P. Krastev, D. Sasselov. I thank my Ph.D. student M. Panayotova and my M.S. students T. Velchev and T. Valchanov for the dedication and the diligence. I thank my colleagues from IA NAO BAS and from Sofia University and my friends for the interest in my research. I am glad that many of the students of my Cosmology and Astrophysics courses at the Physical Department of the Sofia University and at the American University in Bulgaria, Blagoevgrad, shared my fascination with the Universe's secrets and enthusiasm to discover and learn.

I am indebted to my parents and my husband for their help with my children during my visiting positions. I am obliged to my family for the understanding and overall support.

I appreciate the Regular Associateship and the visiting positions at theHigh Energy Section, Abdus Salam International Center for Theoretical Physics, Trieste, the Corresponding Associate position and visiting positions at Theory Division, CERN, the Marie Curie grant and the visiting positions at ULB, Bruxelles. I acknowledge the Danish Governmental Scholarship grant and the work at the Theoretical Astrophysics Center of the Niels Bohr Institute. The heavy numerical analysis was provided thanks to the computational power of the Theoretical Astrophysics Center, Niels Bohr Institute, Copenhagen; Abdus Salam ICTP, Trieste; CERN and Helsinki University.

TABLE OF CONTENTS

LIST OF FIGURES

Figure

LIST OF ABBREVIATIONS

CMB Cosmic Microwave Background

BBN Big Bang Nucleosynthesis

LSS large scale structure

CNB cosmic neutrino background

DM dark matter

DE dark energy

DR dark radiation

FD Fermi-Dirac

ChT chiral tensor

BSMs Beyond Standard Models

SCM Standard Cosmological Model

SM Standard Model

CPV CP-violation

BV B-violation

LHC Large Hadron Collider

LEP Large Electron-Positron Collider

SFC Scalar Field Condensate

SN Super Nova

CHAPTER I

Introduction

The thesis is dedicated to nonequilibrium processes and their cosmological role for the origin, chemical composition and structure of the matter content of the Universe. This research was inspired by the contemporary experimental, observational and theoretical indications for necessity of beyond the Standard Models Physics. In particular, the detection of neutrino oscillations and the precision measurements of the baryon density providing observational evidence for baryon asymmetry, as well as the search for new chiral tensor particles at ATLAS, provoked our investigations of the cosmological importance and cosmological constraints on the corresponding beyond standard model processes and particles.

1.1 Precise, Complimentary and Unique Physical Knowledge from Cosmology

During the last decades Cosmology has experienced a tremendous progress, and has become *a precision science, providing information about Universe characteristics and Nature's physical laws.*

Contemporary Standard Cosmological Model (SCM) (*Zeldovich and Novikov*, 1983; *Dolgov et al.*, 1991; *Kolb and Turner*, 1990; *Liddle*, 1998; *Gorbunov and Rubakov*, 2011a,b), also called Λ Cold Dark Matter (ΛCDM) model, is based on the General Relativity, Astrophysics, High Energy Physics, Thermodynamics and Statistical Physics, and is supported by huge amount of observational data.

Cosmic Microwave Background (CMB), Big Bang Nucleosynthesis (BBN) and large scale structure (LSS) surveys and measurements of Hubble expansion are the main observational pillars of contemporary Cosmology. Mainly due to the detection and investigation of the Universe expansion, CMB, light elements abundance measurements and BBN model, LSS surveys and LSS formation studies, we possess *precise knowledge about the main universe characteristics.* Cosmology *provides complementary knowledge* to fundamental physics (to the knowledge which we get at laboratories).

Besides, the observational data corresponds to different epochs of the universe evolution, i.e. we can "observe" not only present dynamics, structure and physical conditions of the universe, but also these of its earlier stages. For example, the information from the light element abundance measurements corresponds to the first minutes of the universe, CMB data give a glimpse of the epoch when Universe was ~ 380000 years old, while the contemporary telescopes give an insight of the galaxy formation epoch, from the time when the Universe was 11–12 billion years old till present.Hence, contemporary SCM provides useful test also for processes and particles present at high energies and densities, typical for its early stages. Thus, besides being a powerful complementary tool for search of physical laws, Cosmology *provides unique physical information* relevant at very high energies, densities and pressures beyond the reach of colliders and accelerators. I.e. the Universe is the ultimate unique laboratory to reveal the physical secrets of Nature at extreme conditions *unreachable by physics experiments.*

Cosmology also *tests new physics* - physics Beyond Standard Models (BSMs) i.e. beyond Electro Weak Model (called Standard Model (SM) and beyond SCM, also called Λ Cold Dark Matter (ΛCDM) model.

Physics BSMs, is required for the explanation of the experimental physics data, astrophysical and cosmological observational data. Namely, the contemporary SCM, contains considerable BSMs components - the so called *dark energy (DE) and dark matter (DM),* both with yet unrevealed nature, alas. These constitute 96% of the matter content in the universe today, and play a considerable role only at the matter dominated epoch. Recently, experimental and observational data indicated an existence of excess relativistic component, called dark radiation (DR), which is important at early stages.

BSMs physics is needed also for revealing the characteristics of the *inflaton* (the particle/field responsible for inflationary expansion stage) and its nature, as well as *for proposing CP-violation (CPV) and B-violation (BV) mechanisms*, responsible for baryogenesis. Thus, new processes, mechanisms, interactions and particles are expected to be the necessary ingredients for inflation and baryon asymmetry generation, which are the most widely accepted today hypotheses providing natural explanations of numerous intriguing observational characteristics of the Universe.

The inflationary hypothesis (*Linde et al.*, 1991) explains naturally and elegantly the initial conditions of the Universe in the pre-Friedmann epoch, namely: the extraordinary *homogeneity and isotropy* of the Universe; its *extremely high isotropy* at the Cosmic Microwave Background (CMB) formation epoch; its *unique flatness* and the *initial density inhomogeneities necessary for the generation of the pattern of observed structures.* It evades the problem of singularity of the Friedman expansion. Besides, an inflationary stage explains the *lack of topological defects* in the Universe.

Central role in inflationary models is played by the inflaton. At the end of inflation coherent oscillations of this scalar field around its equilibrium point create the particles of the high energy plasma of the early Universe. This reheating process after inflation defines the highest temperature and density reached at the radiation dominated stage of the Universe evolution. Useful analytical formulae for the probability of particle creation in different cases, interesting for Cosmology, were derived and applied for reheating *Dolgov and Kirilova* (1990) and baryogenesis (*Dolgov and Kirilova*, 1991). In the fifth chapter we discuss the role of particle creation processes for baryogenesis.

Baryogenesis models explain the locally observed predominance of matter over antimatter, usually considered as a global characteristic, i.e. matter-antimatter asymmetry of the Universe.

The Standard Model of elementary particles, as well as SCM, describes enormous quantity of experimental data. The *large number of its parameters, however, and also its principal problems*, makes actual the search of new physics beyond BSMs. Besides, there exist numerous *indications and evidences for physics BSMs*, coming from physics experiments, astronomical observations from ground-based and cosmic telescopes and missions, from theoretical and phenomenological physical astrophysical and cosmological models.

Alas, after many years of research there are no firm experimental detection of these BSMs candidates (DM, DE, inflaton, ets.), only experimental and observational constraints on the hypothetical candidates or/and theories exist.

The only exceptions at present are: the robust experimental detection of BSMs physics - the *detection of neutrino oscillations* and the only robust observational evidence for BSMs - the *measured value of the baryon density* (unnaturally big to be explained without new physics). The studies of neutrino oscillations, baryogenesis and leptogenesis are among the most actual problems of contemporary Physics, Neutrino Physics, Astrophysics and Cosmology.

The thesis is dedicated mainly to studies of *processes at the early Universe stage important for the Universe matter content*, namely: *processes important for baryogenesis*, determining the baryonic content and matter-antimatter asymmetry, leptogenesis and constraints on lepton content of the Universe, and to *processes involving neutrino oscillations* during nucleosynthesis epoch, defining the chemical composition of the Universe, processes with chiral tensor particles, presenting extension of the Standard Model matter content, which belongs to the fundamental representation of SU(2) group. We will discuss in the first 3 chapters the processes connected with neutrino oscillations, leptogenesis and leptonic density and in the following two chapters baryogenesis processes.

The biggest hopes for an experimental discovery of physics BSMs are connected with the Large Hadron Collider (LHC), that will reach at its second run the highest energies reached till now at terrestrial experiments. This makes the study of physics processes BSMs very actual at present. The seventh chapter is dedicated to the investigation of chiral tensor particles, presenting a natural extension of the SM, whose search is now conducted at ATLAS experiment of LHC.

1.2 Relevance and Originality of the Research Topics of the Thesis

The thesis is dedicated to the investigation of nonequilibrium processes and interactions, representing physics BSMs, their cosmological role and the cosmological constraints.

The main aim is to improve the knowledge about the physical conditions at different epochs of the Universe and to provide cosmological constraints on BSMs physics, thus contribute to fundamental physics knowledge.The concrete choice of the topics of investigation is provoked by their actuality, the accumulation of huge observational and experimental data and development of research methods during the last decades. Nonequilibrium processes were not systematically studied as the equilibrium ones were. This was the other reason to dedicate our efforts to these nonequilibrium processes.

The investigations, underlying the thesis, include the study of:

– *processes involving neutrino*, especially nonequilibrium electron-sterile neutrino oscillations, and their astrophysical and cosmological effects and constraints, spectrum distortion of neutrino, neutrino-antineutrino asymmetry enhancement, production of sterile neutrino, etc.;

– *processes important for the* cosmological nucleosynthesis, which determine the *chemical content of the baryonic component* of our Universe, in particular processes changing the Universe dynamics and processes influencing the pre-BBN nucleons kinetics;

– *processes concerning lepton asymmetry and baryon asymmetry* of the Universe: namely processes of the interplay between neutrino oscillations and lepton asymmetry, the processes of enhancement of lepton asymmetry, processes important or responsible for the generation of the baryon asymmetry of the Universe and for reheating;

– *processes involving new chiral tensor particles*, carriers of a centi-weak interaction and their cosmological role, etc.

Some of the discussed processes (like neutrino oscillations) have been meanwhile established. Others, predicted on the basis of physical, astrophysical or/and cosmological considerations, remain under discussion and are searched at experiments and by astrophysical observations. Most of them are among the hot topics of contemporary Physics, Astropartical Physics and Cosmology.

1.2.1 BSMs processes involving neutrino and their cosmological effects and constraints

Studies involving neutrino are very actual because of neutrino important astrophysical and cosmological role, as well as because of neutrino importance in fundamental physics theory. Deep connection exist between the neutrino physical characteristics, studied by Particle Physics and main fields of research of Astrophysics and Cosmology: solar physics, stellar evolution, Super Nova (SN) physics, nucleosynthesis, CMB, structure formation in the Universe, DM problem, etc.

Since the first theoretical ideas about neutrino of Pauli in 1930 and its detection in 1953 Neutrino Physics and Astrophysics have achieved serious results. *Neutrinos characteristics were studied at earth reactors and accelerators*: neutrino helicity, the participation in weak neutral currents, the existence of 3 light flavor neutrino types by Large Electron-Positron Collider (LEP) experiments. Besides, *neutrinos from astrophysical sources*: neutrino from the Sun, the atmosphere, supernova SN1987, extra-galactic and geo-neutrinos were detected.

We have been already the lucky witnesses of the experimental establishment of the BSMs physics in the neutrino sector - neutrino oscillations. 40 years after neutrino oscillations were theoretically proposed as a solution for the solar neutrino problem, they have been established experimentally. A detail review of the main experimental and theoretical results of neutrino physics may be found in *Strumia & Vissani*, 2006.

Solar neutrino experiments found *an energy dependent deficit of electron neutrinos coming from the Sun*, compared to the predictions of the standard solar model (*Bahcall*, 1989). SNO proved that solar neutrino deficit is not due to the imperfect astrophysical knowledge about the Sun. Atmospheric neutrino anomaly was found by atmospheric neutrino experiments. In 1998 Super-Kamiokande obtained an evidence of atmospheric flavor neutrino oscillations.

Neutrino oscillations suggested by solar and atmospheric neutrino experiments, were studied by terrestrial experiments, K2K, Minos, T2K, OPERA, KamLAND, which confirmed their existence. Thus, in the period 1998-2003 neutrino oscillations have been definitely experimentally established.

Experimental data on neutrino oscillations firmly determined three neutrino mixing angles and two mass differences, corresponding to the existence of at least two non-zero neutrino masses. Thus, the neutrino experimental data ruled out the Standard Models assumptions about zero neutrino masses and mixing and about flavor lepton number conservation. The detection of neutrino oscillations presents the first experimentally established physics BSMs.

The dominant oscillation channels have been proved to be flavor neutrino oscillations. For a review on neutrino oscillations in the early Universe and references see *Dolgov* (2002); *Kirilova* (2001c); *Kirilova and Frere* (2012); *Kirilova* (2015)) and the introductory part of the next chapters (2.1, 2.2, 3.1 and 3.2). Cosmological BBN considerations were the first to exclude two of the possible sterile solutions to the solar neutrino problem - large mixing angle solution (*Barbieri and Dolgov*, 1990; *Enqvist et al.*, 1992) and low mixing angle solution (*Kirilova and Chizhov*, 1997, 1998, 2000), years before the analysis of solar neutrino oscillations experiments data pointed to the preferred flavor oscillation channels. The role of eventual subdominant active-sterile neutrino oscillation channels is studied now.

Cosmology provides valuable information about the properties of the very elusive particles - the *neutrinos* and BSMs physics in the neutrino sector *due to the considerable influence of neutrino on the processes during different epochs of the universe evolution*, which have observable relics. Theoretically predicted relic neutrinos from the neutrino decoupling epoch of the early universe, corresponding to cosmic times ≤ 1 s and energies several MeV, which constitute the cosmic neutrino background (CNB) have not been detected yet. However, strong observational evidence for CNB and stringent cosmological constraints on relic neutrino characteristics exist from BBN, CMB and LSS data.

The role of neutrinos in Cosmology has been intensively studied: it has been understood that neutrinos had a considerable role during the early stage of the Universe, namely radiation dominated (RD) stage, when light neutrinos were essential ingredients in the universe density, determining the dynamics of the universe. [1] Neutrinos *played an essential role in different processes as for example in BBN, leptogenesis and baryogenesis, the formation of CMB.* In particular, electron neutrino participated in the pre-BBN neutron-proton transitions and nucleons freezing, and thus influenced considerably the primordial production of the light elements. Hence, BBN is very sensitive to neutrino characteristics: neutrino density of different neutrino types, neutrino-antineutrino asymmetries, the presence of light sterile neutrino, deviations from thermal equilibrium of neutrino, neutrino decays, etc.

At later stages of the Universe ($T \leq$eV) relic neutrinos, contributed to the matter density because at least one of the neutrino species became non-relativistic (using the information about neutrino mass differences from the neutrino oscillations data), influenced the formation of galaxies and their structures, influenced CMB anisotropies.

Sterile neutrino (right-handed neutrino) presents the simplest extension of SM particle content. It is proposed by many BSM theories. Depending on its mass scale it may have many important cosmological applications: it may provide neutrino mass generation, KeV sterile neutrino present warm DM candidate (*Kuzenko*, 2009), eV sterile neutrinos may explain the DR problem in Cosmology and the experimental data of short base line experiments, LSND, MiniBoone (*Abazajian et al.*, 2012), sterile neutrino provide the possibility of baryogenesis through leptogenesis, etc.

Thus, possible future detection of the relic neutrinos and the sterile neutrinos will provide precious cosmological information.

At present CMB and LSS data, provide constraints on neutrino masses, number of neutrino species and neutrino number density during the CMB and the LSS formation epochs. For a review see *Lesgourgues and Pastor* (2006, 2012). The determinations of light elements abundances and BBN theory predictions put stringent constraints on neutrino characteristics: neutrino number density, effective number of relativistic

[1] DE and DM, if existing, had negligible dynamical influence at RD stage.

neutrino types, lepton asymmetry in neutrino sector, sterile neutrino characteristics, neutrino mass differences and mixing, deviations from thermal equilibrium, neutrino decay parameters, etc. In particular, cosmological constraints on number of neutrino types (*Shvartsman*, 1969) were proposed decades before the establishment of LEP constraints on light neutrino types.

Thus, on one hand Cosmology and Astrophysics provide knowledge about the properties of neutrino, which is complementary to the information coming from experimental Particle Physics. In many cases Cosmology allows to obtain constraints on neutrino characteristics in the range of their values unreachable by direct experimental search, like very small masses, small mass differences, etc. On the other hand it is important, exploring the cosmological influence of neutrino, to gain unique information about the physical conditions of the very young hot Universe.

In particular, neutrino oscillations effects in the early Universe and the cosmological constraints on oscillation parameters were systematically studied since the 80ies of the previous century.

In the thesis we discuss the established and hypothetical BSMs neutrino characteristics. Chapters 2, 3 and 4 are dedicated to our studies of the cosmological role of neutrinos and the cosmological constraints on neutrino characteristics.

Namely, **in chapter 2** we describe our study of the cosmological role of light non-thermalized sterile neutrino, non-equilibrium active-sterile neutrino oscillations, neutrino non-equilibrium decays and possible tiny lepton asymmetry in the neutrino sector. [2] For the description of the evolution of the studied non-equilibrium processes we proposed and used precise kinetic approach. Kinetic equations for the density matrix of the neutrino in momentum space describing the evolution of the non-equilibrium oscillating neutrino in the early Universe were derived (*Kirilova and*

[2]In previous literature mainly equilibrium case was studied (fast oscillations, thermalized sterile neutrino, fast thermalization of neutrino decay products, chemical potentials for the account of lepton asymmetry, etc.).

Chizhov, 1997, 1998b) and used to study the cosmological influence of nonequilibrium neutrino oscillations during BBN epoch. This approach allowed simultaneous account for the Universe expansion, neutrino oscillations and neutrino interactions with the hot plasma at the radiation dominated stage of the Universe evolution.

As a result of the precise numerical analysis we managed to study more precisely than in previous works the depletion of the active neutrino number densities and the increase of the effective number of the relativistic degrees of freedom due to active-sterile neutrino oscillations and to reveal two *qualitatively new effects of active-sterile neutrino oscillations*, namely: (i) production of a considerable distortion in the active neutrino energy spectrum due to non-equilibrium neutrino oscillations and (ii) possibility for neutrino-antineutrino asymmetry growth in resonant active sterile neutrino oscillations.

We obtained contemporary cosmological constraints on neutrino properties, on the basis of astrophysical and cosmological data, in particular, cosmological constraints on the number of neutrino families, neutrino mass differences and mixing, lepton asymmetry hidden in the neutrino sector, sterile neutrino possible characteristics, deviations of equilibrium in the neutrino sector, neutrino decay parameters.

Most of the cosmological constraints in this thesis were obtained on the basis of BBN considerations.

1.2.2 Processes influencing Big Bang Nucleosynthesis and their BBN constraints

The origin of the chemical content of the Universe is one of the basic cosmological questions. The explanation of the observed light element abundances in the Universe by cosmological nucleosynthesis *(BBN) is one of the great achievements of the SCM.* BBN presents one of the first evidences for the existence of an early hot period in the evolution of the Universe (together with the detection of CMB).

According to the standard cosmological model in an early period of our Universe, at energies 1 – 0.1 MeV, the conditions were favorable for a nuclear synthesis of light elements deuterium D, the isotopes of helium, ^{3}He and ^{4}He, and ^{7}Li to proceed. As a result of BBN, lasting just few minutes, the baryon matter of our Universe is mainly hydrogen-helium one, with tiny traces of D and ^{7}Li.

BBN today is a very *precise quantitative theory of cosmological nucleosynthesis.* For contemporary status of BBN see *Iocco et al.* (2009); *Olive et al.* (2000); *Coc et al.* (2014) and the review and references in 3.1. *BBN is experimentally confirmed theory*: at the corresponding energies the cross sections of the reactions are studied at laboratories. It explains with remarkable precision the observational data on the light elements. Thanks to that good accordance between BBN theory predictions and the observational facts, we know the physical conditions of the Universe (in the pre-BBN and BBN epoch), corresponding to the period from the first seconds to the first 30 minutes of the Universe evolution.

BBN is the *most precision cosmological test of fundamental Physics and BSMs Physics* studied thoroughly. Among the light elements produced primordially helium-4 is the most sensitive to the relativistic density and to the pre-BBN nucleons kinetics. It is the most exactly measured element, precisely calculated and with a simple post-BBN evolution. Therefore, it is appropriate for a precision probe of the conditions of the universe in the BBN epoch. BBN produced He-4 is the best speedometer and leptometer.

In particular, the production of He-4, besides being sensitive to the speed of the Universe expansion, is very sensitive to the interactions of nucleons involving neutrino, hence, it is sensitive to the characteristics of neutrino. It tests neutrino properties beyond SM like number of neutrino types, spectrum distortions of neutrinos, asymmetry in neutrino sector, etc. BBN provides the most stringent constraints on the lepton asymmetry of the Universe.

Chapters 3 and 4 of the thesis are dedicated to BBN, lepton asymmetry and processes in modified BBN models (with additional particles, with active-sterile neutrino oscillations, with lepton asymmetry).

In the third chapter of the thesis we investigate the effect of nonequilibrium neutrino oscillations on the expansion rate of the Universe and on the pre-BBN kinetics of nucleons. The production of helium-4 in modified BBN with nonequilibrium electron sterile neutrino oscillations is calculated for several hundreds different sets of oscillation parameters and for different level of initial population of the sterile neutrino state. BBN constraints on neutrino degrees of freedom in case of neutrino oscillations are presented.

Enormous overproduction of helium (up to 32% in the case of the resonant neutrino oscillations and up to 12.8% in the non-resonant one) is found possible, due to the precise kinetic approach we have used for the description of the neutrino oscillations and their effects on electron neutrino in the early Universe. The accepted in previous literature maximum overproduction was just 5% (mainly due to the account of the dynamical effect of oscillations). Thus, we have proven that maximal overproduction of helium-4 due to neutrino oscillations is 6 times bigger than obtained in studies not accounting for the exact kinetics of the oscillating neutrino, and especially not accounting for the spectrum distortion of the electron neutrino spectrum caused by neutrino oscillations.

The possibility for big overproduction of helium allowed, correspondingly, considerable strengthening of the existing then cosmological constraints on neutrino oscillation parameters. On the basis of the observational data on primordially produced helium-4, coming form BBN light elements data analysis and CMB data on the baryon and photon density, we have obtained the most precise and most stringent cosmological constraints on electron-sterile neutrino mixing and squared mass differences existing in literature. These cosmological constraints were obtained years before the results of neutrino oscillations experiments pointed to the oscillation parameters range, which excluded the electron-sterile channel as dominant for the solution of the solar neutrino anomaly.

The dependence of these cosmological constraints on the initial population of the sterile state was studied. Qualitatively new conclusions concerning this dependence were obtained. In contrast to the conclusions of previous studies that the non-zero initial population of the sterile neutrino may only relax the constraints, we have proved, that the constraints can be relaxed or strengthened depending on the interplay between the kinetic and the dynamical effects of non-zero population of the sterile neutrino state.

The dependence of these cosmological constraints on the lepton asymmetry have been studied in our works as well (see next subsection).

The light elements abundances produced in the standard BBN depend on one parameter - the baryon-to-photon ratio. BBN allows to define the density of baryons during BBN epoch. Deuterium is the best baryometer among the light elements produced primordially. Besides, recent CMB anisotropy measurements, as well, allowed to determine the baryon density with comparable to BBN precision. We have studied the baryon density in modified BBN model with neutrino oscillations. The possibility of relaxation of the BBN constraint on the baryon density in modified models of BBN, containing Physics beyond SM, especially neutrino oscillations has been discussed.

Although the baryon-to-photon number is measured with high precision by different means and at different epochs of the Universe, the exact baryogenesis and leptogenesis mechanisms are not known and appropriate B-violation and CP-violation processes are not detected. Many different types of baryogenesis and leptogenesis models exist in literature. We have proposed and studied numerically baryogenesis model with scalar field condensate (*Kirilova and Chizhov*, 1996b, 2000b), compatible with inflation and the low reheating temperature (see 1.2.4). A mechanism for leptogenesis in MSW resonant active-sterile neutrino oscillations was found in our works (*Kirilova and Chizhov*, 1996a, 1997, 2000a) and will be discussed in the following subsection.

1.2.3 Processes with lepton asymmetry and its cosmological effect and constraints. Asymmetry–neutrino oscillations interplay

Studying lepton asymmetry is necessary because of its important role in physical theories and in Cosmology, in particular in baryogenesis models, in primordial nucleosynthesis, for structure formation in the Universe. Knowledge about lepton asymmetry and its nature would help for precise determination of cosmological parameters, etc. Besides, as mentioned already, relic asymmetry can suppress or enhance neutrino transitions in the early Universe and influence BBN constraints on neutrino oscillations.

Lepton asymmetry of the Universe is usually assumed to be of the order of the baryon asymmetry. However, big lepton asymmetry can hide in the neutrino sector. There are known different possibilities for the origin of big lepton asymmetry, proposed by different BSMs (*Dolgov*, 2002; *Sarkar*, 1996): GUT, leptogenesis due to out of equilibrium decays of heavy Majorana neutrinos (*Fukugita and Yanagida*, 1986; *Murayama et al.*, 1993), in a scenario of baryogenesis with baryonic charge condensate (*Dolgov and Kirilova*, 1991), in fast resonant neutrino oscillations (*Foot et al.*, 1996). We have found (*Kirilova and Chizhov*, 1997, 1996a) the possibility for considerable (by several orders of magnitude) asymmetry growth in resonant electron-sterile oscillations at small neutrino mixings and small mass differences. We established the instability region of the oscillations parameters where such growth is possible.

Although direct measurements of L are not yet possible, constraints on L value exist on the basis of its effect on different processes, which have left observable traces in the Universe.

The role of $L > 0.01$ in BBN have been studied systematically in numerous works since the pioneer works of (*Wagoner et al.*, 1967; *Reeves*, 1972). Its effect on the Universe dynamics and on nucleons kinetics in the pre-BBN epoch have been investigated, and on the basis of BBN considerations stringent constraints on its value have been obtained. See the review of *Simha and Steigman* (2008) and the references and the review part of chapter 4.

In the thesis an original study of the cosmological effects of tiny lepton asymmetries $|L| << 0.01$ is provided. The results of our analysis of the interplay between lepton asymmetry and neutrino oscillations are presented. Indirect kinetic effect of such asymmetries on BBN via neutrino electron-sterile neutrino oscillations was found considerable. The possibility of tiny lepton asymmetries $|L| << 0.01$ (which do not have dynamical or direct kinetic effect on BBN) to influence BBN through its effect on neutrino oscillations is established for a first time.

The possibilities of small lepton asymmetries, depending on its value and on the neutrino oscillations parameters, to enhance, suppress or stop neutrino oscillations, have been analyzed. The possibility of lepton asymmetry to enhance neutrino oscillations is a qualitatively new effect, found in our numerical study (*Kirilova and Chizhov*, 1998b) and explored further in ref. (*Kirilova*, 2012). The possibility of enhancement of neutrino oscillations is due to a qualitatively new type of resonant oscillations transfer in the presence of small lepton asymmetry - "spectrum wave resonance", proposed in our work (*Kirilova and Chizhov*, 1998b), which we were able to find due to the precise kinetic approach used for the description of the interplay between oscillating neutrino and lepton asymmetry.

Besides, we have investigated how the presence of L (relic or produced in neutrino oscillations) changes the BBN cosmological constraints. The asymmetry growth was shown to lead to underproduction of helium in BBN, and correspondingly, to relaxation of the cosmological constraints on oscillation parameters. The effect of small relic asymmetries on helium overproduction and subsequently on the cosmological constraints on oscillations have not been studied before and was believed to be negligible. We have numerically studied the role of tiny lepton asymmetries $|L| \leq 10^{-4}$ in BBN with nonequilibrium neutrino oscillations for numerous sets of oscillation parameters. We have found the parameters range where cosmological constraints on oscillation parameters are strengthened, relaxed or evaded due to lepton asymmetry. Empirical relations, between the oscillations parameters values and the lepton asymmetry value have been obtained on the basis of the exact numerical analysis corresponding to the different cases. For big L that suppresses oscillations new cosmological constraints on oscillation parameters by L are found.

The possibility of relic lepton asymmetry to relax BBN constraints on neutrino oscillations was further explored in connection with the DR problem. A principal solution of DR problem was proposed – relaxation of the BBN constraints on eV sterile neutrino by preventing its thermalization in neutrino oscillations due to the presence of relic lepton asymmetry, large enough to suppress neutrino oscillations. The value of the lepton asymmetry necessary to relax the stringent BBN constraints on eV sterile neutrino was estimated.

A way to obtain stringent BBN cosmological bound on the value of the lepton asymmetry was proposed on the basis of indirect kinetic effect of lepton asymmetry via active-sterile neutrino oscillations. Lepton number of the Universe has not been measured directly, hence, the constraints on its value provide valuable information about this characteristic of the Universe. Thus, eventual future detection of the active-sterile neutrino oscillations will provide an upper limit on the value of lepton asymmetry of the Universe. We have calculated BBN bound on L assuming the values of electron-sterile neutrino oscillations proposed in ref. (*Holanda and Smirnov*, 2011).

The fifth and the sixth chapters of the thesis are dedicated to the processes important for the generation and distribution of the baryonic component of the Universe.

1.2.4 Processes important for baryogenesis. Baryon-antibaryon asymmetry of the Universe and LSS periodicity

The baryon number density of the Universe is measured with high precision by different independent means. The baryonic component constitutes around 5% of the total energy density of the Universe. Besides, antibaryons, except the secondaries, have not been detected in our Galaxy. At present the reason for the observed baryon asymmetry its value and sign is not known. Though the baryon component is small part of the total energy density of the Universe, baryons excess is unexpectedly big - it does not follow naturally form the initially baryon-antibaryon symmetric state of the Universe.

Usually it is assumed that the locally observed asymmetry is a global feature. Unlike the case with BBN, for which precision theory and observational data exist, there is not an accepted theory of baryogenesis, yet. It is known that baryogenesis should have occurred at higher energies and, correspondingly, higher temperatures in the early universe in the period after the inflation and before BBN. [3] Different types of baryogenesis mechanisms exist, like GUT baryogenesis, electroweak baryogenesis (*Kuzmin et al.*, 1985b), baryo-through-lepto-genesis (*Fukugita and Yanagida*, 1986), Affleck-Dine baryogenesis (*Affleck and Dine*, 1985), etc. For a review see refs. (*Dine and Kusenko*, 2004; *Buchmuller et al.*, 2005; *Dolgov*, 1992).

GUT baryogenesis, historically the first baryogenesis scenario, and the most natural versions of the EW baryogenesis are disfavored by experimental data. Baryogenesis-through-leptogenesis and AD baryogenesis scenario are the most promising today baryogenesis scenarios.

Affleck-Dine baryogenesis is compatible with inflation and the low reheating temperature of the Universe (*Dine and Kusenko*, 2004; *Enqvist and Mazumdar*, 2003), it

[3] The presence of the baryon asymmetry as an initial condition is theoretically not aesthetical and also not possible in case of inflation, because it would have washed out any baryon excess existing, or produced, before the inflationary epoch.

can produce simultaneously the observed baryon asymmetry and the dark matter.

In the 5th chapter we discuss and study numerically the Scalar Field Condensate (SFC) baryogenesis model, which is among the preferred today baryogenesis models, based on the Affleck-Dine scenario.

We present the results of analytical and numerical analysis of the generated baryon charge and its evolution on the parameters of the model (the characteristics of the baryon charge carrying scalar field – its mass, decay time, self coupling constants, as well as the Hubble constant at the inflationary stage and the gauge coupling).

We proved that particle creation processes by the time-varying scalar field are important for the evolution and the generated final value of the baryon charge and should be accounted for precisely. For the analytical account of the particle creation processes we have used the rate calculated in the perturbation theory. We proposed also exact numerical account of the particle creation processes.

Our numerical analysis of SFC baryogenesis model comprised hundred sets of model parameters and needed several thousands CP hours.

We have proved that for natural range of model parameters it is possible to generate the observed value of the baryon asymmetry in the SFC baryogenesis model.

Inhomogeneous SFC baryogenesis and antimatter in the Universe

Search for antimatter in Cosmic ray and gamma-ray data by ground based detectors, balloons and spacecraft provided constraints on the fraction of antimatter allowed in our Galaxy. Namely, it was found that small quantities of antimatter are allowed within our Milky Way galaxy (anti-stars, a globular anti-cluster), i.e. in our vicinity there exist enormous asymmetry between matter and antimatter. However, neither observational data nor theory exclude categorically the existence of large quantities of antimatter at distances higher than 10-20 Mpc, corresponding to nearby clusters of galaxies.

Therefore, it is interesting to study possible separation mechanisms between matter and antimatter domains. There are different possible inhomogeneous baryogenesis models discussed in literature (for a review see (*Dolgov*, 1992)) that can predict the existence of astronomically considerable quantities of antimatter.

In the the sixth chapter we study inhomogeneous Scalar Field Condensate baryogenesis model and show that it is capable to explain the locally observed asymmetry and at the same time to predict existence of antimatter domains in the Universe providing sufficient separation between regions of matter and antimatter. Different possibilities of CP-violation are discussed. Observational constraints on inhomogeneous models from CMB, LSS, BBN, CR and gamma ray data are discussed and applied to obtain an indication about the size of the predicted by the model antimatter domains and the distance to them (*Kirilova*, 2003b).

Inhomogeneous SFC baryogenesis and very large-scale structure of the Universe

According to the contemporary theory of structure formation in the Universe, based on the standard cosmological model with cold dark matter, a purely gravitational mechanism is not sufficient to explain the formation of giant voids and giant shells, as well as their possible spatial periodicity (*Broadhurst et al.*, 1990; *Ettori et al.*, 1995). A principal possibility for the formation of the quasi-periodicity of the baryonic matter and the very large scale of the LSS of the Universe of $\sim 120 - 130h^{-1}$ Mpc has been proposed (*Chizhov and Dolgov*, 1992). We have studied such possibility within the inhomogeneous SFC baryogenesis scenario (described in the sixth chapter).

1.2.5 Processes with new chiral tensor particles

The new chiral tensor (ChT) particles were first predicted in an extension of SM from theoretical considerations by Chizhov (1993). These heavy bosons are predicted to be the carriers of new interaction, however in contrast to the gauge bosons, they have only chiral interactions with light fermions, through tensor anomalous coupling.

Today it is known that the existence of particles of this type does not contradict the contemporary experimental data and their presence is able to explain several anomalies in Particle Physics. The search for new chiral bosons continues to be of great interest. These bosons have unique properties, which will help to disentangle them from other widely discussed hypothetical particles at hadron colliders (see Chizhov, 2006, 2007a, 2007b, 2008; Chizhov et al. 2008). At present the search of the chiral bosons is conducted by the international collaboration ATLAS at LHC.

In the thesis the cosmological role and place of the chiral tensor particles in the Universe history have been studied (see seventh chapter and *Chizhov and Kirilova* (2009)). We discuss an extended BSMs model with new ChT particles. The influence of these particles on the early Universe history and evolution is studied. It is shown that ChT particles slightly speed up the Hubble expansion. Their characteristic processes are calculated and the time of their creation, annihilation and decay is defined. The time interval of efficiency of these particles in the Universe evolution is determined for the accepted values for their masses and couplings. Cosmological BBN constraint on the strength of their interaction is obtained – centi-weak interactions, which is in accord with the theoretical and experimental findings.

The discussed model of BSM physics with additional chiral tensor bosons is allowed from cosmological point of view and its unique predictions hopefully will be tested soon at the new run of LHC.

1.3 Main Objectives, Goals and Methods of the Research Underlying the Thesis.

This thesis has the objectives to provide interdisciplinary study of actual problems of contemporary Physics, Astropartical Physics and Cosmology and to obtain cosmological constraints on new Physics.

1.3.1 Main objectives and goals

The main aims of our study are:

(i) to investigate the properties of neutrino and its astrophysical and cosmological effects

(ii) to investigate active-sterile neutrino oscillations and their cosmological effects and constraints

(iii) to investigate alternative cosmological nucleosynthesis models containing Physics BSMs and to obtain cosmological constraints on their characteristics on the basis of observational data

(iv) to study the asymmetries of the Universe - lepton asymmetry and baryon asymmetry, their cosmological effects and observational constraints

(v) to study the relationship between neutrino oscillations and lepton asymmetry

(vi) to study the cosmological role of eventual relic lepton asymmetry, bigger than the baryon asymmetry, during BBN and analyze the change of the cosmological constraints on neutrino oscillations in the model of BBN with lepton asymmetry

(vii) to propose a solution to the DR problem

(viii) to study the possibility for leptogenesis in resonant neutrino active-sterile neutrino oscillations

(ix) to study mechanisms for baryogenesis, explaining the observed locally baryon-antibaryon asymmetry

(x) to study inhomogeneous baryogenesis models able to predict antimatter domains in the Universe and to obtain constraints on their parameters using observational data (light elements abundance at different redshifts, CMB anisotropy measurements, large-scale structure surveys of the Universe)

(xi) to study the possibility to explain the quasi-periodicity in the distribution of the visible baryonic matter and the existence of super-structures in the large-scale structure of the Universe

(xii) to investigate the cosmological role of chiral tensor particles and provide cosmological constraints on their interactions

1.3.2 Approaches and methods used

The studies underlying the thesis concern processes at high energies and densities, corresponding to early Universe stages (BBN, baryogeneis, leptogenesis, inflation, etc.). The investigation of these stages require the unified power of physical sciences. Thus, the methods of Astroparticle Physics, Cosmology, Quantum Field Theory, Theoretical Physics and Phenomenology were the main tools of our investigations.

We have used theoretical and phenomenological approach in our studies. Modified cosmological models were constructed in which the SCM was extended to contain: additional sterile neutrino, chiral tensor particles, neutrino oscillations, both lepton asymmetry and neutrino oscillations, increased baryonic content, etc.

For probing the cosmological role of different processes in most cases numerical analysis and evolutionary analysis was used.

Cosmological constraints were obtained by comparative analysis of the observational data and the predictions of the theoretical models, containing BSMs Physics.

1.4 Structure and Content of the Thesis

The thesis consists of 8 chapters, bibliography, list of figures, list of abbreviations and acknowledgements sections.

The first chapter of the thesis presents introduction to the topics discussed in the thesis, their actuality, originality, the main objectives and goals.

In the introductory part of **the second chapter** of the thesis the main established and predicted by Standard Models neutrino characteristics are discussed. The role of neutrino in the early Universe is reviewed, relic neutrino characteristics and the formation of the cosmic neutrino background and its evolution from the early universe stages till today are described. The influence of flavor and sterile neutrino on the Universe expansion rate and on BBN are discussed and cosmological constraints on neutrino are reviewed. A precise kinetic approach for the analysis of the propagation of nonequilibrium oscillating neutrino in the early Universe is proposed. A model of non-equilibrium electron-sterile neutrino oscillations is presented and numerically studied. The cosmological effects of these nonequilibrium neutrino oscillations are analyzed, namely neutrino spectrum distortion, depletion of neutrino number density and the neutrino-antineutrino asymmetry growth due to oscillations. The more general case of partially filled sterile neutrino is studied as well.

The third chapter of the thesis is dedicated to modified models of BBN. First a short review of the standard BBN model and the contemporary observational data on light elements abundances are presented. The main predictions and constraints of standard BBN are discussed. The major part of the chapter is dedicated to production of helium-4 in modified BBN with nonequilibrium electron sterile neutrino oscillations. The production of helium is numerically studied in non-resonant and resonant oscillations case and for the whole parameters range of the oscillations model and for different level of initial population of the sterile neutrino state. The maximum overproduction of He is determined. Cosmological constraints on electron-sterile neutrino mixing and squared mass differences are obtained. The dependence of the cosmological constraints on the initial population of the sterile state is studied. The possibilities of relaxation of the BBN constraint on neutrino oscillations and on the baryon density in modified models of BBN containing Physics beyond SM, are investigated.

The fourth chapter is dedicated to lepton asymmetry, neutrino oscillations and BBN. First I review the known basic cosmological effects of L on processes in the

Universe. The cosmological constraints on L on the basis of standard BBN model are shortly discussed. Then the results of our analysis of the interplay between lepton asymmetry and $\nu_e \leftrightarrow \nu_s$ neutrino oscillations are presented. The numerical study of the growth of asymmetry in resonant oscillations allowed us to determine the instability region and the maximum asymmetry growth. A new type of resonant oscillations transfer in the presence of small lepton asymmetry - "spectrum wave resonance" is found. Modified BBN model with neutrino electron-sterile oscillations and small lepton asymmetry is considered and the indirect kinetic effect of lepton asymmetries (relic or oscillations generated) on the production of helium-4 is studied. The change of cosmological constraints on oscillation parameters due to lepton asymmetry is numerically studied. New cosmological constraints on oscillations parameters in case of lepton asymmetry big enough to stop oscillations are obtained. The possibility of relic lepton asymmetry to relax BBN constraints on neutrino oscillations is explored in connection with the DR problem. A principal solution of DR problem was proposed. BBN bound on L in case of electron-sterile neutrino oscillations are obtained.

The fifth chapter discusses the baryon asymmetry and its generation. We describe and study numerically Scalar Field Condensate baryogenesis model. We present the results of analytical and numerical analysis of the generated baryon charge and its evolution on the parameters of the model (the characteristics of the baryon charge carrying scalar field – its mass, decay time, self coupling constants, as well as the Hubble constant at the inflationary stage and the gauge coupling). We discuss the important role of the precise account for the particle creation processes by the time-varying scalar field.

In the sixth chapter we discuss the possibility of baryon inhomogeneities at large scale and their explanation in inhomogeneous SFC baryogenesis models. First inhomogeneous SFC baryogenesis model capability to produce antimatter regions, safely separated from the matter ones is studied. Different possibilities of CP-violation are discussed corresponding to different size of the predicted domains of matter and antimatter and different distance between them. We discuss the observational constraints from CMB anisotropy data, CR and gamma-ray data and BBN for each separate case.

Inhomogeneous SFC baryogenesis is shown capable to explain also the observed quasi-periodicity in the distribution of the visible matter in the Universe and the generation of super-structures.

In the seventh chapter we discuss processes with chiral tensor particles.

We discuss an extended BSMs model with new ChT particles. The influence of these particles on the early Universe history and evolution is studied. It is shown that these particles slightly speed up the Hubble expansion. Their characteristic processes with the particles of the hot Universe plasma are calculated and the time of their creation, annihilation and decay is defined. The time interval of efficiency of these particles in the Universe evolution is determined for the accepted values for their masses and couplings. Cosmological constraint on the strength of their interaction is obtained – centi-weak interactions, which is in accord with the theoretical and experimental findings.

In the eighth chapter we present our conclusions and an overview of the main results and achievements. The publications, underlying the thesis are listed. Part of the international conferences, symposiums and workshops, where the results presented in this thesis were discussed are given, as well.

CHAPTER II

Processes involving neutrino. Nonequilibrium Neutrino Oscillations and Their Cosmological Effects

2.1 Introduction

Neutrinos cosmological role has been systematically studied: It has been understood that neutrinos had a considerable role in the universe evolution during its early stages, namely, neutrino was essential relativistic component and defined the universe dynamics, CMB formation epoch, neutrino participated in reactions with nucleons and influenced considerably BBN, neutrino might be responsible for leptogenesis and baryogenesis. Depending on their mass neutrinos were important also during later stages of the universe, influencing the formation and evolution of the large scale structure and being a good candidate for the dark matter (DM) in the universe. Thus, the possible future detection of the relic neutrinos will provide precious information about the first seconds of the universe evolution.

Meanwhile *neutrino physics and astrophysics have achieved serious results.* Since the first idea about neutrino existence, presented in the now famous Pauli's letter of 1930, and since neutrinos first direct detection in 1953 by Reines and Cowan, Neutrino

Physics and Astrophysics has passed a long and fruitful path.

Neutrinos from earth reactors and accelerators. To mention just several of its road marks: neutrino helicity measurements first made in 1957 by Goldhaber et al.; the existence of 2 types of neutrinos predicted in 1960 by Lee and Yang and the detection of muon neutrino in 1962 by L. Lederman, M. Schwartz and J. Steinberger; the hypothesis of neutrino oscillations proposed by B. Pontecorvo in 1958; the participation of neutrino in weak neutral currents, found in 1973; the existence of 3 light flavor neutrino types, confirmed by LEP experiments in 1993; studies of neutrino mass by double beta decay experiments; studies of neutrino oscillations at terrestrial experiment (in other terms studies of "man-made" neutrinos from controlled sources) CHORUS, NOMAD, LSND, K2K, Minos, OPERA, reactor-based experiments KamLand, CHOOZ, MiniBoone reactor long baseline neutrino oscillations experiments, etc.

Neutrinos from astrophysical sources. Besides neutrinos from earth reactors and accelerators, we have detected and studied *neutrinos from astrophysical sources*, namely from the Sun, from the atmosphere, from supernova SN1987, extragalactic neutrinos and geo-neutrinos from the Earth interiors. Neutrinos from the Sun and the atmosphere were intensively studied. Since the first solar neutrino experiment - the chlorine Homestake experiment by R. Davis in 1960's it was found (and confirmed by the following solar neutrino experiments like gallium radiochemical experiments Gallex, SAGE, water Cherenkov experiments Kamiokande) that *there exists an energy dependent deficit of electron neutrinos coming from the Sun*, compared to the predictions of the standard solar model. Another anomaly, atmospheric neutrino anomaly, was found in neutrino fluxes from the atmosphere by IMB, and confirmed by Kamiokande, MACRO and SOUDAN experiments.

These *solar and atmospheric neutrino anomalies were successfully explained in terms of neutrino oscillations.* In 1998 Super-Kamiokande obtained the evidence of atmospheric flavor neutrino oscillations, which pointed to non-zero neutrino mass.

The flavor neutrino oscillations, suggested by solar and atmospheric neutrino experiments, were confirmed by neutrino terrestrial experiments. The atmospheric neutrino oscillations were confirmed by the earth based experiment K2K and Minos. In 2002 the heavy water Cherenkov experiment SNO provided the evidence of flavor-transformation of solar neutrinos, thus allowing solar neutrino oscillations to be established independently of the solar model. The ground based experiment KamLAND gave an evidence of reactor flavor antineutrino oscillations.

Thus, solar neutrino problem, atmospheric neutrino anomaly and the positive results of terrestrial neutrino experiments were resolved by the phenomenon of neutrino oscillations. The dominant oscillation channels have been proved to be flavor neutrino oscillations. A nice detail review of the main experimental and theoretical results of neutrino physics may be found in e.g. *Strumia and Vissani* (2010).

Thus, a strong evidence for *non-zero neutrino mass and mixing* has been provided by solar, atmospheric and terrestrial neutrino oscillation experiments in recent years. The existence of 3 mass differences requires that at least 2 neutrinos have mass.

The next subsections are dedicated to the main established and predicted by SMs neutrino characteristics. The role of neutrino in the early Universe is discussed. SCM predictions about relic neutrino characteristics and the formation of the cosmic neutrino background and its evolution are presented. The established BSMs physics in neutrino sector - neutrino oscillations - is discussed. The propagation of oscillating neutrino in the early Universe is shortly reviewed in section 2. Section 2.2 describes our model of non-equilibrium electron-sterile neutrino oscillations. Section 3 discusses the found in our analysis effects of electron-sterile neutrino oscillations, namely neutrino spectrum distortion, depletion of neutrino number density and the neutrino-antineutrino asymmetry growth due to oscillations. In section 4 the spectrum distortion due to oscillations in the more general case of partially filled sterile neutrino is presented.

2.1.1 Neutrinos in the Standard Model and beyond

According to the Standard Model, neutrinos are massless, spin 1/2 fermions, which have weak interactions, i.e. they belong to SU(2)$_W$ doublets. There exist 3 neutrino flavors of weakly interacting light neutrinos, namely electron neutrino ν_e, muon neutrino ν_μ and tau neutrino ν_τ. The most precise experimental measurement of the number of light (with $m < m_Z/2$) neutrino types comes from four LEP experiments, and gives $N_\nu = 2.984 \pm 0.008$ (*Adeva et al.*, 1989).

Besides, BSMs physics predicts other types of neutrinos, not coupled to Z, called "sterile" ν_s, i.e. SU(2)$_W$ singlets, not having the ordinary weak interactions. Sterile neutrinos may be produced in GUT models, in models with large extra dimensions, Manyfold Universe models, mirror matter models, or by neutrino oscillations, etc.

It is extremely difficult to obtain experimental information about ν_s. Hence, the cosmological information about sterile neutrino is very valuable. The existing and the established in our works stringent cosmological bounds on the number of neutrino families and on sterile neutrino will be discussed in detail in the following sections.

However, there are robust experimental evidence for BSMs physics in the neutrino sector: Neutrinos oscillate, i.e. their mass eigenstates do not coincide with their flavor eigenstates, there exist neutrino mixing and non-zero neutrino mass differences. Neutrino oscillations data proved that neutrinos are massive. The origin of neutrino masses is still unknown. Various mass generation mechanisms, usually involving the introduction of extra particles, are discussed.

2.1.1.1 Neutrino oscillations

Neutrino Puzzles

The theme of neutrino oscillations is with us more than fifty years, since the hypothesis for them was proposed (*Pontecorvo*, 1958a,b, 1968). They were studied experimentally and theoretically and their cosmological and astrophysical effects have been considered in numerous publications as far as their study helps to go deeper into the secrets of neutrino physics and neutrino mass pattern.

In the 90ies there were known three main *experimental indications* that neutrinos oscillate, namely: the solar neutrino deficit (an indirect indication) (*Cleveland and others Homestake Coll.*, 1995; *Hampel and others (GALLEX Coll.)*, 1996; *Abdurashitov and others (SAGE Coll.)*, 1996; *Fukuda and others (Kamiokande Coll.)*, 1996), the atmospheric neutrino anomaly (an indirect indication) (*Fukuda and others (Kamiokande Coll.)*, 1994; *Becker-Szendy and others (IBM Coll.)*, 1995; *Allison and others (Soudan-2 Coll.)*, 1997) and the LSND experiment results (a direct indication) (*Athanassopoulos and others (LSND Coll.)*, 1996) .

(a) **Solar neutrino deficit:** Experiments using different techniques had detected electron neutrinos from the Sun, at a level significantly lower than the predicted on the basis of the Standard Solar Model and the Standard Electro Weak Theory. Moreover, there existed incompatibility between Chlorine and Kamiokande experiments data, as well as problems for predicted berilium and borum neutrinos in the gallium experiments (*Hampel and others (GALLEX Coll.)*, 1996; *Bahcall*, 1989).

It was realized that by changing the solar model it is hardly possible to solve these problems (*Bahcall and Pinsonneault*, 1995), (*Berezinsky et al.*, 1996). Therefore, it was necessary to find a solution beyond the Standard Electroweak Model. The only known natural solutions then were the energy dependent Miheyev-SMirnov-Wolfenstein (MSW) neutrino transitions in the Sun interior (see refs. (*Mikheyev and Smirnov*, 1985; *Wolfenstein*, 1978)), the "just-so" vacuum oscillations solutions and the hybrid solutions of MSW transitions + vacuum oscillations type (*Krastev and Petcov*, 1996; *Berezhiani and Rossi*, 1995; *Hata and Langacker*, 1995; *Dar and Shaviv*, 1996).

(b)**Atmospheric neutrino anomaly:** Underground experiments on atmospheric neutrinos had observed disappearance of muon neutrinos (*Fukuda and others (Kamiokande Coll.)*, 1994; *Becker-Szendy and others (IBM Coll.)*, 1995; *Allison and others (Soudan-2 Coll.)*, 1997), which was in contradiction with the theoretically expected flux of muon neutrinos from primary cosmic rays interacting in the atmosphere.

(c)**Los Alamos LSND experiment** claimed evidence for the oscillation of $\tilde{\nu}_\mu$ into $\tilde{\nu}_e$, with a maximal probability of the order of 0.45×10^{-2}. A complementary ν_μ into ν_e oscillation search, with completely different systematics and backgrounds, also showed a signal, which indicated the same favored region of oscillation parameters (*Athanassopoulos and others (LSND Coll.)*, 1996).

There existed yet another **observational suggestion for massive neutrinos and neutrino oscillations** - the **dark matter problem**. Models of structure formation in the Universe at the time indicated that the observed hierarchy of structures is reproduced best by an admixture of about 20% hot dark matter to the cold one (*Primack et al.*, 1995; *Caldwel and Mohapatra*, 1993; *Wright et al.*, 1992). Light neutrinos with mass in eV range were the only particle dark matter candidates, that were actually known to exist and were the most plausible candidates provided by particle physics since the early studies (*Drees*, 1996). Actually, most popular then hot plus cold dark matter models assumed that two nearly degenerate massive neutrinos each with mass around 2 eV play the role of the hot dark matter.

In case one takes seriously each of these experiments pointing to a neutrino anomaly and the neutrino oscillation solution to them, a fourth neutrino seems inevitable. In the case of only three species of light neutrinos with normal interactions and a see-saw hierarchy between the three masses, it is hardly possible to accommodate all the oscillations data simultaneously.

The successful attempts to reconcile the LSND results with neutrino oscillation solutions to the solar and atmospheric neutrino problems usually contained fourth ultra-light sterile neutrino species, or inverted neutrino mass hierarchy. However, an additional light (with mass less than 1 MeV) flavor neutrino is forbidden both from cosmological considerations and the experiments on Z decays at LEP (*Adeva et al.*, 1989). Hence, it was reasonable to explore in more detail the possibility for an additional light *sterile* neutrino. [1]

Therefore, it was interesting to obtain precise information about the cosmologically allowed range for the neutrino mixing parameters and thus present an independent test for the solutions of the discussed neutrino puzzles.

The results of our study of the cosmological effects of neutrino oscillations (to be discussed in more detail in the following sections and in chapter 3) allowed to exclude almost completely LOW active-sterile solution in addition to the already excluded by cosmology LMA active-sterile solution to the solar neutrino puzzle and active-sterile solution to the atmospheric neutrino puzzle. Cosmological indications, (*Barbieri and Dolgov*, 1990, 1991; *Enqvist et al.*, 1992, 1990a) including our results, (*Kirilova and Chizhov*, 1997, 1998c, 2000a), preceded by several years the experimental results which pointed to the flavor mixing solution of the first two anomalies and provided precious complementary information to the neutrino oscillations experimental data.

Moreover, the very small values of mass differences, which can be explored by the oscillations cosmological effects (like the ones discussed in our model) still are beyond the reach of present and near future experiments.

The present day status of LSND and other recent experiments pointing to the necessity of active-sterile neutrino oscillations and eV sterile neutrino will be discussed in more detail below and in chapter 4 in connection with the DR problem.

Neutrino oscillation parameters

Neutrinos oscillate, i.e. their mass eigenstates ν_j do not coincide with the flavor

[1] Besides, GUT theories ($SO(10), E_6$, etc.) and SUSY theories predict the existence of a sterile neutrino. Moreover, models of singlet fermions, which explain the smallness of sterile neutrino mass and its mixing with the usual neutrino were proposed (*Chun et al.*, 1996).

eigenstates ν_f, there exist neutrino mixing and non-zero neutrino mass differences:

$$\nu_f = \sum_{i=1}^{3} U_{fi}\nu_i, \quad \delta m_{ij}^2 = m_j^2 - m_i^2 \neq 0, \ (i \neq j) \tag{2.1}$$

Then in the simple two-neutrino oscillation case in vacuum, the probability of a given neutrino type in an initially homogeneous neutrino beam of the same type is:

$$P_{ff} = 1 - \sin^2 2\vartheta \sin^2(\delta m^2 t/4E), \tag{2.2}$$

where E is the neutrino energy, δm^2 and ϑ are the oscillation parameters, correspondingly, the neutrino squared mass difference and the mixing angle.

In general neutrino oscillations occur in medium. The medium distinguishes between different neutrino types due to different interactions and changes the oscillation pattern (*Wolfenstein*, 1978; *Mikheyev and Smirnov*, 1985). Neutrino oscillations in medium are called "matter oscillations". Matter oscillation parameters are expressed through the vacuum ones and the characteristics of the medium.

Solar and atmospheric neutrino anomalies were resolved by neutrino oscillations, confirmed by the terrestrial neutrino oscillations experiments. The dominant neutrino oscillation channels have been proved to be flavor neutrino oscillations. The global analysis of current neutrino oscillations experimental data, including SNO, Borexino, SuperKamika, Chlorine, Gallium and SKI+SKII+SKIII, MINOS, T2K and Kamland data, provided precision information about neutrino mass differences and mixing (*Nakamura and Petcov*, 2012; *Capozzi et al.*, 2014),ν_e in the Sun oscillate into ν_μ and ν_τ, the corresponding oscillating parameters are:

$$\delta m_{12}^2 \sim 7.5 \times 10^{-5}\mathrm{eV}^2, \sin^2\theta_{12} \sim 0.3$$

Atmospheric muon neutrinos oscillate mainly into tau neutrinos with almost maximal mixing.

$$|\delta m^2_{31}| \sim 2.4 \times 10^{-3}\mathrm{eV}^2,$$

$$\sin^2\theta_{23} \sim 0.455$$

The θ_{13} was recently measured. First indications of a non-zero value were obtained by T2K, MINOS and Double CHOOZ Experiment. Combined analysis of the data from T2K, MINOS, Double Chooz, Daya Bay and RENO experiments found non-zero value at 7.7 sigma (*Machado et al.*, 2012):

$$\sin^2\theta_{13} \sim 0.024$$

The pattern of neutrino mixing is drastically different from the pattern of quark mixing. The masses of neutrino are much smaller than those of quarks and charged leptons.

This well-established 3-neutrino oscillations pattern, however, cannot accommodate for the data from: LSND, its successor MiniBoone, and short base line experiments.

The analysis of these neutrino oscillations data suggested the existence of 1 or 2 light sterile neutrinos, participating in oscillations with the flavor ones with sub-eV mass and differences of mass squared close to eV^2 (*Kopp et al.*, 2011).

Neutrino mass

Since 1998 the neutrino oscillation data firmly established that at least 2 neutrino species have non-zero mass. Neutrino oscillations data cannot determine the absolute mass scale. From atmospheric neutrino oscillations data lower mass limit is obtained: at least one type of neutrino has mass exceeding 0.048 eV. For 3 massive neutrinos with mass m, the neutrino energy density today is expected to be $\Omega_\nu = 3m/(93.14h^2$ $\mathrm{eV}^2)$. Hence, the neutrino oscillations data put lower limit on the energy density of relic neutrino: $\Omega_\nu > 0.003$.

The absolute neutrino mass has not been directly measured yet, neutrinoless double beta decay and beta decay experiments set an upper limit to the neutrino mass. For example the Mainz (*Krauz et al.*, 2005) and Troitsk (see e.g. (*Aseev and others (Troitsk Collaboration)*, 2011)) Tritium decay experiments limit the electron neutrino mass correspondingly $m < 2.05$ eV at 95% C.L.

Neutrino oscillations data provided information about the mass differences and mixing, while the ordering of neutrino masses is not known because of the unknown sign of δm_{13} and δm_{23}. So there exist the following possibilities for the neutrino mass spectrum: the *normal hierarchy* $m_1 < m_2 << m_3$ and the *inverted hierarchy* $m_3 << m_1 < m_2$. Neutrino masses may be small - of the order of δm_{23} but also they may be big and almost degenerate: $m_1 \sim m_2 \sim m_3 >> \delta m_{23}$.

Much more stringent mass limits are due to cosmology, which measures neutrino mass indirectly and provides the most stringent available now constraints on the total neutrino mass: $m < 0.66$ eV, corresponding to $\Omega_\nu < 0.02$

While cosmology cannot distinguish yet between eventual Dirac or Majorana nature of neutrino, it provides the most stringent constraints also on the number of neutrino families, neutrino mass differences and mixing, neutrino chemical potentials, which will be discussed in the thesis.

2.1.2 Relic neutrino predicted by Standard Cosmological Model

According to the SCM (*Zeldovich and Novikov*, 1983) at early radiation dominated stage of the Universe neutrinos were kept in thermal equilibrium due to their standard weak interactions with other particles while their interaction rates were faster than the expansion rate of the universe

$$\Gamma \sim \sigma(E) n_\nu(T) > H. \tag{2.3}$$

Hence, neutrino had an equilibrium Fermi-Dirac energy distribution

$$n_\nu^{eq} = (1 + \exp((E - \mu)/T))^{-1}. \tag{2.4}$$

The energy contribution ρ_ν of the light neutrino species to the energy density of the universe in relativistic species at that stage was comparable to the CMB photons one: $\rho_\nu \sim \rho_\gamma$. Hence, at early stages neutrino influenced the expansion rate of the universe H considerably, where:

$$H = \sqrt{8\pi G_N \rho/3} \tag{2.5}$$

The dynamical effect of equilibrium neutrino is usually parameterized by the effective number of the relativistic neutrino species N_{eff}:

$$\rho_\nu = 7/8(T_\nu/T)^4 N_{eff} \rho_\gamma(T). \tag{2.6}$$

As the universe expanded and cooled, particle densities diluted and the weak interactions became slower than expansion, i.e. ineffective to keep neutrino in good thermal contact with the plasma. Thus, at $T \sim 3$ MeV muon and tau neutrino decoupled and at ~ 2 MeV electron neutrino decoupled and since then they are free streaming, i.e. formed the cosmic neutrino background (CNB).

Due to neutrinos negligible masses they kept their equilibrium Fermi-Dirac (FD) spectrum after decoupling while their temperature decreased with the expansion and cooling of the universe.

During e^+e^- - annihilation, the photons were heated and since then neutrino temperature is lower than the CMB one

$$T_\nu = (4/11)^{1/3} T_{cmb}, \tag{2.7}$$

the number density per flavor is $n_\nu = 3/11 n_\gamma$, neutrino density is:

$$\rho = 7/8(4/11)^{4/3} N_{eff} \rho_\gamma(T). \tag{2.8}$$

Since the neutrino decoupling was close to e^+e^--annihilation, which proceeded at ~ 0.5 MeV, neutrinos shared a small part of the released entropy [2] due to non-instantaneous ν decoupling and flavor oscillations, and thus neutrinos were slightly heated (*Dolgov et al.*, 1997b; *Mangano et al.*, 2005). The account for these effects and for the QED finite temperature effects slightly changed neutrino number density and neutrino energy density. The neutrino distribution was negligibly distorted, the change may be described by changing the effective number of relativistic neutrino species

$$N_{eff} = 3.046.$$

Today SCM predicts CNB with the following characteristics: number density (per 3 neutrino species) comparable to the CMB photons one $n_{CMB} = 411$ cm^{-3}: $n_\nu + n_{\bar{\nu}} = 339.3$ cm^{-3}, and temperature slightly smaller than CMB temperature: $T_\nu \sim 1.9K$.

Thus, although relic neutrinos contributed considerably to the universe dynamics while $m_\nu << T_\nu$ because they are numerous, the relic neutrinos today contribute negligible part to the total energy density due to their low temperature. Namely: $\Omega_\nu(t_0) \sim 10^{-5}$.

Summarizing, the standard cosmological model predicts CNB, which has formed close to the BBN epoch, with a temperature today slightly smaller than the CMB one, negligible chemical potential, and negligible nonthermal features. Nice detail reviews of relic neutrinos can be found in refs. (*Dolgov*, 2002; *Lesgourgues and Pastor*, 2006; *Hannestad*, 2010).

Direct CNB detection has not been performed. It is difficult because, though

[2] This is still unobservable by present observations.

numerous, neutrinos have weak interactions and relic neutrinos are with low energy today $\sim 10^{-4}$ eV. Neutrino detectors today are able to catch neutrinos with considerable energy, like neutrinos from supernovas' bursts, from the Sun, etc.

In some near future, hopefully, appropriate detector facilities will be able to study the cosmological neutrinos, which will provide a glimpse into the first seconds of the universe existence (the epoch of CNB formation).

Fortunately, at present *indirect CNB detection* is possible due to CNB cosmological effects, i.e. its effect on BBN, CMB, LSS, etc. The closeness of neutrino decoupling to the BBN epoch is one of the reasons for the big influence of neutrino on BBN and the numerous BBN constraints on neutrino properties, which will be discussed in the following chapters.

2.1.3 Possible deviations of relic neutrino spectrum from Fermi-Dirac distribution

There exist different possibilities for deviations of the relic neutrino energy spectrum from the equilibrium Fermi-Dirac (FD) distribution (*Kirilova and Chizhov*, 2010). Among them are nonequilibrium neutrino oscillations, non-equilibrium neutrino decays, non-zero lepton asymmetry, etc.

Lepton asymmetry

One possible source of ν spectrum distortion (SD) is the existence of *non-zero relic neutrino asymmetry.* Such asymmetry might be generated in resonant MSW active-sterile oscillations after neutrino decoupling.

Asymmetry in the neutrino sector is strongly constrained by BBN considerations: flavor ν oscillations with parameters favored by the atmospheric and solar neutrino data establish an equilibrium among active neutrino species before BBN epoch. Hence, the stringent BBN limit to ν_e degeneracy applies to all flavors.

However, there still exists a possibility of lepton asymmetry in the post-BBN epoch, which has not been much explored.

Neutrino oscillations

Non-equilibrium neutrino oscillations present another source of deviation of neutrino distribution from the equilibrium FD form.

It is known that flavor oscillations slightly shift neutrino FD distribution because of the almost equal temperature of the different neutrino species, which equality is due to their very close decoupling times.

Active-sterile oscillations effective before neutrino decoupling also slightly influence active neutrino distributions, because the flavor states are refilled due to interactions with the plasma.

In contrast, active-sterile nonequilibrium oscillations $\nu_e \leftrightarrow \nu_s$, proceeding after ν_e decoupling, i.e. $\delta m^2 \sin^4(2\vartheta) \leq 10^{-7}\text{eV}^2$ and provided that ν_s state is not in equilibrium,[3] may cause strong energy SD and ν_e depletion and generate $\nu_e - \bar{\nu}_e$ asymmetry.

Hence, due to $\nu_f \leftrightarrow \nu_s$, CNB may be considerably depleted (*Kirilova and Chizhov*, 2010). When oscillating neutrino reach statistical equilibrium, the active species may be depleted by a factor $p/(p+k)$, here p is the number of active neutrino flavors participating in oscillation with k sterile neutrino species. Besides, CNB may be less energetic with an energy spectrum distorted from the equilibrium FD one. In the case of such oscillations future prospects of observing CNB may be even worse than the predicted by standard cosmological paradigm. On the other hand eventual future observations of SD of relic neutrino will allow to peek into the well hidden realm of sterile neutrino.

Decays of neutrino

Eventual non-equilibrium decays of neutrino or decays of particles into neutrino

[3] which is an expected natural possibility, because ν_s decouples much earlier in the universe evolution and since then flavor neutrinos have been heated by the annihilation processes, taking place till flavor neutrino's later decoupling.

also have been discussed as a potential reasons for deviation of the relic neutrino spectrum from FD form. See for example (*Dolgov and Kirilova*, 1988; *Kirilova*, 2009) and the references there in.

2.2 Propagation of the oscillating neutrino in the early Universe

The *thermal background in the early Universe strongly affects the propagation of neutrinos* (*Nötzold and Raffelt*, 1998; *Harris and Stodolsky*, 1978; *Stodolsky*, 1987). Differences in the interactions with the particles from the plasma lead to different average potentials V_f for different neutrino types (the electron neutrinos and antineutrinos receive extra contribution from charged current interactions with electrons, in comparison with muon and tau neutrinos. The sterile neutrino does not feel the medium, hence $V_s = 0$. Then:

$$V_f = q \pm l \tag{2.9}$$

$$q = -bET^4/(\delta m^2 M_W^2) \tag{2.10}$$

$$l = -aET^3 L^\alpha/(\delta m^2) \tag{2.11}$$

where $f = e, \mu, \tau$, L^α is given through the fermion asymmetries of the plasma, a and b are positive constants different for the different neutrino types, $-l$ corresponds to the neutrino and $+l$ to the antineutrino case.

Thus in the Sun, where $l >> q$ neutrino and antineutrino experience an opposite effect. However, in the early Universe q is the leading term, unless l is assumed unusually large, i.e. $L >> B$.

In the adiabatic case the effect of the medium can be formally hidden in the oscillation parameters δm^2 and ϑ by introducing matter oscillation parameters. They are expressed through the vacuum ones and through the characteristics of the medium, like its density and temperature. In the early Universe the matter mixing angle is given by

$$\sin^2\vartheta_m = \sin^2\vartheta/[\sin^2\vartheta + (q \mp l - \cos 2\vartheta)^2]. \tag{2.12}$$

In general the medium suppresses oscillations by decreasing their amplitude. There also exists a possibility of enhanced oscillation transfer in case a resonant condition between the parameters of the medium and the oscillation parameters holds. For the early Universe the resonant condition is:

$$q \mp l = \cos 2\vartheta. \tag{2.13}$$

Then the mixing in matter becomes maximal, independently of the value of the vacuum mixing angle, i.e. resonant transfer takes place. For $q = 0$ this is the well known Mikheyev-Smirnov-Wolfenstein effect (*Mikheyev and Smirnov*, 1985; *Wolfenstein*, 1978).

At high temperature of the early Universe and in case of a lepton asymmetry of the order of the baryon one, $q > l$. So for $\delta m^2 < 0$ resonance transfer is possible both for neutrino and antineutrino. At low T, however, $l > q$, and as can be seen from the resonant condition, if $\delta m^2 > 0$ a resonance transfer in the neutrino ensemble can take place, while for $\delta m^2 < 0$ – the resonance transfer is possible only for the antineutrinos.

This simplified behavior is characteristic in the equilibrium situation, when working in terms of mean neutrino energy is acceptable. When spectrum distribution of neutrino in the early universe is taken into account the behavior is more complicated. For example, it is possible to observe simultaneous resonance transfer also in the $\delta m^2 < 0$ case (*Kirilova and Chizhov*, 1998b; *Kirilova*, 2011c, 2012), as will be discussed in chapter 4.

In the following sections we discuss a model of nonequilibrium neutrino oscillations and provide an exact analysis of the neutrino evolution using kinetic equations for the neutrino density matrix for each momentum mode. The main effects of nonequilibrium oscillations are discussed.

2.2.1 Electron-sterile neutrino oscillations in the early Universe

In refs. (*Kirilova and Chizhov*, 1997, 1998c, 2000a, 2001a) we explored the cosmological effect of *nonequilibrium neutrino oscillations* $\nu_e \leftrightarrow \nu_s$ in the early Universe, and in particular on the primordial nucleosynthesis and obtained cosmological constraints on the neutrino mixing parameters.

The nonresonant case in the early Universe medium corresponds to the resonant case in the Sun, therefore, the obtained information was of special interest for finding a solution to the solar neutrino problem.

We discussed the special case of *nonequilibrium oscillations* between weak interacting electron neutrinos and sterile neutrinos for *small mass differences* δm^2.

The case of large δm^2 was already sufficiently well studied (*Barbieri and Dolgov*, 1990; *Enqvist et al.*, 1992; *Shi*, 1996). Oscillations between active and sterile neutrinos, effective before neutrino freezing at 2 MeV, leading to ν_s thermalization before 2 MeV had been studied there. Equilibrium oscillations were considered with rates of oscillations and neutrino weak interactions greater than the Universe expansion rate.

We explored nonequilibrium oscillations between electron neutrinos ν_e and sterile neutrinos ν_s for the case when ν_s do not thermalize till ν_e decoupling at 2 MeV and oscillations become effective after ν_e decoupling. Such kind of *late active-sterile neutrino oscillations in vacuum* was first precisely studied in (*Kirilova*, 1988) using an accurate kinetic approach for the description of oscillating neutrinos.

However, the thermal background in the pre-nucleosynthesis epoch effects the propagation of neutrino (*Weldon*, 1982; *Nieves*, 1989; *Lausman and Weert*, 1987; *Pal and Pham*, 1989; *Langacker et al.*, 1983; *Barger et al.*, 1980) and, therefore, the account of the neutrino interactions with the primeval plasma is important (*Nötzold and Raffelt*, 1998; *Harris and Stodolsky*, 1978; *Stodolsky*, 1987; *Barbieri and Dolgov*, 1990; *Enqvist et al.*, 1990a; *Sigl and Raffelt*, 1993).

The precise kinetic consideration of late electron-sterile neutrino oscillations in a medium was first provided in ref. (*Kirilova and Chizhov*, 1996a, 1997). It was proved that in case when the Universe expansion, the neutrino oscillations and the neutrino interactions with the medium have comparable rates, their effects should be accounted for simultaneously, using exact kinetic equations for the neutrino density matrix.

Moreover, energy distortion and asymmetry between neutrinos and antineutrinos play a considerable role in case of nonequilibrium oscillations. As far as both neutrino collisions and active-sterile neutrino oscillations distort the initially equilibrium momentum distribution of active neutrino, the momentum degree of freedom in the description of neutrino must be accounted for. Therefore, for the case of nonequilibrium oscillations the evolution of neutrino ensembles should be studied using the exact kinetic equations for the *density matrix of neutrinos in momentum space.* This precise kinetic approach allowed an exact investigation of the influence of neutrino oscillations (*Kirilova*, 1988; *Kirilova and Chizhov*, 1996a, 1997). The following effects of the neutrino oscillations were discovered and studied: depletion of the neutrino number densities, the energy distortion and the generation of asymmetry, for each separate momentum of the neutrino ensembles.

In a cycle of works (*Kirilova and Chizhov*, 1997, 1998c,b, 2000a) the matteroscillations between left-handed electron neutrinos ν_e and nonthermalized sterile neutrinos ν_s in the early Universe plasma was studied. The case when ν_s do not thermalize till 2 MeV and the oscillations become effective after ν_e decoupling was discussed.

As far as for this model the rates of expansion of the Universe, neutrino oscillations and neutrino interactions with the medium may be comparable, we have analyzed the kinetic equations for neutrino density matrix, accounting *simultaneously* for all processes. The evolution of neutrino ensembles was described numerically by integrating the kinetic equations for the neutrino density matrix in *momentum* space for small mass differences $\delta m^2 \leq 10^{-7}$ eV^2.

This approach allowed us to study precisely the evolution of the neutrino number densities, energy spectrum distortion and the asymmetry between neutrinos and antineutrinos due to oscillations for each momentum mode.

2.2.2 Nonequilibrium neutrino oscillations - our model

The model of nonequilibrium oscillations between weak interacting electron neutrinos ν_e and sterile neutrinos ν_s for the case when ν_s do not thermalize till ν_e decoupling at 2 MeV and oscillations become effective after ν_e decoupling is proposed and described in detail in *Kirilova and Chizhov* (1996a, 1997). The main assumptions are the following:

- Singlet neutrinos decouple much earlier, i.e. at a considerably higher temperature than the active neutrinos do: $T^F_{\nu_s} > T^F_{\nu_e}$, and hence,

$$\delta N_s = \rho_{\nu_s}/\rho_{\nu_e} < 1 \tag{2.14}$$

.

This is a natural assumption, as far as sterile neutrinos do not participate into the ordinary weak interactions. In the models predicting singlet neutrinos, the interactions of ν_s are mediated by gauge bosons with masses $M = \mathcal{O}(1 \text{ TeV})$. Therefore, in later epochs after their decoupling, their temperature and number densities are considerably less than those of the active neutrinos due to the subsequent annihilations and decays of particles that have additionally heated the nondecoupled ν_e in comparison with the already decoupled ν_s.

The transitions between different neutrino flavours were proved to have negligible effect on the neutrino number densities and on primordial nucleosynthesis because of the very slight deviation from equilibrium in that case $T_f \sim T'_f$ (f is the flavour index) *Dolgov* (1981); *Langacker et al.* (1986); *Dolgov et al.* (1997a). Hence, for simplicity we neglect flavour neutrino oscillations.

- We consider oscillations between ν_s ($\nu_s \equiv \tilde{\nu}_L$) and the active neutrinos, according to the Majorana&Dirac ($M\&D$) mixing scheme with mixing present in the electron sector $\nu_i = \mathcal{U}_{il}\ \nu_l$, $l = e, s$:

$$\begin{aligned} \nu_1 &= c\nu_e + s\nu_s \\ \nu_2 &= -s\nu_e + c\nu_s, \end{aligned}$$

where ν_s denotes the sterile electron antineutrino, $c = \cos(\vartheta)$, $s = \sin(\vartheta)$ and ϑ is the mixing angle in the electron sector, the mass eigenstates ν_1 and ν_2 are particles with masses correspondingly m_1 and m_2.

The nonresonant oscillations case corresponds to $\delta m^2 = m_2^2 - m_1^2 > 0$. This in the small mixing angle limit corresponds to a sterile neutrino heavier than the active one.

In this model the *element of nonequilibrium is introduced by the presence of a small singlet neutrino density* at 2 MeV $n_{\nu_s} \ll n_{\nu_e}$, when the oscillations between ν_s and ν_e become effective. In order to provide such a small singlet neutrino density the sterile neutrinos should have decoupled from the plasma sufficiently early in comparison to the active ones and should have not regained their thermal equilibrium till 2 MeV *Kirilova* (1988), *Kirilova and Chizhov* (1996a, 1997). Therefore, as far as the oscillations into ν_e and the following noncoherent scattering off the background may lead to the thermalization of ν_s, two more assumptions were made to ensure the nonequilibrium case to have place:

- Neutrino oscillations should become effective after the decoupling of the active neutrinos, $\Gamma_{osc} \geq H$ for $T \leq 2$ MeV, which is realizable for $\delta m^2 \leq 1.3 \times 10^{-7}$ eV^2 *Kirilova and Chizhov* (1996a, 1997).

- Sterile neutrinos should not thermalize [4] till 2 MeV when oscillations become effective, i.e. the production rate of ν_s (whatever its origin) must be smaller than the expansion rate.

These assumptions define the allowed range of oscillation parameters for our model (*Kirilova and Chizhov*, 1996a, 1997):

$$\sin^2(2\vartheta)\delta m^2 \leq 10^{-7}\text{eV}^2. \tag{2.15}$$

2.2.2.1 Electron neutrino decoupling

Decoupling occurs when the neutrino weak interaction rate $\Gamma_w \sim E^2 n_\nu(E)$ becomes less than the expansion rate $H \sim \sqrt{g}T^2$. We assumed that electron neutrinos decouple at 2 MeV, as predicted in SCM. However, the neutrino decoupling process is more complicated. It has been discussed in literature in detail *Dolgov and Zeldovich* (1989); *Rana and Mitra* (1991); *Kostelecky and Samuel* (1995). Most of electron neutrinos decouple at about 2 MeV. Nevertheless, due to the fact that weak interaction rate is greater at a higher energy, some thermal contact between neutrinos from the high energy tail of the neutrino spectrum and high energy plasma remains after 2 MeV. In case these high energy neutrinos begin to oscillate before their decoupling, the account of the dependence of decoupling time on the neutrino momentum will be essential for our model. Otherwise, in case these neutrinos do not start oscillating before decoupling, there will be no harm considering them decoupled earlier, as far as they preserve their equilibrium distribution anyway due to their extremely small mass.

[4] The problem of sterile neutrino thermalization was discussed in the pioneer work of *Manohar* (1987) and in following publications (*Barbieri and Dolgov*, 1990; *Enqvist et al.*, 1990a).

In *Kirilova and Chizhov* (1997) we have checked analytically and numerically that neutrinos from high-energy tail start to oscillate much later than they decouple for the range of oscillation parameters considered in our model. It can easily be understood from the fact that the oscillation rate decreases with energy $\Gamma_{osc} \sim \delta m^2/E_\nu$ and, therefore, neutrinos with higher energies begin to oscillate later, namely when Γ_{osc} exceeds the expansion rate $H \sim \sqrt{g}T^2$. Hence, the precise account for the momentum dependence of the decoupling does not change the results of our model but unnecessarily complicates the analysis and leads to an enormous increase of the calculation time. Therefore, in what follows we have assumed a fixed decoupling time instead of considering the real decoupling period - i.e. we have accepted that the electron neutrinos have completely decoupled at 2 MeV.

2.2.2.2 The kinetics of nonequilibrium oscillating neutrino

As far as for the nonequilibrium model discussed the rates of expansion of the Universe, neutrino oscillations and neutrino interactions with the medium may be comparable, *we have derived kinetic equations for neutrinos accounting simultaneously for the participation of neutrinos into expansion, oscillations and interactions with the medium.*

All possible reactions of neutrinos with the plasma were considered, namely: reactions of neutrinos with the electrons, neutrons and protons, neutrinos of other flavours, and the corresponding antiparticles, as well as self interactions of electron neutrinos. These equations contain all effects due to first order on G_F medium-induced energy shifts, second order effects due to non-forward collisions, and the effects non-linear on the neutrino density matrices like neutrino refraction effects in a medium of neutrinos.

In the case of nonequilibrium active-sterile oscillations the density matrix of neutrinos may considerably differ from its equilibrium form. [5] Then, for the correct

[5] When neutrinos are in equilibrium their density matrix has its equilibrium form, namely $\rho_{ij} = \delta_{ij}\exp(\mu/T - E/T)$, so that one can work with particle densities instead of ρ. In an equilibrium

analysis of nonequilibrium oscillations, it is important to work in terms of density matrix of neutrinos in momentum space (*Dolgov*, 1981; *Kirilova*, 1988; *Sigl and Raffelt*, 1993; *Kirilova and Chizhov*, 1996a, 1997). Therefore, we have provided a proper kinetic analysis of the neutrino evolution. We have derived the kinetic equations for the *neutrino density matrix for each momentum mode* of the nonequilibrium oscillating neutrinos in the primeval plasma of the Universe in the epoch previous to nucleosynthesis, i.e. consisting of photons, neutrinos, electrons, nucleons, and the corresponding antiparticles. They have the form:

$$\frac{\partial \rho(t)}{\partial t} = Hp\,\frac{\partial \rho(t)}{\partial p} + i\left[\mathcal{H}_o, \rho(t)\right] + i\left[\mathcal{H}_{int}, \rho(t)\right] + \mathrm{O}\left(\mathcal{H}^2_{int}\right), \tag{2.16}$$

where p is the momentum of electron neutrino and ρ is the density matrix of the massive Majorana neutrinos in momentum space.

The first term in the equation describes the effect of expansion, the second is responsible for oscillations, the third accounts for forward neutrino scattering off the medium and the last one accounts for second order interaction effects of neutrinos with the medium. $\mathcal{H}_o$ is the free neutrino Hamiltonian:

$$\mathcal{H}_o = \begin{pmatrix} \sqrt{p^2 + m_1^2} & 0 \\ 0 & \sqrt{p^2 + m_2^2} \end{pmatrix},$$

while $\mathcal{H}_{int} = \alpha\ V$ is the interaction Hamiltonian, where $\alpha_{ij} = U^*_{ie} U_{je}$.

$$V = G_F\left(+\mathcal{L} - Q/M_W^2\right) \tag{2.17}$$

V in the interaction basis plays the role of an induced squared mass for electron

background, the introduction of flavour oscillations slightly shifts ρ from its diagonal form, due to the extreme smallness of the neutrino mass in comparison with the characteristic temperatures and to the fact that equilibrium distribution of massless particles is not changed by the expansion (*Dolgov*, 1981).

neutrinos:

$$\mathcal{H}_{int}^{LR} = \begin{pmatrix} V & 0 \\ 0 & 0 \end{pmatrix}.$$

Hence, V is the time varying (due to the Universe cooling) effective potential, induced by the interactions of neutrino with the medium through which it propagates. Since ν_s does not interact with the medium it has no self-energy correction, i.e. $V_s = 0$. The first 'local' term in V accounts for charged-current and neutral-current tree-level interactions of ν_e with medium protons, neutrons, electrons and positrons, neutrinos and antineutrinos. It is proportional to the fermion asymmetry of the plasma $L = \sum_f L_f$, which is usually taken to be of the order of the baryon one (i.e. $B - L$ conservation is assumed).

$$L_f \sim \frac{N_f - N_{\bar{f}}}{N_\gamma} T^3 \sim \frac{N_B - N_{\bar{B}}}{N_\gamma} T^3 = \beta T^3.$$

The case with $L >> B$ have been also considered, see chapter 4. The second 'nonlocal' term in V arises as an W/Z propagator effect, (*Nötzold and Raffelt*, 1998; *Harris and Stodolsky*, 1978; *Stodolsky*, 1987; *Barbieri and Dolgov*, 1990) and has different behavior with the temperature: $Q \sim E_\nu T^4$

For the early Universe conditions both terms must be accounted for because although the second term is of the second power of G_F , the first term is proportional to the first power of G_F and to the small value of the fermion asymmetries. Moreover, the two terms have different temperature dependence and an interesting interplay between them during the cooling of the Universe is observed. In case of $L \sim B$, at high temperature the nonlocal term dominates, while with the Universe cooling in the process of expansion the local term becomes more important.

The last term in the Eq. (2.16) describes the weak interactions of neutrinos with the medium. For the weak reactions of neutrinos with electrons and positrons

$$e^+e^- \leftrightarrow \nu_i\tilde{\nu}_j, \tag{2.18}$$

$$e^\pm\nu_j \rightarrow e'^\pm\nu'_i \tag{2.19}$$

it has the form

$$\begin{aligned}
&\int \mathrm{d}\Omega(\tilde{\nu}, e^+, e^-)\left[n_{e^-}n_{e^+}\mathcal{A}\mathcal{A}^\dagger - \frac{1}{2}\left\{\rho,\ \mathcal{A}^\dagger\bar{\rho}\mathcal{A}\right\}_+\right] \\
+\ &\int \mathrm{d}\Omega(e^-, \nu', e'^-)\left[n'_{e^-}\mathcal{B}\rho'\mathcal{B}^\dagger - \frac{1}{2}\left\{\mathcal{B}^\dagger\mathcal{B},\ \rho\right\}_+ n_{e^-}\right] \\
+\ &\int \mathrm{d}\Omega(e^+, \nu', e'^+)\left[n'_{e^+}\mathcal{C}\rho'\mathcal{C}^\dagger - \frac{1}{2}\left\{\mathcal{C}^\dagger\mathcal{C},\ \rho\right\}_+ n_{e^+}\right],
\end{aligned}$$

where n is the number density of the interacting particles,

$$\mathrm{d}\Omega(i,j,k) = \frac{(2\pi)^4}{2E_\nu}\int \frac{\mathrm{d}^3p_i}{(2\pi)^3\ 2E_i}\frac{\mathrm{d}^3p_j}{(2\pi)^3\ 2E_j}\frac{\mathrm{d}^3p_k}{(2\pi)^3\ 2E_k}\delta^4(p_\nu + p_i - p_j - p_k)$$

is a phase space factor, $\mathcal{A}$ is the amplitude of the process $e^+e^- \rightarrow \nu_i\tilde{\nu}_j$, $\mathcal{B}$ is the amplitude of the process $e^-\nu_j \rightarrow e'^-\nu'_i$ and $\mathcal{C}$ is the amplitude of the process $e^+\nu_j \rightarrow e'^+\nu'_i$. They are expressed through the known amplitudes $\mathcal{A}_e(e^+e^- \rightarrow \nu_e\tilde{\nu}_e)$, $\mathcal{B}_e(e^-\nu_e \rightarrow e^-\nu_e)$ and $\mathcal{C}_e(e^+\nu_e \rightarrow e^+\nu_e)$:

$$\mathcal{A} = \alpha\ \mathcal{A}_e,\ \mathcal{B} = \alpha\ \mathcal{B}_e,\ \mathcal{C} = \alpha\ \mathcal{C}_e.$$

Analogues equations hold for the antineutrino density matrix, the only difference being in the sign of the lepton asymmetry: L_f is replaced by $-L_f$. Neutrino and antineutrino ensembles evolve differently as far as the background is not CP symmetric.

Medium terms depend on neutrino density, thus introducing a nonlinear feedback mechanism. The evolution of neutrino and antineutrino ensembles is coupled and it must be considered simultaneously. Hence, it is expected that oscillations may change neutrino-antineutrino asymmetry and it in turn affects oscillations.

We have analyzed the evolution of the neutrino density matrix for the case when oscillations become noticeable after electron neutrinos decoupling, i.e. after 2 MeV. Then the last term in the kinetic equation can be neglected. So, the equation (2.16) results into a set of coupled nonlinear integro-differential equations with time dependent coefficients for the components of the density matrix of neutrino. It is convenient instead of $\partial/\partial t$ to use $\partial/\partial\mu$, where $\delta = m_n - m_p$ and

$$\mu^2 = \sqrt{16\pi^3 g/45}\ (\delta^2/M_{Pl})\ t.$$

Then, we obtain:

$$\begin{pmatrix} \rho'_{11} \\ \rho'_{22} \\ \rho'_{12} \\ \rho'_{21} \end{pmatrix} = \begin{pmatrix} 0 & 0 & +iscV & -iscV \\ 0 & 0 & -iscV & +iscV \\ +iscV & -iscV & -iM & 0 \\ -iscV & +iscV & 0 & +iM \end{pmatrix} \begin{pmatrix} \rho_{11} \\ \rho_{22} \\ \rho_{12} \\ \rho_{21} \end{pmatrix}, \qquad (2.20)$$

where prime denotes $\partial/\partial\mu$ and $M = \delta m^2/(2E_\nu) + (s^2 - c^2)V$.

The neutrino kinetics down to 2 MeV does not differ from the standard case, i.e. electron neutrinos maintain their equilibrium distribution, while sterile neutrinos are absent. So, the initial condition for the neutrino ensembles in the interaction basis can be assumed of the form:

$$\varrho = n_\nu^{eq} \begin{pmatrix} 1 & 0 \\ 0 & 0 \end{pmatrix}$$

where $n_\nu^{eq} = \exp(-E_\nu/T)/(1 + \exp(-E_\nu/T))$.

Analytical solution in case of matter oscillations is not possible without drastic assumptions. [6] Therefore, we have numerically explored the problem, using the Simpson method for integration and the fourth order Runge-Kutta algorithm for the solution of the differential equations.

We have analyzed the evolution of nonequilibrium oscillating neutrinos by numerically integrating the kinetic equations (2.20) for the period after the electron neutrino decoupling till the freeze out of the neutron-proton ratio (n/p-ratio), i.e. for the temperature interval $[0.3, 2.0]$ MeV. The oscillation parameters range studied was $\delta m^2 \in [10^{-11}, 10^{-7}]$ eV^2 and $\vartheta \in [0, \pi/4]$.

The distributions of electrons and positrons were taken to be the equilibrium ones. Really, due to the enormous rates of the electromagnetic reactions of these particles the deviations from equilibrium are negligible.

We have neglected the distortion of the neutrino spectra due to residual interactions between the electromagnetic and neutrino components of the plasma after 2 MeV. This assumption was justified by accurate studies (*Dolgov et al.*, 1997a; *Dolgov and Fukugita*, 1992b), where it was shown that the relative corrections to ν_e density due to spectrum distortion is less than 1 % and the effect on the primordial helium abundance is negligible.

We have simultaneously solved the equations governing the evolution of neutrino ensembles and those describing the evolution of the nucleons (see the next section). The neutron and proton number densities, used in the kinetic equations for neutrinos, were substituted from the numerical calculations in a BBN code accounting for neutrino oscillations.

[6] In the case of vacuum neutrino oscillations this equation was analytically solved and the evolution of density matrix was given explicitly in *Kirilova* (1988).

2.3 Cosmological Effects of Active-Sterile Neutrino Oscillations

In our works three *main effects of neutrino nonequilibrium oscillations* were revealed and precisely studied, namely electron neutrino depletion, neutrino energy spectrum distortion and the generation of asymmetry between neutrinos and their antiparticles.

2.3.1 Depletion of ν_e population due to oscillations

As far as oscillations become effective when the number densities of ν_e are much greater than those of ν_s, $N_{\nu_e} \gg N_{\nu_s}$, the oscillations tend to reestablish the statistical equilibrium between different oscillating species. As a result N_{ν_e} decreases in comparison to its standard equilibrium value due to oscillations in favor of sterile neutrinos. (Note, that while electron neutrinos are in thermal equilibrium with the plasma no dilution of their number density is expected as far as the equilibrium is kept due to the annihilations of the medium electrons and positrons.)

The effect of depletion may be very strong (up to 50%) for relatively great δm^2 and maximal mixing. Our study of this effect is more precise than previous ones concerning depletion of electron neutrino population due to oscillations (*Enqvist et al.*, 1992), due to the accurate kinetic approach used.

In case of oscillations effective after the neutrino freeze out, electron neutrinos are not in thermal contact with the plasma and, therefore, the electron neutrino state, depleted due to oscillations into steriles, cannot be refilled by electron-positron annihilations. That irreversible depletion of ν_e population exactly equals the increase of ν_s one (see Fig. 2.1). The number of the effective degrees of freedom do not change due to oscillations in that case, as far as the electron neutrino together with the corresponding sterile one contribute to the energy density of the Universe as

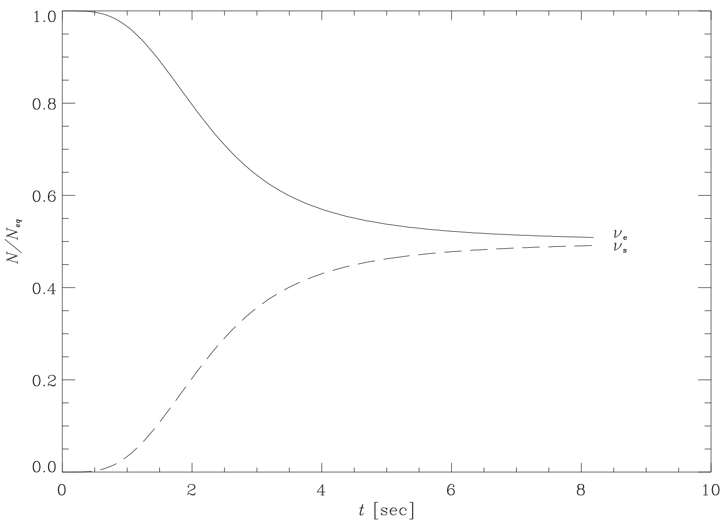

Figure 2.1: The curves show the evolution of the electron neutrino number density (the solid curve) and the sterile neutrino number density (the dashed curve) in the case of the nonresonant active-sterile neutrino oscillations for a maximal mixing and $\delta m^2 = 10^{-8}$ eV^2. The reduction of the active neutrino population is exactly counterbalanced by a corresponding increase in the sterile neutrino population. Figure from ref. *Kirilova and Chizhov* (1998c).

one neutrino unit, even in case when the sterile neutrinos are brought into chemical equilibrium with ν_e. Note the essential difference from the case of electron neutrinos in thermal equilibrium, when the oscillations into sterile neutrinos bring an additional degree of freedom into thermal contact.

The following figures illustrate our results concerning electron neutrino depletion due to neutrino oscillations. In Fig. 2.2 the curves represent the evolution of the electron neutrino number density in the discussed model with a fixed mass difference $\delta m^2 = 10^{-8}$ eV^2 and for different mixings. The numerical analysis showed that for small mixing, $\sin^2(2\vartheta) < 0.01$, the results do not differ from the standard case, i.e. then oscillations may be neglected.

In Fig. 2.3 the evolution of the electron neutrino number density is shown for a nearly maximum mixing, $\sin^2(2\vartheta) = 0.98$, and different squared mass differences. Our analysis has proved, that for mass differences $\delta m^2 < 10^{-11}$ eV^2, the effect of

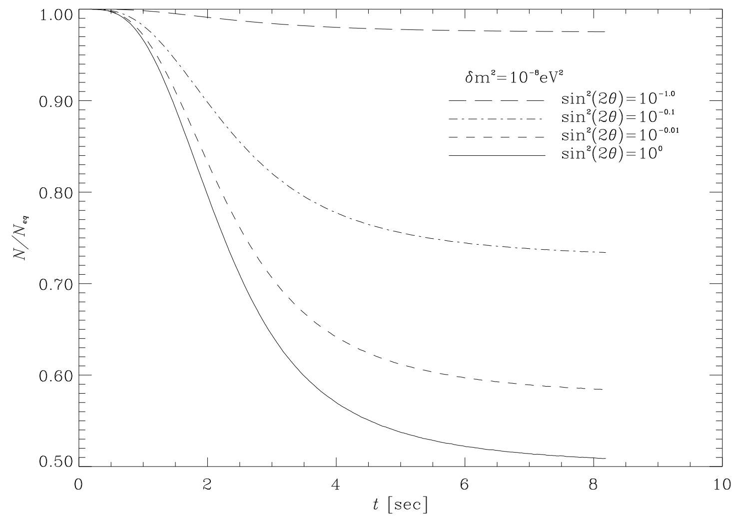

Figure 2.2: The curves represent the calculated evolution of the electron neutrino number density in the discussed model of active-sterile neutrino oscillations with a mass difference $\delta m^2 = 10^{-8}$ eV^2 and different mixing, parametrized by $\sin^2(2\vartheta)$, namely: 1, $10^{-0.01}$, $10^{-0.1}$ and 0.1. Figure from ref. *Kirilova and Chizhov* (1998c).

oscillations is negligible for any ϑ.

In the non-resonant oscillation case the depletion of the electron neutrino increases with the increase of the mass differences and with the increase of the mixing.

The depletion of the electron neutrino number densities due to oscillations into sterile ones strongly affects the $n \leftrightarrow p$ reactions rates. It leads to an effective decrease in the weak processes rates, and, hence, to an increase of the freezing temperature of the n/p-ratio and the corresponding overproduction of the primordially produced ^4He (see chapter 3).

2.3.2 Distortion of the energy distribution of neutrinos

This effect was first discussed in *Dolgov* (1981) for the case of flavour neutrino oscillations. However, as far as the energy distortion for that case was shown to be negligible (*Dolgov*, 1981; *Dolgov et al.*, 1997a; *Dolgov and Fukugita*, 1992b), it was not paid the necessary attention it deserved. The distortion of the neutrino spectrum

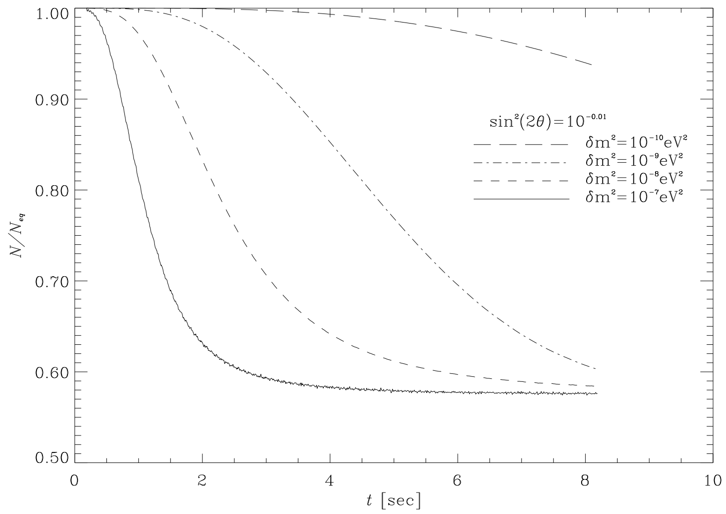

Figure 2.3: The curves show the evolution of the electron neutrino number density in the discussed model of nonresonant active-sterile neutrino oscillations for a nearly maximum mixing, $\sin^2(2\vartheta) = 0.98$, and different squared mass differences δm^2, namely 10^{-7}, 10^{-8}, 10^{-9} and 10^{-10} in eV^2. Figure from ref. *Kirilova and Chizhov* (1998c).

was not discussed in publications concerning active-sterile neutrino oscillations, and was thought to be negligible.

In *Kirilova* (1988) it was first shown that for the case of $\nu_e \leftrightarrow \nu_s$ vacuum oscillations this effect is considerable and may even exceed that of an additional neutrino species. In *Kirilova and Chizhov* (1996a, 1997) we have studied this effect for the case of neutrino oscillations in a medium and have shown that its influence on BBN is the dominant one in case of electron-sterile neutrino oscillations.

Evolution of the distortion

The evolution of the distortion was found to be the following:

Neutrinos with different momentum begin to oscillate at different temperatures and with different amplitudes. First the low energy part of the spectrum is distorted, and later on this distortion concerns neutrinos with higher and higher energies. This behavior is natural, as far as neutrino oscillations affect first low energy neutrinos, $\Gamma_{osc} \sim \delta m^2/E_\nu$.

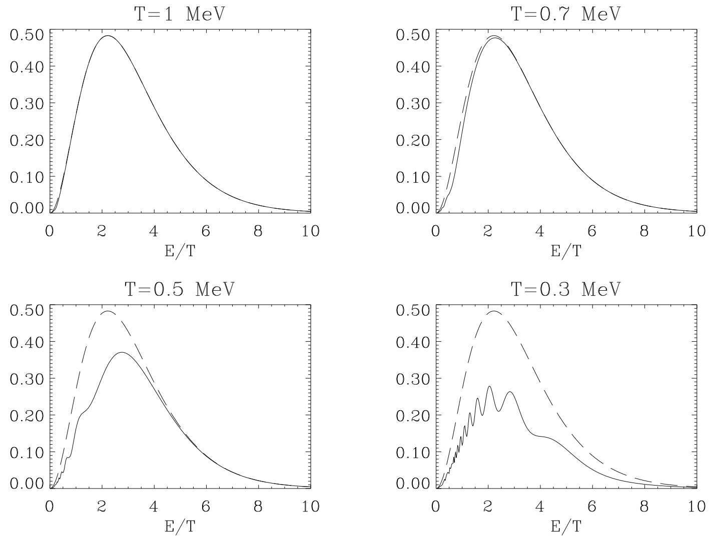

Figure 2.4: The figures illustrate the evolution of the energy spectrum distortion of active neutrinos $x^2\rho_{LL}(x)$, where $x = E_\nu/T$, for the case of nonresonant ν_e-ν_s oscillations with a maximal mixing and $\delta m^2 = 10^{-8.5}$ eV^2, at different temperatures: $T = 1$ MeV (a), $T = 0.7$ MeV (b), $T = 0.5$ MeV (c), $T = 0.3$ MeV (d). Figure from ref. *Kirilova and Chizhov* (1998c).

The Figures 2.4 present the snapshots of the evolution of the energy spectrum distortion of active neutrinos $x^2\rho_{LL}(x)$, where $x = E_\nu/T$, for maximal mixing and $\delta m^2 = 10^{-8.5}$ eV^2, at different temperatures: $T = 1$ MeV (a), $T = 0.7$ MeV (b), $T = 0.5$ MeV (c), $T = 0.3$ MeV (d).

As can be seen from the figures, the distortion down to temperatures of 1 MeV is not significant as far as oscillations are not very effective and/or the weak residual interactions with the background still can compensate for the difference. However, for lower temperatures the distortion increases and at 0.5 MeV is strongly expressed. Its proper account is important for the correct determination of oscillations role in the kinetics of n-p transitions during the freeze out of nucleons at about 0.3 MeV.

SD is much strongly expressed in the resonant oscillation case than in the nonresonant case. In the figure 2.5 the energy distortion of active neutrinos for the resonant neutrino oscillations case is presented.

SD effect on BBN

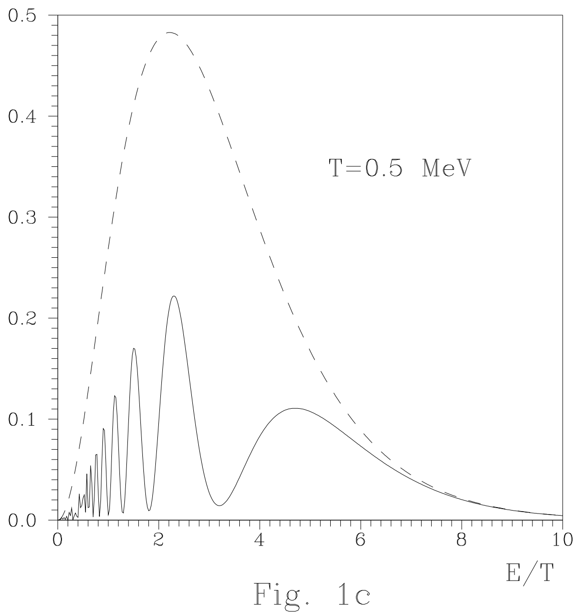

Figure 2.5: The figure shows the energy distortion of active neutrinos $x^2\rho_{LL}(x)$, where $x = E_\nu/T$, for the case of nonequilibrium neutrino oscillations, $\delta m^2 = -10^{-8}$, $\vartheta = \pi/8$ at temperature: $T = 0.5\ MeV$ (b). Figure from ref. *Kirilova and Chizhov* (1997).

The effect of the distortion of the energy distribution of neutrinos on helium-4 production is two-fold. On one hand an average decrease of the energy of active neutrinos leads to a decrease of the weak reactions rate, on the other hand, there exists an energy threshold for the reaction $\tilde{\nu}_e + p \to n + e^+$. *The total effect of the distortion of the energy distribution is an increase in the produced helium* (see chapter 3).

Our analysis has shown that the account for the nonequilibrium distribution by shifting the effective temperature and assuming the neutrino spectrum of equilibrium form, often used in literature (see for example *Shi et al.* (1993)), may give misleading results for the case of oscillations with small squared mass differences $\delta m^2 < 10^{-7}$ eV^2. The effect cannot be absorbed merely in shifting the effective temperature and assuming equilibrium distributions. For larger neutrino mass differences oscillations are fast enough and the naive account is more acceptable, provided that ν_e have not decoupled.

2.3.3 Asymmetry growth in active-sterile neutrino oscillations

The problem of asymmetry generation in different contexts was discussed by several authors. The possibility of an asymmetry generation due to CP-violating flavour oscillations was proposed in (*Khlopov and Petcov*, 1981). Later estimations of an asymmetry due to CP-violating MSW resonant oscillations were provided (*Langacker et al.*, 1987; *Kuo and Panteleone*, 1989).

The problem of asymmetry was considered in connection with the exploration of the neutrino propagation in the early Universe CP-odd plasma in (*Barbieri and Dolgov*, 1990; *Enqvist et al.*, 1990a), and this type of asymmetry was shown to be negligible. However, in following publications it was realized (*Foot et al.*, 1996; *Foot and Volkas*, 1997; *Shi*, 1996; *Kirilova and Chizhov*, 1996a), that asymmetry can grow to a considerable values.

The phenomenon of amplification of the asymmetry in resonant neutrino oscillations for the case of small mass differences $\delta m^2 \leq 10^{-7}$ eV^2 and its important effect on primordial production of helium was found in refs (*Kirilova and Chizhov*, 1996a, 1997). The possibility of asymmetry growth for big mass differences, $\delta m^2 \geq 10^{-5}$ eV^2, was discussed in (*Foot et al.*, 1996; *Foot and Volkas*, 1997; *Shi*, 1996).

Our approach (working with the *self consistent kinetic equations for neutrinos in momentum space*) allowed precise description of the asymmetry evolution, as far as it enabled us to calculate the behavior of the asymmetry at each momentum. This is important particularly when the distortion of the neutrino spectrum is considerable.

Asymmetry role in non resonant oscillation case

We have explored accurately the effect of the asymmetry in the nonresonant case for all mixing angles and for small mass differences $\delta m \leq 10^{-7}$ eV^2. The numerical analysis showed that when the lepton asymmetry is accepted initially equal to the baryon one, (as is usually assumed for the popular $L - B$ conserving models), *the effect of the asymmetry is small for all the discussed parameters range.* And although the asymmetry is not wiped out by the coupled oscillations, as stated by some authors (*Enqvist et al.*, 1990a), nonresonant neutrino oscillations really cannot generate large neutrino-antineutrino asymmetry in the early Universe.

This result is in accordance with the conclusions concerning asymmetry evolution in (*Barbieri and Dolgov*, 1991; *Enqvist et al.*, 1990a; *Kirilova and Chizhov*, 1996a, 1997).

We have also checked that the neutrino asymmetry even in the case of initial neutrino asymmetry by two orders of magnitude higher does not have significant effect on the cosmologically produced ^4He (see next chapters). Therefore, for such small initial values of the lepton asymmetry, the neutrino asymmetry should be better neglected when calculating primordial element production for the sake of computational time.

However, for higher values of the initial asymmetry its effect could be significant, and should be studied in detail. The asymmetry evolution and its effect on He-4 production for unusual high initial values of the lepton asymmetry ($L >> B$) will be discussed in chapter IV.

Asymmetry role in resonant oscillation case

In case of resonant neutrino oscillations *the asymmetry effect is noticeable.* Even when the asymmetry is assumed initially negligibly small (of the order of the baryon one), *it may be considerably amplified at resonant transition* due to different interactions of neutrinos and antineutrinos with the CP-odd medium. The value of the asymmetry may increase by several orders of magnitude, oscillating and sign changing. (The description of this behavior needs very high accuracy and thus complicates strongly the numerical analysis.)

It was proven numerically, that in the case of small mass differences we discussed and naturally small initial asymmetry, the *growth of the asymmetry is up to 5 orders* *of magnitude*. Hence, beginning with asymmetries of the order of the baryon one, the asymmetry does not grow enough to influence *directly* the kinetics of the $n - p$ transitions.

However, we have shown that even in case when the value of the asymmetry does not become considerable enough to have some direct noticeable effect, on primordial nucleosynthesis for example, *the asymmetry term at the resonant transition determines the evolution of the neutrino density matrix*. (As far as the leading order terms, namely of oscillation effects and interaction with the medium, compensate each other at resonant transition.) Most often the asymmetry term effectively suppresses the transitions of active neutrinos (antineutrinos) thus weakening the effect of neutrino depletion at resonance.

Asymmetry growth effect on BBN

The evolution of neutrino may drastically differ from the case without account of asymmetry growth. The maximal asymmetry effect is around 10% decrease of the overproduction of Y_p in comparison with the case of BBN with oscillations but without the asymmetry account.

The total effect of oscillations on BBN, with the complete account of the asymmetry effects, is still overproduction of helium-4, in comparison to the standard value, although smaller at small mixing angles than in the calculations neglecting asymmetry. Therefore, nucleosynthesis constraints on the mixing parameters of neutrino may be alleviated considerably due to the asymmetry effect. We will discuss asymmetry evolution and its effects in more detail in the following chapters.

2.4 Neutrino Spectrum Distortion Due to Oscillations in Case of Non-Zero Initial Population of the Sterile Neutrino State

The degree of population of ν_s at the onset of neutrino oscillations, δN_s, may be different depending on the concrete model of ν_s production. For example, they are naturally produced in GUT models (*Brahmachari*, 1999), in models with large extra dimensions (*Dvali and Smirnov*, 1999) and Manyfold Universe models (*Arkani-Hamed et al.*, 2000), in mirror matter models (*Li and Yang*, 1956; *Berezhiani and Mohapatra*, 1995). They may be produced also in $\nu_{\mu,\tau} \leftrightarrow \nu_s$ oscillations in the preceding epoch and partially thermalized before the nucleosynthesis epoch.

In refs. (*Kirilova*, 2004b) and (*Kirilova*, 2007) we have explored ν_e spectrum distortion for different degree of population of the sterile neutrino state δN_s and estimated the kinetic effect of oscillations on primordial abundance of ^{4}He for different δN_s. We considered δN_s as a free parameter and, varying its value in the range $[0, 1]$ with a step 0.1, provided the numerical analysis of the spectrum distortion and the change of the kinetic effect of oscillations.

As mentioned already, it is not possible to describe analytically, without some radical approximations, the non-equilibrium picture of active–sterile neutrino oscillations, producing non-equilibrium neutrino number densities and distorting the neutrino spectrum. Satisfactory precise analytical description was found only for the case of relatively fast oscillations proceeding before neutrino freezing, with $\delta m^2 > 10^{-6}$ eV^2 and small mixing angles (*Dolgov and Villante*, 2004).

Therefore, we have provided a self-consistent numerical analysis of the evolution of the oscillating neutrinos ρ and $\bar{\rho}$ in the high-temperature Universe, using the following coupled integro-differential equations describing the kinetics of the neutrino ensembles in terms of the density matrix of neutrino ρ and anti-neutrino $\bar{\rho}$.

$$\frac{\partial \rho(t)}{\partial t} = H p_\nu \, \frac{\partial \rho(t)}{\partial p_\nu} + \\ + i\left[\mathcal{H}_o, \rho(t)\right] + i\sqrt{2} G_F \left(\pm \mathcal{L} - Q/M_W^2\right) N_\gamma \left[\alpha, \rho(t)\right] + \mathrm{O}\left(G_F^2\right), \qquad (2.21)$$

where $\alpha_{ij} = U^*_{ie} U_{je}$, p_ν is the momentum of electron neutrino. The plus sign in front of $\mathcal{L}$ corresponds to the neutrino ensemble, the minus sign - to the anti-neutrino ensemble.

Mixing just in the electron sector is assumed: $\nu_i = U_{il}\ \nu_l$ $(l = e, s)$.

The initial condition for the neutrino ensembles differs from the one discussed previously in section 2.8. In the interaction basis it is of the form:

$$\rho = n_\nu^{eq} \begin{pmatrix} 1 & 0 \\ 0 & S \end{pmatrix}, \qquad (2.22)$$

where $n_\nu^{eq} = \exp(-E_\nu/T)/(1 + \exp(-E_\nu/T))$, while S measures the degree of population of the sterile state. $\mathcal{H}_o$ is the free neutrino Hamiltonian. $\mathcal{L}$ is proportional to the fermion asymmetry of the plasma and is essentially expressed through the neutrino asymmetries:

$$\mathcal{L} \sim 2L_{\nu_e} + L_{\nu_\mu} + L_{\nu_\tau}, \qquad (2.23)$$

$$L_{\mu,\tau} \sim (N_{\mu,\tau} - N_{\bar{\mu},\bar{\tau}})/N_\gamma \qquad (2.24)$$

$$L_{\nu_e} \sim \int \mathrm{d}^3 p (\rho_{LL} - \bar{\rho}_{LL})/N_\gamma. \qquad (2.25)$$

The equations are for the neutrino density matrix *in momentum space*, which allows to describe precisely the kinetic effects: spectrum distortion and neutrino-antineutrino asymmetry growth due to oscillations. For the description of the spectrum 1000 bins were used in the nonresonant oscillations case, and from 5000 to 10 000 in the resonant one. These equations provide a simultaneous account of the different competing processes, namely: neutrino oscillations, Universe expansion, neutrino forward scattering, nucleons transformations.

The analysis was performed for all mixing angles ϑ and mass differences $\delta m^2 \leq 10^{-7}$ eV^2. The analyzed temperature interval was $[2.0, 0.3]$ MeV, because at temperatures higher than 2 MeV the deviations from the standard BBN model without oscillations are negligible in the discussed model of oscillations.

The results of our numerical analysis on spectrum distortion at different δN_s are illustrated in the Figs. 2.6, 2.7 and 2.8, where snapshots of the evolution of the energy spectrum distortion of the electron neutrino at different temperatures 1, 0.7 and 0.5 MeV for different initial populations of the sterile state are shown. At each temperature we have plotted the spectrum for three different levels of initial population of the sterile neutrino, namely $\delta N_s = 0.0, 0.5, 0.8$.

The oscillations parameters were $|\delta m^2| = 10^{-7}$ eV^2 and $\sin^2 2\vartheta = 0.1$. At each δN_s the characteristic behavior of the spectrum distortion due to oscillations is observed: the low energy part of the spectrum is distorted first (as far as low energy neutrinos start to oscillate first) and later the distortion penetrates more and more noticeably into the more energetic part of the spectrum.

As expected, *the spectrum distortion becomes less expressed with the increase of the degree of population of the sterile neutrino state* δN_s. Correspondingly, then the kinetic effect on primordial nucleosynthesis decreases.

We have found that the neutrino energy spectrum $n_\nu(E)$ may strongly deviate from its equilibrium form during all the period of interest (2 MeV – 0.3 MeV) even for considerably large δN_s. For example, in the resonant case it may play a considerable role even for very big $\delta N_s \sim 0.8$. Hence, it may be expected that the spectrum distortion will constitute the dominant effect on the overproduction of ^{4}He, caused by neutrino oscillations (as is proven in the next chapter).

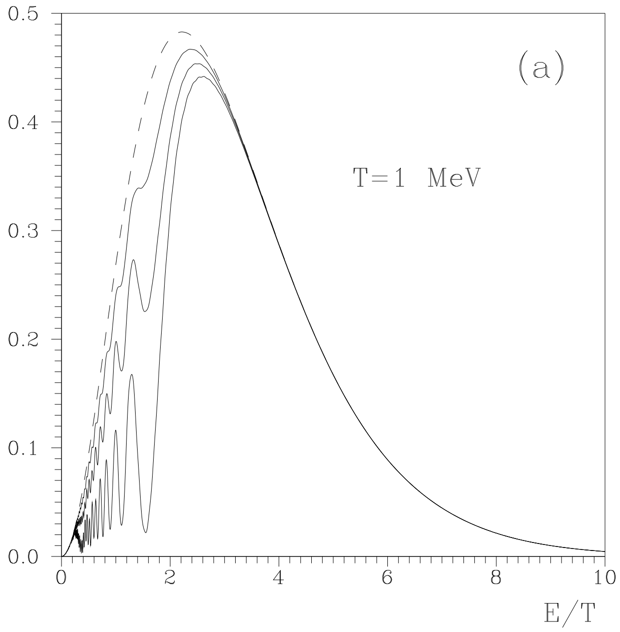

Figure 2.6: The figure illustrates the degree of distortion of the electron neutrino energy spectrum $x^2\rho_{LL}(x)$, where $x = E/T$ at a characteristic temperature 1 MeV, caused by resonant oscillations with a mass difference $\delta m^2 = 10^{-7}$ eV^2 and $\sin^2 2\vartheta = 0.1$ for different initial sterile neutrino populations, correspondingly $\delta N_s = 0$ (the lower curve), $\delta N_s = 0.5$ and $\delta N_s = 0.8$ (the upper curve). The dashed curve gives the equilibrium neutrino spectrum for comparison. Figure from ref. *Kirilova* (2007).

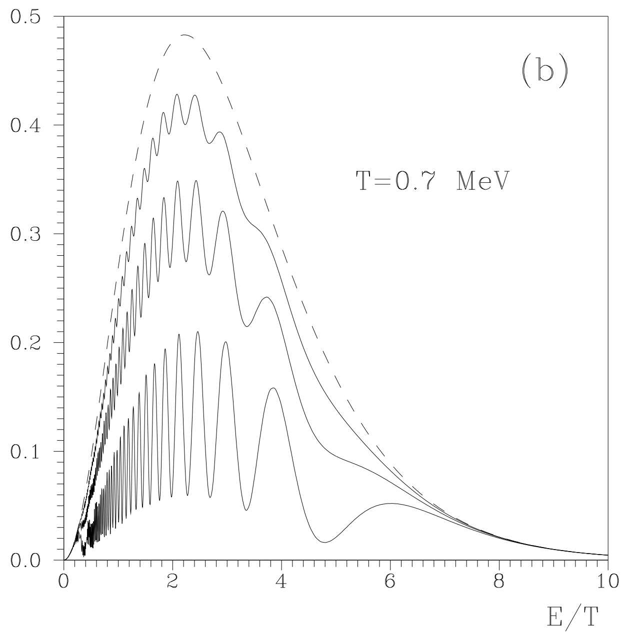

Figure 2.7: The figure illustrates the degree of distortion of the electron neutrino energy spectrum $x^2\rho_{LL}(x)$, where $x = E/T$ at a characteristic temperature 0.7 MeV, caused by resonant oscillations with a mass difference $\delta m^2 = 10^{-7}$ eV^2 and $\sin^2 2\vartheta = 0.1$ for different initial sterile neutrino populations, correspondingly $\delta N_s = 0$ (the lower curve), $\delta N_s = 0.5$ and $\delta N_s = 0.8$ (the upper curve). The dashed curve gives the equilibrium neutrino spectrum for comparison. Figure from ref. *Kirilova* (2007).

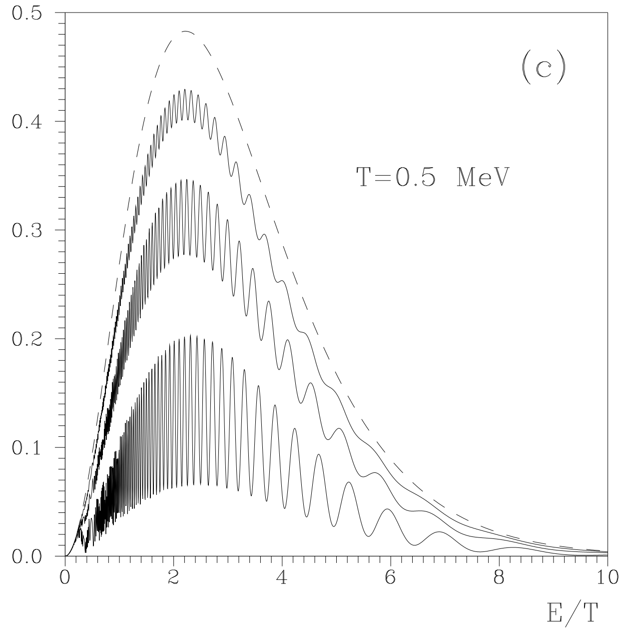

Figure 2.8: The figure illustrates the degree of distortion of the electron neutrino energy spectrum $x^2\rho_{LL}(x)$, where $x = E/T$ at a characteristic temperature 0.5 MeV, caused by resonant oscillations with a mass difference $\delta m^2 = 10^{-7}$ eV^2 and $\sin^2 2\vartheta = 0.1$ for different initial sterile neutrino populations, correspondingly $\delta N_s = 0$ (the lower curve), $\delta N_s = 0.5$ and $\delta N_s = 0.8$ (the upper curve). The dashed curve gives the equilibrium neutrino spectrum for comparison. Figure from ref. *Kirilova* (2007).

2.5 Conclusion

The exact kinetic analysis of the neutrino evolution, discussed in this section reveals important features of nonequilibrium oscillations, that cannot be caught otherwise.

In conclusion, our numerical analysis showed that the nonequilibrium electron-sterile neutrino oscillations can considerably deplete the number densities of electron neutrinos (antineutrinos) and distort their energy spectrum, even in case of big δN_s. Besides, the resonant active-sterile neutrino oscillations can cause neutrino-antineutrino asymmetry growth up to several orders of magnitude.

We have been able to find these qualitatively new effects of spectrum distortion and asymmetry growth thanks to the exact kinetic approach used. The quantitative study was provided for all the range of the model's parameters and also for $1 \geq \delta N_s \geq 0$.

The strength and cosmological importance of these neutrino oscillations effects is illustrated in the following two chapter, where their influence on the primordial production of ^4He and on neutrino-antineutrino asymmetry is explored and BBN constraints on oscillation parameters and on lepton asymmetry are obtained.

CHAPTER III

Production of He-4 in BBN with neutrino oscillations and BBN Cosmological Constraints on Neutrino Oscillations

3.1 Introduction

Big Bang Nucleosynthesis provides one of the most sensitive probes of the physical conditions of the early Universe. Besides, although small, the uncertainties of the primordial abundances values extracted from observations still leave a room for physics beyond the standard model. Thus BBN is often used to constrain new physics, in particular it is used to constrain neutrino oscillations.

Neutrino oscillations between active and sterile neutrino may considerably effect the early Universe, as discussed in the previous chapter. They are capable of exciting additional light particles into equilibrium, thus, affecting the expansion rate H; they may distort neutrino energy spectrum and generate neutrino-antineutrino asymmetry. Thus, electron neutrino – sterile neutrino oscillations $\nu_e \leftrightarrow \nu_s$, influence the weak interaction rates of ν_e and, hence, the kinetics of nucleons at the pre-BBN epoch. Hence, both dynamical effect of oscillations and their kinetic effect influence the primordial nucleosynthesis.

Among the light elements produced primordially, ^{4}He is the most abundantly produced, most precisely measured and calculated, and usually it is the chosen element to probe neutrino oscillations effect on BBN and to obtain BBN constraints on neutrino oscillations.

The effect of oscillations on nucleosynthesis has been discussed in numerous publications starting with the original works (*Dolgov*, 1981; *Kirilova*, 1988; *Khlopov and Petcov*, 1981; *Langacker et al.*, 1987; *Kuo and Pantaleone*, 1989).

First detail kinetic calculation of primordial yield of helium for the case of the nonequilibrium oscillations in vacuum, accounting for the neutrino energy spectrum distortion due to flavor oscillations and active-sterile was made, correspondingly, by *Dolgov* (1981) and *Kirilova* (1988).

The matter oscillations effect on BBN has been previously considered by many authors (*Barbieri and Dolgov*, 1990, 1991; *Enqvist et al.*, 1990a, 1992; *Cline*, 1992; *Shi*, 1996; *Langacker et al.*, 1986; *Dolgov and Fukugita*, 1992a). In these works mainly the excitation of an additional degree of freedom due to oscillations (causing an increase of the effective degrees of freedom g) and the corresponding increase of the Universe expansion rate $H \sim \sqrt{g}$, leading to an overproduction of helium-4 was discussed. The excluded regions for the neutrino mixing parameters were obtained from BBN constraint on the neutrino types: $N_\nu < 3.4$, (*Barbieri and Dolgov*, 1990; *Enqvist et al.*, 1990a). First successful account for the electron neutrino depletion due to oscillations was made in refs. (*Barbieri and Dolgov*, 1990) and (*Enqvist et al.*, 1990a).

Calculations of helium production within the full Big Bang Nucleosynthesis code with oscillations were provided also in *Shi et al.* (1993), however, there the momentum degree of freedom of neutrino was not considered and a simplifying account of the nonequilibrium was used - by merely shifting the neutrino effective temperature and working in terms of equilibrium particle densities.

In a cycle of papers (*Kirilova and Chizhov*, 1996a, 1997, 1998c,b, 2000a, 2001a;

Kirilova, 2003a, 2007; *Kirilova and Panayotova*, 2006) we provided a detail numerical study of the influence of the nonequilibrium $\nu_e \leftrightarrow \nu_s$ oscillations on the primordial production of ^4He. In our works we have for a first time precisely calculated the influence of oscillations on the primordially produced helium-4 using the exact kinetic equations in momentum space for the neutron number density and the density matrix of neutrino, instead for their particle densities.

A simultaneous numerical analysis of the neutrino and neutrons evolution was provided by a numerical integration of the kinetic equations *for each momentum mode*.

The exact kinetic approach enabled us to account precisely for the important effects of neutrino oscillations (neutrino population depletion, distortion of the neutrino spectrum and the generation of neutrino-antineutrino asymmetry) on the kinetics of neutron-to-proton transitions during the primordial nucleosynthesis epoch and correspondingly on the cosmological ^4He production.

This enabled us to investigate the zone of very small neutrino mass differences down to 10^{-11} eV^2, which has not been reached before.

The proper consideration of the spectrum distortion and accounting for the neutrino forward scattering processes off the background particles was first provided in *Kirilova and Chizhov* (1996a) and *Kirilova and Chizhov* (1997) for some neutrino mixing parameters. In *Kirilova and Chizhov* (1998c, 2000a) we provided precise numerical analysis of the influence of oscillations on the production of He-4 within a detail numerical BBN model with nonresonant and resonant nonequilibrium neutrino oscillations. The analysis of *Kirilova and Chizhov* (1997) was expanded for the full space of the mixing parameters values.

It was shown that the neutrino population depletion and spectrum distortion play an important role. The asymmetry effect, in case the lepton asymmetry is accepted initially equal to the baryon one, was proved important in resonant neutrino oscillations case and negligible in the non-resonant oscillations case for the discussed range of δm^2.

Constant helium contours in the mass difference – mixing angle (δm^2 - ϑ) plane were calculated for the full range of the parameter values of our model. No matter what will be the preferred primordial helium value, favored by future observations, it will be possible to obtain the excluded region of the mixing parameters using the results of our survey.

Thanks to the exact kinetic approach precise cosmological constraints on the neutrino mixing parameters were obtained. Cosmological constraints on neutrino oscillations parameters, based on BBN and ^{4}He observational data, have been discussed also in the review papers *Dolgov* (2002); *Kirilova* (2001c, 2004a, 2015).

In this chapter we will discuss a modification of the standard model of cosmological nucleosynthesis - *BBN with neutrino oscillations* and the cosmological constraints on neutrino oscillations parameters that we have obtained. In the next section we describe the standard BBN model. Then in the third section we present our results concerning the effects of $\nu_e \leftrightarrow \nu_s$ oscillations on the primordial production of helium. In the fourth and fifth sections we present the derived cosmological constraints on neutrino oscillations parameters: the non-resonant oscillations case is discussed in the fourth section, then in the fifth section the results for the resonant neutrino oscillation case are presented. Possible relaxation of the cosmological constraints is discussed in the sixth section. The maximum helium overproduction in the modified BBN with neutrino oscillations is given in the seventh section. The eighth section is dedicated to BBN with initially non-zero population of the sterile neutrino state, the SD of neutrino due to neutrino oscillations in that case and the BBN constraints on neutrino oscillations. The results and conclusions are presented in the last section.

3.2 Standard Big Bang Nucleosynthesis

According to the standard cosmological model in the early period of our Universe, while it cooled from $T \sim 10^{10}$ K till 10^9 K, corresponding to cosmic time $t \sim 1$ sec till the first minutes after the Big Bang, the conditions were favorable for a nuclear synthesis of light elements to proceed. During these first minutes several light elements were synthesized in a process called Big Bang Nucleosynthesis: deuterium D, the isotopes of helium, ^3He and ^4He, and ^7Li. So, as a result of BBN, lasting just a few minutes, roughly a quarter of the baryonic matter of the universe was converted to ^4He, while the rest was left as hydrogen H and, hence after the BBN period the baryon matter of our Universe is mainly hydrogen-helium one, with tiny traces of D and ^7Li.

The idea about the production of elements through thermonuclear reactions in the hot ylem during the early stages of the Universe expansion has been first proposed by G. Gamow and studied in the 1930s and 1940s (*Gamow*, 1935, 1942, 1946). George Gamow and his collaborators Herman and R. Alpher in the period 1946-48 provided the first calculations of BBN nucleosynthesis. On the basis of BBN considerations the existence of CMB, its isotropy and temperature T_{cmb}, as artefact from the early BBN epoch was predicted. This early BBN model contained most of the basic ideas of modern BBN theory, such as the importance of weak interactions and the dependence of primordially produced abundances on the baryon density. The first precise standard BBN code was worked out by Wagoner and his collaborators in 1969 and since then BBN codes were proposed to calculate the primordially produced nuclei abundances with higher and higher accuracy.

BBN has been developed to become today a very precise and qualitative theory of cosmological nucleosynthesis. BBN now is recognized as the greatest success of the contemporary cosmology. This elegant famous theory is capable to explain **quanti-**

tatively with remarkable precision the inferred from observational data primordial abundances of the light elements *Boesgaard and Steigman* (1985); *Malaney and Mathews* (1985); *Sarkar* (1996); *Pagel* (1997). Thanks to that good accordance between theory predictions and the observational facts, we nowadays believe to have understood well the physical conditions of the nucleosynthesis epoch, corresponding to the first minutes of the Universe evolution. Moreover, BBN model and the observational data on light elements is used as a most precision cosmological test of Beyond the Standard Physics models. For recent review on BBN see (*Iocco et al.*, 2009).

3.2.1 Qualitative description. Preliminaries.

According to the standard cosmological model BBN started when the universe had cooled enough for protons and neutrons to combine into deuterium nuclei:

$$p + n \to D + \gamma$$

At earlier times corresponding to higher T the entropy was too high so that the back reaction was very fast and no considerable quantities of D were formed. So this reaction is called the D bottleneck. After it fast nuclear reactions proceeded. The BBN reactions are over 100, however the most important among them are 11 reactions leading to formation of the light elements abundances, that followed the weak reactions leading to the neutron-proton freezing before the start of nuclear synthesis.

The production of the primordially produced elements depend on the conditions of the early Universe plasma during BBN, i.e. the density and the temperature during its first minutes, the cooling rate $H = 8/3\pi G\rho$, the characteristics of neutrino (number of neutrino species, degeneracy, spectrum distribution, oscillations..), etc. According to the most recent measurements of light elements produced in BBN, their primordial number densities relative to H span more than 9 orders of magnitude: from $^4He/H_{|p} \sim 0.1$, $D/H_{|p} \sim 2.5 \times 10^{-5}$ to $^7Li/H_{|p} \sim 1.6 \times 10^{-10}$.

The observational primordial abundances nicely fit the predicted values by the standard BBN theory and present one of the first evidences for the existence of an early hot period in the evolution of the Universe.

Thus, knowing the primordial abundances, obtained on the basis of measurements and extrapolations, and comparing them to BBN predicted values, it is possible to obtain information about different characteristics of the Universe during BBN epoch. In particular, the primordially produced D, thanks to the high sensitivity of its production on the baryon density, is known to be the best baryometer among the light elements, while ^{4}He being highly sensitive to the Universe expansion rate and the rates of the neutron-proton transitions in the pre-BBN epoch is a very good speedometer and leptometer (*Kirilova*, 2011a). Both the baryon density and the expansion rate and the lepton number provide fundamental cosmological information. Besides, BBN provides the most effective test for physics beyond the Standard Model. In this chapter and chapter 4 and 7 cosmological constraints on beyond the SM physics, based on BBN consideration, are derived.

3.2.2 BBN - the best baryometer

The produced abundances of the light elements in the standard BBN depend on the baryon-to-photon ratio $\eta = n_b/n_\gamma$, where n_b and n_γ are the number densities of baryons and of photons, correspondingly.

The consistency between theoretically obtained and observationally measured abundances of the light elements produced in BBN at a redshift $z \sim 10^9$ determines η:

$$5.7 \times 10^{-10} \leq \eta \leq 6.7 \times 10^{-10}$$

at 95% CL. When substituting n_γ by the value fixed by the measured CMB temperature, the range of the baryon mass density is:

$$3.9 \times 10^{-10} \leq \rho_b \leq 4.6 \times 10^{-31}\text{g cm}^{-3}.$$

$$0.021 \leq \Omega_b h^2 \leq 0.025.$$

where $\Omega_b h^2 = 3.65 \times 10^7 \eta$, and $\Omega_b = \rho_b/\rho_c$ is the fraction of the present density contributed by baryons.

Even more exact measurements of η are provided by deuterium measurements towards low metallicity quasars, which provide a key baryometer at the time of BBN with a precision of 5% (see *Pettini et al.* (2008), 2012. The D abundance determinations provides an estimate of the mean baryon density of the Universe:

$$\Omega_b h^2 = 0.021 \pm 0.001$$

$$\eta = (5.7 \pm 0.3) \times 10^{-10}$$

at 68% CL and

$$\eta = (6 \pm 0.3) \times 10^{-10}$$

$$\Omega_b h^2 = 0.021 \pm 0.002$$

at 95% CL. BBN determination is in a good agreement with the CMB determined value of the baryon density.

This result is important for our understanding of the matter budget of the Universe. The baryonic density is around 4.6% of the total density, i.e. it is considerably bigger than the density of luminous matter 0.5%, but considerably smaller than the density of gravitating matter, consisting $\sim$ 25% of the density of our Universe $\Omega_m \sim 0.25$. And considerably smaller than the total density of the Universe $\Omega = 1$.

Different independent pieces of evidence exist about the predominant density of a nonbaryonic dark matter (DM) and dark energy (DE). The combined analysis of CMB measurements, Large Scale Structure (LSS) results and Super Nova data point that 22% of the total density of the Universe is in a form of dark nonbaryonic matter, and the predominant density - 73% is in a form of dark energy. Hence, according to today's observational data almost 96% of the Universe density is in a form yet undetected in laboratories. [1]

Thus, although we have determined the baryon density of the Universe with a extremely high precision, we have not yet solved the challenging riddles of the Universe connected with baryons: Why the baryon density, typical for the planets, the stars, etc., is just a tiny component $< 5\%!$ of the total Universe density? What is the physical nature of the non-baryonic components of the Universe?

Another baryons connected riddle is the existence of asymmetry between baryons and antibaryons. We do not know if this is just a local or a global asymmetry, neither we know what was the exact mechanism of its generation or the exact mechanism of the separation of regions of matter from antimatter.

Usually it is assumed that the locally observed asymmetry is a global feature. However, neither theory nor observations exclude categorically big quantities of antimatter at distances higher than 20 Mpc from our galaxy. Small quantities of antimatter (stars, a globular cluster) are even allowed within our Milky Way galaxy.

The fifth and the penultimate chapter of the thesis is dedicated to the baryon asymmetry of the Universe and mechanisms of its generation. In subsection 3.7 the possibility of relaxation of the BBN constraint on the baryon density in modified models of BBN containing physics beyond SM is presented.

[1] The predominant part of the gravitating matter is non-baryonic, in a form of the so called dark matter, and it should be predominantly cold, for the successful formation of galaxies to have taken place. Different DM candidates exist like: WIMPS, KeV mass inert neutrino, axions, neutralino, gravitino, etc. Modified gravitational theories are developed to escape the need of DM. At present the experimental search for DM candidates is still without a rigid positive result, alas.

3.2.3 BBN - the best speedometer and leptometer

BBN is also the ultimate speedometer of the Universe. Among the light elements produced primordially helium-4 is the best speedometer. It is the most exactly measured element, precisely calculated, and besides it has simple post-BBN evolution - it is only produced in stars.

It is measured in HII extragalactic regions usually of dwarf galaxies with low metallicity Z. The post-BBN evolution of ^{4}He is also simple - it is always enriched due to the chemical evolution in galaxies and stars. Hence, the measured abundance should be extrapolated to zero Z to account for the stellar enrichment. [2]

Untill recently, it was considered that the primordial helium is known with 3% precision. The new measurements and the more careful analysis of the data (*Izotov and Thuan*, 2010; *Aver et al.*, 2010), pointed to a higher central value of the observed helium-4 compared to the theoretical predictions and to a higher systematic uncertainty, i.e. 5% uncertainty.

The accepted now conservative mean value of primordially produced helium is:

$$Y_p = 0.2565 \pm 0.006.$$

The error is dominated by systematics.

The theory of standard BBN predicts its primordially produced value with extremely high precision better than 0.1%:

$$Y_p = 0.2486 \pm 0.0002$$

The consistency of the theoretical and observational results is very high. Therefore it was and is used for a precision probe of the conditions of the universe in the pre-BBN

[2]Linear correlations between helium-4, (Y) and metals Z (C, N and O) is used to derive the primordial mass fraction.

and the BBN epoch.

Helium-4 is highly sensitive to the Universe expansion rate H and the rates of the neutron-proton transitions Γ_w in the pre-BBN epoch

$$n + e^- \leftrightarrow p + \nu_e \tag{3.1}$$

$$n + \bar{\nu}_e \leftrightarrow p + e^+ \tag{3.2}$$

$$n \leftrightarrow p + e^- + \nu_e. \tag{3.3}$$

Therefore, it is considered a very good speedometer and leptometer. To a good first approximation all neutrons left after the pre-BBN nucleons freezing epoch bind into helium. Primordial element abundances depend primarily on the neutron-to-proton ratio at the weak freeze out ($(n/p)_f$-ratio) of the reactions interconverting neutrons and protons. Hence, the produced helium essentially depends on the *competition between the expansion rate H and the weak interaction rate Γ_w* $Y_p = (H(\rho(g), \Gamma_w)$, which determine the freezing temperature of neutrons T_f:

$$H \sim \rho_r^{1/2} \sim \sqrt{g}_{eff} G_N T_f^2 = \Gamma_w \sim G_F^2 T_f^5, \tag{3.4}$$

where ρ_γ and ρ_ν are the photon and neutrino energy densities, correspondingly,

$$\rho_r = \rho_\gamma + \rho_\nu = [1 + 7/8(4/11)^{4/3} N_{eff}]\rho_\gamma, \tag{3.5}$$

$$g_{eff} = 11/2 + 7/4 N_{eff}, \tag{3.6}$$

and the weak processes rate is $\Gamma_w \sim G_F^2 T^5$.

Further evolution is due only to the neutron decays

$$n \to p + e + \tilde{\nu}_e$$

that proceed till the effective synthesis of deuterium begins. The expansion rate exceeds considerably the decay rate for the characteristic period before the nucleons freeze out, decays are not essential and therefore, they can be accounted for adiabatically.

To a first approximation it can be expressed by:

$$Y_p = 2(n/p)_f/(1 + (n/p)_f) \times \exp(-t/\tau_n) \sim 0.25, \tag{3.7}$$

where $(n/p)_f \sim \exp(-\delta m/T_f)$ is the neutron-to proton freezing ratio, $\delta m = m_n - m_p = 1.293$ MeV is the mass difference of neutron and proton, $\tau_n = 880$ s is the mean lifetime of the neutron. In the standard (non-degenerate) BBN, assuming equilibrium distributions of particles and 3 generations, $g_{eff} = 10.75$.

The presence of additional light particles during pre-BBN and BBN epoch increases g_{eff} and lead to faster expansion, earlier freeze-out of nucleons and hence, overproduction of helium-4. Thus, limits on particles proposed by new physics (like supersymmetric scenarios, mirror models, large dimensions, etc.) are obtained on the basis of observational data of primordially produced helium-4.

Different non-standard physics processes may also lead to an increase of the effective degrees of freedom, and hence, can be constrained by BBN. In particular active-sterile neutrino oscillations may provoke the equilibration of a sterile neutrino, and thus, they are strongly constrained by BBN. The presence of additional chiral tensor particles also are strongly constrained by BBN considerations (to be dicussed in seventh chapter).

Besides this dynamical effect, non-standard physical processes may effect directly or indirectly the kinetics of the n-p transitions during the pre-BBN epoch, and this way influence the production of light elements. Again, on the basis of the observational data of helium-4 strong constraints on the parameters of such models can be obtained.

In the following sections of this chapter and in chapter 4 modified BBN models with neutrino oscillations and lepton asymmetry are considered. New BBN constraints on neutrino oscillations and on lepton asymmetry, based on the dynamical and the kinetic effects of neutrino oscillations and lepton asymmetry, are derived.

3.3 BBN with Nonequilibrium Oscillating Neutrino

BBN predictions and constraints may considerably differ if active-sterile oscillations took place during BBN. Flavor oscillations influence BBN negligibly, because flavor neutrinos differ slightly due to their close decoupling temperatures.

On the contrary, active-sterile oscillations may considerably effect BBN. In particular, they may cause an increase of H, because they may bring additional light sterile neutrinos into equilibrium and thus increase N_{eff} by δN_s, which effects BBN (see Dolgov, 1981) and is usually called "dynamical" effect. This causes an overproduction of $Y_p \sim 0.013\delta N_s$. Besides, $\nu_e \leftrightarrow \nu_s$ oscillations may *considerably influence nucleons kinetics during BBN* mainly via spectrum distortion of the electron neutrino participating into the kinetics of nucleons (see e.g. Kirilova & Chizhov, 1996, 1997, 1998, 2000). This leads to a decrease of weak interaction rates, causing earlier n/p freezing and He-overproduction.

The *depletion of the electron neutrino number densities* due to oscillations into sterile ones strongly affects the $n \leftrightarrow p$ reactions rates. It leads to an effective decrease in the processes rates, and hence to an increase of the freezing temperature of the n/p-ratio and the corresponding *overproduction of the primordially produced* ^4He.

The effect of the *distortion of the energy distribution of neutrinos* has two aspects:

On one hand an average decrease of the energy of active neutrinos leads to a decrease of the weak reactions rate, $\Gamma_w \sim E_\nu^2$ and subsequently to an increase in the freezing temperature and the produced helium.

On the other hand, there exists an energy threshold for the reaction $\tilde{\nu}_e + p \to n + e^+$. And in case when, due to oscillations, the energy of the relatively greater part of neutrinos becomes smaller than that threshold the n/p- freezing ratio decreases leading to a corresponding decrease of the primordially produced helium-4, *Dolgov and Kirilova* (1988). The numerical analysis showed that the latter effect is less noticeable compared with the former ones.

Thus the final effect of SD is an *overproduction of the primordially produced* ^4He.

The dynamical δN_s and the kinetic δN_{kin} effect on BBN, can be denoted by a change of the relativistic degrees of freedom.

$$\delta N_{eff}^{BBN+osc} = \delta N_{eff} + \delta N_{kin} + \delta N_s, \tag{3.8}$$

Hence, BBN constraints (including bounds on ν characteristics) become more stringent than standard BBN ones and dependent on oscillation parameters. For example, the bound $\delta N_{eff} < 1.6$ changes: From $\delta N_{eff}^{BBN+osc} < 1.6$, there follows that

$$\delta N_{eff} < 1.6 - \delta N_{kin}(\vartheta, \delta m^2, \delta N_s) - \delta N_s. \tag{3.9}$$

3.3.1 Kinetic equations for the evolution of nucleons. Numerical analysis.

In our works we explored BBN model with electron-sterile neutrino oscillations numerically using exact kinetic equations for the description of the evolution of nucleons number densities and for the evolution of the neutrino density matrix in momentum space. This enabled us to analyze precisely the influence on BBN of the neutrino depletion, neutrino SD and the generation of asymmetry in the neutrino sector due to neutrino oscillations.

We provided accurate numerical analysis of the evolution of neutron number density till its freeze-out.

For simplicity we assumed mixing just in the electron sector, $\nu_i = U_{il}\ \nu_l\ (l = e, s)$. The kinetic equations, describing simultaneously the evolution of the neutrino and antineutrino density matrix ρ and $\bar{\rho}$ and of the neutron number density in momentum space n_n for the case of oscillating neutrinos $\nu_e \leftrightarrow \nu_s$, read:

$$\begin{aligned}
&\frac{\partial \rho(t)}{\partial t} = H p_\nu\ \frac{\partial \rho(t)}{\partial p_\nu} + \\
&+i\left[\mathcal{H}_o, \rho(t)\right] + i\sqrt{2} G_F \left(\pm\mathcal{L} - Q/M_W^2\right) N_\gamma \left[\alpha, \rho(t)\right] + \mathrm{O}\left(G_F^2\right), \qquad (3.10)
\end{aligned}$$

$$\begin{aligned}
&(\partial n_n/\partial t) = H p_n\ \ (\partial n_n/\partial p_n) + \\
&+\int \mathrm{d}\Omega(e^-, p, \nu)|\mathcal{A}(e^- p \to \nu n)|^2 \left[n_{e^-} n_p (1-\rho_{LL}) - n_n \rho_{LL}(1-n_{e^-})\right] \\
&-\int \mathrm{d}\Omega(e^+, p, \tilde{\nu})|\mathcal{A}(e^+ n \to p\tilde{\nu})|^2 \left[n_{e^+} n_n (1-\bar{\rho}_{LL}) - n_p \bar{\rho}_{LL}(1-n_{e^+})\right]. \ (3.11)
\end{aligned}$$

where $\alpha_{ij} = U_{ie}^* U_{je}$, p_ν is the momentum of electron neutrino, n stands for the number density of the interacting particles, $\mathrm{d}\Omega(i, j, k)$ is a phase space factor and $\mathcal{A}$ is the amplitude of the corresponding process. The sign plus in front of $\mathcal{L}$ corresponds to neutrino ensemble, while minus - to antineutrino ensemble.

In case of initially empty sterile neutrino state the initial condition for the neutrino ensembles in the interaction basis is assumed of the form:

$$\rho = n_\nu^{eq} \begin{pmatrix} 1 & 0 \\ 0 & 0 \end{pmatrix}$$

where $n_\nu^{eq} = \exp(-E_\nu/T)/(1 + \exp(-E_\nu/T))$. The initial values for the neutron, proton and electron number densities are their equilibrium values.

The neutron and proton number densities, used in the kinetic equations for neutrinos eq. 3.10, were substituted from the numerical calculations of neutron and proton number density evolution. On the other hand, ρ_{LL} and $\bar{\rho}_{LL}$ at each integration step was taken from the simultaneously performed integration of the set of equations 3.10 and 3.11. I.e. we have selfconsistently and simultaneously followed the evolution of neutrino ensembles and the nucleons.

The first term on the right-hand side of the equation for neutrons describes the effect of expansion while the next ones – the processes 3.1 and 3.2 directly influencing the nucleon density.

It differs from the standard BBN one equation only by the substitution of ρ_{LL} and $\bar{\rho}_{LL}$ instead of $n_\nu^{eq} = [1 - \exp(E_\nu/T)]^{-1}$. Besides, contrary to the standard model, the neutrino and antineutrino density matrices differ $\bar{\rho}_{LL} \neq \rho_{LL}$, because of the different reactions with the CP-odd plasma of the pre-nucleosynthesis epoch. The equations account for the final state Pauli blocking for neutrinos and electrons.

Eq. 3.10 results into a set of coupled nonlinear integro-differential equations with time dependent coefficients for the components of the density matrix of neutrinos: four equations for the components of the neutrino density matrix, and another four for the antineutrino density matrix for each momentum mode. However, due to conservation of the total neutrino number density in the discussed model, the number of the equations can be reduced to 6 equations for each momentum mode of neutrinos and antineutrinos. Thus, for nonresonant case with 1000 bins for the description of the neutrino energy spectrum we have solved 6001 equations simultaneously, when describing also the SD of neutrino, instead of 7 (when working with the mean p of neutrino).

Particle number densities per unit volume are expressed as $N = (2\pi)^{-3} \int \mathrm{d}^3p\, n(p)$. Performing the integration one gets the final equations for the time evolution of the neutron number density:

$$
\begin{aligned}
(\partial N_n/\partial t) &= -3HN_n + G_F^2\,\frac{g_V^2+3g_A^2}{\pi^3}\,T^5\ \times \\
\times\ &\Big\{N_p\int_0^\infty [1-\rho_{LL}(x)]\,\frac{\mathrm{e}^{-x-y}}{1+\mathrm{e}^{-x-y}}\,f(x,y)\mathrm{d}x \\
-\ &N_n\int_0^\infty \rho_{LL}(x)\,\frac{1}{1+\mathrm{e}^{-x-y}}\,f(x,y)\mathrm{d}x \\
+\ &N_p\int_{(1+\zeta)y}^\infty \bar{\rho}_{LL}(x)\,\frac{1}{1+\mathrm{e}^{-x+y}} f(x,-y)\mathrm{d}x \\
-\ &N_n\int_{(1+\zeta)y}^\infty [1-\bar{\rho}_{LL}(x)]\,\frac{\mathrm{e}^{-x+y}}{1+\mathrm{e}^{-x+y}}\,f(x,-y)\mathrm{d}x\Big\}
\end{aligned}
\tag{3.12}
$$

where $f(x,y) = x^2(x+y)\sqrt{(x+y)^2+\zeta^2y^2}$ and $y = (\delta+m_e)/T$, $\zeta = m_e/\delta$, $\delta = m_n - m_p$.

The first term on the right-hand side describes the dilution effect of expansion, the next describes the weak processes, as pointed above.

3.3.2 Numerical analysis

We have numerically integrated this equation for the temperature range of interest $T \in [0.3, 2.0]$ MeV for the full range of oscillation parameters of our model. The value of $\rho_{LL}(x)$ at each integration step was taken from the simultaneously performed integration of the set of equations evolution of neutrino and the nucleons was followed self consistently.

As initial values at $T = 2$ MeV for the neutron, proton and electron number densities we have taken their equilibrium values. Although the electron mass is comparable with the temperature in the discussed temperature range, the deviation of the electron density from its equilibrium value is negligible due to the enormous rate of the reactions with the plasma photons (*Dolgov*, 1981).

The parameters values of the BBN model, used in our calculations, were the following: the mean neutron lifetime $\tau = 887$ sec, which corresponds to the weighted average value in 1998, the effective number of relativistic flavour types of neutrinos during the nucleosynthesis epoch N_{eff} was assumed equal to the standard value 3. This is a natural choice in good agreement with the BBN arguments (*Shvartsman*, 1969) and with the precision measurements of the Z decay width at LEP (*Adeva et al.*, 1989). [3]

3.4 Overproduction of He-4 and Cosmological Constraints on Oscillation Parameters. Nonresonant Case of Neutrino Oscillations

3.4.1 Production of primordial He-4 in presence of nonresonant neutrino oscillations. $\delta N_s = 0$.

Our numerical analysis showed that the kinetic effects due to oscillations (neutrino population depletion and distortion of neutrino spectrum) play an important role and lead to a considerable overproduction of helium. The results of the numerical integration are illustrated in Figure 3.1.

In Figure 3.2 the dependence of the frozen neutron number density relative to nucleons $X_n = N_n/(N_p+N_n)$ on the mixing angle for different fixed δm^2 is illustrated. The dependence of the frozen neutron number density relative to nucleons $X_n = N_n/(N_p+N_n)$ on the δm^2 for fixed different mixing angles, is presented in Figure 3.3.

As it can be seen from the figures, it becomes almost negligible (less than 1%) for mixings as small as 0.1 for any δm^2 of the discussed range of our model. The value of the frozen n/p-ratio is a smoothly increasing function of the mass difference. Our

[3] Possibilities for somewhat relaxation of that kind of bound in modifications of the BBN model have been discussed. An example of such modification was BBN with decaying particles (*Terasawa and Sato*, 1987; *Dolgov and Kirilova*, 1988; *Dodelson et al.*, 1994).

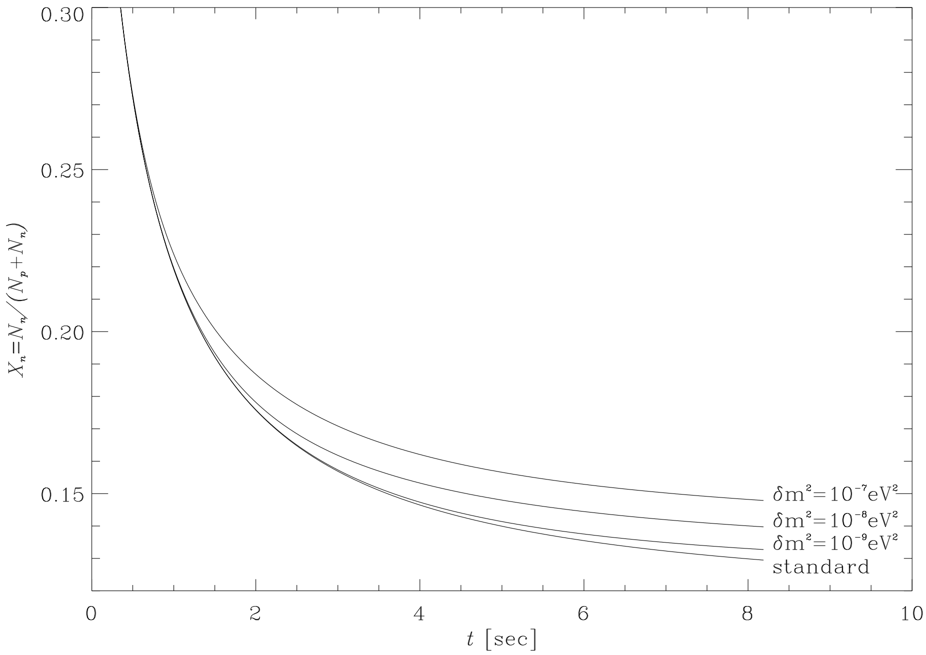

Figure 3.1: The evolution of the neutron number density relative to nucleons $X_n(t) = N_n(t)/(N_p + N_n)$ for the case of nonresonant oscillations with maximal mixing and different δm^2 is shown. For comparison the standard model curve is plotted also. Figure from ref. *Kirilova and Chizhov* (1998c).

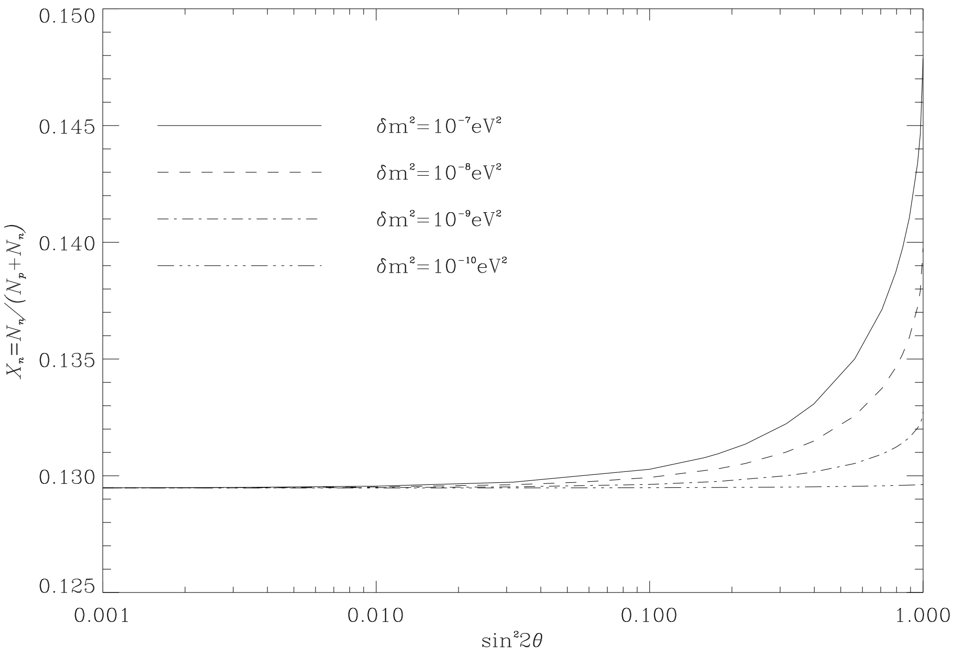

Figure 3.2: The frozen neutron number density relative to nucleons $X_n = N_n/(N_p + N_n)$ dependence on the mixing angle for different fixed δm^2. Figure from ref. *Kirilova and Chizhov* (1998c).

analysis showed that the effect of oscillation for δm^2 smaller than 10^{-10} eV^2 even for maximal mixing is smaller than 1%. The nonresonant oscillations with $\delta m^2 \leq 10^{-11}$ eV^2 do not have any observable effect on the primordial production of elements, i.e. the results coincide with the standard model values with great accuracy.

From the numerical integration for different oscillation parameters we have obtained the primordial helium yield $Y_p(\delta m^2, \vartheta)$, which is illustrated by the surface in Figure 3.4.

Some of the constant helium contours calculated in the discussed model of cosmological nucleosynthesis with nonresonant neutrino oscillations on the $\delta m^2 - \vartheta$ plane are presented in Figure 3.5.

Thus, the total effect of nonequilibrium neutrino oscillations on BBN is an overproduction of helium in comparison to the standard BBN value. The overproduction increases with the increase of the mass differences and the increase of the mixing.

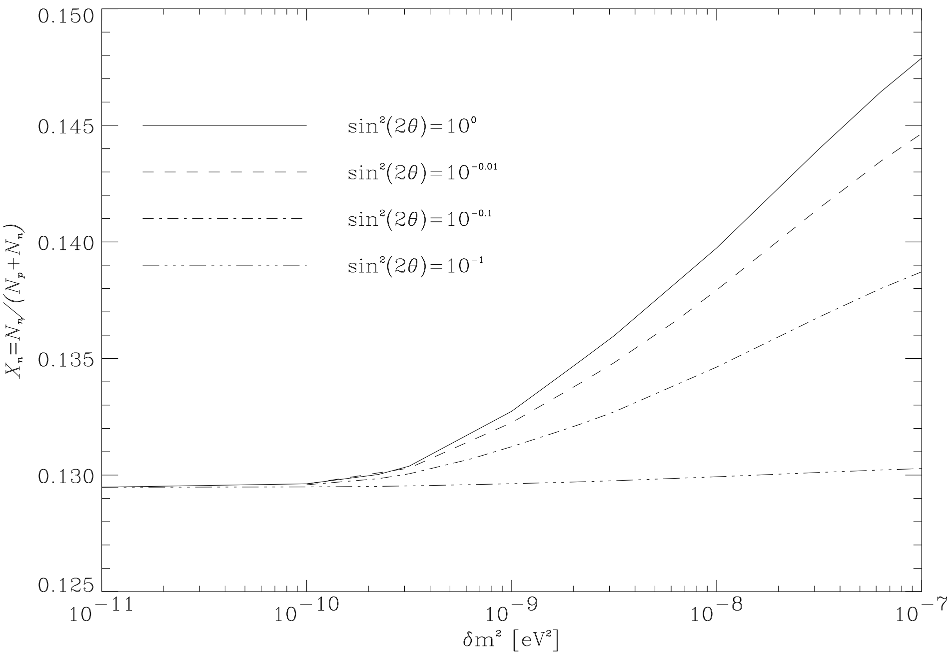

Figure 3.3: The figure illustrates the dependence of the frozen neutron number density relative to nucleons $X_n = N_n/(N_p + N_n)$ on the mass difference for different mixing angles.Figure from ref. *Kirilova and Chizhov* (1998c).

This is an expected result in agreement with the qualitative considerations based on analytic estimations of the effect. The effect of oscillations is maximal at maximal mixing for the nonresonant case of neutrino oscillations.

The account for *asymmetry* showed a slight predominance of neutrinos over antineutrinos, not leading to a noticeable effect on the production of helium in case initially the lepton asymmetry is accepted initially equal to the baryon one. So, the effect of asymmetry is proved to be negligible for all the discussed parameter range, i.e. for any ϑ and for $\delta m^2 \leq 10^{-7}$ eV^2.

In the non-resonant oscillations case we have investigated also the case of higher than the baryon one initial lepton asymmetry. The results pointed that lepton asymmetry initially by three orders of magnitude higher have noticeable effect on the cosmologically produced ^4He and should be accounted for properly even in the non-resonant case, *Kirilova and Chizhov* (1998b), *Kirilova* (2012) (see next chapter).

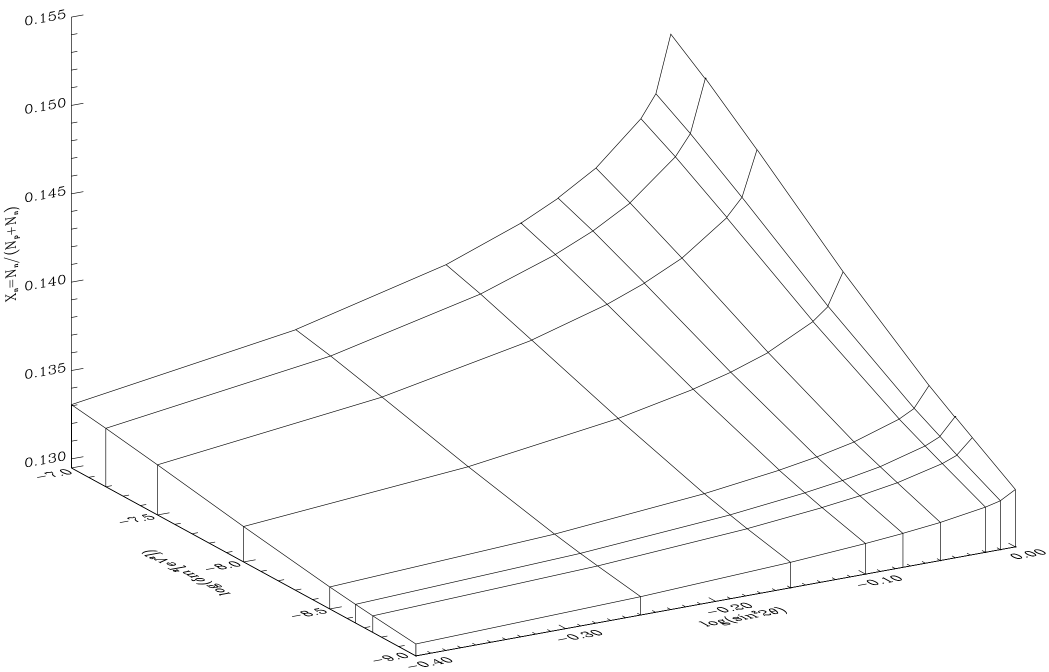

Figure 3.4: The dependence of the primordially produced helium on the oscillation parameters is represented by the surface $Y_p(\delta m^2, \vartheta)$. Figure from ref. *Kirilova and Chizhov* (1998c).

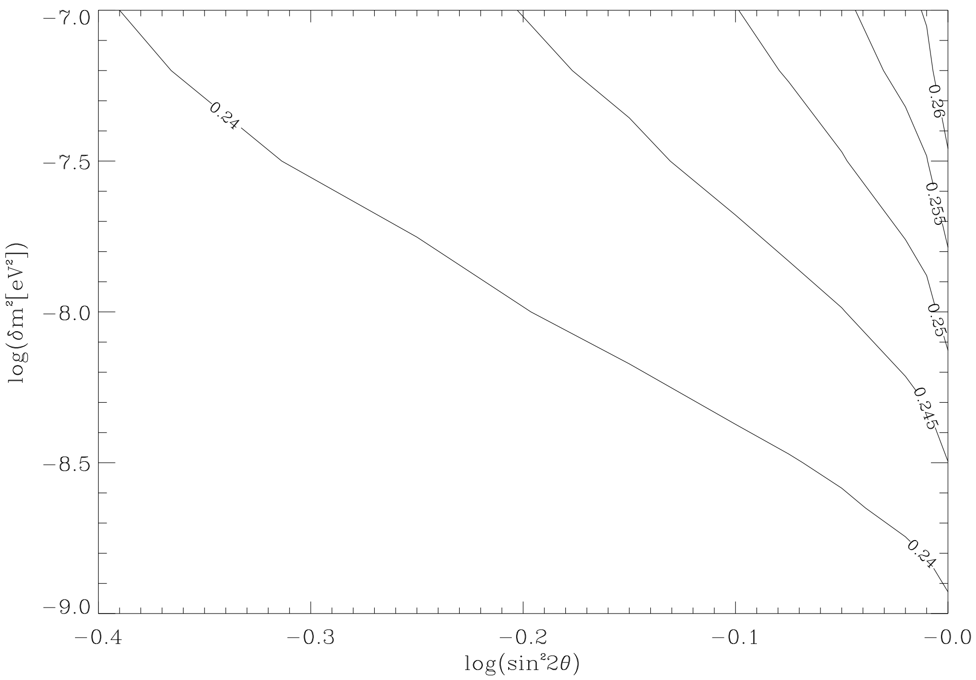

Figure 3.5: On the $\delta m^2 - \vartheta$ plane some of the constant helium contours calculated in the discussed model of cosmological nucleosynthesis with nonresonant neutrino oscillations are shown. Figure from ref. *Kirilova and Chizhov* (1998c).

3.4.2 Cosmological constraints on oscillating neutrino

On the basis of the analysis of neutrino oscillations effect on He-4 production and the observational data on He-4 precise BBN constraints on neutrino oscillation parameters were obtained.

On the basis of these results, requiring an agreement between the theoretically predicted and the observational values of helium, it is possible to obtain cosmological constraints on the neutrino mixing parameters.

The primordial helium values extracted from observations differ considerably due to systematic errors, *Sasselov and Goldwirth* (1995). Therefore, we considered it useful to provide the precise calculations for helium contours up to 0.26. So, whatever the primordial abundance of ^4He will be found to be in future (within this extreme

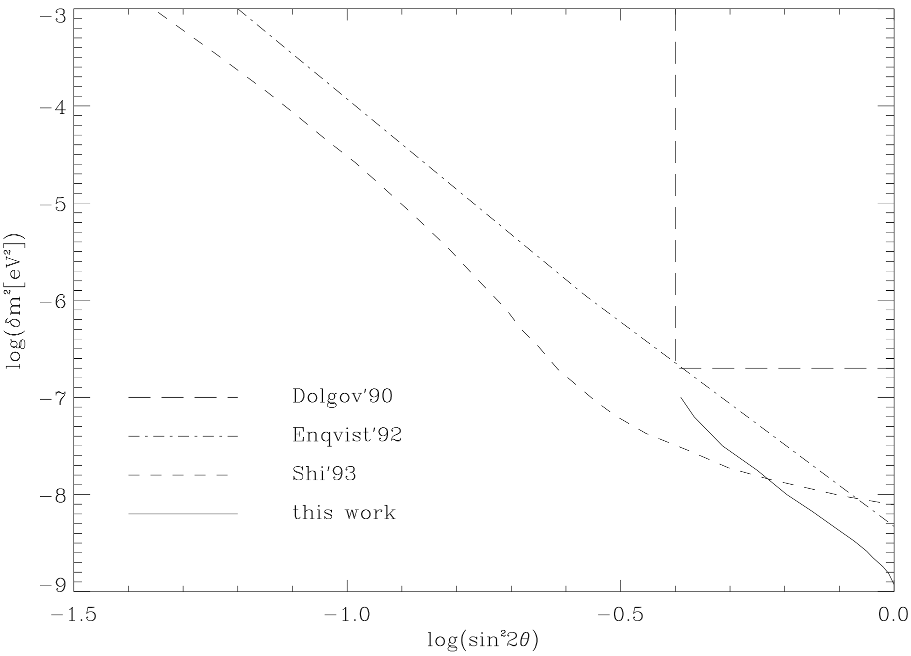

Figure 3.6: The curves, corresponding to helium abundance $Y_p = 0.24$, obtained in the present work and in previous works, analyzing the nonresonant active-sterile neutrino oscillations, are plotted on the $\delta m^2 - \vartheta$ plane. Figure from ref. *Kirilova and Chizhov* (1998c).

range) the results of our calculations may provide the corresponding bound on mixing parameters of neutrino for the case of nonresonant active-sterile oscillations with small mass differences.

Assuming the conventional observational bound on primordial ^4He $Y_p = 0.24$, the cosmologically excluded region for the oscillation parameters on the plane $\sin^2(2\vartheta)$ - δm^2 in Fig. 7 is situated to the right of the $Y_p = 0.245$ curve, which gives 5% overproduction of helium in comparison with the accepted 0.24 observational value.

3.4.3 Comparison with previous studies

For comparison the curves, corresponding to helium abundance $Y_p = 0.24$, obtained in ref. (*Kirilova and Chizhov*, 1998c), and in previous works, analyzing the nonresonant active-sterile neutrino oscillations, are plotted in Figure 3.6.

Our results are in good accordance with the estimations of *Barbieri and Dolgov* (1990) and the numerical analysis of *Enqvist et al.* (1992). These authors estimated the effect of excitement of an additional degree of freedom due to oscillations, and the corresponding increase of the Universe expansion rate, leading to an overproduction of helium-4. The excluded regions for the neutrino mixing parameters were obtained from the requirement that the neutrino types should be less than 3.4: $N_\nu < 3.4$. In these works the depletion effect was considered. The asymmetry was neglected and the distortion of the neutrino spectrum was not studied because the kinetic equations for neutrino mean number densities were considered.

The results of *Shi et al.* (1993), as can be seen from the figure, differ both from the ones of the previously cited works and from our results. The account for nonequilibrium oscillations merely by shifting the effective neutrino temperature is not acceptable for a large range of model parameters.

As can be seen from the curves, for large mixing angles, we exclude $\delta m^2 \geq 10^{-9}$ eV^2, which is much stronger constraint than the previously existing. This more stringent constraints obtained in our work for the region of great mixing angles and small mass differences is due to the more accurate kinetic approach we have used and to the precise account of the effects of neutrino depletion, energy distortion and asymmetry due to oscillations on BBN production of He-4.

It is interesting to compare cosmological constraints with the experimentally found possible solutions to the observed neutrino anomalies: BBN considerations were the first to exclude two of the possible solutions of the solar neutrino problem - large mixing angle solution.We are in a good accordance with the results of active-sterile neutrino oscillation models with higher mass differences, it is obvious that a natural extrapolation of our excluded zone towards higher mass differences will rule out partially the possible solution range for large mixing angles. Besides, we have excluded LOW mixing angle solution years before the analysis of solar neutrino oscillations experiments data pointed to the preferred flavor oscillation channels.

The MWS small mixing angle nonadiabatic solution is out of the reach of our model.

In our toy model we have not accounted for flavor oscillations. BBN constraints on oscillation parameters, accounting for the flavor mixing were obtained in refs (*Dolgov and Villante*, 2004; *Dolgov*, 2002). These bounds are reasonably accurate for large mass differences in case of efficient repopulation of active neutrinos.

In conclusion, we have made a precise survey of the influence of the discussed type of oscillations on the cosmological production of helium-4. We have calculated the evolution of the corresponding neutron-to-proton ratio from the time of freeze out of neutrinos at 2 MeV till the effective freeze out of nucleons at 0.3 MeV for the full range of model parameters. As a result we have obtained the dependence $Y_p(\delta m^2, \vartheta)$ and constant helium contours on the $\delta m^2 - \vartheta$ plane. Requiring an agreement between the observational and the theoretically predicted primordial helium abundances, we have calculated accurately the excluded regions for the neutrino mixing parameters, for different assumptions about the preferred primordial value of helium.

The obtained BBN cosntraints on the electron-sterile oscillations parameters are the most stringent known in literature.

3.5 Overproduction of He-4 and Cosmological Constraints on Oscillation Parameters. Resonant Case of Neutrino Oscillations

3.5.1 Production of primordial He-4 in presence of resonant neutrino oscillations. $\delta N_s = 0$

In a cycle of works (*Kirilova and Chizhov*, 1997, 1998c, 2000a, 2001a; *Kirilova*, 2004b, 2007; *Kirilova and Panayotova*, 2006; *Kirilova*, 2012; *Kirilova and Chizhov*, 2010; *Kirilova*, 2011c) we have explored the influence of the resonant active-sterile neutrino oscillations $\nu_e \leftrightarrow \nu_s$, on BBN and particularly on He-4.

The *resonant* neutrino oscillations case is a much more complicated, than the nonresonant one, as far as rapid growth of asymmetry for certain sets of parameters is typical there (*Kirilova and Chizhov*, 1996a). First numerical calculations of the BBN with resonant neutrino oscillations accounting for the asymmetry growth were provided in refs. (*Kirilova and Chizhov*, 1996a, 1997). The phenomenon of the oscillation-generated asymmetry growth was registered there and it was shown that following the behavior of the neutrino-antineutrino asymmetry at each momentum is important, particularly, when the distortion of the neutrino spectrum is considerable. The effect of the neutrino-mixing-generated asymmetry was shown to be considerable – up to about 10% relative decrease in helium-4 in comparison with the case with oscillations but without the asymmetry account.

Detailed studies of the BBN with resonant neutrino oscillations accounting properly for the asymmetry growth were provided for a wider set of oscillation parameters in refs. (*Kirilova and Chizhov*, 2000a; *Kirilova*, 2011c, 2004b, 2007, 2012). The evolution of the neutrino ensembles was followed selfconsistently with the evolution of the nucleons, using exact kinetic equations for the neutrino density matrix and the nucleon number densities in momentum space, from the time of neutrino decoupling till the freeze-out of nucleons at 0.3 MeV.

We have used exact kinetic approach, which enabled us to study precisely the neutrino depletion, spectrum distortion and neutrino oscillations generated asymmetry due to oscillations at each momentum mode.

BBN production of He-4 was calculated accounting both for the spectrum distortion and for the neutrino asymmetry dynamical evolution *at each momentum mode.* We have calculated the dependence of the primordially produced helium-4 on the oscillation parameters $Y_p(\delta m^2, \vartheta)$ for the full range of mixing parameters of the model, namely for $\sin^2(2\vartheta)$ ranging from 10^{-3} to maximal mixing and

$$10^{-11}\mathrm{eV}^2 \leq \delta\mathrm{m}^2 \leq 10^{-7}\mathrm{eV}^2$$

, and for zero sterile neutrino initial population. For smaller mixing parameters the effect on helium-4 was shown to be negligible *Kirilova and Chizhov* (1996a).

Our results are based on several hundreds of $\delta m^2 - \vartheta$ combinations. The necessary accuracy for description of the SD in the resonant case was much higher than that in the nonresonant one. We used between 5000 and 10 000 bins in case of considerable resonant growth of asymmetry, correspondingly he number of the equations solved increased up to 10 times in comparison with the nonresonant case of neutrino oscillations.

In the next figure 3.7 the evolution of the neutron number density relative to nucleons $X_n(t) = N_n(t)/(N_p + N_n)$ for the nucleosynthesis model with vacuum nonequilibrium oscillations and for the case of resonant oscillations in medium with $\delta m^2 = -10^{-8}$ and $\vartheta = \pi/8$ is presented. The curve corresponding to the standard nucleosynthesis model is given as well for comparison.

The dependence of the BBN produced He-4 on the oscillation parameters was studied.

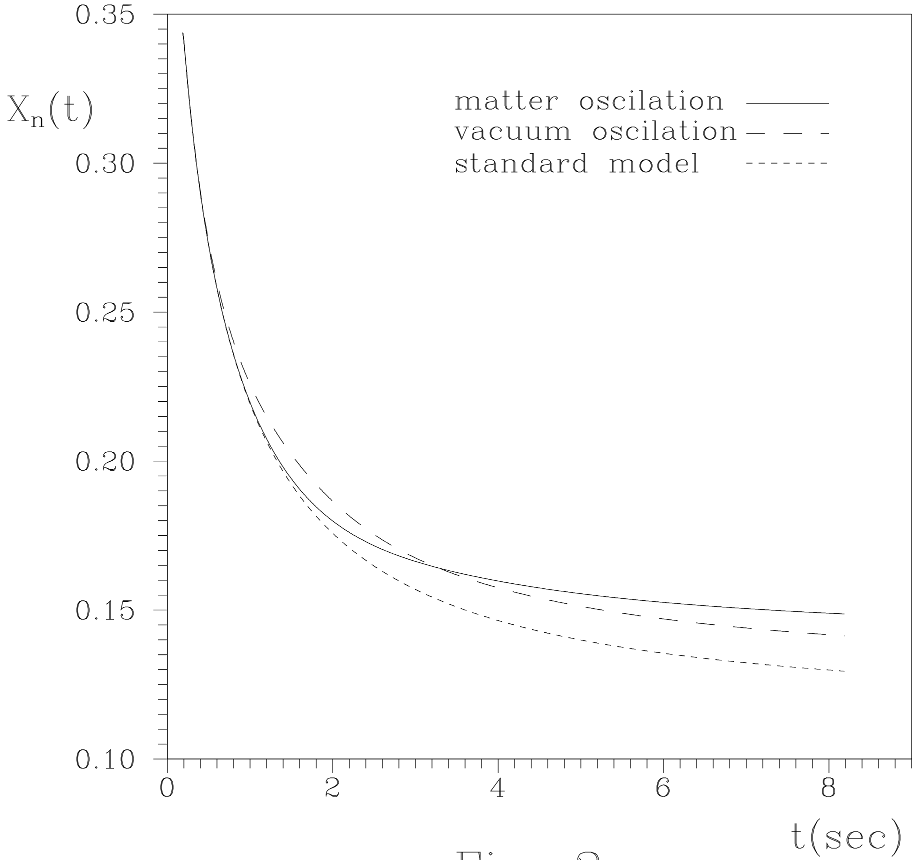

Fig. 2

Figure 3.7: The curves represent the evolution of the neutron number density relative to nucleons $X_n(t) = N_n(t)/(N_p + N_n)$ for the nucleosynthesis model with vacuum nonequilibrium oscillations and for the case of nonequilibrium oscillations in medium, $\delta m^2 = -10^{-8}$, $\vartheta = \pi/8$. For comparison the curve corresponding to the standard nucleosynthesis model is shown. Figure from ref. *Kirilova and Chizhov* (1997).

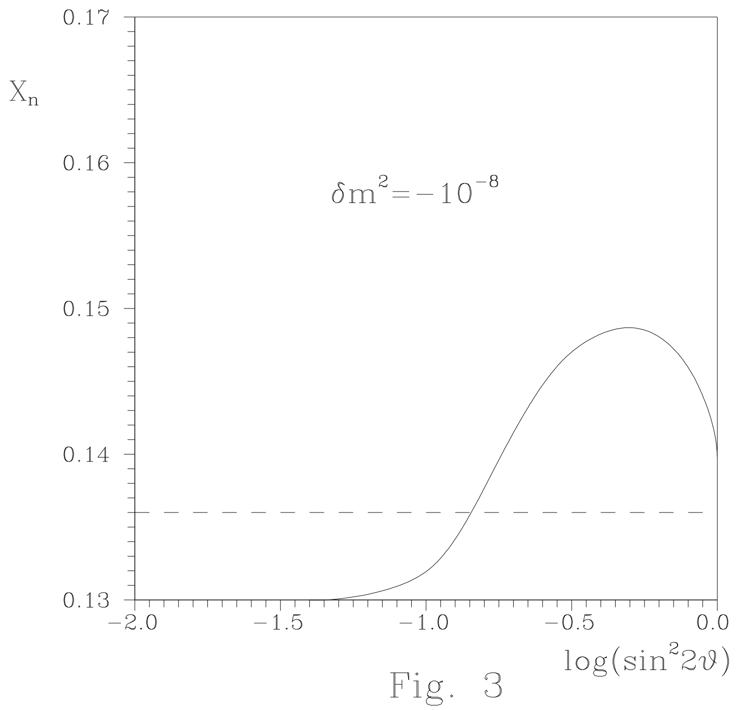

Figure 3.8: The figure illustrates the dependence of the neutron number density relative to nucleons $X_n = N_n/(N_p+N_n)$ on the mixing angle for $\delta m^2 = -10^{-8}$. Figure from *Kirilova and Chizhov* (1997).

The next figure 3.8 shows the dependence of the neutron number density relative to nucleons $X_n = N_n/(N_p + N_n)$ on the mixing angle for $\delta m^2 = -10^{-8}$.

The major effects, of the discussed resonant $\nu_e \leftrightarrow \nu_s$ oscillations with small mass differences on helium-4 production, are due to the depletion of the ν_e population due to oscillations, neutrino spectrum distortion and the neutrino asymmetry growth due to oscillations.

We have found that beginning with asymmetries of the order of the baryon one, the asymmetry does not grow enough to influence *directly* the kinetics of the $n - p$ transitions. Consequently, the apparently great asymmetry effect (as illustrated in Fig. 3.11) is totally due to the *indirect* effects of the asymmetry on BBN. The maximal asymmetry effect is around 10% ‘underproduction’ of Y_p in comparison with the case of BBN with oscillations but without the asymmetry account.

The total effect of oscillations, with the complete account of the asymmetry effects, is still overproduction of helium-4, in comparison to the standard BBN value, although considerably smaller at small mixing angles than obtained in the calculations neglecting asymmetry.

3.5.2 Cosmological constraints on oscillating neutrino

We have obtained iso-helium contours on the $\delta m^2 - \vartheta$ plane. Cosmological constraints on oscillation parameters, more precise than the existing ones were obtained, due to the exact kinetic approach and the proper account for the neutrino spectrum distortion and the oscillations generated asymmetry. These constraints are better by almost an order of magnitude than the existing ones for the neutrino squared mass differences at large mixing angles.

The next figure 3.9 the first BBN constraints, we have obtained for the case of resonant $\delta m^2 < 0$ and nonresonant $\delta m^2 > 0$ neutrino oscillations, corresponding to helium abundance $Y_p = 0.245$, are presented.

In ref. (*Kirilova and Chizhov*, 2000a) from the numerical integration for the full range of oscillation parameters we have obtained the primordial helium yields $Y_p(\delta m^2, \vartheta)$. Some of the iso-helium contours calculated in the discussed model of cosmological nucleosynthesis with resonant neutrino oscillations are presented on the plane $\delta m^2 - \vartheta$ in figure 3.10.

The primordial helium values extracted from observations during the last 10 years differ considerably. At present the primordial helium values extracted from observations are believed to have considerable systematic errors. Therefore, we considered it useful to provide the exact calculations for various iso-helium contours up to 0.26. Knowing more precisely the primordial helium-4 value from observations, it will be possible to obtain the excluded region of the mixing parameters using the results of this survey. The cosmologically excluded region for the oscillation parameters is situated on the plane $\delta m^2 - \vartheta$ to the right of the $Y_p = const$ curves.

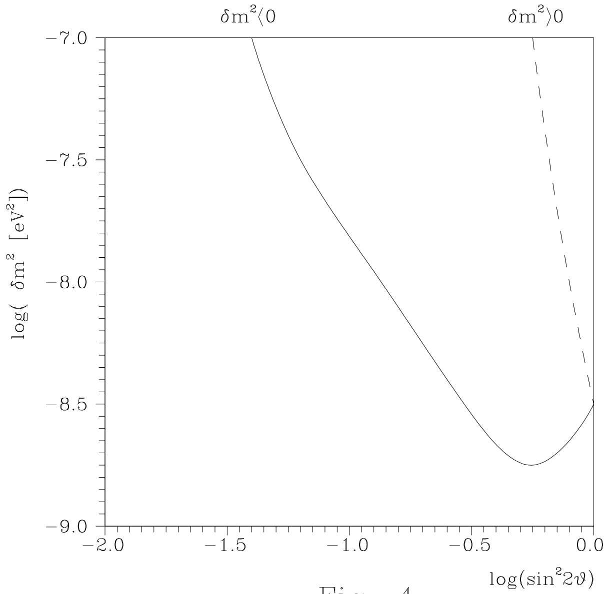

Figure 3.9: Exclusion regions for oscillation parameters are shown for the case of resonant $\delta m^2 < 0$ and nonresonant $\delta m^2 > 0$ neutrino oscillations. The curves correspond to helium abundance $Y_p = 0.245$. Figure from ref. *Kirilova and Chizhov* (1997).

For example, assuming the 'low' observational value of primordial ^4He $Y_p \cong 0.234$, the cosmologically excluded region for the oscillation parameters is situated on the plane $\delta m^2 - \vartheta$ to the right of the $Y_p = 0.245$ curve, which gives 5% overproduction of helium in comparison with this observational value.

3.5.3 Comparison with previous studies

In figure 3.11 a comparison between the curves, corresponding to helium abundance $Y_p = 0.24$, obtained in the present work and in previous works (*Enqvist et al.*, 1992; *Shi et al.*, 1993), analyzing the resonant active-sterile neutrino oscillations, is presented. In *Enqvist et al.* (1992) the excluded regions for the neutrino mixing parameters were obtained from the requirement that the neutrino types should be less than 3.4: $N_\nu < 3.4$. The depletion effect was considered, while the neutrino-antineutrino asymmetry was neglected, and the distortion of the neutrino spectrum was not studied, instead the kinetic equations for neutrino mean number densities

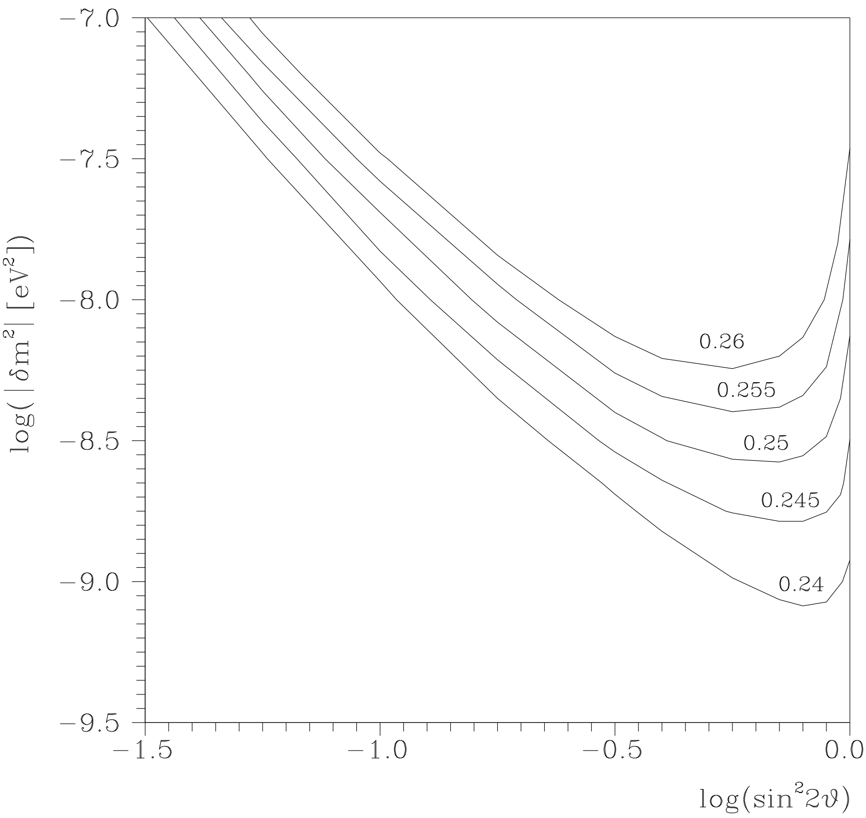

Figure 3.10: On the $\delta m^2 - \vartheta$ plane iso-helium-4 contours $Y_p = 0.24,\ 0.245,\ 0.25,$ 0.255 and 0.26, calculated in the discussed model of BBN with active-sterile resonant neutrino oscillations are shown. For fixed primordial helium-4 value, the area to the left of the corresponding curve gives the allowed region of the oscillation parameters. Figure from ref. *Kirilova and Chizhov* (2000a).

were used.

The dashed curve, presenting our results without the account of asymmetry effect, is in a good accordance with the results of *Enqvist et al.* (1992), where asymmetry was neglected. The difference between the two curves shows explicitly the effect of the proper account of the neutrino spectrum spread and spectrum distortion, which was provided in our work (solid curve). On the other hand, the difference between our curves, the solid and the dashed one, presents the net asymmetry effect.

The results of *Shi et al.* (1993) are not correct: There exists discrepancy between the results of *Shi et al.* (1993) and those of other studies. Moreover, the results of *Shi et al.* (1993) are not consistent even between themselves concerning resonant and nonresonant case. As is well known from the analytical formulae the results for the resonant case $\delta m^2 < 0$ coincide with those for the nonresonant one $\delta m^2 > 0$ at maximal mixing. This fact is illustrated in figure 3.12 of resonant and nonresonant oscillations for all studies, except ref. (*Shi et al.*, 1993).

As is seen from the iso-helium contours for $Y_p = 0.24$, for *large mixing angles* we exclude mass differences $\delta m^2 \geq 8.2 \times 10^{-10}$ eV^2, which is an order of magnitude stronger constraint than the previously existing. This more stringent constraint for mass differences, obtained in our work for the region of large mixing angles is due to the more accurate kinetic approach we have used and to the precise account of neutrino depletion and energy distortion.

At *small mixing angles* the account of the oscillations generated asymmetry leads to an alleviation of the BBN constraints in comparison with the previous works *Enqvist et al.* (1992); *Shi et al.* (1993). It is easy to understand, as far as the asymmetry growth results in suppression of oscillations and, hence, less strongly pronounced overproduction of helium-4 due to oscillations than in the case without the asymmetry account.

In conclusion, we have shown that both the spectrum distortion and neutrino

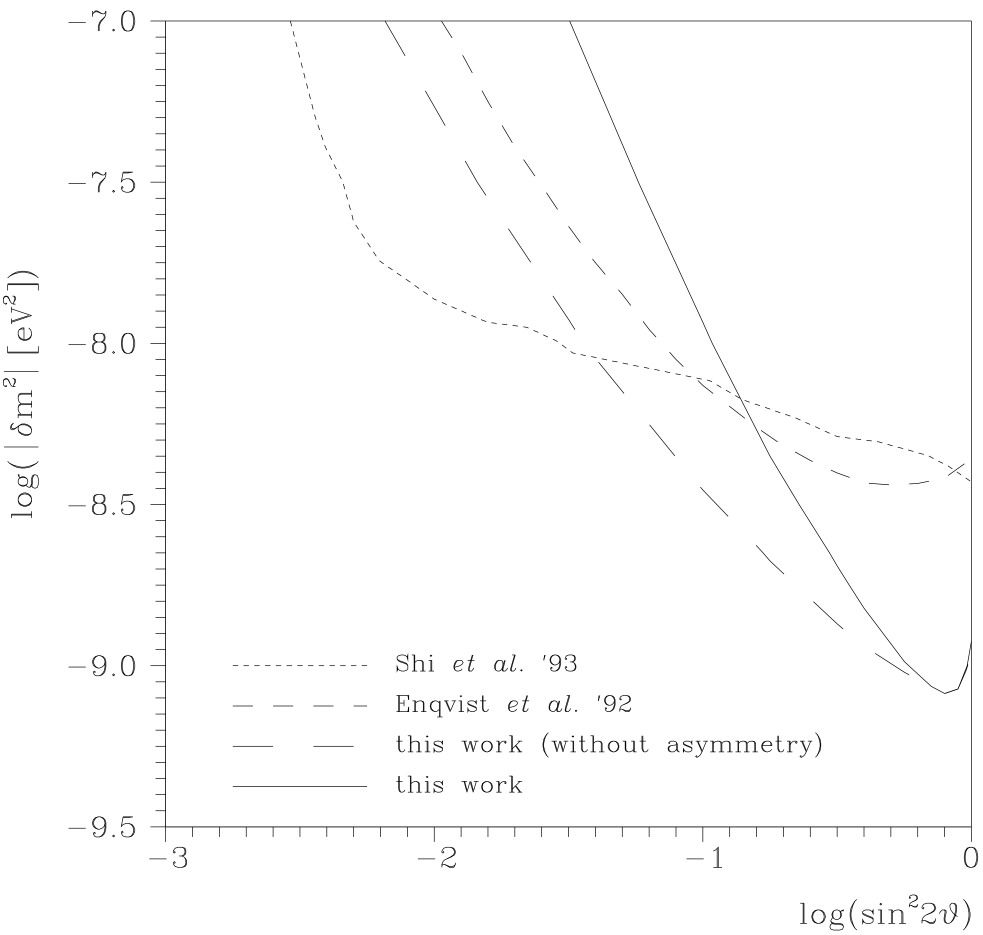

Figure 3.11: In the figure a comparison between the results concerning primordial helium-4 production, obtained in the present work and previous works *Enqvist et al.* (1992); *Shi et al.* (1993), is presented. The dashed curve shows our results in case without asymmetry effect account. It is in a good accordance with the results of *Enqvist et al.* (1992), where asymmetry was neglected. The difference between the two curves shows explicitly the effect of the proper account of the spectrum spread of neutrino, which was provided in our work. On the other hand, the difference between our curves, the solid and the dashed one presents the net asymmetry effect. The artistic curve of Shi et al. *Shi et al.* (1993) is obviously inconsistent with the results of other works and we will leave it without a comment. Figure from ref. (*Kirilova and Chizhov*, 2000a).

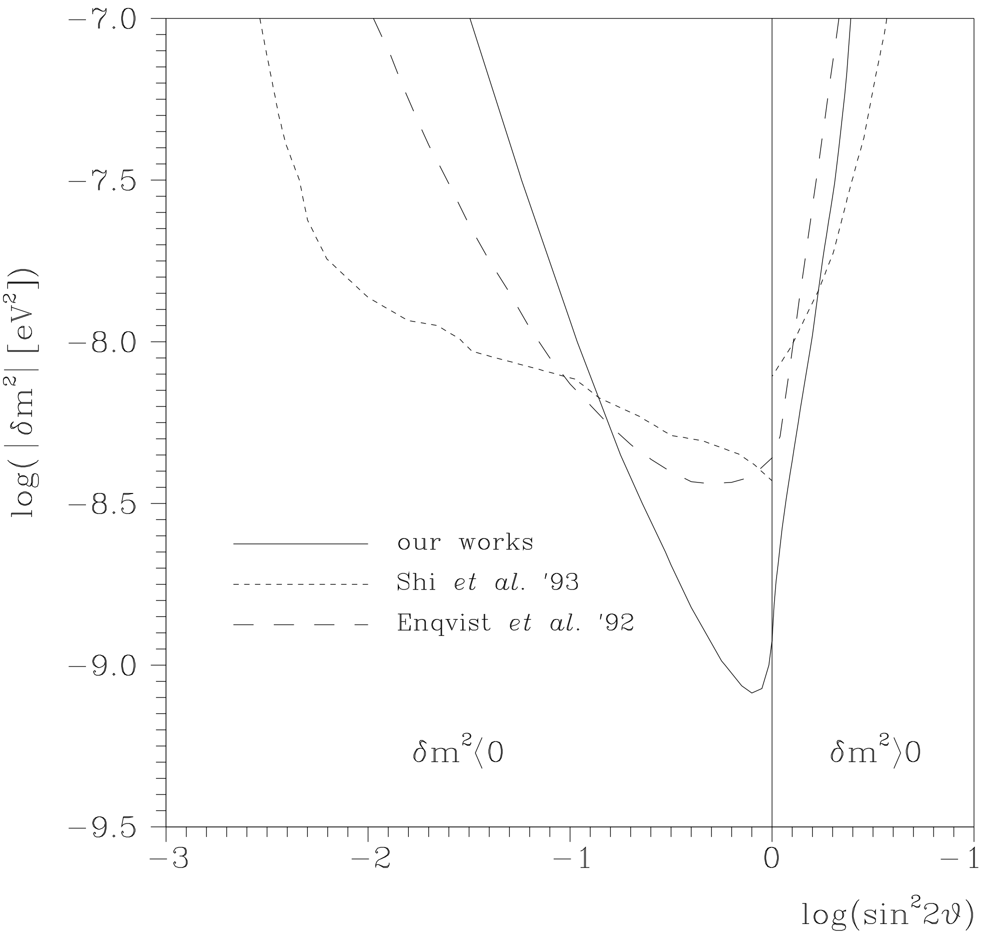

Figure 3.12: Combined iso-helium contours $Y_p = 0.24$, for the resonant oscillations, $\delta m^2 < 0$, and the nonresonant ones, $\delta m^2 > 0$, calculated in previous studies *Enqvist et al.* (1992); *Shi et al.* (1993); *Kirilova and Chizhov* (1998c) and in this work, are presented. The discontinuity of the curve of Shi et al. *Shi et al.* (1993) reveals the discrepancy between their own results for the resonant and nonresonant case. Figure from ref. *Kirilova and Chizhov* (2000a).

mixing generated asymmetry should be accounted for properly in models of BBN with resonant neutrino oscillations, as far as their effect is considerable.

We have calculated different iso-helium contours for the resonant case of neutrino oscillations with small mass differences and obtained the cosmological constraints, better by an order of magnitude than the existing ones due to the exact kinetic approach both to the neutrino evolution and to the nucleons freeze-out.

3.6 Remarks on Possible Change of BBN Constraints

3.6.1 Change of BBN constraints on neutrino oscillations parameters

Several possibilities for modification of the BBN model exist that may considerably change the BBN constraints on neutrino oscillations parameters. Here we list the most popular ones: the additional sterile neutrino population present initially and initial (relic) lepton asymmetry.

Additional sterile population:

Additional sterile population, present before oscillations become effective, may either strengthen or relax BBN constraints on $\nu_e \leftrightarrow \nu_s$ oscillations parameters due to the interplay between its dynamical and kinetic effect, as discussed already in chapter 2. For more detail see subsection 3.8. The BBN constraints for different sterile neutrino population values were obtained in refs. (*Kirilova*, 2004b; *Kirilova and Panayotova*, 2006; *Kirilova*, 2007; *Panayotova*, 2011).

In case of relaxed BBN constraints, namely $\delta N_{eff} < 1.7$, they may be expressed by the 5% Y_p overproduction contour for $\delta N_s = 0.7$, presented in Fig.2. of (*Kirilova and Panayotova*, 2006), see also (*Panayotova*, 2011).

Role of lepton asymmetry L:

The BBN constraints discussed till now concern the case of negligible lepton asymmetry of the order of the baryon one. However, L contained in neutrinos may be large, as discussed in the next chapter. Accurate numerical modeling of BBN with L and oscillations has shown that the dynamically generated asymmetry in oscillations leads to relaxation of constraints at small mixings, while initially present lepton asymmetry $|L| \sim 10^{-6}$ is able to relax BBN constraints at large mixings and strengthen them at small mixings. Large enough initial lepton asymmetry may alleviate BBN constraints (*Kirilova and Chizhov*, 1998b; *Kirilova*, 2011c).Initial asymmetry for certain range of parameters is capable also to enhance neutrino oscillation and, thus, increase the overproduction of Y_p in BBN with neutrino oscillations, and, correspondingly, to strengthen the cosmological constraints on oscillation parameters. The role of lepton asymmetry, either dynamically generated or initially present on BBN and cosmological constraints is discussed in detail in the fourth chapter.

3.6.2 Constraints on the baryon density in BBN with electron-sterile neutrino oscillations

The baryon density range obtained from different kind of observational data measurements circa 2001 differed from the one determined from BBN. Therefore, it was interesting to consider possible relaxations of the BBN bounds.

The model of BBN with late active-sterile neutrino oscillations predicts primordial He-4 increase. Besides, D yield should increase due to the shorter time of its destruction, while Li-7 may be expected to increase as a result of shortened time of Be-7 production. The primordial helium production in this BBN model is a function of the oscillation parameters and of the baryon density. So, the observed D, Li-7 and He-4 abundances in case of oscillations of neutrino require lower baryon density than that in the standard BBN.

Using the constraints on oscillation parameters from the combined analyses of the oscillations experiments data and the observational data on primordially produced light elements it is possible to constrain the range of the baryon density.

In ref. (*Kirilova*, 2001b) we reanalyzed standard BBN cosmological constraints on $\Omega_b h^2$ and showed that the modified BBN model with neutrino oscillations may permit wider range for the baryon density.

The allowed variation of the baryon density in the BBN model with neutrino oscillations obtained on the basis of $\delta Y_p/Y_p = 5\%$ overproduction of He-4 is found to be:

$$\Omega_b h^2 \geq 0.005. \tag{3.13}$$

where Ω_b is the baryon density expressed as a fraction of the critical density, h is the Hubble parameter in units of 100 km/s/Mpc.

More stringent limit is obtained if D and Li-7 data are taken into account, namely:

$$\Omega_b h^2 \geq 0.011. \tag{3.14}$$

For comparison the *standard BBN* extreme range for the BBN baryon density at that time (2001) was $0.016 \leq \Omega_b h^2 \leq 0.025$. Thus, this modification of BBN permits wider range than the standard BBN. Hence, this modified BBN model with neutrino oscillations proposes relaxation of the BBN constraints on the baryon content of the Universe.

The results of our analysis indicated that nonstandard BBN likely can resolve some of the discrepancies between standard BBN predictions and other data and reduce the tension between them in case such tension persists.

The relaxed constraints on the baryon density may be useful also for constraining or relaxing chemical evolution models *Klecker et al.* (2001); *Busemann et al.* (2001); for constraining alternative models with new physics.

3.7 Maximal Overproduction of He-4 in BBN with Late Neutrino Oscillation

The maximum overproduction of helium-4 in cosmological nucleosynthesis with active–sterile neutrino oscillations, $\nu_e \leftrightarrow \nu_s$, efficient after decoupling of electron neutrino, was analyzed in *Kirilova* (2003a), *Kirilova* (2001a). The kinetic effects on primordial nucleosynthesis due to neutrino spectrum distortion, caused by oscillations, were precisely taken into account. The overproduction of the primordial ^{4}He, $\delta Y_p = Y_p^{osc} - Y_p$ in the presence of $\nu_e \leftrightarrow \nu_s$ oscillations was calculated for mass differences $\delta m^2 \leq 10^{-6}$ eV^2 and $0 \leq \vartheta \leq \pi/4$. Several hundreds of $\delta m^2 - \vartheta$ combinations were explored.

We have used the data from the precise calculations of the n/p-freezing provided for the non-resonant case in *Kirilova and Chizhov* (1998c) and for the resonant case in *Kirilova and Chizhov* (2000a). As far as it is the essential for the production of ^{4}He. The neutron decay was accounted adiabatically till the beginning of nuclear reactions at about 0.09 MeV.

We have found that the effect of oscillations becomes very small (less than 1%) for small mixings: as small as $sin^2 2\vartheta = 0.1$ for $\delta m^2 = 10^{-7}$ eV^2, and for small mass differences: $\delta m^2 < 10^{-10}$ eV^2 at maximal mixing. For very small mass differences $\delta m^2 \leq 10^{-11}$ eV^2, or at very small mixing angles $\sin^2 2\vartheta \leq 10^{-3}$, the effect on nucleosynthesis becomes negligible.

In the non-resonant case the oscillation effect increases with the increase of the oscillation parameters, hence it is maximal at maximal mixing and greatest mass differences. In Fig. 3.13 (the lower curve) the maximal relative increase in the primordial ^{4}He as a function of neutrino mass differences at maximal mixing is presented:

$$\delta Y_p^{max}/Y_p = \delta Y_p^{osc}/Y_p(\delta m^2)_{|\theta=\pi/4}$$

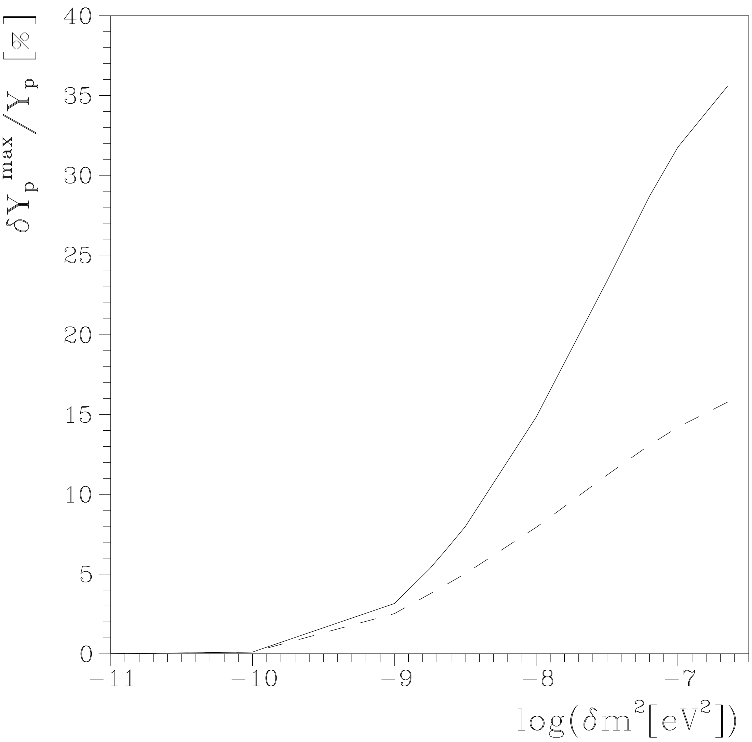

Figure 3.13: Maximum primordial ^{4}He abundance for the resonant (upper curve) and the non-resonant oscillation case (lower curve), as a function of the neutrino mass differences. The non-resonant case is calculated at maximum mixing, while in the resonant case the helium abundance is calculated at the resonant mixing angle for the corresponding mass difference. Figure from ref. *Kirilova* (2003a).

It is seen that for maximal mixing, the oscillation effect becomes greater than 5% (the one corresponding to one additional neutrino type) already at $|\delta m^2| \geq 3 \times 10^{-9}$ eV^2 (in the resonant case) and $\delta m^2 \geq 6 \times 10^{-9}$ eV^2 (in the non-resonant one). It continues to grow up with the increase of the mass differences, and at $|\delta m^2| \sim 10^{-7}$ eV^2 is several times bigger: $\delta N_k^{max} \sim 3$ in the non-resonant case and $\delta N_k^{max} \sim 6$ for the resonant one.

Further increase of the mass differences, however, will lead to oscillations effective before electron neutrino decoupling, and therefore, to a smaller spectrum distortion effect, because the interactions with the plasma will lead to faster thermalization of the sterile state. Hence, the effect on helium will decrease with further increase

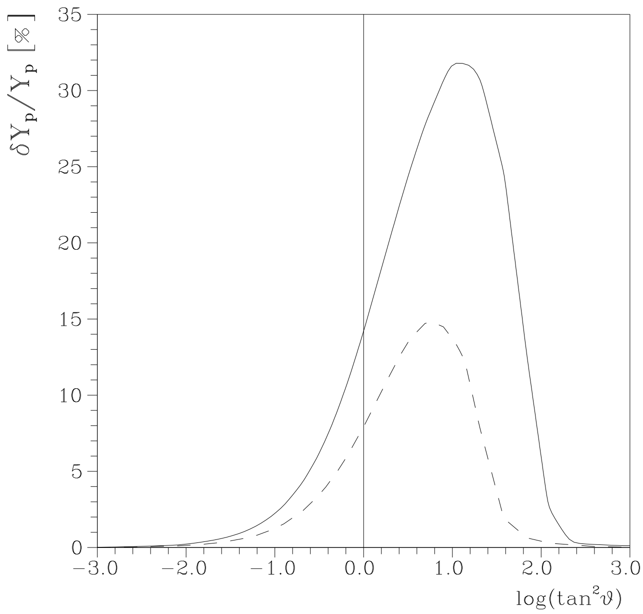

Figure 3.14: The dependence of the relative increase of primordial helium on the mixing angle for the resonant (r.h.s.) and non-resonant (l.h.s.) oscillation case. The upper curve corresponds to $\delta m^2 = 10^{-7}$ eV^2, the lower one to $\delta m^2 = 10^{-8}$ eV^2. Figure from ref. *Kirilova* (2003a).

of $|\delta m^2|$ and finally reach an overproduction of 5% again, corresponding to a full thermalization of the sterile state and its equilibrium spectrum.

In Fig. 3.14 we present a combined plot (for the resonant and the non-resonant oscillation case) of δY_p dependence on the mixing angle for $\delta m^2 = 10^{-7}$ eV^2 and $\delta m^2 = 10^{-8}$ eV^2. While in the non-resonant case the oscillations effect increases with the increase of the mixing (see l.h.s of 3.14), in the resonant case for a given δm^2 there exists some resonant mixing angle, at which the oscillations are enhanced by the medium (due to the MSW effect), and hence, the overproduction of ^{4}He is greater than that corresponding to the vacuum maximal mixing angle. This behavior of the helium production on the mixing angle is illustrated in the r.h.s. of the figure.

The upper curve in Fig. 3.13 shows the maximal relative increase in the resonant oscillations case as a function of mass differences. Each maximum ^{4}He value corresponds to the resonant mixing angle for the concrete mass difference:

$$\delta Y_p^{max}/Y_p = Y_p^{osc}(\delta m^2, \vartheta_{\delta m}^{res})$$

As can be seen from Figs. 3.13 and 3.14, a considerable overproduction can be achieved: in the resonant case up to 32% and in the non-resonant one – up to 14%. So, the net effect of spectrum distortion of electron neutrino due to oscillations on the production of ^{4}He may be considerable and several times larger than the effect due to excitation of one additional neutrino type.

In conclusion, this study has shown that considerable Y_p overproduction may result from the electron neutrino spectrum distortion due to $\nu_e \leftrightarrow \nu_s$ oscillations. The overproduction is maximal for the case of initially empty sterile neutrino state, considered here. The dependence of ^{4}He overproduction on the degree of population of the sterile neutrino state before $\nu_e \leftrightarrow \nu_s$ oscillations was considered (*Kirilova*, 2004b, 2007) and is discussed in the following subsection. The results of this analysis can be useful for constraining nonstandard physics, predicting active-sterile neutrino oscillations, like extra-dimensions, producing oscillations, supernova bursts employing oscillations, etc.. It can be of interest also for models of galactic chemical evolution.

3.8 The Effect of Neutrino Spectrum Distortion on BBN in the General Case of Non-Zero Initial Population of the Sterile Neutrino

Numerical analysis of He-4 production in the presence of $\nu_e \leftrightarrow \nu_s$, effective after neutrino decoupling, in the general case of partially filled initially sterile neutrino state $Y_p(\delta N_s, \delta m^2, \sin^2 2\vartheta)$ was provided in several works (*Kirilova*, 2004b, 2007, 2006;

Kirilova and Panayotova, 2006).

3.8.1 BBN with $\nu_e \leftrightarrow \nu_s$ and non-empty initially ν_s

Effects on BBN

Initially present $\delta N_s \neq 0$ has two-fold effect on He-4 (*Kirilova*, 2004b):

(a)**Dynamical effect:** $\delta N_s \neq 0$ increases the energy density by

$$\delta\rho = 7/8(T_\nu/T_\gamma)^4 \delta N_s \rho_\gamma,$$

thus modifying the cosmic expansion rate at RD stage $H = \sqrt{8\pi\rho/3M_p^2}$. This reflects into higher freezing temperature of the nucleons and overproduction of ^{4}He. The dynamical effect of initially present δN_s on primordial ^{4}He production will be denoted further on by δY_d. Due to this effect *strengthening of the cosmological bounds* with respect to the ones calculated at $\delta N_s = 0$ should be expected.

The approximate fit to the exact numerical results is:

$$\delta Y_p \sim 0.013 \delta N_s.$$

The maximum helium overproduction corresponding to $\delta N_s = 1$ is $\sim 5\%$.

In case of $\nu_{\mu,\tau} \leftrightarrow \nu_s$ oscillations the dynamical effect is the only effect of initially non-zero δN_s.

In the case of $\nu_e \leftrightarrow \nu_s$ oscillations *with almost equilibrium neutrino energy distribution*, i.e. oscillations taking place before neutrino decoupling, this is the leading effect as well. This effect can be accounted for simply by adding the initial δN_s value to the one produced in oscillations. So, in both these cases the rescaling of the existing constraints is rather straightforward.

(b)**Kinetic effects:** In the nonequilibrium $\nu_e \leftrightarrow \nu_s$ oscillations case, **the presence of partially populated ν_s suppresses the oscillations effects on pre-**

BBN nucleons kinetics *Kirilova* (2004b). Further on this kinetic effect is denoted by δY_k^s, while the kinetic effects of oscillations are denoted by δY_k ($\delta Y_k = \delta Y_k^0 + \delta Y_k^s$). In terms of the effective degrees of freedom

$$\delta N_k = \delta N_k^0 + \delta N_k^s$$

$$\delta Y_k \sim 0.013 \times \delta N_k$$

and δN_k^0 is the kinetic effect corresponding to zero initial population of the sterile state.

Kinetic effects are a result of energy spectrum distortion of ν_e caused by oscillations between active and sterile neutrino, and to a smaller degree are due to the neutrino-antineutrino asymmetry, generated in oscillations.

It has been shown by precise numerical analysis that δN_k depends strongly on the initial population of the sterile neutrino at BBN. Larger δN_s decreases the kinetic effects, because the element of initial non-equilibrium between the active and the sterile states is less expressed. Hence, for any specific value of δN_s it is necessary to provide a separate analysis.

In the case $\delta N_s = 1$, ν_s are in equilibrium (the sterile state is as abundant as the electron one), the n–p kinetics does not feel the oscillations, and hence $\delta N_k = 0$. The final effect is only due to the dynamical effect, i.e. $\delta N_{tot} = 1$.

In the case $\delta N_s = 0$ the kinetic effect of oscillations δN_k for given fixed mixing parameters reach their highest value, δN_k^{max}, as far as the non-equilibrium element (the difference between the sterile and active neutrino number densities at the beginning of oscillations) is the greatest.

Results of the numerical analysis

For different δN_s we have calculated precisely the n/p-freezing, essential for the production of helium, down to temperature 0.3 MeV. Then we have calculated Y_p, accounting adiabatically for the following decay of neutrons till the start of nuclear reactions, at about 0.1 MeV.

It was numerically proven that larger δN_s leads to a decrease of the kinetic effects of oscillations and to a decrease of the overproduction of ^{4}He by oscillations with respect to the case of initially zero δN_s, i.e. $\delta N_k < \delta N_k^0$, where δN_k^0 the kinetic effect corresponding to zero initial population of the sterile state presents in fact the maximal kinetic effect at a given set of oscillation parameters. [4]

We have found that *neutrino spectrum distortion effect on BBN is very strong even when there is a considerable population of the sterile neutrino state before the beginning of the electron–sterile oscillations.* It always gives positive δN_k, which for a large range of initial sterile population values, are bigger than 1. The kinetic effects are the strongest for $\delta N_s = 0$:

$$Y_p^{max}(\delta N_s, \delta m^2, \sin^2 2\vartheta) = Y_p(0, \delta m^2, \sin^2 2\vartheta).$$

They disappear for $\delta N_s = 1$, when ν_e and ν_s states are in equilibrium, and the total effect reduces to the SBBN with an additional neutrino.

In Fig. 3.15 we present the frozen neutron number density relative to nucleons $X_n^f = N_n^f / N_{nuc}$ as a function of the sterile neutrino content at neutrino decoupling for a resonant and a nonresonant oscillation case. The oscillation parameters are $\delta m^2 = 10^{-7}$ eV^2 and $\delta m^2 = -10^{-7}$ eV^2 and $\sin^2 2\theta = 10^{-1}$. As far as $\delta Y_p / Y_p = \delta X_n^f / X_n^f$, the results are representative for the overproduction of primordially produced helium.

The dotted curve presents only the effect (a), due to the energy density increase $X_n^f = f(\delta N_s)$, the dashed curves present the pure kinetic effects (b) $X_n^f = f(\delta N_{kin})$, while the solid lines give the total effect. The upper dashed and solid curves correspond to the resonant oscillations case, the lower ones to the non-resonant oscillations

[4]For $\nu_e \leftrightarrow \nu_s$ oscillations effective after ν_e decoupling, these kinetic effects δN_k^0 can be considerable, as large as $\delta N_k^0 \sim 6$.

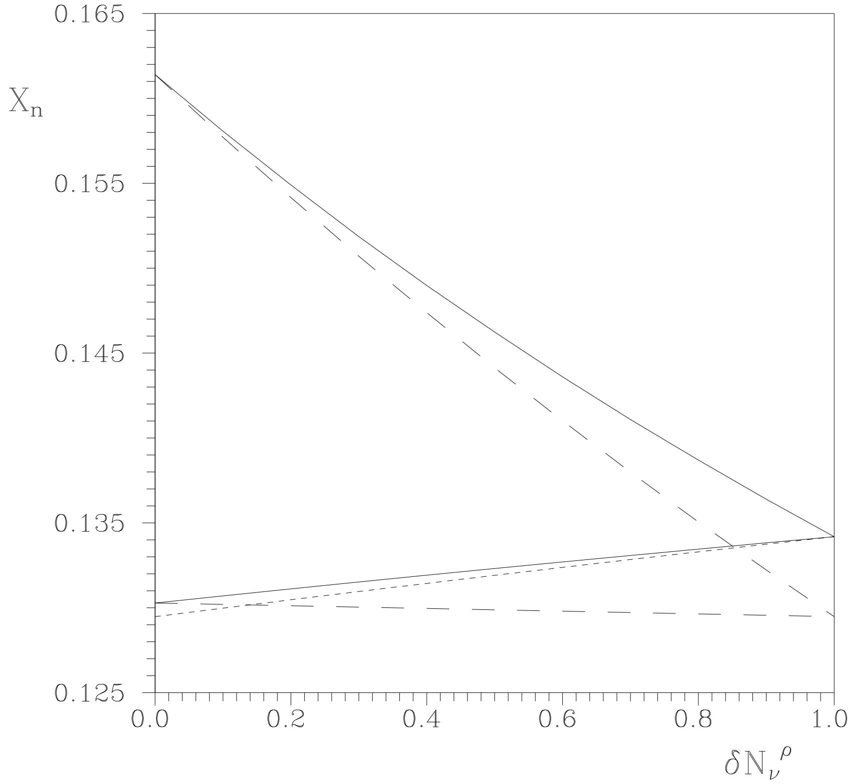

Figure 3.15: The solid curves present frozen neutron number density relative to nucleons $X_n^f = N_n^f/N_{nuc}$ as a function of the sterile neutrino initial population. The dashed curves present only the kinetic effect, while the dotted curve presents the effect due to the energy density increase. The upper two curves (dashed and solid) correspond to the resonant case, the lower dashed and solid curves - to the nonresonant one. Figure from *Kirilova* (2004b).

one.

The analysis for these concrete oscillation parameters, shows that the overproduction of helium is strongly suppressed with the increase of δN_s for the resonant case, while in the non-resonant case it increases with δN_s. This is a result of the fact that, in the resonant case, the kinetic effects (b) of spectrum distortion are the dominant contribution to the overproduction of helium, even for very large degree of population of the sterile state, while in the non-resonant case the main contribution comes from the increase of degrees of freedom already at very small δN_s.

3.8.2 Interplay between dynamical and kinetic effect of oscillating neutrino

SD and its kinetic effect decrease with the increase of initial population of ν_s. The interplay between the kinetic effect of oscillations and the dynamical effect of the additional sterile state on BBN has been thoroughly studied (Kirilova, 2004, 2007). A good approximation to the exact (numerically calculated) interplay between the effects was derived:

$$\delta N_k(\vartheta, \delta m^2) = \delta N_k^{max}(\vartheta, \delta m^2)(1 - \delta N_s), \tag{3.15}$$

where δN_{kin}^{max} is the maximal kinetic oscillations effect for zero initial population of the sterile neutrino $\delta N_s = 0$. Then the change of the helium production is given by:

$$\delta Y_p \sim 0.013[\delta N_k^{max} + \delta N_s(1 - \delta N_k^{max})] \tag{3.16}$$

Hence, *although the kinetic effect always decreases with increasing the population of the inert neutrino, the behavior of the total effect on BBN is more complicated.* In case $\delta N_{kin}^{max} > 1$ the increase of inert population decreases the kinetic effect and the total effect decreases, which leads to a relaxation of BBN constraints on oscillation parameters. While, when the oscillation parameters are such that $\delta N_{kin}^{max} < 1$, the increase of the inert population leads to an increase of the total effect and strengthening the BBN constraints.

An empirical approximation formula to the exact calculated result is:

$$\delta Y_p = 0.013[\delta N_k^{max}(1 - \delta N_s) + \delta N_s],$$

where δN_{kin}^{max} is the value calculated in the case of oscillations with an initially empty sterile state, i.e.

$$\delta N_{tot} = \delta N_k^{max}(1 - \delta N_s) + \delta N_s.$$

It is a good approximation for the non-resonant case and a rather rough one for the resonant case: the deviation from the exactly calculated helium given in Fig. 3.15 may be up to $\delta Y_p/Y_p \sim 0.8\%$. Still, it can give some idea of $\delta Y_p/Y_p$ dependence on δN_s.

For other mixing parameters, the kinetic oscillation effects in the non-resonant case can be also considerable. The kinetic effect can be as high as $\delta N_k \sim 3$ for initially empty sterile state. Hence, in the non-resonant case the spectrum distortion effects may be the dominant one even for much larger δN_s than in the case illustrated in Fig. 3.15.

Interplay between the effects and helium BBN production For each concrete δN_s value a detailed numerical analysis is necessary to reveal the interplay of effects (a) and (b) and their influence on primordial production of ^{4}He.

The next figure shows the influence of different effects on helium-4 production Y_p. The dotted curve present the kinetic effect, the dashed curve – the dynamical effect of initially present ν_s. There is an interplay between the two effects due to the dependence of the kinetic effect on the initial population of ν_s.

There is an interplay between the two types of effects (a) and (b), induced by non-zero δN_s. The total effect depends on the concrete values of the oscillation

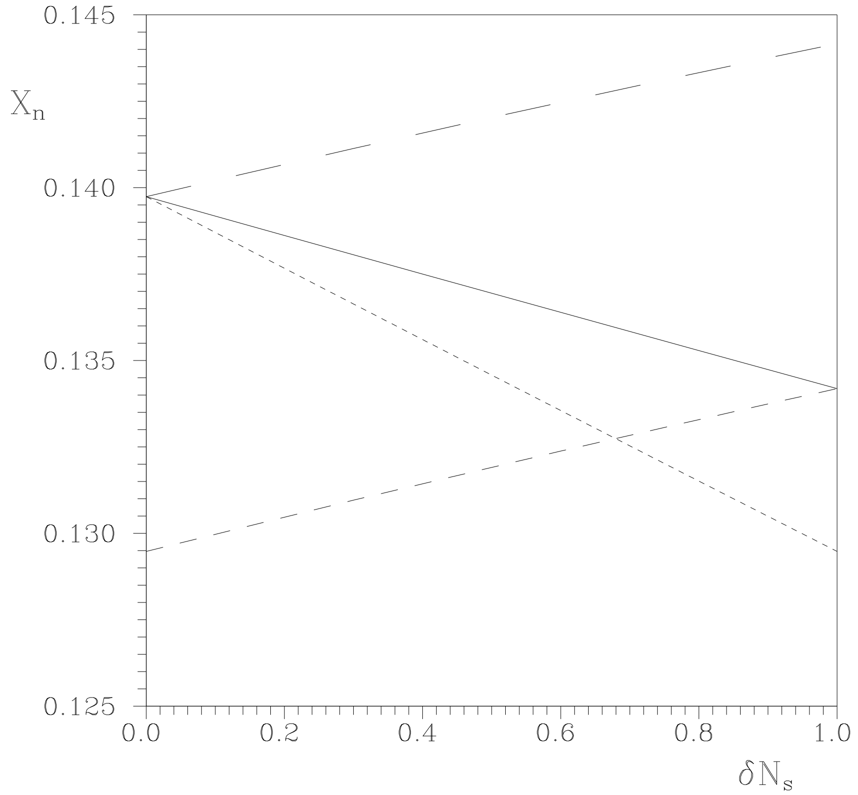

Figure 3.16: The solid curve presents frozen neutron number density relative to nucleons $X_n^f = N_n^f/N_{nuc}$ as a function of the sterile neutrino initial population, at $\delta m = \pm 10^{-8}$ eV^2, $\sin^2 2\theta = 1$. The dotted curve presents the kinetic effect, while the lower dashed curve presents energy density increase effect. The uppermost long dashed curve corresponds to the total effect when the decrease of the kinetic effect is not accounted for, i.e. in case the effects were additive. Figure from ref. *Kirilova* (2004b).

parameters and δN_s. *The shift of the constraints may be expected in either direction (relaxing or constraining the existing constraints)* and its analysis requires numerical study, accounting precisely for ν_e energy spectrum distortion and the suppression of the kinetic effects (*Kirilova*, 2006, 2004b, 2007; *Kirilova and Panayotova*, 2006).

Using the approximate empirical formula giving the dependence of Y_p production on the two effects, obtained in ref. (*Kirilova*, 2004b):

$$\delta Y_p = \delta Y_d + \delta Y_k^0 + \delta Y_k^s \sim 0.013 \times (\delta N_s + \delta N_{kin}^0 - \delta N_s \times \delta N_{kin}^0) \tag{3.17}$$

predictions can be made concerning the value and the sign of the ^{4}He overproduction and the direction of the shift of the BBN constraints. Here $\delta Y_p = Y_p - Y_p^{stand}$, $\delta Y_d = 0.013 \times \delta N_s$, $\delta Y_k^0 = 0.013 \times \delta N_{kin}^0$, while $\delta Y_k^s = -0.013 \times \delta N_s \times \delta N_{kin}^0$.

First: The total effect of oscillations for initially non-zero δN_s **on ^{4}He production is smaller than the sum of the energy density increase effect (i)** *δY_d and the maximum kinetic effect of oscillations (ii) δY_k^0* corresponding to zero δN_s, due to the term $\delta N_s \times \delta N_{kin}^0$, expressing the decrease of oscillations kinetic effect with δN_s.

The results of the exact numerical study of the effects (i) and (ii) on ^{4}He overproduction confirm this estimation. In Fig.3.15, 3.16 and Fig. 3.17 the contribution of the different effects on neutron-to-nucleon freezing ratio $X_n = n_n^f/n_{nuc}$ is illustrated.

The dotted curve shows the dependence of the kinetic effect on δN_s, the lower dashed curve gives the energy increase effect. The total effect is presented by the solid curve, which (although has different behavior in the two cases (correspondingly decreasing in Fig. 3.16 or increasing in Fig. 3.17) is situated always considerably lower than the uppermost long-dashed curve presenting the sum of the effect (a) and the maximal effect (b).

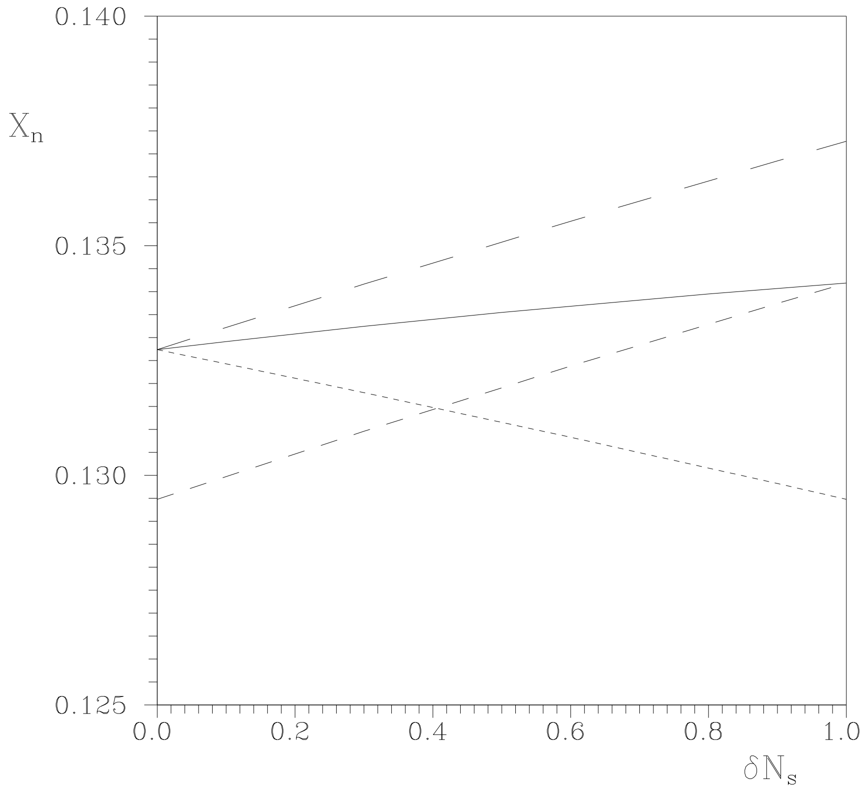

Figure 3.17: The solid curve presents the frozen neutron number density relative to nucleons $X_n^f = n_n^f/n_{nuc}$ as a function of the sterile neutrino initial population, at $\delta m = \pm 10^{-9}$ eV^2, $\sin^2 2\theta = 1$. The dotted curve presents the kinetic effect, while the lower dashed curve presents energy density increase effect. The uppermost long dashed curve corresponds to the total effect if the effects were simply additive. Figure from ref. *Kirilova and Panayotova* (2006).

The uppermost long-dashed curve in the figures presents the overproduction of ^{4}He for such specific situation when the enhancement of the energy density δN_s is due to other additional particles brought partially into equilibrium (like sterile neutrinos in the muon or tau-sectors, or other relic relativistic particles) while the sterile state, which participates further in oscillations with the electron neutrino is initially empty.

However, due to the fact that δN_k is a decreasing function of δN_s, naively adding the two effects $(\delta N_d + \delta N_k^0)$ exaggerates Y_p overproduction, and hence would define stronger bounds than the real ones. *Hence, the cosmological constraints for the os-*

cillations model discussed will be less stringent than in the case of simply additive effects.

Second: The direction of the shift of the constraints should be as follows: in case $\delta N_{kin}^0 \delta N_s < \delta N_s$ the constraints will be strengthened in comparison with the $\delta N_s = 0$ constraints, while in the opposite case they will be relaxed.

In Fig. 3.16 the solid curve, presenting the total effect, is a decreasing function of δN_s because $\delta N_{kin}^0 > 1$, i.e. for that set of oscillation parameters the overproduction of ^{4}He due to oscillations decreases with the increase of the initial population of the sterile neutrino state. Obviously, the suppression effect (ii) dominates. In that case we expect relaxation of the cosmological constraints compared to the case of initially zero population of ν_s.

Fig.2b presents the results for a set of oscillation parameters for which $\delta N_{kin}^0 < 1$. Then, as it is illustrated, the total effect is an increasing function of δN_s, the dynamical effect (i) dominates over (ii), thus the overproduction of ^{4}He increases in respect to the case of $\delta N_s = 0$ and hence, the cosmological constraints must become more stringent with the increase of δN_s. And as far as $\delta N_{kin}^0 = \delta N_{tot}$ at $\delta N_s = 0$, the BBN constraints, corresponding to ^{4}He observational uncertainty expressed as $\delta N_{tot} < 1$, will be strengthened. For example, ^{4}He uncertainty $\delta Y_p \sim 0.007$ corresponds to $\delta N_{tot} \sim 0.54$. Thus at $\delta N_s = 0$ $\delta N_{kin}^0 \sim 0.54 < 1$, and hence strengthening of the cosmological constraints is expected.

The cosmological constraints obtained by a detail numerical study of the effects (i) and (ii) and corresponding to such ^{4}He overproduction and different δN_s values are presented in the next section.

In case of big ^{4}He uncertainty, corresponding to $\delta N_{tot} > 1$, the term (ii) dominates (as illustrated in Fig. 3.16), leading to a decrease of the ^{4}He overproduction due to oscillations and hence, relaxation of the cosmological constraints should be expected. It is interesting to note that contrary to some prejudice, *even for ^{4}He uncertainty* *greater than* 5%, *equivalent to* $\delta N_{tot} > 1$, *cosmological constraints on oscillation parameters still persist, provided that* $\delta N_s < 1$ and that a proper description of the neutrino energy spectrum distortion is made.

3.8.3 Generalized cosmological constraints on neutrino oscillations: relaxed or strengthened

In this subsection, following mainly the results of *Kirilova and Panayotova* (2006); *Kirilova* (2007, 2004b) I show how and to what extend the available cosmological constraints on $\nu_e \leftrightarrow \nu_s$ oscillation parameters, obtained with the assumption $\delta N_s = 0$, are changed in the more general case $\delta N_s \neq 0$.

Here I present the results of the numerical analysis of ^{4}He production in BBN with nonequilibrium $\nu_e \leftrightarrow \nu_s$ oscillations and initially nonzero ν_s population $0 < \delta N_s < 1$ and discuss the generalized cosmological constraints on oscillation parameters. Primordial ^{4}He yield $Y_p(\delta N_s, \delta m^2, sin^2 2\vartheta)$ was calculated at different δN_s values for the set of oscillations parameters of the model: for all mixing angles ϑ and mass differences $\delta m^2 \leq 10^{-7}$ eV^2.

Cosmological constraints on oscillation parameters corresponding to $\delta Y_p/Y_p = 3\%$ overproduction and different initial δN_s were calculated in ref. *Kirilova* (2007). They strengthen with the increase of δN_s. Contrary to the case of 3% overproduction, for which the constraints relax with the increase of δN_s.

A. $\delta N_{tot} < 1$:

For the analysis of the constraints the observational uncertainty of the primordially produced ^{4}He was assumed $\delta Y_p < 0.007$ in correspondence to the accepted then systematic error in the ^{4}He measurements (*Izotov and Thuan* , 2004). Uncertainty $\delta Y_p = 0.007$ corresponds to $\delta Y_p/Y_p \sim 3\%$. Before 2005 3% overproduction was considered a reliable bound for the uncertainty of helium from the observational viewpoint.

Then the maximum possible value of δN_s at BBN epoch was constrained on the basis of BBN considerations: Using the approximate empirical formula

$$\delta Y_p \sim 0.013 \delta N_{tot},$$

$\delta Y_p < 0.007$ corresponds to $\delta N_s < 0.54$. So, in our analysis we have varied δN_s in the range $0.0 \leq \delta N_s \leq 0.5$ with a step 0.1. The case $\delta N_s > 0.54$ corresponds to higher ^{4}He uncertainty and was discussed in more detail in ref. (*Kirilova and Panayotova*, 2006).

This choice of maximum δN_s was also supported by the results of the standard BBN analysis + ^{4}He observational data with an input the baryon density value from WMAP data, which provided bounds on the number of additional neutrino species at BBN in the range $\delta N_{eff} < 0.1 - 0.5$.

In Fig. 3.18 I present the calculated cosmological constraints on oscillation parameters for the $\delta N_s = 0.1$, and $\delta N_s = 0.5$ for the resonant (to the left) and the non-resonant (to the right) oscillation cases. The region upwards of the corresponding curves is cosmologically excluded. The upper dashed curve is for $\delta N_s = 0.1$ case, the lower dashed one – for $\delta N_s = 0.5$. $\delta N_s = 0$ constraints are given for comparison by the solid contours.

The analysis shows that the two effects (i) and (ii) of δN_s, nearly compensate each other for small δN_s values. Hence, the cosmological constraints for $\delta N_s = 0.1$ slightly differ from the ones for $\delta N_s = 0$, as illustrated in Fig.3.18. For $\delta N_s > 0.1$ δY_d noticeably dominates over the suppression term δY_k^s, so the constraints are strengthened. As a whole the cosmological constraints in the resonant case are slightly changed for small mixings compared to the case with initially zero sterile state, while at large mixings in the resonant case and in the non-resonant case the change is more noticeable, and the constraints are becoming more stringent with the increase of δN_s.

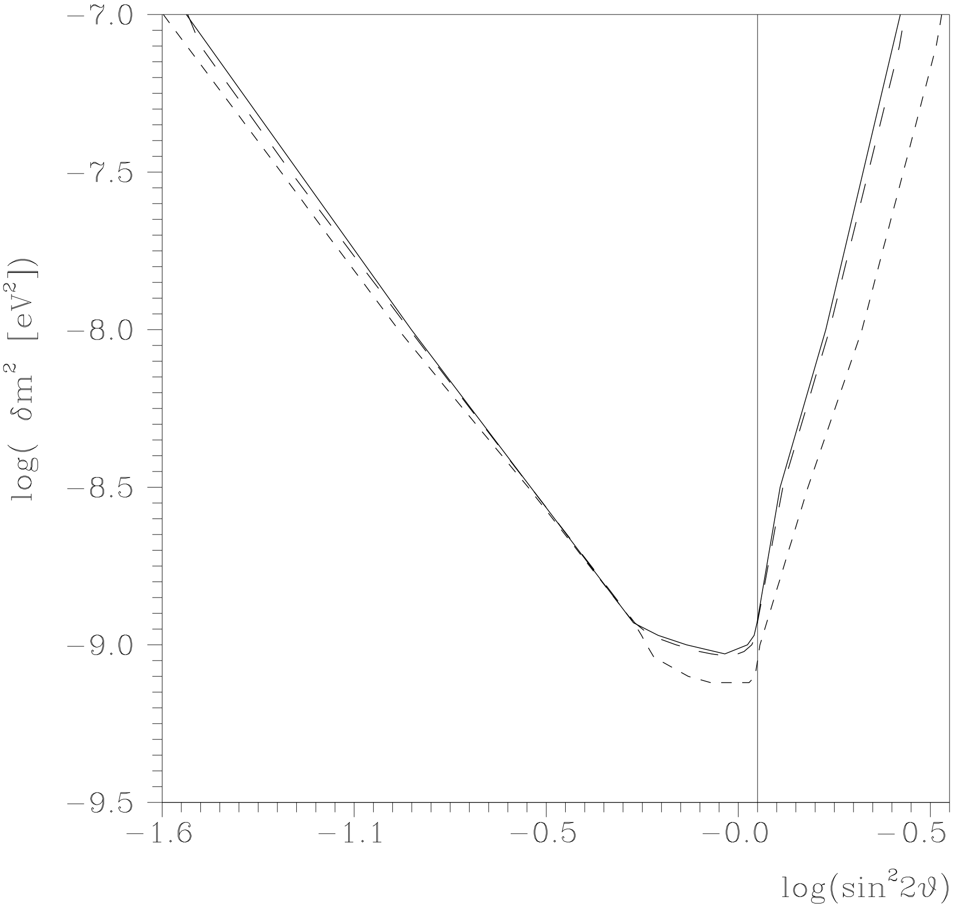

Figure 3.18: The dashed curves present 3% ^{4}He BBN constraints on oscillation parameters for the resonant (l.h.s.) and the non-resonant $\nu_e \leftrightarrow \nu_s$ oscillations (r.h.s.) and for initial degrees of population of the sterile neutrino state $\delta N_s = 0.1$ and $\delta N_s = 0.5$ (the lowest curve). The solid contours present the constraints for $\delta N_s = 0$ case for comparison. Figure from ref. *Kirilova and Panayotova* (2006).

The behavior of the constraints in the resonant case can be understood, having in mind the effect of the oscillations generated neutrino-antineutrino asymmetry, which acts towards relaxing the constraints at small mixings. Similar behavior as the one of the 3% ^{4}He constraints with δN_s will have all the cosmological constraints concerning helium uncertainty corresponding to $\delta N_{tot} < 1$, i.e. $\delta Y_p/Y_p < 5\%$. Namely, they will strengthen when increasing δN_s value.

It is interesting also to discuss *the dependence of the shift* on the value of the helium uncertainty for a fixed value of δN_s. The shift is given by: $\delta N_s - \delta N_s \times \delta N_k^0$ and for $\delta N_{tot} < 1$ case the first term is the dominant one. The shift will increase with the decrease of the uncertainty (decrease of δN_k^0). So, for example for 1% helium constraints the downward shift with δN_s will be greater than the one for 3% constraints, while for 4% constraints it will be smaller. Finally, for $\delta Y_p/Y_p = 5\%$ no shift with δN_s is to be expected, because then the two terms in the shift equation cancel.

B. $\delta N_{tot} > 1$:

In the case of helium uncertainty corresponding to $\delta N_{tot} > 1$, i.e. $\delta Y_p/Y_p > 5\%$, the second term in the shift equation dominates and hence δN_s leads to a relaxation of the constraints proportional to it. I.e. *all isohelium contours situated above the* 5% *one, will be shifted upwards with* δN_s. For a fixed δN_s the absolute shift (depending on δN_k^0) increases with the increase of the uncertainty of helium-4.

So, when increasing the uncertainty of helium for a fixed δN_s value, the absolute value of the downward shift decreases smoothly till zero and then turns into an upward shift and continues to increase. In other words, for a fixed initial population of the sterile neutrino the constraints will strengthen with the increase of helium precision, however, they will be stronger than the corresponding ones for zero initially sterile neutrino state if the helium uncertainty is less than 5%, while they will be relaxed in comparison with the ones for zero initially sterile neutrino state if helium uncertainty is bigger than 5%.

The recent reanalysis of helium observational data of the IT sample, accounting for the stellar absorption in the determinations of Y_p, suggested a higher conservative bound of He and higher systematic errors.

BBN constraints corresponding to $\delta Y_p/Y_p \sim 5\%$ and different ν_s populations were calculated in ref. (*Kirilova and Panayotova*, 2006). These BBN constraints relax with the increase of δN_s.

The constraints for $\delta N_s = 0.5$ and $\delta N_s = 0$ and different He overproduction are illustrated in Fig. 3.19. The two uppermost contours present the constraints for $\delta Y_p/Y_p = 5\%$ overproduction, the two lower curves – for $\delta Y_p/Y_p = 3\%$.

In conclusion *BBN constraints may be either strengthened or relaxed with the increase of the initial population of the sterile state, depending on the level of the He overproduction.* The results are important for studying neutrino properties, for defining the role of the sterile neutrino in resolvingneutrino anomalies, for constraining models with sterile neutrinos during BBN epoch.

We have found that the effect of the neutrino spectrum distortion due to oscillations may be very strong, even for a considerable initial population of the sterile neutrino state. Correspondingly, the kinetic effect of oscillations remain the dominant one even for big δN_s.

The results of this analysis may be applied for different models generating sterile neutrino, like GUT models, mirror models, extra-dimensions models, etc., as far as the initial value of population of the sterile state δN_s depends on the concrete model of its production. These results may be of interest also for mixing schemes in which a portion of ν_s have been brought into equilibrium before neutrino decoupling, due to $\nu_\mu \leftrightarrow \nu_s$ or $\nu_\tau \leftrightarrow \nu_s$ oscillations.

In case the ν_s presence is due to the much earlier (at atmospheric mass difference scale, or LSND) oscillations of $\nu_{\mu,\tau} \leftrightarrow \nu_s$, δN_s may be directly connected with the

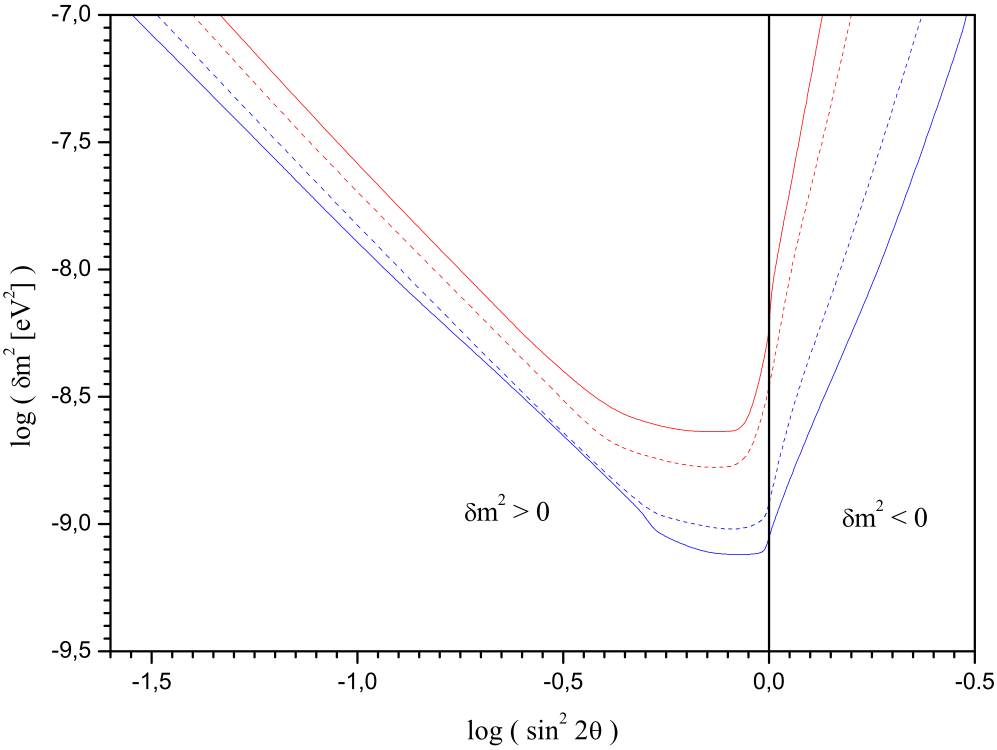

Figure 3.19: The lower dashed curve presents BBN constraints corresponding to 3% He overproduction and $\delta N_s = 0$, while the lowest curve presents the strengthened constraints due to higher δN_s, namely $\delta N_s = 0.5$. The upper curve gives the relaxed 5% He overproduction contour corresponding to $\delta N_s = 0.5$, while the upper dashed curve corresponds to 5% He and $\delta N_s = 0$. Figure from ref. *Kirilova* (2006).

available constraints on the sterile neutrino fraction, deduced from the neutrino oscillations experimental data analysis. So, we hope that the results may be indicative and helpful for choosing among the different possibilities for the sterile fraction in the subdominant active-sterile oscillations used in the oscillation analysis of neutrino anomalies.

3.9 Summary

The primordial production of ^{4}He in the presence of $\nu_e \leftrightarrow \nu_s$ oscillations, effective after electron neutrino decoupling was analyzed. It was shown that the considerable spectrum distortion of the electron neutrino caused by oscillations, which effects the kinetics of the neutron-proton transitions during nucleons freezing, plays the dominant role in the overproduction of ^{4}He due to neutrino oscillations. A precise quantitative study of the maximum overproduction of ^{4}He, accounting for all oscillations effects was provided. Enormous maximum overproduction of ^{4}He (up to 32% in the resonant case and 14% in the non-resonant case) was found possible in case the sterile neutrino state was empty at the start of oscillations.

BBN with nonequilibrium $\nu_e \leftrightarrow \nu_s$ oscillations, in the more general case of non-zero population of ν_s before oscillations $\delta N_s \neq 0$, was discussed. ^{4}He primordial production $Y_p(\delta N_s)$ in the presence of $\nu_e \leftrightarrow \nu_s$ oscillations for different initial populations of the sterile neutrino state $0 \leq \delta N_s \leq 1$ and the full range of oscillation parameters was calculated.

The role of a *non-empty* sterile state before $\nu_e \leftrightarrow \nu_s$ oscillations on primordial production of ^{4}He and on the BBN oscillations constraints was studied.

Two-fold effect of non-zero δN_s on ^{4}He were unrevealed:

(i) it enhances the energy density and hence increases the cosmic expansion rate, leading to Y_p *overproduction.*

(ii) it suppresses the kinetic effects of oscillations on BBN, namely the effects on pre-BBN nucleon kinetics, caused by the ν_e energy spectrum distortion and the $\nu_e - \bar{\nu}_e$ asymmetry generation by oscillations, leading to *decreased* Y_p *production.*

Depending on oscillation parameters one or the other effect may dominate, causing, correspondingly, either a relaxation of the cosmological constraints or their strengthening with the increase of δN_s .

More general BBN constraints on $\nu_e \leftrightarrow \nu_s$ oscillation parameters, corresponding to 3% and 5% Y_p overproduction, for different initial populations of the sterile state were calculated. The 2-neutrino toy model was used to demonstrate the expected shift of the BBN bounds due to non-zero δN_s with respect to the bounds in the $\delta N_s = 0$ case.

The constraints were obtained for the natural assumption, that at BBN epoch the initial lepton asymmetry is of the order of the baryon one. Provided a small lepton asymmetry $L << 0.1$ is present, it may be large enough to relax or alleviate the discussed BBN bounds on neutrino oscillations. [5] For more detail see next chapter.

Cosmological constraints can be relaxed also if the systematic error of Y_p is higher than 0.007. However, it is worth noting that even for helium uncertainty as big as $\delta Y_p \sim 0.01$, and a considerable initial population of ν_s ($\delta N_s < 1$, however) the constraints are not removed. They are relaxed, but still persist (*Kirilova and Panayotova*, 2006).

These cosmological constraints were obtained for the case of 2-neutrino mixing. The account for mixing between active neutrinos in the resonant case has been proved important for the case of oscillations proceeding before neutrino decoupling *Dolgov and Villante* (2004).

Further generalization of the cosmological constraints on non-equilibrium neutrino electron-sterile mixing both for the $\delta N_s = 0$ and for the $\delta N_s \neq 0$ case should

[5]For $\delta N_s = 0$ case it was proven that larger than 10^{-7} lepton asymmetry may strongly suppress oscillations effective after neutrino decoupling and change the constraints, while initial lepton asymmetry larger than $10^{-5} - 10^{-4}$ can alleviate them (*Kirilova and Chizhov*, 1998b, 2001a; *Kirilova*, 2011c, 2012).

include flavor neutrino mixing as well. Qualitatively, for 4-neutrino mixing, the non-equilibrium initial population of the sterile state will cause spectrum distortion not only to electron neutrino but also to the other neutrinos. Then the spectrum distortion and depletion of the electron neutrino will be reduced compared to the 2-neutrino case. Correspondingly, for the case $\delta N_s = 0$ the cosmological constraints on oscillation parameters in 4-neutrino mixing case will be less stringent than the ones presented here. However, the shift of the constraints due to non-zero δN_s will remain proportional to δN_s value and in the same directions as presented here.

The results of this analysis can be useful for constraining nonstandard physics, predicting active-sterile neutrino oscillations, like extra-dimensions, producing oscillations, supernova bursts employing oscillations, etc.. It can be of interest also for models of galactic chemical evolution.

CHAPTER IV

Lepton Asymmetry Generation and Its Cosmological Effects and Constraints. The Interplay Between Lepton Asymmetry and Neutrino Oscillations

4.1 Introduction

Lepton asymmetry of the Universe is usually defined as

$$L = (N_l - N_{\bar{l}})/N_\gamma, \tag{4.1}$$

where N_l is the number density of leptons, and $N_{\bar{l}}$ of antileptons, while N_γ is the number density of photons.

In equilibrium L may be expressed as usual through the chemical potential μ or degeneracy parameter $\xi = \mu/T$:

$$L = 1/12\zeta(3) \sum_i T^3_{\nu_i}/T^3_\gamma (\xi^3_{\nu_i} + \pi^2 \xi_{\nu_i}) \tag{4.2}$$

Direct measurements of the lepton asymmetry magnitude and sign have not been done yet, because Cosmic Neutrino Background has not been detected. There are available just indirect indications and constraints on L through its effect on other processes, which have left observable traces in the Universe, like the abundances of light elements produced in BBN, Cosmic Microwave Background, LSS, etc.

It is traditionally assumed that the lepton asymmetry is of the order of the baryon one, which is measured precisely by different independent means (BBN, CMB, to be discussed in the next chapter) to be

$$\beta = (N_b - N_{\bar{b}})/N_\gamma \sim 6.10^{-10}.$$

However, in general, large lepton numbers L bigger than the baryon number β ($L > \beta$) and even much bigger $L \gg \beta$ are not excluded by any profound theoretical principle.

Universal charge neutrality implies that the lepton asymmetry in the electron sector is $L_e \sim \beta$. Hence, big L may reside in the neutrino sector and L may be many orders of magnitude larger than β. Therefore, L is defined mainly by the sum of the asymmetries in the different neutrino sectors:

$$L \sim \sum L_{\nu_i}.$$

Whatever its value L contribute to the leptonic content of the Universe.

The origin of eventual big lepton numbers is not fully understood. See the review papers (*Dolgov*, 2002; *Sarkar*, 1996). There exist numerous different mechanisms for their generation:

- Large lepton numbers can be consistent with the observed small baryon number for example in the context of Grand Unification Theories;

- There exist different models producing $L \gg \beta$: in the scenario of baryogenesis with baryonic charge condensate (*Dolgov and Kirilova*, 1991), where large and inhomogeneous lepton asymmetry can be produced;

- The out-of equilibrium decays of heavy Majorana neutrinos (*Fukugita and Yanagida*, 1986; *Murayama et al.*, 1993) can produce it as well;

- Resonant neutrino oscillations in CP-asymmetric plasma of the early Universe can create considerable neutrino asymmetry at low temperature (as it was already mentioned in the previous chapters) (*Foot et al.*, 1996; *Kirilova and Chizhov*, 1997, 1996a).

Studying L of the Universe is intriguing and important because of many reasons. Just a short list of some of them reads:

- A significant cosmological effect of L might be expected, having in mind that neutrinos are abundant and large L may be contained in the neutrino sector. Large lepton asymmetry has interesting cosmological implications: in baryogenesis models, for solving the monopole problem, as well as domain wall problem, in primordial nucleosynthesis, for structure formation in the Universe. Besides, as mentioned already in the previous chapters, relic asymmetry can suppress or enhance neutrino transitions in the early Universe.

- Precise determination of neutrino properties is of cosmological importance. As far as the uncertainty of neutrino characteristics leads to large systematic errors in the estimation of cosmological parameters obtained from CMB data. Therefore, knowledge about L and its nature would help to determine them more precisely.

- Knowledge about L magnitude and sign is relevant for baryogenesis through leptogenesis issues, for inhomogeneous BBN models, cosmological models with leptonic domains, etc.

- Studying L and its cosmological influence provides, on the other hand, an opportunity to use cosmology as a probe of neutrino properties.

- Particularly concerning neutrino oscillations: Due to the fact that L is capable of suppressing and inhibiting or enhancing neutrino oscillations, determining L will enlighten our knowledge about the cosmological role of neutrino oscillations.

- L provides a possible solution of the recently found preference or/and indication for additional relativistic density (the so called dark radiation problem).

In the next section we review the basic cosmological effects of L on processes in the Universe and present the indirect kinetic effect of lepton asymmetry, found in our studies. The interplay between small lepton asymmetry and electron-sterile neutrino oscillations $\nu_e \leftrightarrow \nu_s$, effective after neutrino decoupling, is discussed in section 3. A mechanism for generation of neutrino-antineutrino asymmetry is found. In the 4th section cosmological constraints on L on the basis of its dynamical and direct kinetic effect on standard BBN model are shortly discussed. Our results on indirect cosmological effect of small L (relic and oscillations generated) through neutrino oscillations on primordial production of ^4He in BBN with late $\nu_e \leftrightarrow \nu_s$ oscillations is discussed. We present our results concerning the influence of L on the BBN constraints on oscillations. Section 5is dedicated to the BBN constraints on L. Section 6 discusses the problem of radiation density excess and the possibility to solve it using the asymmetry oscillations interplay, which we have proposed. The last section provides the summary.

4.2 Lepton Asymmetry Cosmological Effects

A. Dynamical effect

A well-known cosmological effect of L is the increase of the radiation energy density $\delta\rho_r$, which is usually expressed in terms of the increase of the effective number of the relativistic degrees of freedom δN_{eff}:

$$\delta\rho_r = [1 + 7/8(4/11)^{4/3}\delta N_{eff}]\rho_\gamma, \tag{4.3}$$

$$\delta N_{eff} = 15/7[(\xi/\pi)^4 + 2(\xi/\pi)^2]. \tag{4.4}$$

The increase of the radiation density due to L speeds up the Universe expansion $H = (8/3\pi G\rho)^{1/2}$, delays matter/radiation equality epoch, changes the decoupling temperature of neutrino, which on their turn influence BBN, CMB and the evolution of the density perturbations, and correspondingly the formation of structures in the Universe.

Particularly well studied (using the BBN codes) is L dynamical effect on BBN.

Qualitatively it can be understood from the following considerations: The increase of the expansion rate of the Universe due to L allows less time for the nuclear reactions to proceed. The increase of the cooling rate of the Universe due to L, leads to earlier freezing of the reactions governing neutron-to-proton ratio n/p , i.e. leads to higher freezing ratio $(n/p)_f$, which reflects in higher D and ^4He abundances.

B. Direct kinetic effect.

Lepton asymmetry with a magnitude $|L| > 0.01$ in the ν_e sector exerts a direct kinetic effect on nucleons kinetics and on BBN, because the ν_e participates in the reactions interconverting neutrons and protons (eqs. 3.1, 3.2), changes the number density of ν_e and $\bar{\nu_e}$, alters the reaction rates of neutrino interactions, as far as these rates are extremely sensitive to the neutrino spectrum.

In case of electron neutrino degeneracy the effect on BBN and the outcome of the light elements is L sign dependent. As is obvious, $L > 0$ in the pre-BBN epoch would result into preponderance of protons and reduction of $(n/p)_f$ and thus lead to underproduction of primordial helium-4 abundance, while $L < 0$ would lead to increase of neutrons and overproduction of ^{4}He.

Degenerate BBN has been thoroughly studied since the pioneer papers of refs. *Wagoner et al.* (1967); *Reeves* (1972).

An empirical formula, which provides a fairly good fit (see *Simha and Steigman* (2008)), presents the dependence of the produced primordially ^{4}He, Y_p, on the discussed dynamical and kinetic effect of L:

$$Y_p \sim (0.2482 \pm 0.0006) + 0.0016\eta_{10} + 0.013\Delta N_{eff} - 0.3\xi_{\nu_e} \tag{4.5}$$

As is obvious from eqs. 4.4 and 4.5, Y_p is more sensitive to the kinetic than to the dynamical effect of L (at natural values $\xi_{\nu_e} < 1$).

C. Indirect kinetic effect of lepton asymmetry through neutrino oscillations

Small L, $|L| << 0.01$, that has negligible (A) and (B) effects, in case of late $\nu_e \leftrightarrow \nu_s$ oscillations may considerably influence oscillating ν_e, namely change its evolution, number density, energy distribution, oscillation pattern and, thus through ν_e, influence BBN kinetics (*Kirilova and Chizhov*, 1997, 1998b).

The **effect of small relic** $L << 0.01$ and nonresonant $\nu_e \leftrightarrow \nu_s$ oscillations effective after neutrino decoupling on BBN has been first studied by *Kirilova and Chizhov* (1998b). It was found that $L < 10^{-7}$ is destroyed by these oscillations, while $L \geq 10^{-7}$ *may enhance or suppress them* and through them influence primordially produced elements, see also (*Kirilova and Chizhov*, 2001b).

The **effect of small L generated by oscillations** on ^4He abundance and on cosmological constraints on oscillations was first analyzed in ref. (*Kirilova and Chizhov*, 1997, 2000a, 2001b) and studied for a wider range of model's parameters in (*Kirilova*, 2012).

Late active-sterile oscillations may *induce neutrino-antineutrino asymmetry growth* during the resonant transfer of neutrinos. Indirect kinetic effect of asymmetry generated at relatively big mixing and small mass differences $\delta m^2 < 10^{-7}$ eV^2 was first found by *Kirilova and Chizhov* (1996a, 1997), this dynamically produced asymmetry is not high enough to have dynamical or direct L kinetic effect on the synthesis of light elements, it effects indirectly BBN through its back effect on oscillating neutrinos. It was numerically found (*Kirilova and Chizhov*, 1997, 2000a; *Kirilova*, 2012) that in the case of resonant $\nu_e \leftrightarrow \nu_s$ oscillation effective after neutrino decoupling neutrino-antineutrino asymmetry is amplified by not more than 5 orders of magnitude from an initial value of the order of the baryon one.

Oscillations generated asymmetry *suppresses oscillations at small mixing angles*, leading to noticeable decrease of ^4He production at these mixing angles.

In conclusion, very small asymmetries $10^{-7} < |L| \ll 0.01$, either relic or produced in active-sterile oscillations, may considerably influence oscillating electron neutrino and through it Y_p and BBN.

4.3 Lepton Asymmetry - Neutrino Oscillations Interplay in BBN epoch.

The effect of large L either previously existing or produced by oscillations, which effect directly the kinetic of BBN has been studied in numerous papers. The effect of small relic asymmetry was not so thoroughly studied.

Here we present the results on the interplay between small asymmetries $L << 0.01$ and late $\nu_e \leftrightarrow \nu_s$ oscillations in the early Universe and their effect on BBN, discussed in the original works *Kirilova and Chizhov* (1997, 1998b, 2000a), *Kirilova* (2011c, 2012).

In case of late oscillating active-sterile neutrinos with relic or generated in oscillations L the energy distribution of neutrinos may be strongly distorted from the equilibrium Fermi-Dirac form (*Kirilova and Chizhov*, 2000a). Hence, a precise account for the energy spectrum distortion of the degenerate oscillating neutrinos is necessary for the proper description of the effect of small lepton asymmetry. Particularly, the capability of small relic L to enhance oscillations has essentially spectral character (*Kirilova and Chizhov*, 1998b) and requires a precise kinetic approach, provided in our numerical analysis.

We have studied two different cases of L, namely initially present at the neutrino decoupling epoch, called further on *relic* L, and dynamically generated L by active-sterile neutrino oscillations.

Qualitatively, the effect of L on oscillating neutrino may be understood as follows: As discussed in chapter 2, the average potentials V_f for ν depend on the particle asymmetries of different constituents of the medium and they differ for different neutrino types due to different interactions with the particles of the plasma.

L, as a characteristic of the medium, may suppress oscillations by decreasing their amplitude, or enhance oscillation transfer in case resonant condition (eq. 2.14) between the parameters of the medium and the oscillation parameters holds.

Thus neutrino propagation and resonance in the neutrino sector differs from that of antineutrino for non-zero L. Due to L influence of the ν propagation L may change n_ν, its spectrum distribution and oscillation pattern.

4.3.1 The kinetics of nucleons and the oscillating neutrino in presence of lepton asymmetry

We have used a self consistent numerical analysis describing simultaneously the kinetics of the oscillating neutrinos, the nucleons freeze-out and the asymmetry evolution. The following system of kinetic equations for neutrino density matrix and neutron number densities in momentum space are used to describe the evolution of the system of oscillating neutrinos in the high temperature Universe and lepton asymmetry role in BBN:

$$\begin{aligned}
\partial\rho(t)/\partial t &= Hp_\nu \ (\partial\rho(t)/\partial p_\nu) + \qquad (4.6)\\
&+i\left[\mathcal{H}_o,\rho(t)\right] + i\sqrt{2}G_F\left(\mathcal{L} - Q/M_W^2\right)N_\gamma\left[\alpha,\rho(t)\right] + \mathrm{O}\left(G_F^2\right),\\
\partial\bar\rho(t)/\partial t &= Hp_\nu \ (\partial\bar\rho(t)/\partial p_\nu) + \qquad (4.7)\\
&+i\left[\mathcal{H}_o,\bar\rho(t)\right] + i\sqrt{2}G_F\left(-\mathcal{L} - Q/M_W^2\right)N_\gamma\left[\alpha,\bar\rho(t)\right] + \mathrm{O}\left(G_F^2\right),
\end{aligned}$$

$$L_{\nu_e} = \int \mathrm{d}^3p(\rho_{LL} - \bar\rho_{LL})/N_\gamma \qquad (4.8)$$

$$\begin{aligned}
\partial n_n/\partial t &= Hp_n \ (\partial n_n/\partial p_n) + \qquad (4.9)\\
&+\int \mathrm{d}\Omega(e^-,p,\nu)|\mathcal{A}(e^-p\to\nu n)|^2\left[n_{e^-}n_p(1-\rho_{LL}) - n_n\rho_{LL}(1-n_{e^-})\right]\\
&-\int \mathrm{d}\Omega(e^+,p,\tilde\nu)|\mathcal{A}(e^+n\to p\tilde\nu)|^2\left[n_{e^+}n_n(1-\bar\rho_{LL}) - n_p\bar\rho_{LL}(1-n_{e^+})\right],
\end{aligned}$$

where $\mathcal{L} \sim 2L_{\nu_e} + L_{\nu_\mu} + L_{\nu_\tau}$, $L_{\mu,\tau} \sim (N_{\mu,\tau} - N_{\bar\mu,\bar\tau})/N_\gamma$.

The first two equations describe the evolution of neutrino and antineutrino ensembles. They provide a *simultaneous account* of the different competing processes: expansion (first term), neutrino oscillations (second term), neutrino forward scattering and weak interaction processes. The sterile state was assumed empty at the time of decoupling of the electron neutrino.

Due to the non-zero L term the equations are coupled integro-differential and the numerical task is much complicated than in the case of $L \sim \beta$. Besides, L term leads to different evolution of neutrino and antineutrino due to the different sign with which it enters their equations. (The case of $L \sim \beta$ corresponds to negligible $\mathcal{L}$ term in the potential when the evolution of the neutrino and antineutrino density matrices is identical in the nonresonant oscillations case.)

4.3.2 Nonresonant oscillations case. Results of the numerical analysis

Our numerical analysis for the nonresonant oscillations case with L showed that the coupling between the neutrino and antineutrino ensembles leads to their similar behavior: Whenever the resonance condition is fulfilled for neutrino (or antineutrino), and the ensemble suffers a resonant oscillations, due to the strong coupling between the systems, the antineutrino ensemble too shows the same behavior (after some negligible delay time). The concrete 'spectral' mechanism of that strong coupling between the ensembles in our case is described in detail in section 4.4. This is qualitatively new result, opposite to the traditional naive conclusions (*Enqvist et al.*, 1990b), that the resonance may take place either in the neutrino sector or in the antineutrino one, but not both, based on observations just for a certain parameter values and provided for the mean neutrino momentum, that in the low temperature resonance case (when the nonlocal term is neglected in comparison with the local one).

We studied numerically the evolution of neutrino ensembles, evolution of L and the evolution of nucleons, to reveal L role during pre-BBN epoch for a broad range of oscillation parameters and for the case of relic L in the range $10^{-10} < |L| < 0.01$.The results have almost negligible dependence on the sign of the initial asymmetry, as could be expected from this behavior of the ensembles.

Depending on the oscillation parameters and L values, the following interplay between L and oscillations was observed: relatively large L suppress oscillations, smaller L lead to their resonant enhancement.

4.3.3 Asymmetry generated in resonant oscillations

For the analysis of oscillations generated L we have assumed its initial value $L \sim \beta$.

The numerical analysis was provided for the temperature range [0.3 MeV, 2 MeV] and the full set of oscillation parameters of the electron-sterile oscillations model, and with higher accuracy than in previous studies.

In order to keep the appropriate precision of calculation for the wide range of initial parameter values, we have used a step for the evolution of temperature of the order $10^{-8} - 10^{-6}$ MeV and for the calculation of the neutrino spectrum a step for E_ν/T of the order $10^{-3} - 10^{-4}$.

Active-sterile oscillations proceeding after neutrino decoupling produce ν_s at the expense of active neutrino and thus δN_{eff} does not change. However in that case late oscillations strongly distort neutrino energy spectrum for a wide range of values of oscillations parameters and L. Therefore, a precise description of neutrino momenta distribution is necessary. In our analyses we have used between 1000 and 5000 bins to describe neutrino spectrum distribution in the non-resonant neutrino oscillations case, and up to 10 000 in the resonant case.

Instability region

Resonant oscillations were found capable to amplify L. In the analyzed oscillations case the evolution of L is dominated by neutrino oscillations and typically L has rapid oscillatory behavior: it oscillates and changes sign. We have determined numerically the region of parameter space for which noticeable generation of L is possible. A good approximation to the exact results is:

$$|\delta m^2| \sin^4 2\theta \leq 10^{-9.5} \text{ eV}^2. \tag{4.10}$$

The maximal possible growth of L is 4-5 orders of magnitude. The instability region and the magnitude of L are close to the bounds existing in literature for other oscillation models, see for example *Dolgov et al.* (2000).

L changes energy spectrum distribution and the number densities of electron neutrinos from standard BBN case. This influences the kinetics of nucleons during BBN and changes the production of light elements.

The precise description of the distribution of the neutrino momenta was found extremely important for the correct determination of L evolution in the resonant oscillations case. For some choices of oscillation parameters increasing the resolution of momentum space leads to changes of the oscillatory character of L and diminishes L amplitude. [1] This observation is in accordance with the studies of other authors in other parameter regions corresponding to smaller θ and bigger δm^2 (see *Di Bari and Foot* (2000)).

In the following sections we present the results of a detail numerical study of the effect of this lepton asymmetry-neutrino oscillations interplay on BBN produced ^{4}He. We present the numerical results on the influence of small L on oscillating neutrino and on BBN and show that BBN produced ^{4}He feels extremely small L and represents now the finest known "leptometer".

4.4 BBN with Lepton Asymmetry and Neutrino Oscillations

In the next subsection we present first the available in literature cosmological constraints on L coming from BBN with flavor neutrino oscillations. Then, in the following subsection we discuss our results concerning L and BBN with electron-sterile neutrino oscillations.

4.4.1 Cosmological constraints on lepton asymmetry from standard BBN

At present SBBN provides the most stringent constraints on L on the basis of L dynamical and direct kinetic effect. There exist numerous papers on the subject. I list here only the results of more recent work. For more information and reference of

[1] As a rule in these cases the evolution of the neutrino ensembles is strongly distorted from the expected behavior.

earlier papers see the review (*Dolgov*, 2002).

In case of equilibration of the neutrino oscillation degeneracies due to flavor oscillations before BBN the limit on L in the muon and tau neutrino sector strengthens. Then BBN constraint reads (*Dolgov et al.*, 2002) $|\xi_\nu| < 0.1$. For such a small L the expantion rate remains practically unaffected $\delta N_{eff} \sim 10^{-3}$.

It was realized that the equilibration of the chemical potentials before BBN depends on the value of the yet unknown mixing θ_{13} (*Pastor et al.*, 2009). Besides, since relic L is capable to suppress or enhance oscillations, depending on its value and the values of oscillation parameters, L itself may play the role of an inhibitor or a catalyzer of the equilibration. Hence, different possibilities for the values of chemical potential in different neutrino flavors still may have place.

The analysis on the basis of BBN and the abundances of D and ^4He and CMB/LSS constraints on baryon-to photon value, provided restrictive constraints on the neutrino degeneracy, see for example *Simha and Steigman* (2008). Namely the following constraints were derived for $N_{eff} = 3.3^{+0.7}_{-0.6}$ and different possibilities for the chemical potentials: in case $\xi_{\nu_e} \neq \xi_{\nu_\mu} = \xi_{\nu_\tau}$ $\xi_\nu < 2.3$ corresponding to $L < 5$; in case $\xi_{\nu_e} = \xi_{\nu_\mu} \neq \xi_{\nu_\tau}$ $\xi_{\nu_\tau} < 4$ $L < 7.6$, while in case $\xi_{\nu_e} = \xi_{\nu_\mu} = \xi_{\nu_\tau}$ $0.01 < \xi_\nu < 0.1$ and $L < 0.07$. In the last case practically the rate of expansion does not change, and the small dynamical effect of L corresponding to $\Delta N_{eff} \sim 0.03$ is undetectable by BBN and CMB.

CMB and LSS provide much looser bounds: They feel the change in the total density, i.e. only dynamical effect of L – δN_{eff}. L modifies the power spectra of radiation and matter (*Lesgourgues and Pastor*, 2006). However, today's sensitivity of CMB and LSS data do not allow to probe different flavors. CMB data (including WMAP 5 years data results) combined with LSS data put the bound: $\xi_\nu < 0.7$ and $L < 0.6$ at 2σ level.

In conclusion, depending on the different combinations of observational data sets used and the assumed uncertainties, cosmology provides an upper bound for L in the range $|L_{\nu_{\mu,\tau}}| < 10^{-2} - 10$ and $|L| < 0.01 - 0.2$. These values are many orders of magnitude larger than the baryon asymmetry value.

In the next sections we analyze the indirect kinetic effect of small L on BBN with late neutrino oscillations and present a possibility for much sensitive leptometer capable to constrain tiny L values close to the baryon one. Namely, we describe a model of BBN with late electron-sterile neutrino oscillations, which can 'measure' L bigger than $|L| \geq 10^{-8}$.

4.4.2 Helium production in BBN with neutrino oscillations and L. Different effects of L on neutrino oscillations

To study the lepton asymmetry effect on BBN we have provided a detail numerical analysis of the influence of L on Y_p, because primordially produced ^4He is highly sensitive to the nucleons kinetics during the pre-BBN epoch and besides, it is the most precisely measured element among light elements synthesized during BBN. A recent measurement of Y_p was provided on the basis of 93 spectra of 86 low redshift HII regions (*Izotov and Thuan*, 2010).

Oscillations generated asymmetry and BBN We have calculated precisely for hundreds different sets of model's parameters the neutron to nucleons freezing ratio $X_n^f = n_n^f/(n_n + n_p)^f = f(\delta m^2, \sin^2 2\theta, L)$, which is essentially influenced by oscillations and L. The primordially produced ^4He was estimated from it.

We have precisely followed the evolution of nucleons in the presence of electron-sterile neutrino oscillations in the pre-BBN period for different sets of oscillation parameters and different values of L. The production of ^4He was numerically calculated and compared to the BBN value without asymmetry growth account.

Figure 4.1 illustrates the typical behavior of the frozen neutron number density relative to nucleons when increasing the mixing in case of asymmetry growth (red

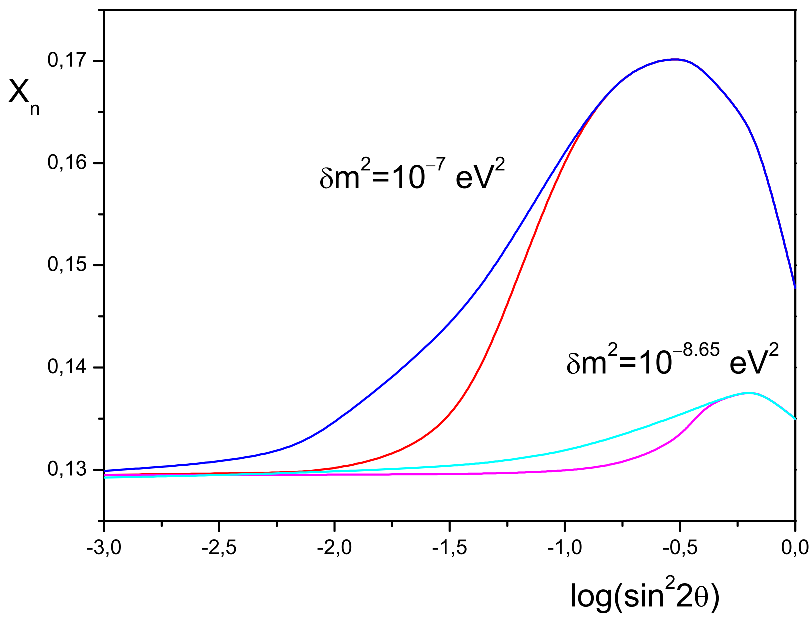

Figure 4.1: The dependence of the frozen neutron number density relative to nucleons on the mixing in case of the account of asymmetry growth (red curves) and in case without asymmetry growth account for two different mass differences $\delta m^2 = 10^{-8}$ eV^2 and $\delta m^2 = 10^{-7}$ eV^2. Figure from ref. (*Kirilova*, 2012).

curves) and in case without asymmetry growth account for two different mass differences. The asymmetry growth takes place at smaller mixing angles when increasing δm^2. Then *due to the asymmetry growth the production of* X_n (correspondingly Y_p) *decreases at small mixing.* The effect of the asymmetry growth on helium production is always towards decreasing of the caused by oscillations overproduction of ^4He, leading to a relaxation of BBN constraints at small mixings.

Thus, the analysis has proven that BBN is sensitive to the oscillations generated asymmetry, which usually grow not more than 5 orders of magnitude and are small $|L| < 10^{-5}$.

Initial asymmetry, nonresonant neutrino oscillations and BBN

We considered the case of nonresonant oscillations $\delta m^2 > 0$ with small mass differences for a wide range of the initial values of L, namely $10^{-10} - 1$, and provided a precise numerical study for $10^{-10} \leq |L| \leq 10^{-4}$, which is the most unexplored part of it.

We assumed no degeneracy of muon and tau neutrinos for simplicity. However, this assumption is not essential. The results can be easily rescaled for the general case of asymmetry in all sectors.

Numerical analysis of $Y_p(\delta m^2, \theta, L)$ dependence has been provided for the entire range of mixing parameters of the model and relic $|L| \geq 10^{-10}$.

In fig. 4.2 the evolution of the neutron number density relative to nucleons $X_n(t) = N_n(t)/(N_p + N_n)$ for the case of oscillations with $\sin^2(2\vartheta) = 10^{-0.05}$ and $\delta m^2 = 10^{-7}$ eV^2 for different values of the initial asymmetry ($L = 10^{-6}$, $L = 10^{-5}$ and $L = 10^{-10}$) is plotted. As is seen from the figures, even relatively small asymmetry ($L = 10^{-6}$) can considerably effect the neutron-to nucleon ratio.

In figure 4.3 the evolution of the neutron number density relative to nucleons $X_n(t) = N_n(t)/(N_p + N_n)$ for the case of oscillations with maximal mixing and $\delta m^2 = 10^{-7}$ eV^2 for different values of the initial asymmetry ($L = 10^{-6}$, $L = 10^{-5}$ and

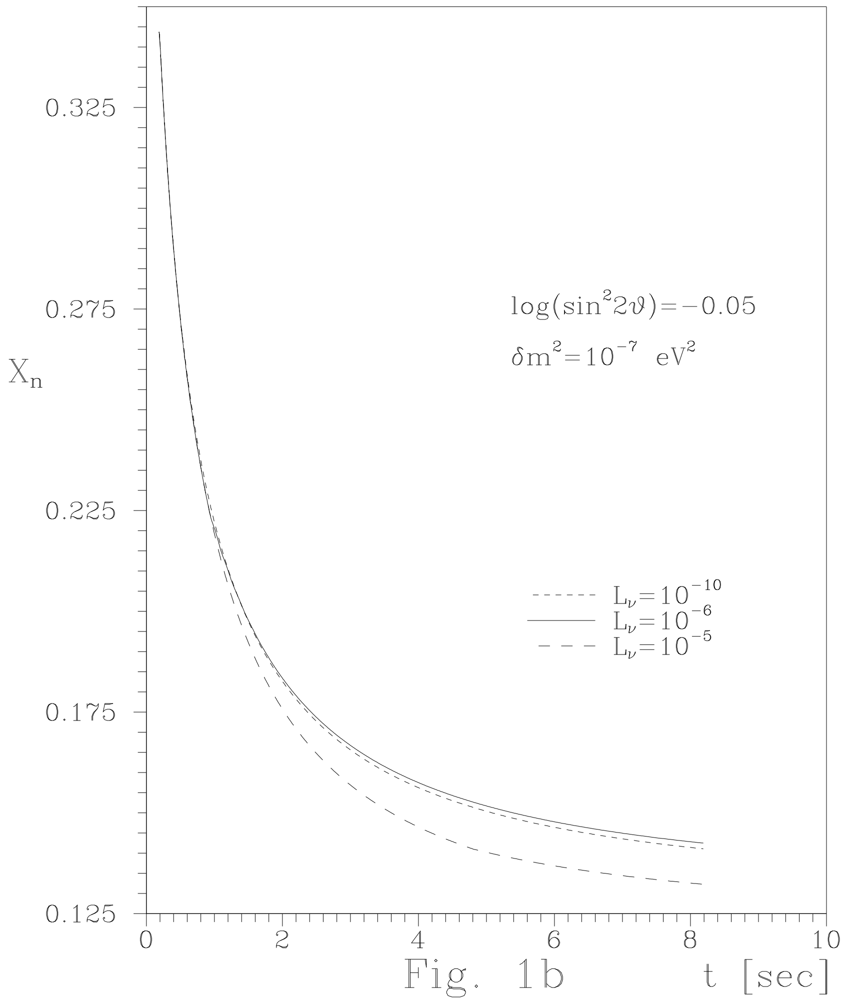

Figure 4.2: The evolution of the neutron number density relative to nucleons $X_n(t) = N_n(t)/(N_p + N_n)$ for the case of oscillations with $\sin^2(2\vartheta) = 10^{-0.05}$ and $\delta m^2 = 10^{-7}$ eV^2 and for initial asymmetry of the order of the baryon one and for $L = 10^{-6}$ and $L = 10^{-5}$ Figure from ref. (*Kirilova and Chizhov*, 1998b).

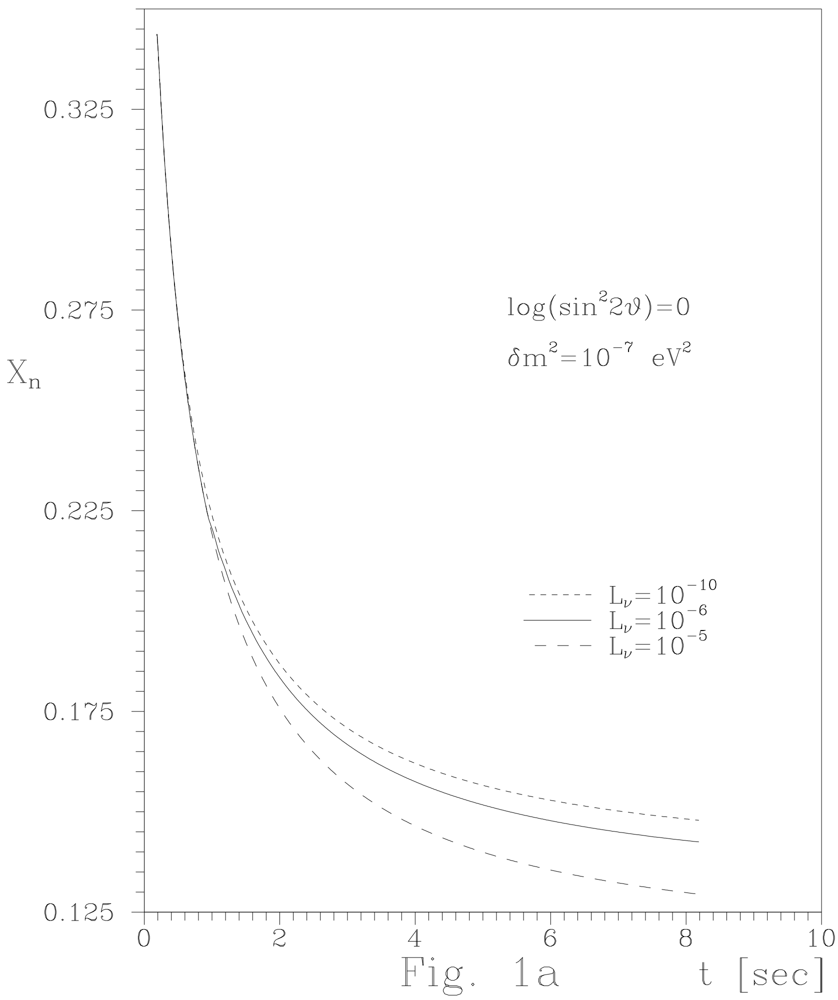

Figure 4.3: The evolution of the neutron number density relative to nucleons $X_n(t) = N_n(t)/(N_p + N_n)$ for the case of oscillations with maximal mixing and $\delta m^2 = 10^{-7}$ eV^2 for different values of the initial asymmetry ($L = 10^{-6}$, $L = 10^{-5}$ and $L = 10^{-10}$). Figure from ref. (*Kirilova and Chizhov*, 1998b).

$L = 10^{-10}$) is plotted.

In some cases, i.e. for maximal mixing (figure 4.3), the presence of L is leading to underproduction of helium-4, while in others (figure 4.2) to its overproduction in comparison with helium yields calculated in models with small asymmetry ($L \sim 10^{-10}$).

In figure 4.4 the dependence of the neutron to nucleon freezing ratio on the mixing angle for $L = 10^{-6}$ for different mass differences $\delta m^2 = 10^{-7}$ eV^2 and $\delta m^2 = 10^{-8}$ eV^2

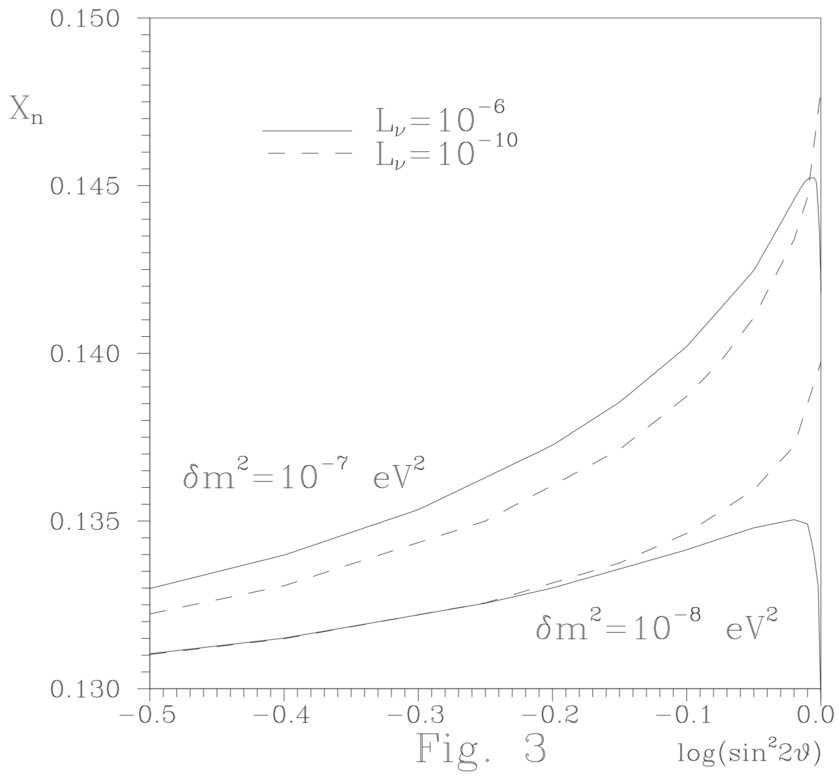

Figure 4.4: The dependence of the neutron to nucleon freezing ratio on the mixing angle for $L = 10^{-6}$ for different mass differences $\delta m^2 = 10^{-7}$ eV^2 and $\delta m^2 = 10^{-8}$ eV^2 is shown. For comparison with dashed lines the corresponding curves with small asymmetry $L = 10^{-10}$ are presented. Figure from ref. (*Kirilova and Chizhov*, 1998b).

is shown. For comparison the corresponding curves with small asymmetry $L = 10^{-10}$ are presented with dashed lines. It is interesting to note, that, as illustrated in this figure depending on the mixing angle, it is possible to reduce or increase the overproduction of helium and correspondingly to weaken or to strengthen the cosmological limits in comparison with the model of BBN with oscillations without a considerable lepton asymmetry. Namely, for large mixing, the presence of neutrino degeneracy of the order 10^{-6}, for example, weakens the oscillation effect of overproducing helium leading to less strong constraints on the mixing parameters. While for smaller mixing angles the same asymmetry enhances oscillations and increases the helium overproduction, leading to stronger limits on mixing parameters.

The indirect kinetic effect on BBN of small *relic* L, $10^{-8} < L << 0.01$, via oscillations was studied in ref. (*Kirilova and Chizhov*, 1998b; *Kirilova*, 2012).

We have found that correct account for the spectral spread of neutrino is very important because of the oscillation-asymmetry interplay, and it is decisive for the realization of low temperature resonance in $\delta m^2 > 0$ case – called further "spectrum wave resonance". In models working with the mean momentum only, the resonance does not have place as far as actually the asymmetry calculated in this approximation reaches zero at resonance.

The calculated ^4He production dependence on oscillation parameters and on L shows that, in case of electron-sterile neutrino oscillations:

i) BBN can feel extremely small L: down to 10^{-8}.

ii) Large enough L change primordial production of ^4He by enhancing or suppressing oscillations.

L role

On the basis of numerical analysis, for the oscillation model discussed, we have found three interesting regions for the range of the lepton asymmetry. Depending on oscillation values $L \geq 10^{-7}$ may enhance oscillations, while $L > 0.1(\delta m^2/\mathrm{eV}^2)^{2/3}$ may suppress oscillations, and asymmetries as big as $L > (\delta m^2/\mathrm{eV}^2)^{2/3}$ inhibit oscillations. L enhancing oscillations leads to a higher production of Y_p. L suppressing oscillations decreases Y_p overproduction by oscillations. L bigger than 10^{-4} leads to a total suppression of oscillations, i.e. to the standard BBN yield of Y_p, without oscillations.

Let us consider nearly maximal mixing: $\sin^2(2\vartheta) = 10^{-0.05}$. Then these regions are as follows.

A. In the range $|L_\nu| \geq 5 \times 10^{-5}$ the asymmetry fully suppresses neutrino oscillations.

The yield of helium-4 coincides with the values obtained in the models of primordial nucleosynthesis without oscillations. Therefore, the nucleosynthesis bounds on the mixing parameters in the presence of such large asymmetries are waved away.

For $|L| \leq 10^{-2}$ the direct kinetic effect of such asymmetries on the neutron-to-proton transfer is almost negligible, i.e. for the range $10^{-4} - 10^{-2}$ the only role of asymmetry is to suppress oscillations.

Asymmetries greater than that effect nucleosynthesis by directly changing the kinetics of nucleons and are exhaustively studied in previous works.Therefore for $|L| > 10^{-4}$ we have not provided detail numerical calculations.

B. The range of smaller than 10^{-4} asymmetries was more appealing to us as far as it was totally unexplored. Therefore, we numerically analyzed the problem for the initial values of the neutrino asymmetry in the range $10^{-10} - 10^{-4}$, and for the full mixing parameter space of the late active-sterile oscillations model, described in *Kirilova and Chizhov* (1997).

The zone $10^{-7} \leq |L| \leq 5 \times 10^{-6}$ is the most interesting one. The asymmetry with magnitudes of that order is strong enough to influence neutrino oscillations although the neutrino asymmetry is too small to effect nucleosynthesis directly. It does effect nucleosynthesis yields in indirect way through its influence on neutrino oscillations pattern. The asymmetry values in that range are able to enhance oscillations. So, depending on the mixing angle for some L in this interval the ensemble of neutrinos expires a resonance. For nearly maximal mixing it is roughly around $L \sim 10^{-6}$. This enhancement of oscillations is big enough to influence considerably the electron neutrino and electron antineutrino number density and spectrum and leads to an enhanced depletion of the number densities of neutrinos and antineutrinos and a decrease in their mean energy, as well as nontrivial evolution of the asymmetry itself. Thus, it influences the helium-4 value, which is extremely sensitive to it. The result is overproduction of helium-4 in comparison with the case of primordial nucleosynthesis in the presence of oscillations with negligibly small L. This on its turn leads to a strengthening of the nucleosynthesis bounds on the neutrino mixing parameters for

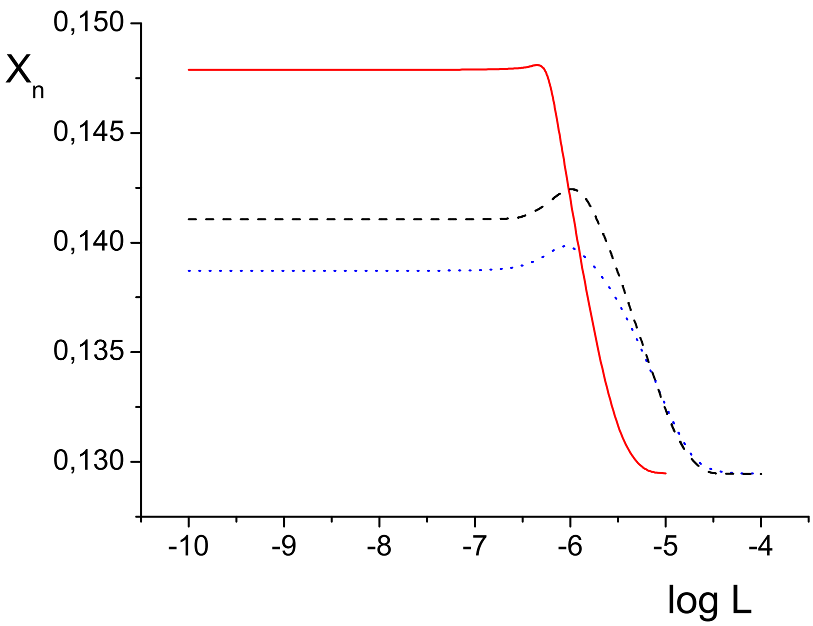

Figure 4.5: Frozen neutron number density relative to nucleons as a function of the relic initial lepton asymmetry for $\delta m^2 = 10^{-7}$ eV^2. The solid curve corresponds to maximal mixing, the dashed curve to $\sin^2 2\theta = 10^{-0.05}$ and the dotted curve to $sin^2 2\theta = 10^{-0.1}$. Figure from ref. (*Kirilova*, 2012).

that certain set of parameters $(L, \delta m^2, \vartheta)$.

C. For small asymmetries $|L| < 10^{-8}$ asymmetry has too week effect on nucleosynthesis to be considered.

Finally, we have calculated the He-4 dependence on the neutrino asymmetry for the whole range of mixing parameters of our model and we have obtained the primordial helium yields $Y_p(L, \delta m^2, \vartheta)$. This enabled us to obtain isohelium contours in the $\delta m^2 - \vartheta$ plane. Some of these constant helium contours, for $L = 10^{-10}$ and $L = 10^{-6}$, are presented in the following subsection.

In Figure 4.5 the dependences of X_n^f on relic L for different mixings (to the left) and different mass differences are presented. For L smaller than $\sim 10^{-7}$ X_n^f keeps unchanged from the case without L. The higher the mixing - the higher is the overproduction of He-4 due to oscillations. Increasing further L for fixed oscillation

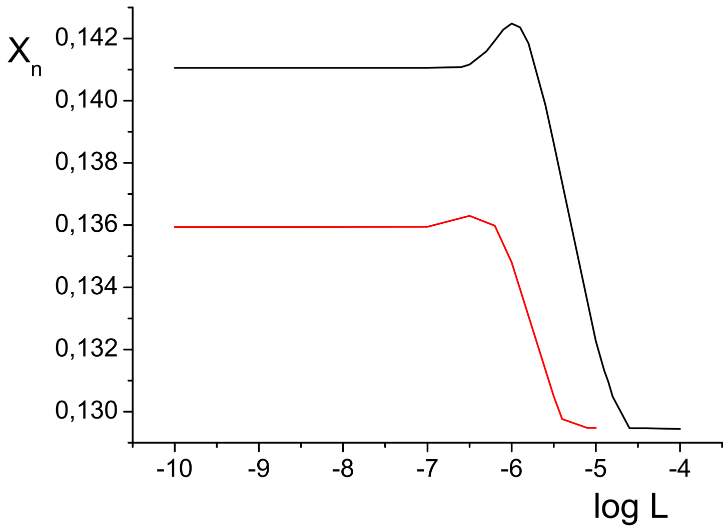

Figure 4.6: Frozen neutron number density relative to nucleons dependence on the initial asymmetry for $\sin^2 2\theta = 10^{-0.05}$ and two different mass differences $\delta m^2 = 10^{-8}$ eV^2 (lower curve) and $\delta m^2 = 10^{-7}$ eV^2 (upper curve). Figure from ref. (*Kirilova*, 2012).

parameters leads first to an increase of helium production, corresponding to the region of parameters space where L enhances oscillations, and then to a decrease of helium production, corresponding to big L suppressing oscillations, and hence to less Y_p overproduction caused by oscillations. At some critical L value defined by the concrete set of oscillation parameters $L_c(\delta m^2, \theta)$ the produced helium reaches its standard BBN value - i.e. L has stopped the oscillations. As is illustrated in the figure, the width of the enhancement region and the height of the overproduction peak is sensitive to the mixing. Bigger values (up to about an order of magnitude) for L_c are necessary to inhibit oscillations when decreasing the mixing.

Figure 4.6 illustrates the dependence of X_n on the initial asymmetry value for a fixed mixing, namely $\sin^2 2\theta = 10^{-0.05}$ and different mass differences $\delta m^2 = 10^{-8}$ eV^2 and $\delta m^2 = 10^{-7}$ eV^2. The enhancement peak due to L is more clearly expressed for higher mass differences, and L_c is bigger for bigger mass differences.

L bigger than $\sim 10^{-4}$ leads to a total suppression of oscillations effect on BBN for late oscillations studied here and hence, eliminates the BBN bounds on oscillation parameters. In that case instead the following approximate bound holds:

$$\delta m^2/\mathrm{eV}^2 < L^{3/2}. \tag{4.11}$$

4.4.3 Spectrum wave resonance

The ability of L within that range to enhance the oscillations looks quite amazing at a first glance. The naive picture one expects as a result of increasing the initial L is a gradual suppression of oscillations proportional to L. As far as L value, calculated for the mean neutrino momentum is by orders of magnitude bigger than the necessary one for a resonance transfer $L \gg L_r$.

However, the detail numerical analysis, accounting for the momentum spread of neutrino ensemble, showed a more complex picture. Varying L for fixed mixing parameters we have observed a resonance region, i.e. an enhancement of oscillations, as seen in the figures. And besides that, when a resonance for a given L value was observed for neutrino it was followed with a negligible time delay by a resonance in antineutrino! This leads to a considerable depletion of number densities and to further overproduction of helium-4. This amazing results can be explained as follows.

The system of nonlinear differential equations cannot be solved analytically without radical assumptions. However, the qualitative behavior of the ensembles and the obtained results concerning helium-4 can be guessed from the following simplified considerations.

The resonant conditions for the neutrino looks like:

$$\cos(2\vartheta)(\delta m^2/2E_\nu) = \sqrt{2}G_F(L - Q/M_W^2)N_\gamma \tag{4.12}$$

while for antineutrino the sign before L term is the opposite one.

For the mean neutrino momenta $\bar{p} = 3.15\ T$ in our model

$$\begin{aligned} |L| &\gg Q/M_W^2 \\ |L| &\gg \cos(2\vartheta)\delta m^2/(2\sqrt{2}E_\nu G_F N_\gamma). \end{aligned}$$

Now let us consider the possibility that at a given temperature, for neutrino of a given momentum $p < \bar{p}$ the resonance condition is fulfilled, i.e. L has the resonance value $L_r(p)$. Then neutrinos with this momentum suffer a resonant transfer, leading to a decrease in the number densities of neutrinos (in favour of the sterile neutrinos). As far as for antineutrinos L has the opposite sign, oscillations remain suppressed, and the number densities of antineutrinos do not change. Hence, the net result is a decrease in L due to this resonant transition. This decrease makes possible the fulfillment of the resonant condition for more energetic neutrinos, leading to further decrease of L and so on; due to this 'resonance wave' passing to neutrinos with higher and higher momenta, the neutrino number densities expire a considerable depletion, consequently, having in mind the small initial values of the neutrino asymmetry ($\delta N_\nu \sim L_\nu N_\nu$) soon this resonant wave leads to a change in the sign of L. This suppresses further resonant transfer for neutrinos, however, for the antineutrino ensemble now there appears the possibility for a resonance. So, the same process follows in the antineutrino ensemble.

The only difference being that contrary to the neutrino system, for antineutrinos the resonance is first fulfilled for the high energy neutrinos and then passes to the low energetic ones - i.e. it reaches more rapidly neutrinos with mean momentum, and the process is more avalanche like. This rapid decrease of antineutrinos leads to a rapid bump of L which again becomes positive.

This pendulum like process proceeds relatively fast, the oscillation of the asymmetry proceeds much faster than the temperature decrease. The total effect is that the resonant transfer both for neutrino and antineutrino system is realized even for a considerable initial asymmetry values (nonresonant ones, when calculated for the mean neutrino momentum), and due to the enhanced transfer of active to sterile neutrinos a considerable 'resonant' production of helium-4 is observed.

We would like to emphasize that the qualitatively new result, namely that small asymmetries may enhance oscillations and consequently to strengthen the nucleosynthesis bounds, was revealed only due to the correct approach accounting for the spectral spread of neutrino momenta and energy spectrum distortion due to oscillations, advocated in our previous papers and in the pioneer work of *Dolgov* (1981). Other studies missed this possibility as far as there it was assumed that neutrino ensemble follows the behavior of average momentum even in the presence of oscillations and asymmetry.

4.4.4 Production of He-4 in BBN with neutrino oscillations and lepton asymmetry

4.4.4.1 Relic lepton asymmetry

We have found that even small asymmetries $|L| > 10^{-7}$ may considerably effect nucleosynthesis (contrary to the conclusions of the previous works) and that asymmetry is also able to *enhance oscillations and consequently to strengthen* the nucleosynthesis bounds on neutrino mixing parameters for concrete regions in the parameter space $(L, \delta m^2, \vartheta)$, besides suppressing oscillations and thus loosening the bounds on mixing parameters from nucleosynthesis. Depending on its value, relic L may change BBN bounds: It relaxes them at large mixings and strengthens them at small mixings *Kirilova and Chizhov* (1998b); *Kirilova* (2006, 2001c); *Kirilova and Chizhov* (2001b); *Kirilova* (2012).

Figure 4.7 presents the dependence of X_n on the mass differences at a fixed non maximal mixing angle and for two different initial L. As illustrated, higher initial L leads to an increase of helium production at bigger mass differences, and reduces he-

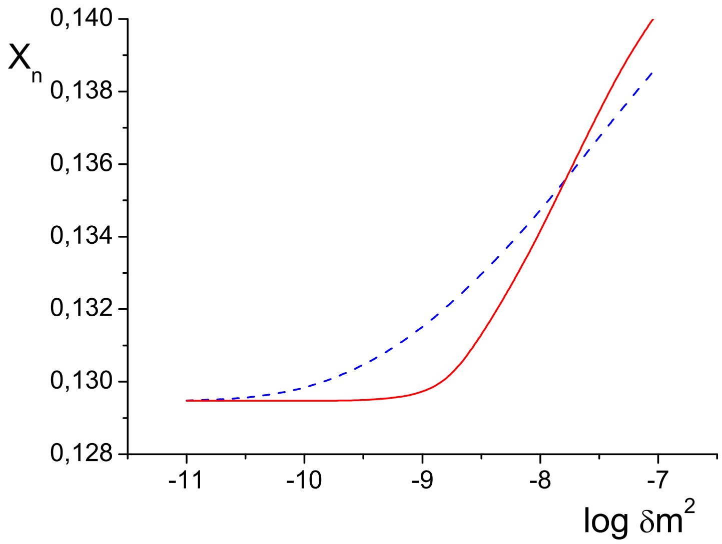

Figure 4.7: The dependence of the frozen neutron number density relative to nucleons on the mass differences at $\sin^2 2\theta = 10^{-0.1}$ and for two different initial lepton asymmetries $L = 10^{-10}$ (the dashed curve) and $L = 10^{-6}$ (solid curve). Figure from ref. (*Kirilova*, 2012).

lium production at smaller mass differences. Correspondingly, increasing L at a fixed mixing leads to relaxation of the bounds at small mass differences and strengthens them for big mass differences.

At maximal mixing, however, bigger L leads to a suppression of the production of helium for all mass differences, and $L = 10^{-5}$ is enough to eliminate oscillations effect, i.e. to eliminate also the constraints on oscillation parameters in the discussed BBN model (see figure 4.8).

Finally in figure 4.9 we present the dependence of the helium production on the mixing angle at different initial L. Bigger L leads to decreasing the production of ^4He with increasing the mixing. I.e. for fixed mass differences, L relaxes the BBN constraints at large mixings. Analysis at bigger mass differences $\delta m^2 > 10^{-8}$ eV^2 has shown that at fixed δm^2 L strengthens the constraints at small mixing. $|L| = 10^{-6}$ relaxes BBN bounds at large mixings and strengthens them at small mixings.

Assuming the conventional observational bound on primordial ^4He $Y_p = 0.24$ the

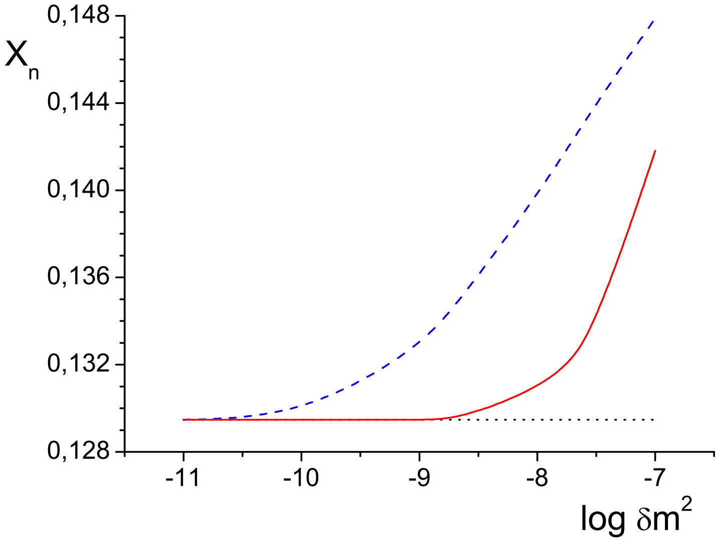

Figure 4.8: The dependence of the frozen neutron number density relative to nucleons on the mass differences at $\sin^2 2\theta = 1$ and for three different initial lepton asymmetries $L = 10^{-10}$ (the dashed curve) and $L = 10^{-6}$ (solid curve) and $L = 10^{-5}$ (the dotted curve).Figure from ref. (*Kirilova*, 2012).

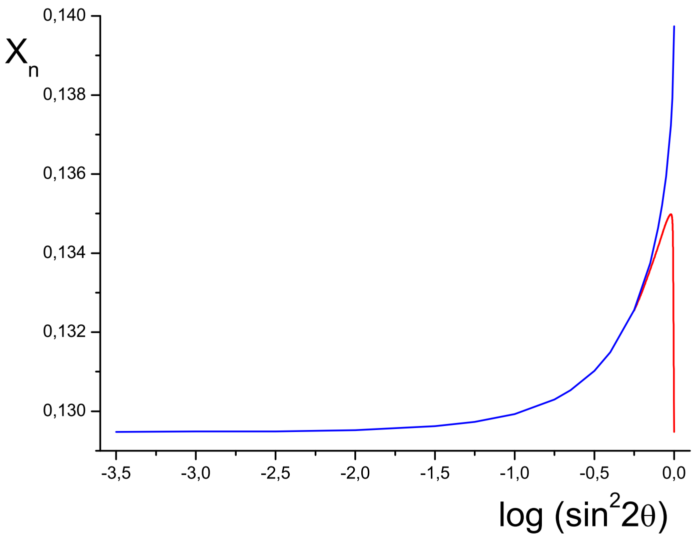

Figure 4.9: The dependence of the frozen neutron number density relative to nucleons on the mixing angle at $\delta m^2 = 10^{-8}$ eV^2 and for two different initial lepton asymmetries $L = 10^{-10}$ (the dashed curve) and $L = 10^{-6}$ (solid curve). Figure from ref. (*Kirilova*, 2012).

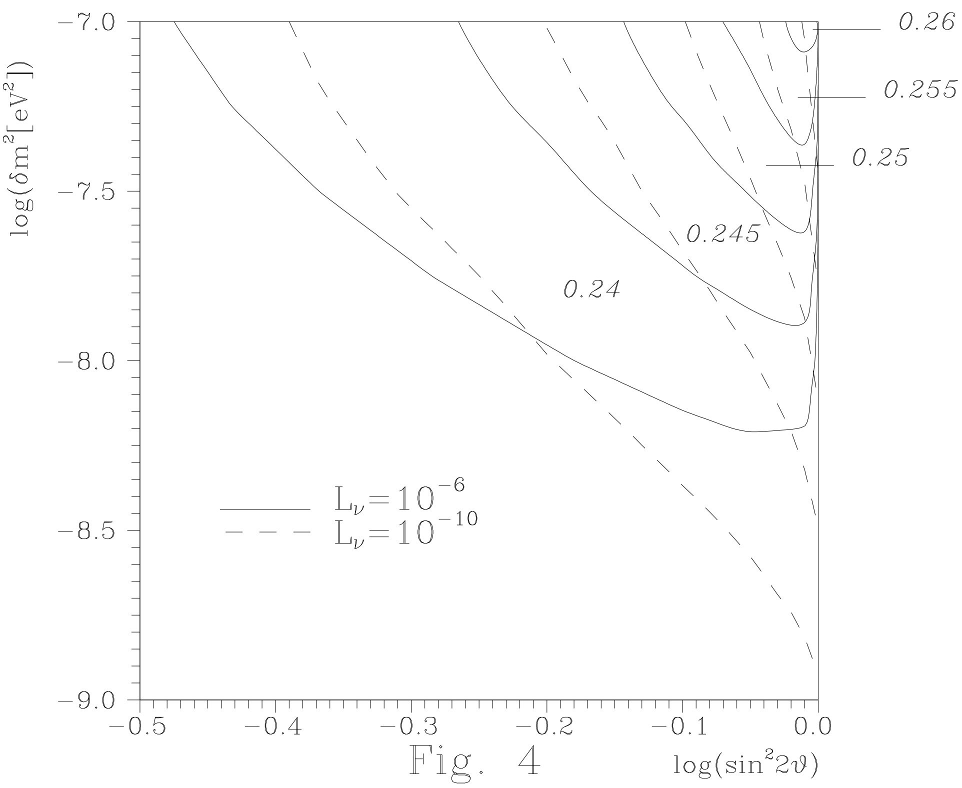

Figure 4.10: on the $\delta m^2 - \vartheta$ plane the constant helium contours calculated in the discussed model of cosmological nucleosynthesis with neutrino oscillations for $L = 10^{-6}$ and $L = 10^{-10}$ are shown. Figure from ref. (*Kirilova and Chizhov*, 1998b).

cosmologically excluded region for the oscillation parameters on the plane $\sin^2(2\vartheta) - \delta m^2$ in figure 4.10 lies to the right of the $Y_p = 0.245$ curve, which gives 5% overproduction of helium in comparison with the standard value. For comparison the curves corresponding to $L = 10^{-10}$ and $L = 10^{-6}$ are plotted.

In fig. 4.10 on the $\delta m^2 - \vartheta$ plane the constant helium contours calculated in the discussed model of cosmological nucleosynthesis with neutrino oscillations for $L = 10^{-6}$ and $L = 10^{-10}$ are shown.

4.4.4.2 Neutrino oscillations generated lepton asymmetry

In case of oscillations generated lepton asymmetry BBN constraints on neutrino oscillations may notably change although the values of the asymmetry are small (*Kir-*

ilova and Chizhov, 1996a, 2000a; *Kirilova*, 2007; *Kirilova and Panayotova*, 2006; *Kirilova*, 2012).

Our investigations and the numerical analysis showed that the dynamically produced asymmetry at small mixing angles suppresses oscillations, which leads to less overproduction of ^4He in comparison with BBN with oscillations but without an asymmetry account. Hence, the bounds on oscillation parameters are alleviated at small mixing angles (*Kirilova and Chizhov*, 2000a; *Kirilova*, 2001c).

Here we present the updated cosmological constraints for electron-sterile oscillation case, accounting precisely for the oscillations generated asymmetry. The dynamical asymmetry effect on BBN via neutrino oscillations is illustrated in comparison with an artificial case without the account of asymmetry in order to extract the net effect of the asymmetry on BBN.

In figure 4.11 the impact in helium-4 due to oscillations and asymmetry is presented as a function of the neutrino square mass differences. For comparison the curve corresponding to the artificial case without the account of the asymmetry is presented also. The difference between the two curves measures the net asymmetry effect on BBN with oscillations. It is obvious, that for the range of oscillation parameters discussed, the total effect of the asymmetry is a reduction in Y_p in comparison with the case without asymmetry account. This reduction can be as big as 10%, which is considerable on the background of our recent knowledge from primordial helium measurements. As it is obvious from the figure, small δm^2 are also constrained from BBN considerations.

In figure 4.12 we present a comparison of the iso-helium-4 contours, $Y_p = 0.245$, for the resonant case, obtained without the account of the asymmetry, with the contours obtained with the account of the asymmetry. The area to the left of the curves is the allowed region of the oscillation parameters.

The apparently great asymmetry effect (as seen from the curves) is totally due

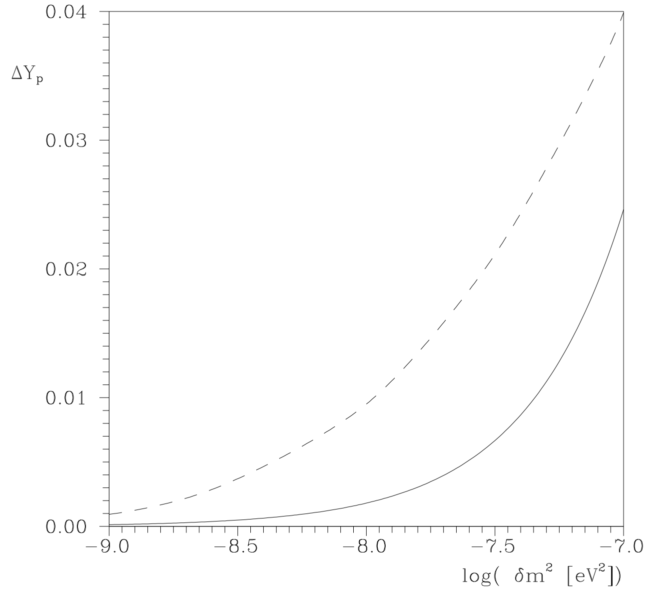

Figure 4.11: The relative change in the primordial yield of helium-4 as a function of the neutrino squared mass differences in case of BBN with oscillations for $\sin^2(2\theta) = 0.05$. The solid curve shows the complete effect of oscillations with the account of the asymmetry. The dashed curve shows solely the effect of oscillations neglecting the asymmetry.

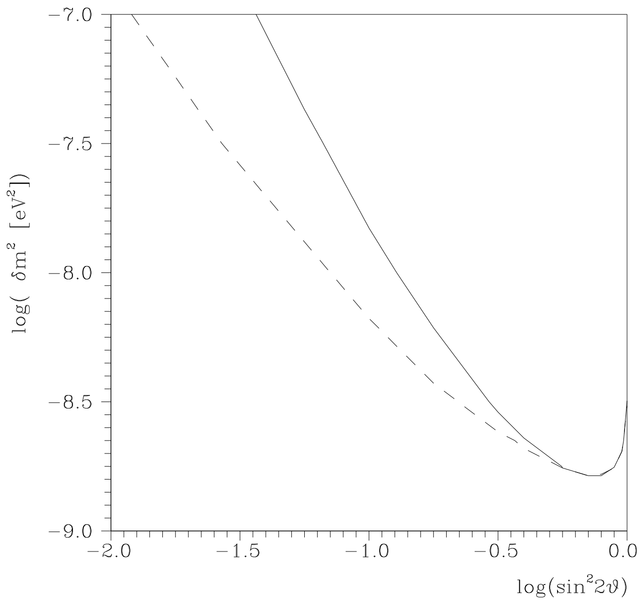

Figure 4.12: On the $\delta m^2 - \theta$ plane iso-helium-4 contour $Y_p = 0.245$, calculated in the discussed model of BBN with active-sterile neutrino oscillations and the account of the complete asymmetry effect, is shown. The dashed curve presents a comparison with the same case, but without the asymmetry account. The area to the left of the curves is the allowed region of the oscillation parameters.

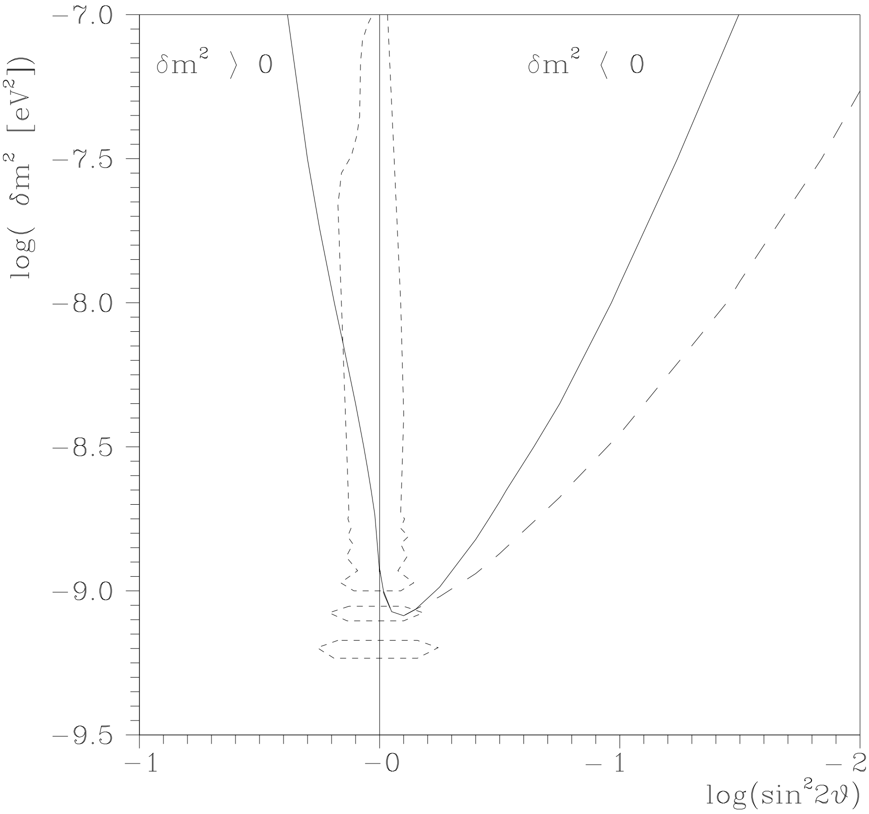

Figure 4.13: Cosmological constraints for the electron-sterile neutrino oscillations, are presented by the solid curves $Y_p = 0.24$. The dashed curve shows the contour without asymmetry account. The dotted curve shows solar neutrino LOW solution.

to the indirect effects of the asymmetry on BBN. The maximal asymmetry effect is around 10% 'underproduction' of Y_p in comparison with the case of BBN with oscillations but without the asymmetry account. The total effect of oscillations, with the complete account of the asymmetry effects, is still overproduction of helium-4, although considerably smaller than in the calculations neglecting asymmetry. Therefore, BBN constraints on the mixing parameters of neutrino are alleviated considerably due to the asymmetry effect.

The updated constraints on active-sterile neutrino oscillations, precisely accounting for the asymmetry generation, spectrum distortion and the depletion of the neutrinos, are presented in fig. 4.13 . The plots correspond to $Y_p = 0.24$. The net *indirect* asymmetry effect on BBN is given for the resonant case by the difference between the dashed curve (without asymmetry account) and the solid one. Due to asymmetry growth account, and the corresponding suppression of oscillations, Y_p overproduction is not so strongly expressed at small mixing angles, hence BBN constraints are alleviated at small mixing angles for $\delta m^2 < 0$.

In the resonant case the cosmological constraints at large mixing are:

$$|\delta m^2| \leq 8.2 \times 10^{-10} \text{ eV}^2. \tag{4.13}$$

In the nonresonant case $\delta m^2 > 0$ an analytical fit to the exact constraints is:

$$\delta m^2 (\sin^2 2\vartheta)^4 \leq 1.5 \times 10^{-9} \text{ eV}^2. \tag{4.14}$$

The constraints in both cases are strengthened compared to the previous ones due to the precise account of the spectrum distortion and to the exact kinetic approach to the neutrinos and nucleons evolution.

In conclusion we would like to stress once again that lepton asymmetries $|L| \geq 10^{-8}$ can both enhance or suppress (completely or partially, depending on the concrete values of the model parameters) neutrino oscillations and consequently can strengthen or weaken oscillation effect on primordial nucleosynthesis. The cosmological constraints in case of proper account of the asymmetry growth are less stringent at small mixing angles (where the growth of asymmetry takes place) in comparison with the case when the asymmetry growth was neglected.

The constraints on the oscillation parameters obtained from nucleosynthesis with lepton asymmetry of the order of the baryon one *Barbieri and Dolgov* (1991); *Enqvist et al.* (1990b); *Kirilova and Chizhov* (1997); *Barbieri and Dolgov* (1990); *Enqvist et al.* (1992, 1990a); *Cline* (1992); *Shi et al.* (1993); *Kirilova and Chizhov* (1998c, 2000a, 2001a) can be considerably changed - either relaxed (or even totally removed) or strengthened for (note!) *not very large* values of the initial lepton asymmetry. This may have interesting astrophysical and cosmological implications.

The constraints and conclusions of previous works concerning asymmetry effect on BBN with oscillations will change considerably when a proper selfconsistent account for (a) the complete effect of the asymmetry (1)-(4) during its whole evolution in nucleosynthesis epoch; (b) the neutrino spectrum distortion; (c) and the exact kinetics of nucleons is provided using the kinetic equations in momentum space. The role of the mixing-generated neutrino asymmetry in BBN is considerable and should be accounted for precisely.

4.5 Cosmological Constraints on Lepton Asymmetry from BBN with Neutrino Oscillations

The detection of the Cosmic Neutrino Background would provide L direct measurement. Till then L is measured indirectly by its influence on observable relics of the Universe. We have studied numerically the special case of influence of very small L on oscillating neutrino and on BBN. Both small neutrino oscillations generated asymmetry and small relic asymmetry influences considerably the primordial production of ^4He in the model of BBN with late electron-sterile neutrino oscillations. The produced primordially ^4He in this model feels extremely small L, namely $10^{-8} \leq L << 0.01$ due to the indirect kinetic effect of L. Hence, BBN with oscillations feels extremely small L and represents now the finest known "leptometer".

Having definite values for the neutrino mixing parameters, it will be possible, on the basis of requirement of agreement between the theoretically calculated and the extracted from observations values of helium-4, to put cosmological constraints on L even within that range of exclusively small magnitudes.

Namely, equation 4.11 can be used to put the following BBN constraint on L: Having the indications for active-sterile oscillations with $\delta m^2 \sim 10^{-5}$ (*Holanda and Smirnov*, 2011) and replacing this value in eq. 4.11, a stringent upper limit on L follows:

$$L < 5.10^{-4}.$$

This limit is much stronger than the one following from standard BBN.

Today it is reasonable to study L, also as a possible solution of the recently found cosmological preference or/and indication for additional relativistic density.

4.6 Lepton Asymmetry and Excess Radiation Density

In recent years an increasing number of *cosmological indications* appeared suggesting excess relativistic density, corresponding to different epochs (*Izotov and Thuan*, 2010; *Aver et al.*, 2010; *Komatsu and others (WMAP)*, 2009).

Namely, recent measurements of primordially produced ^4He, Y_p, and CMB measurements of Y_p pointed to higher values of the effective number of the relativistic degrees of freedom at the BBN epoch, at the CMB formation epoch, and at present epoch (on the basis of LSS survey data) than previously estimated ones and higher than the theoretically predicted standard value for 3 neutrino species $N_{eff} = 3.046$.

Besides, recent analysis of the *combined neutrino oscillation data*, including LSND and MiniBoone requires 1 or 2 additional low mass (sub-eV) sterile neutrinos ν_s, participating into oscillations with flavor neutrinos with higher mass differences values, than the ones required by solar and atmospheric neutrino oscillations experiments *Kopp et al.*, 2011; *Giunti and Laveder*, 2010. These light ν_s brought into equilibrium by oscillations with active neutrinos may be a successful explanation of the excess relativistic density.

It is interesting if cosmology allows 2 light additional sterile neutrinos and if they can explain the excess relativistic density.

It is known that additional light sterile neutrinos with the mixing and mass differences estimated by ν oscillations data with mass differences in the eV range will be brought into equilibrium in the early Universe. BBN favors the presence of one such ν_s but He and D data excludes 3 fully thermalized ν_s. Besides, neutrinos in sub-eV range produce too much hot dark matter (*Hamann et al.*, 2010). Thus, two additional ν_s are in tension both with BBN and with LSS requirements (*Giusarma et al.*, 2011).

Lepton asymmetry, namely its dynamical and direct kinetic effects, has been considered as an explanation of the excess radiation. It was shown that excess radiation cannot be explained by degenerate BBN (*Mangano et al.*, 2012). However, the presence of L may be the solution in case its value is enough to suppress active-sterile oscillations so that ν_s are not fully thermalized. Our estimation (*Kirilova*, 2013) of the value of L necessary to suppress oscillations and achieve the suppression of ν_s production is:

$$|L| \geq 0.08.$$

This is higher than the values discussed by *Hannestad et al.* (2012); *Mirizzi et al.* (2012), that found $|L| > 10^{-2}$. The difference might be due to different approximations used or to the fact that previous studies do not account precisely for the ν energy distribution.

Thus, in modified BBN with ν oscillations and high enough L the models with additional light sterile neutrinos may be allowed. To obtain the exact L value a precise numerical analysis, solving the exact kinetic equations, including all ν species and accounting for all L effects, discussed above, should be provided.

Hence, the excess relativistic density might point to additional sterile neutrinos and the presence of L. However, there exist other possibilities as well, namely: ν active-sterile late oscillations leading to the overproduction of He-4 and thus imitating extra radiation, MeV decaying particles during BBN (*Kirilova*, 2009; *Ruchayskiy and Ivashko*, 2012), or other modifications of the standard cosmological model. Future experimental and observational data will choose among different possibilities. In particular, it is expected that Planck data will be able to check with higher sensitivity the status of extra radiation.

4.7 Summary

Lepton asymmetry of the Universe has not been directly observed. It may be much bigger than the baryon asymmetry, and hidden in the neutrino sector. Since relic neutrino background is not yet detected, the lepton asymmetry in the neutrino sector may be measured/constrained just indirectly, namely by its influence on Universe expansion, Big Bang Nucleosynthesis, Cosmic Microwave Background, LSS, etc.

We discussed the case of small lepton asymmetry influence on the neutrino involved processes in pre-BBN epoch, and particularly on neutrino oscillations and pre-BBN kinetics.

Cosmological influence of such small lepton asymmetries, which do not have direct effect on nucleons kinetics during BBN and are invisible by CMB, was explored and shown to be considerable for certain range of oscillation parameters and L.

It was found that lepton asymmetries as small as 10^{-8} may be felt by BBN in case of neutrino oscillations. The effect of the dynamically generated and initially present L on BBN with oscillations was studied. We have calculated the dependence of primordially produced helium-4 on the parameters of the model $Y_p(L, \delta m^2, \vartheta)$.

Relic L present during BBN, depending on its value, may increase, decrease overproduction of Y_p or reduce it to the standard BBN value. Thus, the presence of an initial asymmetry bigger than the baryon one may considerably change the bounds on oscillation parameters obtained from primordial nucleosynthesis considerations. We have obtained limits on the neutrino mixing parameters corresponding to nucleosynthesis with degenerate neutrinos. Correspondingly, L can strengthen, relax or wave out BBN constraints on oscillations. It relaxes BBN bounds at large mixing and strengthens them at small mixings. Large enough L alleviates BBN constraints on oscillation parameters. In that case, instead, L constraint on oscillation parameters are derived.

An intriguing new result of our analysis is that the lepton asymmetry is able to *enhance oscillations and tighten the nucleosynthesis bounds on neutrino mixing parameters*, besides its well known ability to relax them. We would like to emphasize that the qualitatively new result, namely that small asymmetries may enhance oscillations and consequently to strengthen the nucleosynthesis bounds, was revealed only due to the correct approach accounting for the spectral spread of neutrino momenta and energy spectrum distortion due to oscillations, advocated in our papers.

The evolution of asymmetry growth in case of small mass differences and relatively big mixing angles was studied. The instability region in the oscillation parameter space, where considerable growth of L takes place, was determined numerically. Higher resolution for the description of the neutrino momenta distribution is required for the investigation of the asymmetry behavior in this oscillation parameter region. In the case of relic lepton asymmetry we have determined the parameter range for which L is able to enhance, suppress or inhibit neutrino oscillations.

Oscillations generated asymmetry at small mixing angles decreases the production of Y_p and relaxes BBN constraints at these angles.

Finally we would like to point to the essential differences between our work and the previous ones: we have considered the *nonresonant* case of oscillations with very *small mass differences*; the oscillations proceed effectively relatively late i.e. after neutrino decoupling and the change in the lepton number is dominated *by oscillations*, not by collisions; we have accounted precisely for the *momentum spread* of neutrinos and we have explored very small L and its indirect kinetic effect on BBN via neutrino oscillations.

CHAPTER V

Processes Essential for the Generation of the Baryon Asymmetry of the Universe

5.1 Baryonic Component of the Universe. Introduction.

The baryonic component of the Universe, according to independent observational data, corresponding to different epochs of Universe evolution, constitutes now around 5% of Universe matter budget. A basic cosmological and theoretical physics issue is to explain the presence of the baryon component, its density and the observed locally baryon-antibaryon asymmetry.

5.1.1 Locally observed baryon-antibaryon asymmetry

Amazing and still unresolved mystery of our Universe is the strong predominance of matter over antimatter in our surroundings. The Universe is predominantly baryonic in our vicinity: Cosmic ray (CR) and gamma-ray (GR) observations (within 20 Mpc) indicate that there exist baryon-antibaryon asymmetry in our neighborhood. Namely, the available Cosmic ray (CR) data (*Abe et al.*, 2012; *Adriani and others (PAMELA Coll.)*, 2010; *Mayorov et al.*, 2011; *Alcaraz and others (AMS Coll.)*, 1999; *Kappl and Winkler*, 2014) and gamma-ray (GR) data (*Steigman*, 1976, 2008; *Stecker*, 1985; *von Ballmoos*, 2014) on cosmic/galactic antimatter, obtained from balloons and spacecraft searches (BESS, AMS, PAMELA, etc.), point to a strong *predominance of matter over antimatter in out Galaxy.* [1] Observational evidence for matter-antimatter asymmetry in the Universe has been recently reviewed (*Canetti et al.*, 2012; *Dolgov*, 2014).

Experimental search for antinuclei and $\bar{p}$ in CR:

CR search for anti protons $\bar{p}$ and antinuclei on high-altitude balloons and on spacecraft found $\bar{p}$ with negligible numbers: $\bar{p}/p \sim 10^{-5} - 10^{-4}$ depending on the part of energy spectrum. The detected antiprotons and positrons in the primary CR can be totally due to interactions of primary CR with the interstellar medium.

No antinuclei were observed. Only strong upper limits on anti-He and anti-D were obtained. The bound on cosmic anti-helium is (*Sasaki and others (BESS Collab.)*, 2008):

$$\bar{He}/He < 3.10^{-7}.$$

The search continues at AMS and PAMELA missions as far as an antinuclei detection would be certain signature for antimatter BBN and antistars, because the secondary flux of antinuclei is predicted to be extremely low (*Chardonnet et al.*, 1997).

Thus, CR data indicate that there are no antimatter objects within radius 1 Mpc. [2]

GR data: Gamma ray data, interpreted as a result from annihilation provides constraints on the antimatter fraction in different structures (*Stecker*, 1985; *Steigman*, 1976). No evidence for expected annihilation features in the γ-ray data, which may be created by $\bar{p}p$ annihilations at the borders of the matter antimatter regions, for the period $z < 100$ was found in the cosmic GR background. GR flux in the MeV region excludes significant amounts of antimatter up to the distance of galaxy cluster scales $\sim 10 - 20$ Mpc. This points to the absence of big antimatter objects in our

[1]Still, domains of antimatter are not absolutely ruled out (*Dolgov and Silk*, 1993; *Khlopov et al.*, 2000; *Dolgov*, 2014).

[2]However, recently positron 0.511 MeV line was observed from the galactic bulge, which can be an indication for presence of antimatter.

cluster of galaxies.

Analysis of annihilation features within concrete baryogenesis model and EGRET gamma-ray background data showed that a fraction ($< 10^{-6}$) of antimatter stars in our Galaxy is allowed (*Belotsky et al.*, 2000). Possibility of primordial black holes, antiquasars and antistars was also revealed (*Dolgov and Silk*, 1993). *CR and GR data constrain antimatter fraction at certain scales.*

Other signatures of antimatter are the distortions of the CMB spectrum and the spatial variations of the light elements abundances. The isotropy of CMB rules out large voids between matter and antimatter regions during earlier time. BBN restricts the ammount of annihilation at early epoch and, hence, limits the fraction of antimatter (*Kurki-Suonio and Sihvola*, 2000; *Chechetkin et al.*, 1982).

The observational value of the baryon-antibaryon asymmetry *in our neighborhood* within radius of 1 Mpc is:

$$\beta = (N_B - N_{\bar{B}})/N_\gamma \sim N_B/N_\gamma = \eta \sim 6.1 \times 10^{-10} \tag{5.1}$$

There exist different ways to determine the baryon density. Contemporary observational knowledge on the baryon density of the local Universe is provided mainly on the basis of precise observational data from BBN and CMB. Namely:

(i)**Data based on BBN**

The baryon density is determined from the requirement of consistency between theoretically predicted and observationally measured abundances of the primordially produced light elements. This consistency at BBN epoch $z \sim 10^9$ (*Olive and others*, 2014) requires:

$$5.1 \times 10^{-10} \leq \eta_{BBN} \leq 6.5 \times 10^{-10} \quad at \quad 95\% \quad CL \tag{5.2}$$

(ii)**Deuterium data**

The determined η from measurements of Deuterium towards low metallicity quasars combined with BBN data (*Pettini and Cooce*, 2012) is:

$$\eta_D = 6 \pm 0.3 \times 10^{-10} \quad at \quad 95\% \quad CL \tag{5.3}$$

(iii)**CMB anisotropy data**

CMB anisotropy measurements , allow precise determination of the main Universe characteristics, including the baryon density. Precise determination of η corresponding to $z \sim 1000$ by WMAP9 (*Bennett et al.*, 2012) and Planck (*Ade and others (Planck Coll.)*, 2014, 2015) give:

$$\eta_{WMAP} = 6.16 \pm 0.16 \times 10^{-10} \quad at \quad 68\% \quad CL \tag{5.4}$$

$$\eta_{Planck} = 6.05 \pm 0.09 \times 10^{-10} \quad at \quad 68\% \quad CL \tag{5.5}$$

The observed seemingly small value of β, actually is unexpectedly big: In the framework of the SCM, equal quantities of matter and antimatter at the early hot stage of Universe evolution without BV-processes are expected, which after annihilation result in $\beta \sim 10^{-18}$ today.

We do not know yet if the Universe is globally baryonic ($\beta = const$) or the observed in our vicinity baryon excess is just a local characteristic ($\beta = f(x)$) and perhaps somewhere $\beta < 0$.

In case this locally observed asymmetry is a *global* characteristic of the Universe, i.e. there exists baryon asymmetry of the Universe (BAU). It may be due to the generation of a baryon excess at some early stage of the Universe, that diluted, eventually, during its further evolution gave the value observed today. I.e. baryogenesis mechanisms are required to explain the asymmetric production of matter or/and anti-matter. At present different baryogenesis mechanisms are proposed to explain the generation of the big excess.

The observed asymmetry is the only known "experimental" indication for baryon violation (BV). The unaesthetic assumption that the asymmetry is just an initial condition while baryon number is conserved, shortens by an order of magnitude the inflationary stage, making impossible the successful evolution of the Universe to its present state (*Dolgov et al.*, 1988). BV processes must have proceeded during inflation or after it, in order to generate the observed today baryon asymmetry.

The explanation of the observed asymmetry, its sign and its value, is the main goal of numerous baryogenesis scenarios, like GUT baryogenesis, electroweak baryogenesis (*Kuzmin et al.*, 1985b), baryo-through-lepto-genesis (*Fukugita and Yanagida*, 1986), Affleck-Dine baryogenesis (*Affleck and Dine*, 1985), etc. The chosen by Nature baryogenesis mechanism is not known yet.

Most of the baryogenesis models fulfill Sacharov's conditions for baryogenesis (*Sakharov*, 1967):

- Nonconservation of baryon number.

  Such B-violation is predicted by GUT and by electroweak theory. Inflation also points to necessity of B-violation.

- Violation of symmetry between particles and antiparticles, i.e. breaking of C and CP invariance.

  The mechanisms of CP-breaking can be different, namely: *explicit CP-violation*, by complex parameters in the Lagrangian; spontaneous CP-violation, by a non-zero expectation value of C or P odd scalar field; *stochastic CP-violation*, generated by a complex scalar field, shifted from its equilibrium position.

- Departure from thermal equilibrium.

  This is realized easily in the expanding Universe.

None of these conditions is obligatory. Different baryogenesis scenarios, where some of the Sakharov's requirements are not fulfilled have been discussed in ref. (*Dolgov*, 1992).

5.1.2 Baryogenesis scenarios

Numerous baryogenesis scenarios exist today, see the reviews (*Dine and Kusenko*, 2004; *Buchmuller et al.*, 2005). Different mechanisms for generation both of the baryon asymmetry and the dark matter of the Universe and their dependence on the reheating temperature have been discussed (*Buchmuller et al.*, 2005). The most studied among the baryogenesis scenarios are Grand Unified Theories (GUT) baryogenesis (*Sakharov*, 1967), Electroweak (EW) baryogenesis (*Kuzmin et al.*, 1985b,a), Baryogenesis-through-leptogenesis (often called leptogenesis) (*Fukugita and Yanagida*, 1986), Affleck-Dine (AD) baryogenesis (*Affleck and Dine*, 1985), etc.

GUT baryogenesis is the earliest baryogenesis scenario, proceeding at GUT unification scale M_{GUT}. However, most inflationary models predict reheating temperature below this scale. Besides, successful unification requires supersymmetry. SUSY implies the existence of gravitinos, which are too numerously produced unless the reheating temperature is well below M_{GUT} (*Rubakov et al.*, 1982; *Weinberg*, 1982).

EW baryogenesis is theoretically attractive because it relies only upon weak scale physics and is experimentally testable scenario. For a review see *Rubakov and Shaposhnikov* (1996); *Morrissey and Ramsey-Musolf* (2012). However, the simplest and most appealing version of this scenario cannot generate within the Standard Model the observed value of the baryon asymmetry, because of the insufficient CP-violation induced by CKM phase and the requirement of first order electro-weak transition, possible only for Higgs boson mass considerably smaller than the detected one by ATLAS and CMS collaborations.

EW baryogenesis in Minimal Supersymmetric Standard Model was considered.

Now MSSM window for EW baryogenesis is substantially narrowed by the experimental data from LHC (*Carena et al.*, 2013) and recent electron dipole measurements. The viable parameter space is considerably reduced.

Baryogenesis-through-leptogenesis is a plausible possibility. Baryon asymmetry in this scenario is created before the electroweak phase transition, which then gets converted to the baryon asymmetry in the presence of (B+L) violating anomalous processes. For a review see *Buchmuller et al.* (2005); *Davidson et al.* (2008); *Blanchet and Di Bari* (2012). It has become especially attractive after the discovery of non-zero neutrino masses in neutrino oscillations experiments. Baryogenesis through leptogenesis mechanisms in different extensions of the SM are studied.

Possibilities for falsifying concrete realizations of high scale leptogenesis from recent LHC data have been proposed (*Frere et al.*, 2009).

Neutrino Minimal Standard Model (νMSM) can potentially account simultaneously for baryon and dark matter generation and neutrino oscillations (*Caneti and Shaposhnikov*, 2010). νMSM is testable at colliders and in astrophysical observations. For a recent review and constraints form collider experiments, astrophysics and cosmology see *Canetti et al.* (2013).

AD baryogenesis scenario (*Affleck and Dine*, 1985; *Dine and Kusenko*, 2004) is one of the most promising today baryogenesis scenarios, compatible with inflation. Nice reviews of AD baryogenesis contemporary status can be found in *Dine and Kusenko* (2004); *Enqvist and Mazumdar* (2003). AD baryogenesis has numerous attractive features. A short list of these is as follows:

(i) It is extremely efficient - it can produce equal or much bigger than the observed baryon asymmetry;

(ii) It can be realized at lower energy, i.e. relatively late in the Universe evolution. I.e. it is consistent with the low energy scales after inflation;

(iii) AD condensate can be generated generically in different cosmological models;

(iv) It can explain simultaneously the generation of the baryon and the dark matter in the Universe, and explain their surprisingly close values;

(v) AD model, due to its high efficiency, can be successful even in case of significant production of entropy at late times, predicted by some particle physics models.

The original AD scenario is based on SUSY. In supersymmetric models scalar superpartner of baryons and leptons φ exist. The potential of such scalar field U(φ) may have flat directions, along which the field can have a non-zero vacuum expectation value due to quantum fluctuations during inflation. After inflation φ evolves down to the equilibrium point $\varphi = 0$ and if U(φ) is not symmetric with respect to the phase rotation it acquires non-vanishing and typically large baryon charge. Subsequent B-conserving decay of φ into quarks and leptons transforms baryon asymmetry into the quarks sector. In contrast to other scenarios of baryogenesis, in which the generated asymmetry usually is insufficient, the original Afleck-Dine scenario leads to higher value of β and additional mechanisms are needed to dilute it down to the observed value.

AD mechanism was re-examined in *Dine et al.* (1996).It has been realized that finite energy density of the early Universe breaks SUSY and induces soft parameters in the soft potential along flat directions, which are of the order of the Hubble parameter. Then, contrary to the original AD mechanism the observed value of the baryon asymmetry may be generated, without the requirement of subsequent entropy release. Different issues on AD baryogenesis were presented in *Dolgov and Kirilova* (1989). AD baryogenesis mechanism was used in numerous SM extensions and different inflationary scenarios. Just to list several of the more recent studies: AD in effective supergravity, AD in anomaly mediated SUSY breaking models, AD in SUSY with R-parity violation, AD in D-term inflation, etc. Most of AD baryogenesis models can naturally explain as well the origin of the dark matter in the Universe.

Here and in the next chapter we discuss the scalar field condensate baryogenesis model (SFC baryogenesis), which is among the preferred today baryogenesis scenarios, compatible with inflation. It is based on the Affleck-Dine scenario.

Here we discuss baryogenesis model based on Scalar field condensate (SFC) baryogenesis model first discussed by *Dolgov and Kirilova* (1991) and further studied and numerically analyzed in series of papers (*Kirilova & Chizhov*, 2000), (*Kirilova and Chizhov*, 1996b; *Kirilova*, 2003b) and (*Panayotova and Kirilova*, 2012; *Kirilova and Panayotova*, 2007; *Kirilova*, 2011b). The next section describes the basic features of the model. Numerical analysis of the evolution of the baryon charge carrying scalar field is provided for many different sets of models parameters. The role of particle creation by the time-varying scalar field and a proper account for particle creation is discussed. The dependence of the evolution and of the final value of the baryon excess on the model's parameters is presented.

5.2 Scalar Field Condensate Baryogenesis

The SFC baryogenesis model was first discussed analytically by *Dolgov and Kirilova* (1989, 1991). There it was also shown that the account of particle creation by the time varying scalar field will lead to strong reduction of the produced baryon excess in the Affleck-Dine scenario. Namely, it was proven that fast oscillations of φ result in particle creation due to the coupling of the scalar field to fermions $g\varphi f_1 f_2$, where $g^2/4\pi = \alpha$. For $\lambda_i^{3/4} > g$ the rate of particle creation Γ exceeds the ordinary decay rate of φ at the stage of baryon non-conservation and, therefore, its amplitude is damped. Hence, the baryon charge, contained in the condensate, is reduced due to particle creation at this stage with considerable baryon violation. [3]

[3]In case of $\Gamma = const$ the baryon charge, contained in the condensate, is reduced exponentially and it does not survive till φ decays to quarks and leptons. In case when Γ is a decreasing function of time the damping process may be slow enough for the baryon charge contained in φ to survive until the B-conservation epoch.

It was discussed in detail in (*Dolgov and Kirilova*, 1991) that for a constant Γ this reduction is exponential and generally, for a natural range of the model's parameters, the baryon asymmetry is waved away till baryogenesis epoch as a result of the particle creation processes. Fortunately, in the case when the production rate is a decreasing function of time, the damping process may be slow enough for a considerable range of acceptable model parameters values of m, H, α, and λ, so that the baryon charge contained in ϕ may survive until the advent of the B-conservation epoch.

The temperature of evaporation of the condensate was also discussed.

The precise numerical account for the particle creation processes in SFC baryogenesis was found necessary. In series of papers (*Kirilova and Chizhov*, 1996b), *Kirilova & Chizhov*, 2000, (*Kirilova*, 2003b; *Kirilova and Panayotova*, 2007; *Panayotova and Kirilova*, 2012), we explored numerically SFC baryogenesis model. In this chapter we present the results of our numerical analysis of the evolution of the baryon excess in SFC baryogenesis model and its dependence on the model parameters.

The production of matter-antimatter asymmetry in this scenario proceeds generally at low energies ($\leq 10^9$ GeV). This is of special importance having in mind that the low-temperature baryogenesis scenarios are the preferred ones, as far as for their realization in the postinflationary stage it is not necessary to provide considerable reheating temperature.

The essential ingredients of the SFC baryogenesis model are:

- baryon charged complex scalar field ϕ (scalar superpartner of quarks), present together with the inflaton;
- flat directions in the potential $U(\phi)$;
- BV at microdistances at the inflationary stage;

  The baryon charge of the field is not conserved at large values of ϕ due to B-violating self-interaction terms in the field's potential. Due to that the condensate of a baryon charge (stored in $< \phi >$) is produced during inflation $B \sim H_I^3$.

- decrease of the field's amplitude after inflation;

  After inflation ϕ oscillates around its equilibrium point with a decreasing amplitude, due to (i) Universe expansion and (ii) particle production by the oscillating scalar field.

- fields decay.

  In case the baryon charge contained in ϕ survives until B-conservation epoch t_b, it is transferred to quarks during the decay of the field $\phi \to q\bar{q}l\gamma$ at t_b and an antisymmetric plasma appears. Its charge, eventually diluted further by some entropy generating processes, dictates the observed baryon asymmetry.

5.2.1 Scalar field condensate

The essential ingredient of the model is a scalar field – squark condensate ϕ, with a nonzero baryon charge. It naturally appears in supersymmetric theories and is a scalar superpartner of quarks. The condensate $< \phi > \neq 0$ is formed during the inflationary period as a result of the enhancement of quantum fluctuations of the ϕ field (*Vilenkin and Ford*, 1982; *Linde*, 1982; *Bunch and Davies*, 1978; *Starobinsky*, 1982):

$$< \phi^2 > = H^3 t / 4\pi^2$$

until the limiting value $< \varphi^2 > \sim H^2/\sqrt{\lambda}$ in case that $\lambda\varphi^4$ terms dominate in the potential energy of φ.

The baryon charge of the field is not conserved at large values of the field amplitude due to the presence of the B nonconserving self-interaction terms in the field's potential. As a result, a condensate of a baryon charge (stored in $< \phi >$) is developed during inflation with a baryon charge density of the order of H_I^3, where H_I is the Hubble parameter at the inflationary stage.

5.2.2 Evolution of the baryon asymmetry in SFC baryogenesis model

After inflation ϕ starts to oscillate around its equilibrium point with a decreasing amplitude. This decrease is due to the Universe expansion and to the particle production by the oscillating scalar field. We discuss the more promising case of particle production when ϕ decays into fermions and there is no parametric resonance. (The case of decays into bosons due to parametric resonance, especially in the broad resonance case, will lead to an explosive decay of the condensate, and hence an insufficient baryon asymmetry.)

We study the natural case, when the inflaton density dominates, $\rho_\psi > \rho_\phi$, and after inflation $H = 2/(3t)$, because the Universe is dominated by a coherent oscillations of the inflaton field

$$\psi = m_{PL}(3\pi)^{-1/2}\sin(m_\psi t).$$

Its density diminishes with the expansion according to:

$$\rho = m_\psi^2 M_{Pl}^2 [R_i/R]^3 \tag{5.6}$$

Then in the expanding Universe ϕ satisfies the equation

$$\ddot{\phi} - a^{-2}\partial_i^2\phi + 3H\dot{\phi} + \frac{1}{4}\Gamma\dot{\phi} + U'_\phi = 0, \tag{5.7}$$

where $a(t)$ is the scale factor and $H = \dot{a}/a$.

For spatially homogeneous field the second term vanishes.

The potential $U(\phi)$ is chosen in the form

$$U(\phi) = m^2\phi^2 + \frac{\lambda_1}{2}|\phi|^4 + \frac{\lambda_2}{4}(\phi^4 + \phi^{*4}) + \frac{\lambda_3}{4}|\phi|^2(\phi^2 + \phi^{*2}) \tag{5.8}$$

Baryon charge of the field B is not conserved at large ϕ values due to the B-violating terms in the potential.

The mass parameters of the potential are assumed small in comparison to the Hubble constant during inflation $m \ll H_I$. In supersymmetric theories the constants λ_i are of the order of the gauge coupling constant α. A natural value of m is $10^2 \div 10^4$ GeV.

The initial values for the field variables can be derived from the natural assumption that the energy density of ϕ at the inflationary stage is of the order H_I^4, then $\phi_o^{max} \sim H_I\lambda^{-1/4}$ and $\dot{\phi}_o = 0$.

The term $\Gamma\dot{\phi}$ in the equations of motion explicitly accounts for the eventual damping of ϕ

$$\phi \to \phi exp(-\Gamma t) \tag{5.9}$$

as a result of particle creation processes due to the coupling of the field to fermions $g\phi f_1 f_2$. For $g < \lambda^{3/4}$, Γ considerably exceeds the rate of the ordinary decay of the field:

$$\Gamma_m = \alpha m. \tag{5.10}$$

Fast oscillations of ϕ after inflation result in particle creation due to the coupling of the scalar field to fermions $g\phi\bar{f}_1 f_2$, where $g^2/4\pi = \alpha_{SUSY}$. Therefore, the amplitude of ϕ is damped as

$$\phi \to \phi \exp(-\Gamma t/4)$$

and the baryon charge, contained in the ϕ condensate, is considerably reduced.

5.2.3 Numerical analysis of the evolution of the baryon charge carrying scalar field

We have analyzed semi-analytically and numerically the evolution of the baryon charge carrying scalar field $\phi(t)$ and B(t) using the exact kinetic equations in the period after inflation until the BC epoch. [4] The typical range of energies discussed is $10^{16} - 100$ GeV. We analyzed ϕ and B evolution for natural ranges of values of the model's parameters: $\lambda = 10^{-2} - 5 \times 10^{-2}$, $\alpha = 10^{-3} - 5 \times 10^{-2}$, $H = 10^7 - 10^{16}$ GeV, m = 100 - 1000 GeV. We studied around hundred sets of model's parameters.

Due to the oscillatory character of B, the value of the generated asymmetry is very sensitive to the parameters of the model, as well as to the numerical methods used, and therefore, the problem requires precise studies.

5.2.4 Baryogenesis epoch t_B

When at later stages ϕ relaxes to its equilibrium state, its coherent oscillations produce an excess of quarks over antiquarks (or vice versa) depending on the initial sign of the baryon charge condensate.

This epoch when ϕ decays to quarks with non-zero average baryon charge and thus induces baryon asymmetry we call baryogenesis epoch t_B. This epoch for our model coincides with the advent of the baryon conservation epoch, i.e. the time after which the mass terms in the equations of motion cannot be neglected. In the AD original version this epoch corresponds to energies $10^2 - 10^4$ GeV.

However, as it was already explained, the amplitude of ϕ may be reduced much more quickly due to the particle creation processes and as a result, depending on the model's parameters the advent of this epoch may be considerably earlier.

For the correct estimation of t_B and the value of the generated baryon asymmetry,

[4] In previous studies it was studied semi-analytically.

it is essential to account for the eventual damping of the field's amplitude due to particle production processes by the time-dependent scalar field, which leads to a strong reduction of the baryon charge contained in the condensate.

5.3 The Role of Particle Creation Processes

Particle creation processes by the time dependent scalar field play essential role for the determination of β, hence it is important to account for them as precisely as possible.

The explicit account for the effect of particle creation processes in the equations of motion was proposed in (*Kirilova and Chizhov*, 1996b). The production rate Γ was analytically calculated by *Dolgov and Kirilova* (1990).

In our works, in particular see (*Kirilova and Panayotova*, 2007; *Kirilova and Chizhov*, 1996b) we have accounted for the damping due to particle creation qualitatively: using the perturbation theory approximation for the production rate:

$$\Gamma = \alpha\Omega, \tag{5.11}$$

where the frequency of the scalar field Ω was estimated as $\Omega \sim \lambda^{1/2}\phi$, $g^2/4\pi = \alpha$.

Then we have provided also a precise numerical calculations of Ω and of the particle creation processes, calculating numerically Ω at each step. We solved the system of ordinary differential equations, corresponding to the equation of motion for the real and imaginary part of ϕ, by Runge-Kutta 4th order method for both cases.

We have found that the numerically calculated oscillation frequency of the field for certain model's parameters may be quite different from the analytically estimated one, used in the adiabatical approximation of the particle creation.

We have found that the results for ϕ and B evolution and the final value of B at

BC epoch considerably differ when different accounts for particle creation processes are made.

On the next figures we illustrate the evolution $B(\tau)$ for fixed model's parameters $\lambda_1 = 5 \times 10^{-2}$, $\lambda_2 = \lambda_3 = 5 \times 10^{-4}$, $\alpha = 10^{-3}$, $H = 10^{11} GeV$, $m = 350 GeV$, $\varphi_o = 2^{-1/4} H \lambda^{-1/4}$, and $\dot{\varphi}_o = H^2$, and in two different cases, namely when the particle creation is accounted either numerically or analytically.

The amplitude of B_{num} decreases more sharply than the amplitude of B_{anal} and hence at BC epoch $B_{num} = -2.2 \times 10^{-3}$ and $B_{anal} = -1.7 \times 10^{-2}$. *Therefore, a precise numerical approach for the account of particle creation processes is necessary for constructing a realistic baryogenesis model.*

Using the numerical account for Γ we have calculated the dependence $B(\alpha)$, namely $B(\tau)$ was calculated for $\alpha = 10^{-3}, 10^{-2}, 5 \times 10^{-3}$ and fixed other parameters. The next figure illustrates the dependence of B on α.

With increasing α, B evolution becomes shorter and the final B decreases.

In cases of more effective particle creation, like the case with flat directions in the potential, or in the case when ϕ decays spontaneously into bosons due to parametric resonance, the discussed mechanism of the baryon asymmetry generation is not efficient.

5.4 Dependence of the Baryon Charge Contained in the SFC on Model's Parameters - Numerical Results

We have numerically explored the SFC baryogenesis model for numerous sets of model's parameters, within their natural range of values. In several works (*Kirilova and Panayotova*, 2007, 2013; *Panayotova and Kirilova*, 2012) we have presented our results concerning β dependence on gauge coupling constant α, Hubble constant during inflation H_i, mass of the condensate m and self coupling constants λ_i. Namely:

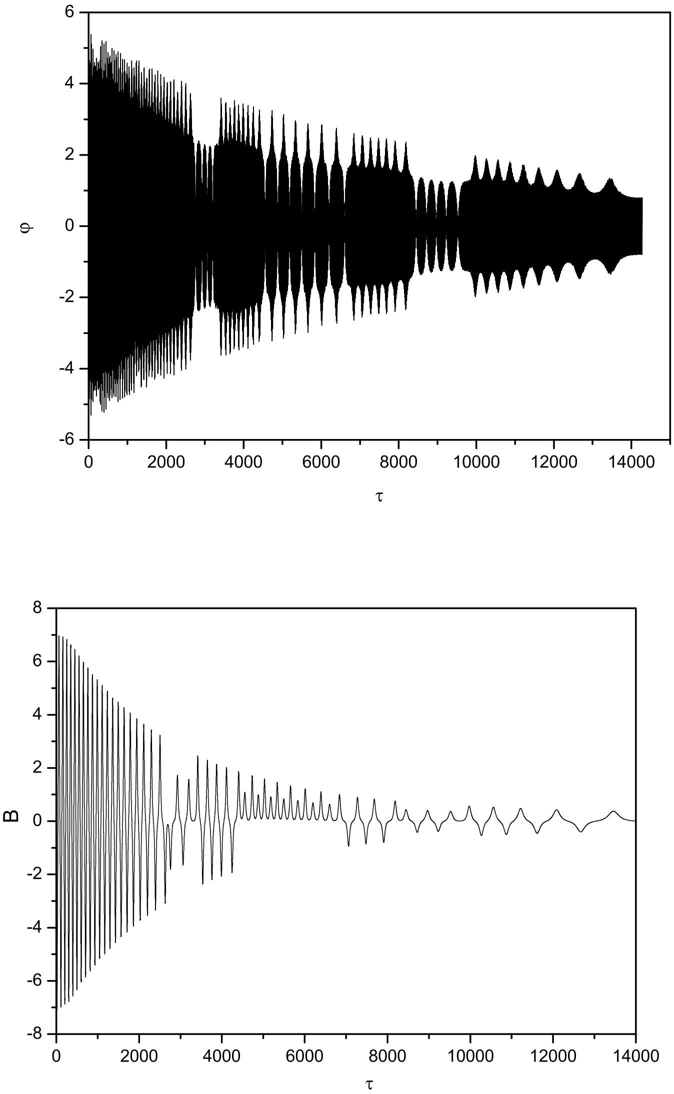

Figure 5.1: The evolution of the scalar field $\varphi(\tau)$ and the baryon charge $B(\tau)$ for $\lambda_1 = 5\times10^{-2}$, $\lambda_2 = \lambda_3 = 5\times10^{-4}$, $\alpha = 10^{-3}$, $H = 10^{11}GeV$, $m = 350GeV$, $\varphi_o = 2^{-1/4}H\lambda^{-1/4}$, and $\dot{\varphi}_o = H^2$. The particle creation processes are accounted analitically. Figure from ref. (*Kirilova and Panayotova*, 2007).

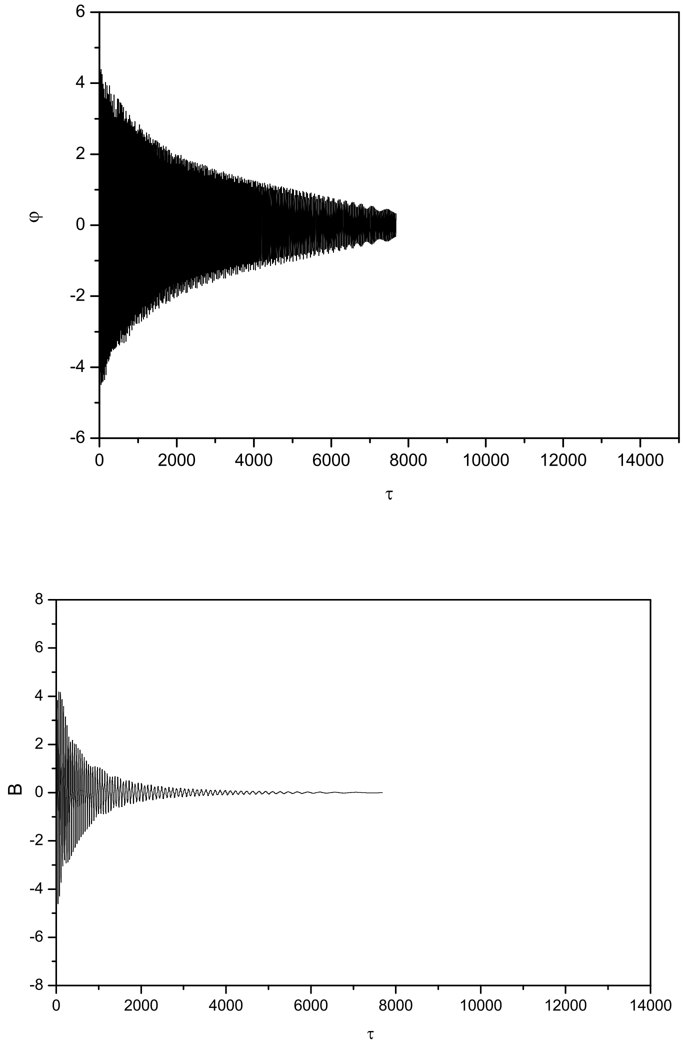

Figure 5.2: The evolution of the scalar field $\varphi(\tau)$ and baryon charge $B(\tau)$ for $\lambda_1 = 5 \times 10^{-2}$, $\lambda_2 = \lambda_3 = 5 \times 10^{-4}$, $\alpha = 10^{-3}$, $H = 10^{11} GeV$, $m = 350 GeV$, $\varphi_o = 2^{-1/4} H \lambda^{-1/4}$, and $\dot{\varphi}_o = H^2$. The particle creation processes are accounted numerically. Figure from ref. (*Kirilova and Panayotova*, 2007).

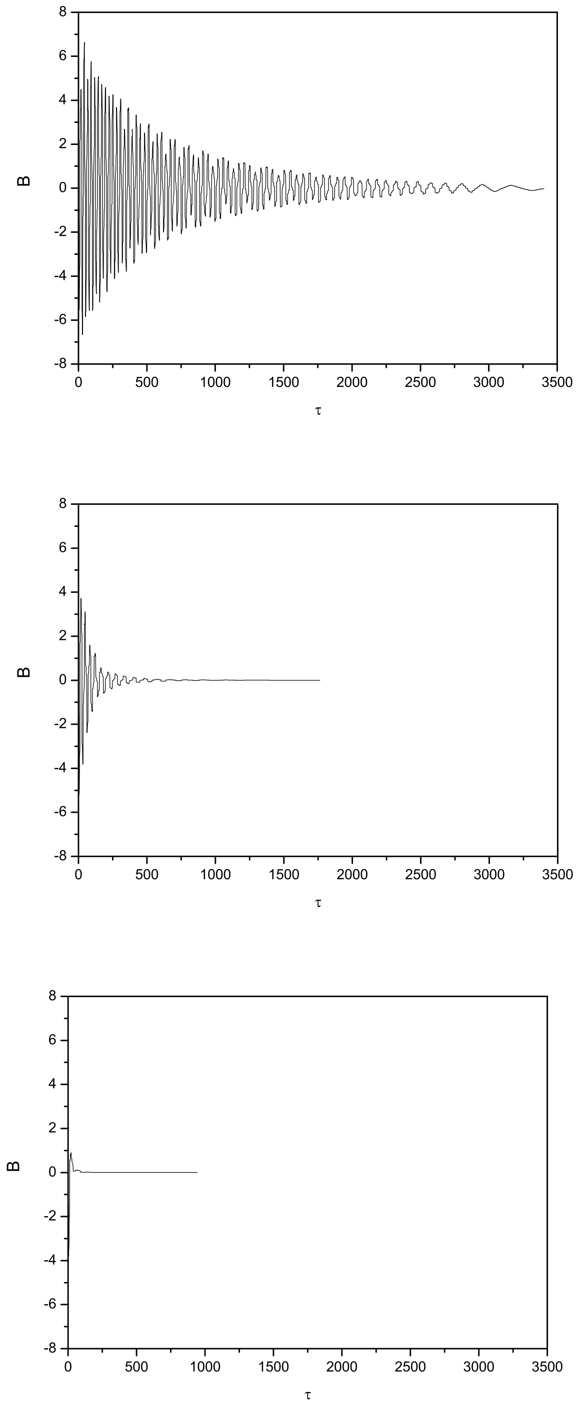

Figure 5.3: The evolution of the baryon charge $B(\tau)$ for $\lambda_1 = 5 \times 10^{-2}$, $\lambda_2 = \lambda_3 = 5 \times 10^{-4}$, $H = 10^{10}GeV$, $m = 350GeV$, $\alpha = 10^{-3}, 10^{-2}, 5 \times 10^{-2}$. Figure from ref. (*Kirilova and Panayotova*, 2007).

(i) **Dependence on the value of the Hubble constant** H_I:

We have followed the evolution $B(t)$ varying H_I for fixed values of the other parameters. We have explored the evolution of the field and the baryon charge $B(t)$ contained in it varying the Hubble constant at the inflationary stage H_I for fixed values of the other parameters.

Our detail analysis for numerous different parameters of the SCF model shows that *B evolution becomes longer and the final B value decreases with the increase of H_I.* This result is in agreement with previous numerical and analytical studies. Qualitatively, this dependence is an expected result because the initial value of ϕ is proportional to H_I and particle creation, which reduces β is proportional to φ, $\Gamma \sim \Omega \sim \varphi$. Thus, the bigger H_I - more efficient is the decrease of β due to particle creation.

(ii) **Dependence on the mass m of the condensate**:

The dependence of the final baryon charge on m for fixed λ_1, λ_2, λ_3, α and H_I has been discussed by *Kirilova and Panayotova* (2007, 2013).

It has been found that in general B decreases with the increase of m. This behavior is more clearly and more strongly expressed for big values of H_I and then corresponds to the expected one from analytical estimations (Namely, as far as m defines the onset of BC epoch: $t_s \sim 1/\alpha m$, and hence for lower values of m, B evolution is longer and the final B value is smaller.)

For smaller values of H_I the dependence is weaker and not so straightforward and clear.

(iii) **Dependence on gauge coupling constant** α:

Using the numerical account for Γ we have calculated $B(t)$ for α varying in the range $10^{-3} - 10^{-2}$ and fixed other parameters. The dependence of B on α is very strong, as can be expected, knowing that particle creation processes play essential role for the evolution of the field and the baryon charge, contained in it, and keeping in mind that the analytical estimation is $\Gamma = \alpha\Omega$.

With increasing α, B evolution becomes shorter and the final B decreases.

(iv) **Dependence on the self-coupling constants**

The dependence of the baryon charge, at the B-conservation epoch, on the value of the coupling constants λ_i was first discussed in (*Panayotova and Kirilova*, 2014). Our extended analysis confirms that the final B value decreases when increasing λ_1 and B evolution becomes shorter. The effect provides a difference in the final B value of an order of magnitude.

The results of the extended analysis showed that the final value of B may be much sensitive to λ_2 and λ_3 than previously estimated. Namely, we have found that the final values of B may differ up to 3 orders of magnitude even for small changes of these parameters (measuring the B-violating terms in the potential).

Thus, we have found that although the dependence of baryon generation on the self-coupling constants is important for determination of the parameters range for the successful baryogenesis model.

5.5 Estimation of the Generated Baryon Asymmetry

In order to estimate the baryon asymmetry on the basis of the obtained results for the produced baryon density it is necessary to know the temperature of the relativistic plasma after the decay of φ and the decay of the inflaton.

In case the inflaton energy density dominates until the decay of φ, i.e. prior to reheating, $\rho_\psi > \rho_\varphi$, the entropy is mainly defined by the relativistic particles from inflaton decay. Thus, the temperature after the decay of ψ at t_ψ will be approximately

$$T_R \sim (\rho_\psi)^{1/4} = (\rho_\psi^0)^{1/4}(t_0/t_\psi)^{1/2}. \tag{5.12}$$

Then the baryon asymmetry will be given by:

$$\beta \sim N_B/T_R^3 \sim (B/H_I)(M_{Pl}/t_\psi)^{1/2} \tag{5.13}$$

The baryon asymmetry may be also expressed through the reheating temperature after the decay of the inflaton:

$$\beta \sim N_B/T_R^3 \sim BT_R/H_I \tag{5.14}$$

From these estimations it is seen that the later the inflaton decays the smaller the produced β will be. Also, the lower the reheating temperature after inflaton decay the lower the produced baryon asymmetry will be. Knowing that the reheating temperature should be sufficiently low to avoid gravitino ptoblem, i.e. in our model it should be several orders or more lower than the value of H_I, and having the results for B it is easy to obtain the value of the observed baryon asymmetry for different sets of parameters in this model.

Our analysis shows that for a natural range of SCB model's parameters, a value of β of the order of the observed one may be obtained. The SCF baryogenesis model can serve as a successful baryogenesis, compatible with inflation.

Of course H_I, the decay time of ψ and the value of the reheating temperature may be different in different inflationary scenarios. We would like only to note that the results of the numerical analysis of the SCF baryogenesis model are encouraging. The analysis points that this model provides an opportunity to produce baryon asymmetry β, consistent with its observed value for natural values of the model's parameters. Therefore, this model deserves further considerations.

5.6 Summary

We have provided precise analysis of the homogeneous SFC baryogenesis model. The post-inflationary evolution of the baryon charge carrying scalar field was followed both semi-analytically and numerically using exact kinetic equations.

It was found that the analytical estimations of the baryon charge evolution and its final value in SFC baryogenesis model may considerably differ from the exact numerically calculated ones. Hence, in several works we have numerically explored the SFC baryogenesis model for numerous sets of model's parameters.

It was shown that particle creation processes play essential role for the B evolution and its final value. It may lead to a considerable decrease of the field's amplitude for large g or/and H values, which reflects finally into strong damping of the baryon charge carried by the condensate. We have accounted precisely for particle creation processes: we have obtained self-consistently the frequency Ω and the rate Γ from the exact numerical analysis of the field's evolution. Numerically calculated Ω may be quite different from the analytical estimation. Thus, the numerical approach for the calculation of Γ was proved necessary.

The precise numerical account for particle creation points to stronger and earlier reduction (up to two orders of magnitude) of the B excess in comparison with the case of analytical account of particle creation processes.

We have investigated the dependence of the evolution of the field and the evolution of the baryon charge contained in it, as well as the final value of the baryon charge on the model's parameters: the gauge coupling constant α, the Hubble parameter at the inflationary stage H_I, the mass m and the self-coupling constants λ_i. Qualitative dependance of the final B on these parameters have been found. Namely, it was shown that the produced baryon excess is a strongly decreasing function of α and also a decreasing function of H_I. The dependence on m is not so straightforward. For small m values B decreases with m increase, however for larger m the dependence is more complicated.

We have found that due to the oscillatory character of the baryon charge stored in the scalar field, the generated baryon asymmetry is sensitive both to small shifts of the model's parameters and to the numerical methods used. Nevertheless, the main trend of the behavior of the final baryon excess B on the parameters' values can be determined.

The analysis may be used to indicate the values of the model's parameters for which baryon asymmetry β, consistent with its observed value, may be produced in a given inflationary scenario.

The results of this analysis may be used for constructing realistic SCF baryogenesis models. Moreover, assuming SCM baryogenesis and assuming a concrete inflationary scenario, from the observed value of the baryon asymmetry it is possible to put cosmological constraints on the model's parameters, provided by physics theories, i. e. constrain physics beyond Standard model.

On the other hand, it is expected that future searches for experimental and observational signatures of physics beyond the standard model, as well as searches for antimatter and dark matter, and also the more precise future cosmological and astrophysical data will provide constraints on baryogenesis models and hopefully soon will point to the baryogenesis mechanism realized in Nature.

CHAPTER VI

Processes Essential for the Generation of the Baryon Inhomogeneities in the Universe

In this chapter we discuss inhomogeneous baryogenesis model, based on SFC baryogenesis. First we discuss the possibility of primary antimatter in the Universe. We study numerically the evolution of the baryon density space distribution and the possibility of SFC baryogenesis model to provide a mechanism for efficient separation of matter from antimatter domains in the Universe. Predicted antimatter structures and observational constraints on their size and separation distance are discussed. In the second section we review the observational indication for a very large scale in the large scale structure of the Universe and study the possibility to generate baryon density perturbations in the SFC baryogenesis model, which can explain the observed large scale and the quasi-periodicity of the visible matter. The last section presents a summary of the results.

6.1 Inhomogeneous SCF Baryogenesis Model Predicting Antimatter in the Universe

6.1.1 Possibilities for primary antimatter in the Universe - observational status

Though the available CR and GR data on cosmic/galactic antimatter, obtained from balloons and spacecraft searches (BESS, AMS, PAMELA, etc.), point to a strong *predominance of matter over antimatter in out Galaxy* and the small antimatter constituent may be explained as of secondary origin, a small primary component of antimatter is not excluded.

CR data: Although the measured $\bar{p}$ flux and its spectrum is in agreement with the predicted for secondaries, *extragalactic primary component is not excluded.* On one side, CR at the rigidities accessible to antimatter experiments are expected to be strongly suppressed by galactic, cluster and intergalactic magnetic fields (*Ormes et al.*, 1997). On the other hand the uncertainty of the predicted secondary antimatter is big. Namely, the analysis of uncertainties in the predicted antiproton flux due to spallations of CR on interstellar matter in our Galaxy, including all possible sources of uncertainty, show: $10-25\%$ propagation related uncertainty and 25% related to nuclear reactions (*Donato et al.*, 2001). Hence, primary extragalactic component in $\bar{p}$ cannot be ruled out with high significance. Even in case the propagation parameters were known it is very probable that a fraction of the observed antiprotons are cosmic rays from distant antigalaxies.

The observations do not forbid astronomically significant clumps of antimatter in our dominated by matter Galaxy (*Dolgov*, 2011).

Gamma ray data:

The absence of the expected annihilation features of $\bar{p}p$ annihilations, in the γ-ray data limits the antimatter fraction for different structures (*Steigman*, 1976) and/or the distance to the antimatter domains – $l_b > 10$ Mpc. I.e. we can expect the nearest anti-galaxy to be at least at 10 Mpc distance from our Galaxy.

The mass fraction of antimatter in the two colliding galaxies in the Bullet cluster was estimated to be smaller than 10^{-6} (*Steigman*, 2008).

In case of assumptions of baryosymmetric Universe, adiabatic perturbations and continuous close contact between the antimatter and matter domains, the limit is much stronger – $l_b > 1$ Gpc *Cohen et al.* (1998).

Analysis of annihilation features within concrete baryogenesis model and the EGRET gamma ray background data showed that a fraction ($< 10^{-6}$) of antimatter stars in our Galaxy is allowed (*Belotsky et al.*, 2000).

There are also limits based on BBN considerations, which forbid large fluctuations of the baryon density at distances higher than 1 Mpc. CMB anisotropy data restricts noticeable isocurvature fluctuations larger than 10 Mpc.

Thus, observational data do not rule out antimatter domains in the Unioverse, they constrain antimatter fraction at certain scales. So, it is interesting to explore possibilities for production of antimatter regions in the Universe in the inhomogeneous SFC baryogenesis model and their observational signatures and constraints. Moreover, it has already been shown that SCF inhomogeneous baryogenesis model can naturally explain the generation of small fraction ($< 10^{-6}$) of antimatter stars, primordial antiblackholes, antiquasars, *Dolgov and Silk* (1993), one antimatter globular cluster, allowed by CR and GR data *within our Galaxy.* We have explored bigger antimatter structures, namely *beyond our Galaxy*, at distances typical for galactic clusters, big antimatter structures like antigalaxies, groups and clusters of antigalaxies (*Kirilova and Chizhov*, 1996b; *Kirilova*, 1998a, 2003b) are predicted for natural range of the parameters of the discussed here SFC baryogenesis model.

In case of *local* character of the asymmetry, the problem reduces to finding a natural baryogenesis mechanism able to produce inhomogeneities and baryons and antibaryons at different space regions.

There exist different baryogenesis models, predicting matter and antimatter regions *Dolgov* (1992). In the next sections SFC inhomogeneous baryogenesis model predictions concerning antimatter in the Universe will be presented. The cosmological constraints for different cases of antimatter structures will be discussed.

6.1.2 SFC inhomogeneous baryogenesis model

Attractive features of SFC baryogenesis from the view point of antimatter cosmology are:

- It does not suffer from the basic problems of antimatter cosmology models,

i.e. the causality problem, the annihilation catastrophe problem, the domain walls problem, discussed in detail in (*Steigman*, 1976).

- It generates large antimatter domains and can provide a natural separation between them and the matter domains.

- The characteristic scale of antimatter regions and their distance from matter ones may be in accordance with the observational constraints for natural choice of parameters, as will be shown below.

The necessary conditions for generation of vast separated regions of matter and antimatter by the SFC baryogenesis model are (*Chizhov and Dolgov*, 1992):

(i) initial space distribution at the inflationary stage $\phi(r, t_0)$, $B(r, t_0)$;

(ii) unharmonic potential of the field carrying the baryon charge;

(iii) inflationary expansion of the initially microscopic baryon distribution.

Due to that initially microscopic domains with given B sign evolve into matter and antimatter regions with astronomically considerable size.

6.1.3 Evolution of the baryon density distribution

We studied the evolution of the baryonic space distribution, assuming a monotonic initial distribution of the baryon density within a domain with a certain sign of the baryon number $B(r, t_0) \sim \phi(r, t_0)$. For different sets of parameter values of the model λ_i, α, m/H_i, we have numerically followed the evolution $B(r, t)$ for all initial values of the field $\phi_o^i = \phi(r_i, t_0)$ till t_b.

In case of nonharmonic field's potential, the period depends on the amplitude. In our model the dependence is $\omega \sim \lambda^{1/2}\phi_i(r)$. As a result in different points different periods are observed and the initial smooth distribution $\phi_i(r)$ soon transfers into quasiperiodic. Correspondingly, the spatial distribution of baryons $B(t_b, r)$ is found to be quasiperiodic (*Kirilova and Chizhov*, 1996b; *Kirilova*, 2003b), *Kirilova & Chizhov*, 2000.

The region r_0 which initially was characterized with its baryon excess splits into regions with baryon excess and such of baryon underdensities. Due to the smoothly decreasing baryon density towards the borders between the baryonic and antibaryonic regions, predicted by the model, annihilation is not considerable, and hence the strong GR constraint (*Cohen et al.*, 1998) does not apply. Matter and antimatter domains become separated by large empty from baryons voids, perhaps filled with dark matter.

Due to inflation the regions with different baryon density (overdensity, underdensity or density of antibaryons with size d) becomes macroscopically large $d \rightarrow d\exp(Ht)$. *The characteristic scale between matter and antimatter regions* is a function of the models parameters, $l_b = l(\lambda_i, \phi(r, t_i), t_b, r_0)$, namely: the coupling constants of the potential λ_i, the initial amplitudes of the field $\phi(r, t_i)$, the period of baryogenesis t_b and the characteristic scale of the baryonic spatial variation at the inflationary stage r_o. The provided analysis showed that for a natural choice of the values of these parameters the separation scale may be in the Mpc - 100 Mpc range.

Different cases of CP-violation are possible:

A. *Stochastic CP-violation*: There is no explicit breaking of the CP-symmetry. CP is broken only stochastically at the inflationary stage by the chaotic initial conditions $\phi_i(x) \neq 0$. Due to the quantum fluctuations of the field a baryon charge is generated at micro distances. In different domains it may have different values. On macro distances there is no global BV, i.e. at macro scales the baryon density fluctuations are unobservable. Due to the exponential expansion during the inflationary epoch these microscopic regions become of astronomically considerable size.

The variations of B appear around zero. The initially baryonic domain is broken to baryonic and antibaryonic regions and divided by nearly baryonically empty space. The case is attractive as far as it allows the realization of symmetric Universe without domain walls. However, the resulting fluctuations of the baryon density may be considerable and lead to unacceptably large angular variations of the microwave background radiation.

B. *Stochastic+explicit CP-violation*: The field's equilibrium value is non zero, and the fluctuations of the field around it result into fluctuations of the baryon density around some mean number. Then at t_b the domain with a given sign of explicit CPV may consist predominantly of baryonic regions plus small quantity (for $l \sim 100$ Mpc it is $\sim 10^{-4}$) of antibaryonic ones. Though not so aesthetic, because in that case there should be besides the stochastic CPV discussed, another mechanism of CPV producing the mean baryon density, this case is more promising.

6.1.4 Predicted antimatter structures and observational constraints

Using the constraints from gamma rays and CR data, BBN and CMB anisotropy measurements, we discuss different realizations of the model.

Recent CMB measurements ruled out pure isocurvature perturbations models, so, accordingly, the case when the baryon charge carrying field is the inflaton itself, is excluded. Other possibilities, when besides the inflaton there exists a second scalar field during inflation with the features discussed in our model remain viable. According to the recent mixed isocurvature plus adiabatic models, although the isocurvature contribution is not suggested it has neither been ruled out.

A. **Stochastic CP-violation**

Case A.1. The first most simple case we considered assumed that the overdensity regions correspond to galaxy or antigalaxy superclusters with big voids between with a characteristic size $\sim 120-130$ Mpc. In that case the antimatter domains are roughly of the same scale and the similar density as the matter ones. CR and gamma-ray data constraints are fulfilled. Large variation of the primordially produced elements, should be observable at the corresponding scales. There are no data for the rest light elements at large distances, however the observed D towards high-z quasars shows some deviations from the expected primordial plateau. Alas, in that case the magnitude of the isocurvature perturbations is high and may induce CMB anisotropies not compatible with the data (*Enqvist et al.*, 2000).

Case A.2 Smaller structures of antimatter $< 10-20$ Mpc are possible. The CMB constraint weakens when decreasing the scale. However, CR and gamma-ray data restricts the number of such smaller antimatter objects, not excluding, however, the possibility for their existence. Spatial variations of the light elements are expected also.

B. **Stochastic+explicit CP-violation**:

Case B.1. There exist vast matter superclusters with typical scale D at $L \sim 120$ Mpc separation (as observed), while the antimatter objects are of characteristic scales $d \leq 10^{-4}D$. Hence, depending on the following evolution these antimatter regions may collapse to form small antigalaxies, antistar clusters or vast dense antihydrogen clouds. They are at a safe distance from the matter superclusters about $l_b \sim 60$ Mpc. All the observational constraints may be satisfied.

Case B.2 The scales of the antimatter domains are of galaxy cluster or galaxy scales. As CMB constraints weaken at smaller scales, mainly CR and GR data restricts the number of antimatter object in that case. Different possibilities for antimatter domains may be realized, namely an antimatter galaxy may wonder between galaxy clusters, a globular star anticluster may be found in the space between groups of galaxies.

In conclusion: In general the model proposes the possibility that only our vicinity is baryonic, while globally the Universe may contain considerable quantities of antibaryons, and in the extreme case may be symmetric. The inhomogeneous baryogenesis model may predict different antimatter structures (*Kirilova*, 2003b): antigalactic clusters, antigalaxies situated between clusters of galaxies, antistar globular clusters

The discussed mechanism of separation of matter from antimatter domains could be realized in a variety of models, depending on the type of the baryogenesis model, on the field potential, on the type of the CP-violation, on the initial space distribution of the baryon density at the inflationary stage, etc.

Eventual future positive indications for antimatter at CR experiments on long balloon flights and spacecraft, planning to measure antiproton and positron spectra at wide range of energies ($0.1 - 150$ GeV) (as by PAMELA magnetic spectrometer) and reach a sensitivity for antinuclei at $\sim 10^{-7}$ (AMS magnetic spectrometer), will help to choose among the existing variety of baryogenesis models, give information about their parameters.

Future searches for antimatter among cosmic rays are expected to increase this lower bound of the distance to the antimatter regions (20 Mpc) by nearly an order of magnitude. Namely, the reach of the AntiMatter Spectrometer is expected to exceed 150 Mpc (Ahlen et al. 1982) and its sensitivity is three orders of magnitudes better than that of the previous experiments. Then future experiments on long balloon flights and spacecraft may reveal the secrets of nearby (up to 150 Mpc) antiworlds and may allow to to establish the theory of baryogenesis.

6.2 SFC Baryogenesis and Large Scale Structure of the Universe

6.2.1 Introduction.

The large scale texture of the Universe shows a great complexity and variety of observed structures, it shows a strange pattern of filaments, voids and sheets. Moreover, due to the increasing amount of different types of observational data and theoretical analysis during the last years, it was realized, that *there exists a characteristic very large scale of about* $130h^{-1}$ Mpc in the large scale texture of the Universe.

Below we discuss briefly some of the indications for the presence of the very large scale $120 - 130h^{-1}$ Mpc in the LSS.

- Galaxy deep pencil beam surveys

The galaxy deep pencil beam surveys by (*Broadhurst et al.*, 1988, 1990) found an intriguing periodicity in the very large scale distribution of the luminous matter. The data consisted of several hundred redshifts of galaxies, coming from four distinct surveys, in two narrow cylindrical volumes into the directions of the North and the South Galactic poles of our Galaxy, up to redshifts of more than $z \sim 0.3$, combined to produce a well sampled distribution of galaxies by redshift on a linear scale extending to $2000h^{-1}$ Mpc. The plot of the numbers of galaxies as a function of redshifts displays a remarkably regular redshift distribution, with most galaxies lying in discrete peaks, with a periodicity over a scale of about $130h^{-1}$ Mpc comoving size, extending over 13 periods. Though initially rejected as a statistical anomaly, the periodicity was confirmed by the following studies.

It was realized that the density peaks in the regular space distribution of galaxies in the redshift survey of Broadhurst et al. correspond to the location of superclusters, as defined by rich clusters of galaxies in the given direction (*Bahcal*, 1991).

The survey of samples in other directions, located near the South Galactic pole also gave indications for a regular distribution on slightly different scales near $100h^{-1}$ Mpc, see for example *Ettori et al.* (1995).

This discovery of a large scale pattern at the galactic poles was confirmed in *a wider angle survey* of 21 new pencil beams distributed over 10 degree field at both galactic caps (*Broadhurst et al.*, 1995) and also by the new *pencil-beam galaxy redshift data around the South Galactic pole* region (*Ettori et al.*, 1997).

The analysis of observations of other types of different objects confirm the existence of this periodicity.

- quasars, galaxies and galaxy clusters

Such structure is consistent with the reported periodicity in the distribution of quasars and radio galaxies and Lyman-α forest; the studies on spatial distribution of galaxies (both optical and IRAS) and clusters of galaxies.

An indication of the presence of this characteristic scale in the distribution of clusters has been found also from the *studies of the correlation functions and power spectrum of clusters of galaxies* (*Einasto et al.*, 1994, 1997).

The study of the whole-sky distribution of high density regions defined by very rich Abell and APM clusters of galaxies confirmed from 3-dimensional data the presence of the characteristic scale of about $130h^{-1}$ Mpc of the spatial inhomogeneity of the Universe, found by Broadhurst et al. from the one dimensional study. For a detail list of references on the regularity of the Universe on large scales see (*Einasto et al.*, 1997), *Kirilova & Chizhov*, 2000.

- superclusters

The supercluster distribution was shown also to be not random but rather described as some weakly correlated network of superclusters and voids with typical mean separation of $120h^{-1}$ Mpc. Peculiar velocity information suggests the existence of a large scale superclusters-voids network with a characteristic scale around $130h^{-1}$ Mpc. These results are consistent with the statistical analysis of the pencil beam surveys data, which advocated a regular structure.

- CMB data

The fact that the Universe is not homogeneous and fully isotropic at scales $130h^{-1}$ Mpc does not contradict the observed level of isotropy of the CMB. CBM data favors the presence of a peak at this scale and the subsequent break in the initial power spectrum. Namely, CMB background anisotropy data indicates the presence of a features in the spectrum, consistent with the LSS data, indicating a peak in the matter power spectrum at $k \sim 0.05h$ Mpc^{-1}.

Thus, *the observations and their theoretical analysis present an evidence for the regularity of the supercluster-void network: Different objects trace the same structure, the same high-density regions at large scales, pointing to the real existence of a typical large scale of the matter distribution of the Universe.* Rich superclusters and voids form a quasi-rectangular lattice with a mean separation of rich superclusters across voids of $120 - 130h^{-1}$ Mpc.

However, this scale is significantly larger than the predicted by standard models of structure formation by gravitational instability, see for example (*Eisenstein et al.*, 1998), and is rather to be regarded as a new feature appearing only when very large scales ($> 100h^{-1}$ Mpc) are probed. Cosmological N-body simulations in CDM model showed that the regularity has a probability below 10^{-3} in these models.

6.2.2 Generation of the spatial periodicity. Qualitative description

The problem of the generation of the spatial periodicity in the density distribution of luminous matter at large scales was discussed in numerous publications. It was shown that a random structure could not explain the observed distribution. Statistical analysis of the deviations from periodicity showed that even for a perfectly regular structure a somewhat favored direction and/or location within the structure may be required. The presence of the observed periodicity up to a great distance and in different directions seams rather amazing. Its physical origin, its scale and extend is an open question.

Having in mind this results, we chose another way of exploration, namely, we assumed these as a typical new feature characteristic only for very large scales ($>100h^{-1}$ Mpc) and considered the possibility that density fluctuations required to explain the present cosmological largest scale structures of the universal texture may be a result from a completely different mechanism not necessarily with gravitational origin. Namely, we considered SFC inhomogeneous baryogenesis scenario and we found it capable to answer these questions rather naturally.

A successful baryogenesis mechanism, explaining the observed periodicity, was proposed by *Chizhov and Dolgov* (1992) in the framework of high-temperature baryogenesis scenarios.[1]

According to the discussed mechanism an additional complex scalar field (besides inflaton) is assumed to be present at the inflationary epoch, and it yields the extra power at the very large scale discussed. Primordial baryonic fluctuations are produced during the inflationary period, due to the specific evolution of the space distribution of the complex scalar field, carrying the baryon charge.

[1]By high-temperature baryogenesis scenarios we denote here those scenarios which proceed at very high energies of the order of the Grand Unification scale, and especially the GUT baryogenesis scenarios. In contrast, low temperature baryogenesis scenarios like Affleck and Dine scenario and electroweak baryogenesis, proceed at energies several orders of magnitude lower .

We studied the possibility of generating the periodic space distribution of primordial baryon density fluctuations at the end of inflationary stage, applying this mechanism for the case of low temperature baryogenesis with baryon charge condensate of *Dolgov and Kirilova* (1991).

We provided detail analysis of the evolution of the baryon density perturbations from the inflationary epoch till the baryogenesis epoch and described the evolution of the spatial distribution of the baryon density (*Kirilova*, 2003b; *Kirilova and Chizhov*, 1996b, 2000b).

It was already discussed (*Chizhov and Dolgov*, 1992) that a periodic in space baryonic density distribution can be obtained provided that the following assumptions are realized:

(a) There exists a complex scalar field ϕ with a mass small in comparison with the Hubble parameter during inflation;

(b) Its potential contains nonharmonic terms;

(c) A condensate of ϕ forms during the inflationary stage and it is a slowly varying function of space points.

All these requirements can be naturally fulfilled in SFC baryogenesis and in low temperature baryogenesis scenarios based on the Affleck and Dine mechanism (*Affleck and Dine*, 1985).

In case when the potential of ϕ is not strictly harmonic the oscillation period depends on the amplitude $P(\phi_0(r))$, and it on its turn depends on r. Therefore, a monotonic initial space distribution will soon result into spatial oscillations of ϕ. Correspondingly, the baryon charge, contained in ϕ: $B = i\phi^* \overleftrightarrow{\partial}_0 \phi$, will have quasi-periodic behavior. During Universe expansion the characteristic scale of the variation of N_B will be inflated up to a cosmologically interesting size. Then, if ϕ has not reached the equilibrium point till the baryogenesis epoch t_B, the baryogenesis would make a snapshot of the space distribution of $\phi(r, t_B)$ and $B(r, t_B)$, and thus the present periodic distribution of the visible matter may date from the spatial distribution of the baryon charge contained in the ϕ field at the advent of the B-conservation epoch.

Density fluctuations with a comoving size today of $130h^{-1}$ Mpc reentered the horizon at late times at a redshift of about 10 000 and a mass of $10^{18}M_o$. After recombination the Jeans mass becomes less than the horizon and the fluctuations of this large mass begin to grow. We propose that these baryonic fluctuations, periodically spaced, lead to an enhanced formation of galaxy superclusters at the peaks of baryon overdensity. The concentration of baryons into periodic shells may have catalysed also the clustering of matter coming from the inflaton decays onto these "baryonic nuclei". After baryogenesis proceeded, superclusters may have formed at the high peaks of the background field (the baryon charge carrying scalar field, we discuss). We imply that afterwards the self gravity mechanisms might have optimized the arrangement of this structure into the thin regularly spaced dense baryonic shells and voids in between with the characteristic size of $130h^{-1}Mpc$ observed today.

The analysis showed that in the framework of our scenario both the generation of the baryon asymmetry and the periodic distribution of the baryon density can be explained simultaneously as due to the evolution of the complex scalar field.

Moreover, for a certain range of parameters the model predicts that the Universe may consist of sufficiently separated baryonic and antibaryonic shells, as discussed in the previous section.

The following subsection describes the results of the numerical analysis of the generation of the periodicity of the baryon density and discusses the results.

6.2.3 Generation of the baryon density periodicity. Numerical analysis

In order to explore the spatial distribution behavior of the scalar field and its evolution during Universe expansion it is necessary to analyze eq.(5.7). We have made the natural assumption that initially ϕ is a slowly varying function of the space coordinates $\phi(r,t)$. The space derivative term can be safely neglected because of the exponential rising of the scale factor $a(t) \sim \exp(H_I t)$. Then the equations of motion for $\phi = x + iy$ read

$$\begin{aligned}
&\ddot{x} + 3H\dot{x} + \frac{1}{4}\Gamma_x \dot{x} + (\lambda + \lambda_3)x^3 + \lambda' x y^2 = 0 \\
&\ddot{y} + 3H\dot{y} + \frac{1}{4}\Gamma_y \dot{y} + (\lambda - \lambda_3)y^3 + \lambda' y x^2 = 0
\end{aligned} \tag{6.1}$$

where $\lambda = \lambda_1 + \lambda_2$, $\lambda' = \lambda_1 - 3\lambda_2$.

In case when at the end of inflation the Universe is dominated by a coherent oscillations of the inflaton field $\psi = m_{PL}(3\pi)^{-1/2}\sin(m_\psi t)$, the Hubble parameter is $H = 2/(3t)$. In this case it is convenient to make the substitutions $x = H_I(t_i/t)^{2/3}u(\eta)$, $y = H_I(t_i/t)^{2/3}v(\eta)$ where $\eta = 2(t/t_i)^{1/3}$. The functions $u(\eta)$ and $v(\eta)$ satisfy the equations

$$\begin{aligned}
&u'' + 0.75\ \alpha\Omega_u(u' - 2u\eta^{-1}) + u[(\lambda + \lambda_3)u^2 + \lambda' v^2 - 2\eta^{-2}] = 0 \\
&v'' + 0.75\ \alpha\Omega_v(v' - 2v\eta^{-1}) + v[(\lambda - \lambda_3)v^2 + \lambda' u^2 - 2\eta^{-2}] = 0.
\end{aligned} \tag{6.2}$$

The baryon charge in the comoving volume $V = V_i(t/t_i)^2$ is $B = N_B \cdot V = 2(u'v - v'u)$. The numerical calculations were performed for $u_o, v_o \in [0, \lambda^{-1/4}]$, $u'_o, v'_o \in [0, 2/3\lambda^{-1/4}]$. For simplicity we considered the case: $\lambda_1 > \lambda_2 \sim \lambda_3$, when the unharmonic oscillators u and v are weakly coupled.

For each set of parameter values of the model λ_i we have numerically calculated the baryon charge evolution $B(\eta)$ for hundreds sets of different initial conditions of the field corresponding to the accepted initial monotonic space distribution of the field $\phi(r_i, t_i)$ (see the following figures).

The numerical analysis confirmed the important role of particle creation processes for baryogenesis models and large scale structure periodicity, which were obtained

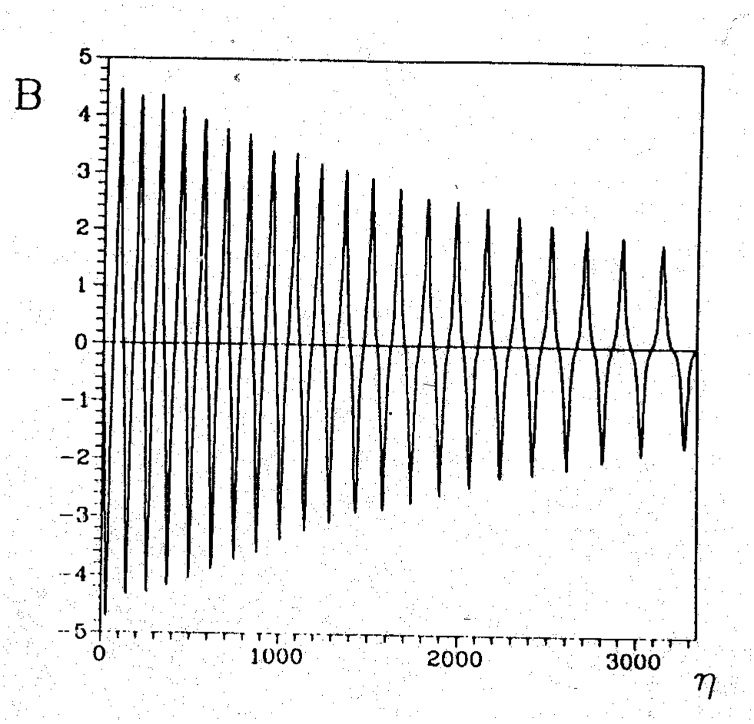

Figure 6.1: The evolution of the baryon charge $B(\eta)$ contained in the condensate $<\phi>$ for $\lambda_1 = 5\times10^{-2}$, $\lambda_2 = \lambda_3 = \alpha = 10^{-3}$, $H_I/m = 10^7$, $\phi_o = H_I\lambda^{-1/4}$, and $\dot{\phi}_o = 0$. Figure from ref. *Kirilova & Chizhov*, 2000.

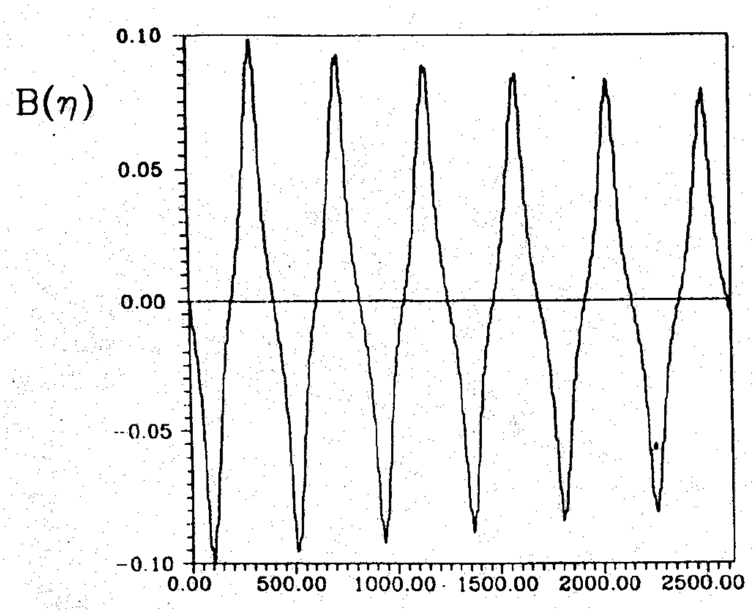

Figure 6.2: The evolution of the baryon charge $B(\eta)$ contained in the condensate $<\phi>$ for $\lambda_1 = 5\times10^{-2}$, $\lambda_2 = \lambda_3 = \alpha = 10^{-3}$, $H_I/m = 10^7$, $\phi_o = \frac{1}{50}H_I\lambda^{-1/4}$, and $\dot{\phi}_o = 0$. Figure from ref. *Kirilova & Chizhov*, 2000.

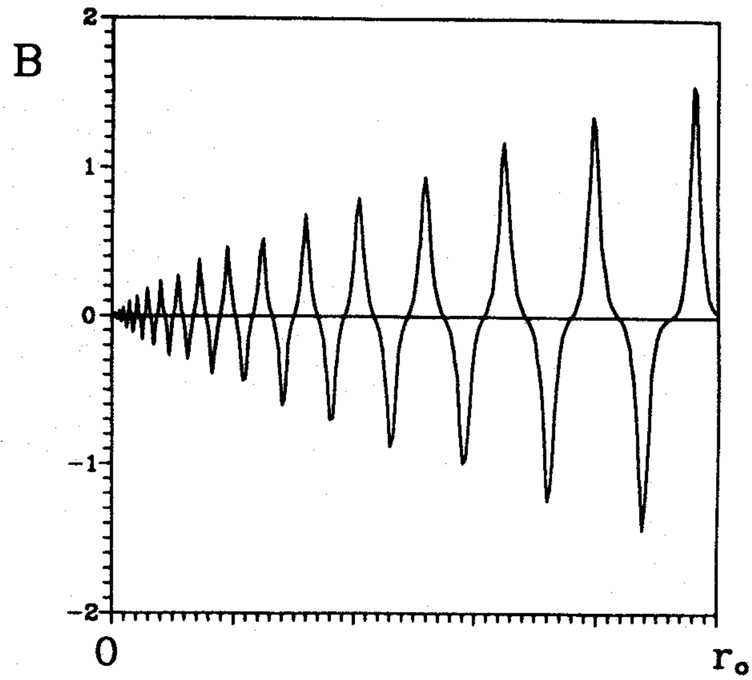

Figure 6.3: The space distribution of baryon charge at the moment of baryogenesis for $\lambda_1 = 5 \times 10^{-2}$, $\lambda_2 = \lambda_3 = \alpha = 10^{-3}$, $H_I/m = 10^7$. Figure from ref. *Kirilova & Chizhov*, 2000.

from an approximate analytical solution. We have accounted for particle creation processes explicitly. It was shown, that the damping effect due to the particle creation is proportional to the initial amplitudes of the field. As far as the particle creation rate is proportional to the field's frequency, it can be concluded that the frequency depends on the initial amplitudes. This result confirms our analytical estimation provided in earlier works.

The space distribution of the baryon charge $B(t_B, r)$ is followed numerically till for the moment t_B. It is obtained from the evolution analysis $B(\eta)$ for different initial values of the field, corresponding to its initial space distribution $\phi(t_i, r)$ (see Fig.6.1. and Fig. 6.2). The calculated space distribution of the baryons at t_B for one set of model's parameters is presented in (Fig.6.3).

Due to the nonharmonic field's potential, the initially monotonic space behavior is quickly replaced by space oscillations of ϕ, because of the dependence of the period on the amplitude, which on its turn is a function of r. As a result in different points different periods are observed and space behavior of ϕ becomes quasiperiodic. Correspondingly, the space distribution of the baryon charge contained in ϕ becomes quasiperiodic as well. Therefore, the space distribution of baryons at the moment of baryogenesis is found to be periodic.

The observed space distribution of the visible matter today is defined by the space distribution of the baryon charge of the field ϕ at the moment of baryogenesis t_B, $B(t_B, r)$. So, that at present the visible part of the Universe consists of baryonic shells, divided by vast underdense regions.

For a wide range of model'sparameters' values the observed average distance of $130h^{-1}$ *Mpc between matter shells in the Universe can be obtained. The parameters of the model ensuring the necessary observable size between the matter domains belong to the range of parameters for which the generation of the observed value of the baryon asymmetry may be possible in the model of scalar field condensate baryogenesis.* This is an attractive feature of this model because both the baryogenesis and the large scale structure periodicity of the Universe can be explained simply through the evolution of a single scalar field.

6.3 Summary and Discussion

Observational cosmic ray, gamma-ray, BBN and CMB data do not rule out antimatter domains in the Universe, separated at distances bigger than 10 Mpc from us. Hence, it is interesting to analyze the possible generation of vast antimatter structures during the early Universe evolution.

First, we discussed a inhomogeneous SFC baryogenesis model, which model provides generation of the small locally observed baryon asymmetry for a natural initial conditions. The characteristic scale of antimatter regions and their distance from the matter ones is in accordance with observational constraints from cosmic ray, gamma-ray and cosmic microwave background anisotropy data.

The model proposes an elegant mechanism for achieving a sufficient separation between regions occupied by baryons and those occupied by antibaryons, necessary in order to inhibit the contact of matter and antimatter regions with considerable density (*Kirilova*, 1998b).

Besides, in some realizations of the model neither explicit, no spontaneous charge asymmetry violation are needed. Charge asymmetry is broken stochastically by quantum fluctuations during inflation. Thus, the domain wall problem is evaded.

According to our model, the visible part of the Universe at present may consist of baryonic and antibaryonic regions, sufficiently separated, so that annihilation radiation is not observed.

Second, we discussed a mechanism for producing baryon density perturbations during inflationary stage and studied the evolution of the baryon charge density distribution in the framework of the low temperature SFC baryogenesis scenario. It was shown that this mechanism may be important for the large scale structure formation of the Universe and particularly, may be essential for understanding the existence of a characteristic scale of $130h^{-1}$ Mpc (comoving size) in the distribution of the visible matter.

The detailed numerical analysis showed that both the observed very large scale of the visible matter distribution in the Universe and the observed baryon asymmetry value could naturally appear as a result of the evolution of a complex scalar field condensate, formed at the inflationary stage.

The SFC baryogenesis deserves further precise numerical studies. On the first place, due to the extreme sensitivity of the generated baryon excess on Γ it is necessary to account as precisely as possible for particle creation processes.

It is interesting to provide a more precise study of the question for different possibilities of particle creation and their relevance for the discussed scenario of baryogenesis and periodicity generation.

In the case of narrow-band resonance decay the final state interactions regulate the decay rate, parametric amplification is effectively suppressed and does not drastically enhance the decay rate. Therefore, we expect that this case will be interesting to explore. Another interesting case may be the case of strong dissipative processes of the products of the parametric resonance. As far as the dissipation reduces the resonant decay rate it may be worthwhile to consider such a model as well.

CHAPTER VII

Processes Involving Chiral Tensor Particles in the Early Universe

7.1 Chiral Tensor Particles in the Early Universe

The new chiral tensor (ChT) particles – a new type of spin-1 particles – are inserted into the standard model of elementary particles to complete the set of Yukawa interactions and realize all possible irreducible representations of the Lorentz group. Such model was first presented by *Chizhov* (1993) and was discussed in more detail in the reviews (*Chizhov*, 1995, 2011).

These chiral tensor particles belong to the fundamental representation of SU(2) Standard Model group, which contains the known fermions and the Higgs doublet.

The introduction of new ChT particles into the standard electroweak model, is based on the experimental fact that such type of particles exist in Nature at the QCD scale as hadron resonances, see *Chizhov* (2004). An extension of the standard model by ChT particles at the electroweak scale is similar to the technicolor idea, which considers hadron resonances like prototypes of the electroweak bosons.

The new ChT particles contribute to the matter tensor in the right-hand side of the Einstein–Hilbert equation, increasing the Universe density and changing the dynamical evolution of the Universe. Besides, they have direct interactions with the particles present at the early stage of the Universe evolution.

Cosmological influence of antisymmetric tensor particles present in the primeval plasma, namely their effects on the Friedmann expansion and on the processes in the early Universe has been considered for a first time in 1994 in the M.S. thesis of T. Velchev under my supervision and then in (*Kirilova et al.*, 1995). Further it was investigated for the updated characteristics of these particles in (*Kirilova and Chizhov*, 1998a), *Chizhov and Kirilova* (2009); *Kirilova and Chizhov* (2009).

In the next section we briefly describe the status of the chiral tensor particles in the extended electroweak model, their experimental constraints, signatures and the possibilities for their detection at the new colliders. In the third section we estimate the characteristic scale of their typical processes and their effect on the expansion rate of the Universe. The BBN constraint on their effective coupling constant is provided in the fourth section. The last section presents our conclusions and vision about future exploration of the ChT particles.

7.2 Status of the Chiral Tensor Particles

According to the extended model with ChT particles (see *Chizhov* (1993, 1995)), the latter are described by an *antisymmetric* tensor fields of a rank two. An antisymmetric tensor field describes two fields with spin one, which are represented by a polar and an axial vectors with respect to spatial transformations. (Unlike the common association of the word *tensor* with particles with spin two, which are described by a second rank *symmetric* tensor, like the graviton.)

7.2.1 Chirality

The new particles have a chiral charge and change the fermion chirality in contrast to the gauge bosons with spin one, which have minimal interactions with fermions and do not change their chirality. They have an anomalous (Pauli) interaction with matter, which provides a distinguishing signature for their detection.

7.2.2 Introduction of chiral tensor particles into the SM

The ChT particles are introduced as doublets $\left(T^{+}_{\mu\nu}T^{0}_{\mu\nu}\right)$, like Higgs particles, due to the same as Higgs chirality property. As a result of their richer interaction possibilities new chiral anomalies appear. The latter are avoided by introducing an additional doublet $\left(U^{0}_{\mu\nu}U^{-}_{\mu\nu}\right)$ with an opposite chiral- and hypercharge. This doubling of doublets concerns also the Higgs sector, thus, similar to the SUSY case, it becomes $\left(H^{+}_{1}H^{0}_{1}\right)$, $\left(H^{0}_{2}H^{-}_{2}\right)$.

Massless tensor particles have just longitudinal degrees of freedom. In order for them to acquire mass a Higgs-like mechanism should be applied. However, in this case the role of the Higgs field will be played by a triplet and a singlet gauge vector particles or by four $SU(2)_L$ singlets (depending on the chiralities of the ChT particles), which supply them with the transverse physical degrees of freedom. Thus, in addition to the discussed Higgs doublets an extra triplet and five singlets, denoted further on by C_μ and P^i_μ $(i = 1, ..., 5)$, correspondingly, should be introduced as well for the two tensor doublets.

However, the doublets doubling may cause a flavor violation in the neutral sector. This can be easily avoided if the doublets H_1 and $T_{\mu\nu}$ interact only with down-type fermions, while the doublets H_2 and $U_{\mu\nu}$ – with up-type ones (*Glashow and Weinberg*, 1977).

7.2.3 Chiral tensor particles degrees of freedom

The antisymmetric tensor particles while massless, have only longitudinal physical degrees of freedom opposite to the case of gauge fields. Therefore, the presence of the two additional tensor doublets, the triplet and singlets gauge vector particles and the extra Higgs doublet leads to an increase of the total effective number of the degrees of freedom

$$g_{ChT} = g_T + g_U + g_C + g_P + g_H = 4 + 4 + 6 + 10 + 4 = 28.$$

The total number of the degrees of freedom, while the additional particles are relativistic, is:

$$g_* = g_{\mathrm{SM}} + g_{ChT} = 106.75 + 28 = 134.75$$

.

7.2.4 Chiral tensor particles masses

As in the SM the particle masses are induced through the Higgs mechanism. The presence of the vacuum expectation values of the two different Higgs doublets leads to different masses for the tensor particles interacting with up- and down-type fermions. Present experimental constraints on the masses of the tensor particles interacting with down type fermions at 95% CL are: $M_{T^0} > 2.85$ TeV and $M_T^+ > 3.21$ TeV (*Aad and others (ATLAS Coll.)*, 2014a,b). Constraints on the masses of tensor particles interacting with up-type fermions are not available yet.

7.2.5 Experimental signatures and constraints

The presence of the ChT particles do not contradict the present experimental data and, moreover, can explain successfully a number of anomalies in the precise low energy physics, namely: *weak radiative pion decay anomaly* (*Chizhov*, 2005), *CVC anomaly in tau decays* (*Chizhov*, 2007), *muon g-2 anomaly* (*Chizhov*, 2009).

Besides the successful explanation of the listed above anomalies, the *tensor interactions do not contradict the precise low energy experiments* like: super-allowed beta decay, muon decay, neutron decay, etc. The results of DELPHI, TWIST and μ_{P_T} experiments do not exclude the presence of these particles with the parameters discussed above.

The chiral tensor particles may be produced and detected at powerful high energy colliders. For example, some feature indicative for the ChT particles was already observed at the Tevatron (*Chizhov*, 2008), however it is not yet confirmed by LHC. The chiral tensor particles, if they exist, should be certainly discovered at the ongoing Large Hadron Collider by CMS and ATLAS experiments at CERN, in case they have the theoretically predicted masses and coupling constants (*Chizhov and Budagov*, 2008). After the first run of the LHC the mentioned above experimental constraints on the tensor particles masses were obtained. This year (2015) began the second run of the experiment, which hopefully will discover the ChT particles or provide new constraints on their characteristics.

7.3 Cosmological Effects of the Chiral Tensor Particles

Here two types of cosmologically important effects of ChT particles are discussed: first, their influence on Universe dynamics due to the increase of the energy density; second, ChT particles directly interact with the other constituents of the early Universe plasma.

7.3.1 ChT particles effect on the Universe expansion

The presence of two doublets of antisymmetric tensor particles and the corresponding additional Higgs doublet, triplet and singlets of gauge vector particles leads to a considerable increase of the energy density of the Universe in comparison with the Standard Cosmological Model case:

$$\rho = \rho_{SCM} + \rho_{ChT}. \tag{7.1}$$

This results in speeding up the Friedmann expansion: $H = \sqrt{\frac{8\pi}{3} G_N \rho}$. At the early stage, while the additional particles are relativistic, their contribution can be expressed through the effective degrees of freedom, namely:

$$\rho_{ChT} = \frac{\pi^2}{30} g_{ChT} T^4, \tag{7.2}$$

where T is the photons temperature. Hence, for cosmic times t later than ChT particles creation time t_c and before ChT particles became non-relativistic or decay, i.e. $t_c < t < t_d$, the Friedmann expansion is speeded up

$$H = \sqrt{8\pi^3 G_N g_*/90}\, T^2 \tag{7.3}$$

where g_* is the total number of the effective degrees of freedom $g_* = 134.75$, as discussed in the previous section.

The temperature-time dependence:

$$t \sim 1/(\sqrt{g_*}\, T^2) \tag{7.4}$$

is also shifted, namely the cosmic time, corresponding to a given temperature, slightly decreases compared to the standard cosmological model case, since $g_* > g_{SM}$.

7.3.2 ChT particles interactions in the early Universe

Through their interactions with the fermions the tensor particles directly influence the early Universe plasma. Analyzing the interactions of the tensor particles, we have estimated the characteristic temperatures and cosmic times of their creation, scattering, annihilation and decay.

ChT particles unfreezing

Tensor particle interactions become effective when the characteristic rates of interactions $\Gamma_{int} \sim \sigma n$ become greater than the expansion rate $H(T)$. At energies greater than the tensor particles masses, the cross sections have the following behavior $\sigma \sim E^{-2}$. Hence, at very high energies tensor particles have been frozen, and with the cooling of the Universe during its expansion, they unfreeze. The temperature of unfreezing T_{eff}, i.e. the temperature corresponding to the beginning of the epoch of particles effectiveness due to a given interaction $i \to f$ is defined from the relation

$$\sigma_{if}(T_{eff})n(T_{eff}) = H(T) \tag{7.5}$$

and the corresponding cosmic time in seconds is estimated as

$$t_{eff} \approx 2.42/\sqrt{g_*}\, T_{eff}^2, \tag{7.6}$$

where T_{eff} is in MeV.

ChT particles creation from fermion-antifermion collisions

The cross-section for the creation of pairs of longitudinal tensor particles from fermion-antifermion collisions is calculated to be:

$$\sigma_c \approx \frac{\pi\alpha^2 \ln(E/v)}{64 \sin^4 \theta_W E^2} \tag{7.7}$$

where the fine-structure constant $\alpha(M_Z) \approx 1/127.9$, the weak-mixing angle $\sin^2\theta_W \approx 0.23136$ and the Higgs vacuum expectation $v \approx 250$ GeV. Thus, the tensor particle creation becomes effective at

$$T < T_c \approx 3.3 \times 10^{16} \text{ GeV} \tag{7.8}$$

which corresponds to cosmic times $t > t_c \approx 1.9 \times 10^{-40}$ s.

Fermions scattering on ChT particles

The fermions scattering on tensor particles has a cross-section

$$\sigma_s \approx \frac{\pi\alpha^2}{192\sin^4\theta_W E^2} \tag{7.9}$$

It becomes effective at $T < T_s \approx 3.4 \times 10^{14}$ GeV and $t > t_s \approx 1.8 \times 10^{-36}$ s.

ChT particles annihilations

Tensor particles annihilations proceed till

$$t_a \approx 2.42/(\sqrt{g_*}\, T_a^2[\mathrm{MeV}])\ \mathrm{s} \approx 2.3 \times 10^{-14}\ \mathrm{s} \tag{7.10}$$

where $T_a = 2M_T$ and we have assumed $M_T = 3$ TeV.

ChT particles decays

The decay width of the tensor particles is

$$\Gamma \approx \alpha M_T/\sin^2\theta_W \approx 102\ \mathrm{GeV}. \tag{7.11}$$

The lifetime and the corresponding cosmological temperature are $t_d = 6.5 \times 10^{-27}$ s and $T_d = 5.7 \times 10^9$ GeV.

The decay time is much earlier than the annihilation time, hence the tensor particles disappear from the cosmic plasma mainly by decay. The period of their effectiveness is the period from the time of their creation to the moment of their decay, i.e. during the very early stage of the Universe evolution:

$$t_c = 1.9 \times 10^{-40}\ \mathrm{s} < t < t_d = 6.5 \times 10^{-27}\ \mathrm{s}.$$

The corresponding energy range spreads from 10^{16} GeV down to 10^9 GeV. So, the ChT particles decay safely early so that their decay products do not disturb BBN and CMB.

On the other hand they are present at energies typical for inflation, Universe reheating, lepto- and baryogenesis, et cetera. The ChT particles eventual role in these processes is to be explored in future studies. We would like only to mention here that the extended model with ChT particles proposes new source for CP-violation due to the richer structure of particles and interactions, and therefore, may present a natural mechanism for leptogenesis and baryogenesis scenarios.

7.4 BBN Constraint on the ChT Particles Interactions Strength

In the discussed extended model with the ChT particles right-handed neutrinos interact with the chiral tensor particles and in case the neutrinos are light they can be produced through ChT particles exchange. Then it is straightforward to obtain rough cosmological bound on the coupling constant of the ChT particles G_T on the basis of BBN considerations (*Dolgov*, 2002).

Using the BBN bound on the additional light neutrinos

$$N_{eff} = g_R (T_{\nu_R}/T_{\nu_L})^4 < 1 \tag{7.12}$$

and assuming three light right-handed neutrinos, it follows that

$$3(T_{\nu_R}/T_{\nu_L})^4 < 1, \tag{7.13}$$

which puts a constraint on the decoupling/freezing of the right-handed neutrinos. The temperature of freezing T_f of ν_R may be determined using the BBN constraint and entropy conservation relation $gT^3 = const$, namely

$$T_{\nu_R}/T_{\nu_L} = (\frac{43}{4}/g_*(T_f))^{1/3} < 0.76. \tag{7.14}$$

Then the rough constraint on the ChT particles decoupling temperature is:

$$T_f > 140 \text{ MeV}. \tag{7.15}$$

On the other hand the decoupling temperature of a given species is connected with its interactions coupling strength, hence

$$(G_T/G_F)^2 \sim (T_f/3 \text{ MeV})^{-3},$$

where we assume 3 MeV as the decoupling temperature of the active neutrino species. Then the constraint on the ChT coupling is:

$$G_T < 10^{-2} G_F. \tag{7.16}$$

In case of two light right-handed neutrinos, the corresponding constraints on the decoupling temperature is:

$$T_f > 100 \text{ MeV}, \tag{7.17}$$

which slightly changes the constraint on the coupling. These two cases provide BBN constraints in agreement with the value of the G_T provided from the experimental data discussed in the second section. So *BBN cosmological constraint points as well to the possibility of a centi-weak tensor interactions.*

Considerably looser BBN bound will follow in case of only one light right-handed neutrino species, as seen from the above considerations, namely $G_T \leq G_F$. Vice versa, the eventual future detection of the ChT particles and determination of their coupling constant may point to the number of the light right-handed neutrino species.

7.5 Summary

As has been discussed, the existence of chiral tensor particles does not contradict the experimental data of the precise low energy experiments like: super-allowed beta decay, muon decay, neutron decay, etc. Moreover, chiral tensor particles help to explain some anomalies in the precision low energy physics, namely, the weak radiative pion decay anomaly, the CVC anomaly in tau decays, the muon g-2 anomaly, etc. Besides, the inclusion of the ChT particles helps to solve the hierarchy problem (*Chizhov and Dvali*, 2011).

It is remarkable that chiral tensor particle anomalous interactions with matter provide a distinguishing signature for their detection. The new particles may be produced and detected at powerful high energy colliders. Particularly, if they exist, they should be certainly discovered at the ongoing Large Hadron Collider by CMS and ATLAS experiments at CERN, in case they have the mentioned above masses and coupling constants. At present the search of these particles is conducted in the ongoing experiments of the ATLAS Collaboration at LHC. First experimental results provided constraints on the tensor particle masses.

As demonstrated in this work, these particles are allowed by cosmology, as well. BBN cosmological considerations allow a centi-week tensor interactions strength. ChT particles cause a slight increase of the Friedmann expansion. This dynamical cosmological effect is due to the density increase caused by the introduction of the new particles, and correspondingly the change of the temperature-time dependence. The characteristic interactions of the chiral tensor particles in the early Universe plasma were calculated. The period of effectiveness of the interactions with the other Universe constituents was determined. This period lasts from the time of their creation till their decay, namely:

$$t_c = 1.9 \times 10^{-40} \text{ s} < t < t_d = 6.5 \times 10^{-27} \text{ s} \tag{7.18}$$

The corresponding energy range is from 10^{16} GeV (typical for the inflationary period) down to 10^9 GeV, which according to us is very promising for theoretical speculations involving the chiral tensor particles concerning inflationary models, reheating scenarios, baryogenesis, leptogenesis scenarios, etc.

In conclusion: The existence of the chiral tensor particles is allowed from cosmological considerations and welcomed by the particle physics phenomenology.

Hopefully, in future more particle physics experiments will pay attention to the experimental exploration of the characteristics of the chiral tensor particles and they will be included in the theoretical models of the early Universe evolution as well.

CHAPTER VIII

Summary and Conclusions

Main results and achievements

The main results and achievements of the research work, on which this thesis is based are summarized below.

Nonequilibrium neutrino oscillations

1. We have *proposed precise kinetic approach for the description of the evolution of the non-equilibrium oscillating neutrino.* We have derived kinetic equations for the density matrix of neutrino in momentum space accounting simultaneously for the Universe expansion, neutrino oscillations and the interactions of neutrino and the nucleons. These equations provided an accurate description of the evolution of the neutrino depletion, neutrino energy distribution and the neutrino-antineutrino asymmetry.

2. We have constructed and explored a *model of nonequilibrium electron-sterile neutrino oscillations*, effective after active neutrino decoupling in the early Universe. The qualitative numerical analysis of neutrino oscillations effects was provided for the whole range of neutrino oscillations parameters of the model and for different initial population of the sterile neutrino $0 \leq \delta N_s < 1$.

3. Thanks to the exact kinetic approach used we have found *quantitatively new effects caused by nonequilibrium neutrino oscillations.* We have established that the nonequilibrium active-sterile neutrino oscillations lead to *considerable distortion of the energy spectrum of electron neutrinos (antineutrinos)* and depletion of their number densities. The distortion decreases with the increase of δN_s.

4. We have found that resonant MSW nonequilibrium active-sterile neutrino oscillations lead to *enhancement of the neutrino-antineutrino asymmetry.*

i) In case of small mass differences and relatively big mixing angles the maximal possible growth of L was found to be *by 4-5 orders of magnitude.*

ii) The *instability region in the oscillation parameter space*, where considerable growth of L takes place, was determined.

For the proper description of the asymmetry behavior in this oscillation parameter region high resolution for the description of the neutrino spectrum distribution is required.

BBN with nonequilibrium neutrino oscillations

5. We have constructed and studied numerically a model of BBN with nonequilibrium $\nu_e \leftrightarrow \nu_s$ neutrino oscillations, effective after electron neutrino decoupling.

i) We have proposed *precise kinetic approach for the simultaneous description* of the evolution of the non-equilibrium oscillating neutrino and the evolution of the nucleons.

ii) The primordial production of ^{4}He in the presence of oscillations was numerically analyzed for hundreds sets of oscillations parameters values in non-resonant and resonant oscillation case.

iii) It was shown that the total effect of neutrino oscillations for the whole parameters range of the model is overproduction of ^{4}He.

iv) The effects of neutrino oscillations on BBN were numerically studied.

– It was found that the kinetic effect due to the distortion of the electron neutrino energy spectrum, caused by nonequilibrium $\nu_e \leftrightarrow \nu_s$ oscillations, plays the dominant role for the overproduction of ^{4}He.

– It was found that the asymmetry growth due to resonant $\nu_e \leftrightarrow \nu_s$ neutrino oscillations takes place at small mixing and in that range of parameters of the model the production of ^{4}He is reduced in comparison to the case without an account of asymmetry growth. However, this asymmetry effect is subdominant.

6. A precise quantitative study of the *maximum overproduction of* ^{4}He, accounting for all oscillations effects was provided. Enormous maximum overproduction of ^{4}He (up to 32% in the resonant case and 14% in the non-resonant case) was found possible. It was shown that the net effect of spectrum distortion on the production of ^{4}He may be several times larger than previously accepted in literature maximal overproduction due to the dynamical effect of an additional neutrino type.

Cosmological constraints on neutrino oscillations parameters ($\delta N_s = 0$ case)

7. We have calculated isohelium contours in the δm^2 - θ plane for 3%, 5% and 7% helium uncertainties. Observational data on primordial ^{4}He and D were used to determine the cosmologically allowed range for oscillation parameters. We have obtained cosmological constraints on nonequilibrium $\nu_e \leftrightarrow \nu_s$ neutrino oscillations, which are:

– *more stringent by an order of magnitude towards small mass differences in comparison with previous studies.* This is a result of the precise account of the strong kinetic effect of neutrino spectrum distortion caused by active-sterile oscillations, while previous studies considered the integral effects like neutrino number density depletion and shift of the temperature of otherwise equilibrium neutrino spectrum;

– at the time (1996-2000) by *4 orders of magnitude stronger than the experimentally available constraints.* They excluded almost completely the LOW electron-sterile solution, in addition to the sterile LMA solution already excluded in previous investigations, years before the analysis of solar neutrino oscillations experiments data pointed to the preferred flavor oscillation channels. Thus, these cosmological constraints served as indicators for the mixing pattern of neutrinos.

In the resonant case we have obtained precise cosmological constraint on neutrino oscillation parameters δm^2 and θ accounting for the dynamical evolution of the neutrino asymmetry, its interplay with oscillations and its effect on primordial production of ^{4}He. It was found that the account for asymmetry growth relaxes the cosmological constraints at small mixing.

8. We have *studied different possibilities of change of the BBN constraints on neutrino oscillations.* Namely, *additional sterile population*, which due to the interplay between its dynamical and kinetic effect could either increase or decrease ^{4}He overproduction and thus strengthen or relax the constraints; *presence of relic lepton asymmetry*, which depending on its value is able to enhance, suppress or even stop the neutrino oscillations.

Non-zero population of sterile neutrino and BBN with neutrino oscillations

9. BBN with nonequilibrium $\nu_e \leftrightarrow \nu_s$ oscillations, in the more general case of initially (at the start of the neutrino oscillations) non-zero population of ν_s before oscillations $\delta N_s \neq 0$, was numerically explored.

i) ^{4}He primordial production was calculated for different initial populations of the sterile neutrino state $0 \leq \delta N_s < 1$ and the full range of oscillation parameters of the model of nonequilibrium electron-sterile neutrino oscillations.

ii) An exact numerical analysis of δN_s effects on pre-BBN nucleons freezing and the production of ^{4}He in BBN with oscillations was provided. It was found for a first time that δN_s has two-fold effect on ^{4}He:

– enhancement of the cosmic expansion rate, leading to Y_p *overproduction.*

– suppression of the kinetic effects of oscillations, caused by the ν_e energy spectrum distortion and the $\nu_e - \bar{\nu}_e$ asymmetry generation by oscillations, leading to *decreased* Y_p *production.*

Depending on oscillation parameters and δN_s one or the other effect may dominate, causing, correspondingly, either increase or decrease of Y_p overproduction.

10. Isohelium contours corresponing to to 3% and 5%, 7% and 9% overproduction of Y_p were determined. More general BBN constraints on $\nu_e \leftrightarrow \nu_s$ oscillation parameters, corresponding to 3% and 5% Y_p overproduction, for different initial populations of the sterile state $0 \leq \delta N_s < 1$ were calculated. It was found that cosmological constraints may be relaxed or strengthened by non-zero δN_s. The possibility to suppress the kinetic effect and relax the cosmological constraints due to non-zero δN_s was revealed for a first time.

Small lepton asymmetry and BBN with neutrino oscillations

11. We have provided a detail numerical study of the *interplay between small lepton asymmetry* $|L| << 0.01$, either relic (initially present) or dynamical (generated by MSW active-sterile neutrino oscillations) *and* $\nu_e \leftrightarrow \nu_s$ *oscillations* for the whole parameters range of the model of nonequilibrium nonresonant $\nu_e \leftrightarrow \nu_s$ neutrino oscillations. We have found that there are significant modifications of neutrino number densities and energy distributions over a large range of values of the initial asymmetry.

12. We have shown that relic L is able to enhance (an intriguing qualitatively new effect), suppress or inhibit neutrino oscillations. We have determined the parameter ranges for which L enhance, suppress or inhibit neutrino oscillations.

On the basis of the numerical analysis we have obtained empirical relations between oscillations parameters and lepton asymmetry value (that provide relatively good fit to the exact results) corresponding to the qualitatively different types of lepton asymmetry effect.

13. We have found that the capability of small lepton asymmetry *to enhance oscillations* is *due to a new type of resonance* in the neutrino oscillations - spectrum wave resonance.

We would like to emphasize that this phenomenon and the enhancement of neutrino oscillations by lepton asymmetry was revealed due to the correct account for the spectral spread of neutrino momenta and energy spectrum distortion due to oscillations, advocated in our papers.

14. The *indirect kinetic effect* (via neutrino oscillations) *of lepton asymmetries* $|L| << 0.01$ *on BBN* and especially on helium production, was numerically analyzed in a model of cosmological nucleosynthesis with $\nu_e \leftrightarrow \nu_s$ neutrino oscillations. Both the case of oscillations generated asymmetry and the case of initially present (relic) asymmetry were studied.

The account of spectrum distortion of the oscillating neutrinos as well as the selfconsistent account of neutrinos and nucleons evolution was proved essential for revealing the indirect kinetic effect of small lepton asymmetries.

i) It was found that relic L, due to its effect on neutrino oscillations and on neutrino number densities, may increase, decrease overproduction of Y_p or reduce it to the standard BBN value.

ii) It was found that the neutrino-antineutrino asymmetry, generated at small mixing angled by resonant neutrino oscillations, reduces the overproduction of Y_p at these mixing angles.

15. We have studied and established the possible change of the BBN constraints on neutrino oscillations due to small lepton asymmetries. BBN limits on the oscillation parameters derived for the case of lepton asymmetry of the order of the baryon one are considerably altered by asymmetries $|L| > 10^{-8}$: they may be strengthened, relaxed or waved out.

i) The capability of lepton asymmetry to enhance neutrino oscillations and consequently to *tighten* the nucleosynthesis bounds on neutrino mixing parameters is revealed for a first time.

ii) Large enough L is capable to alleviate BBN constraints on oscillation parameters. In that case, instead, new constraint is derived: the oscillations parameters are constrained by L.

iii) It particular, it was found that relic $L \sim 10^{-6}$ relaxes BBN bounds at large mixing and strengthens them at small mixing.

16. On the basis of the interplay between L and neutrino oscillations stringent cosmological bounds on L may be obtained. For example from the indications for active-sterile oscillations with $\delta m^2 \sim 10^{-5}$ a stringent upper limit on L follows: $|L| < 5 \times 10^{-4}$ (stronger than standard BBN limit $|L| < 0.01$).

17. We have proposed the ability of L to suppress neutrino oscillations as a possible solution of the recently found indication for additional relativistic density. We have estimated the value of L necessary to suppress neutrino oscillations and thus to inhibit the sterile neutrino thermalization through active-sterile neutrino oscillations and, thus, evade the stringent BBN constraints.

SFC baryogenesis model and particle creation processes

18. We have provided precise analysis of the SFC baryogenesis model, based on the Affleck-Dine baryogenesis scenario. The post-inflationary evolution of the baryon charge carrying scalar field ϕ was followed both semi-analytically and numerically using exact kinetic equations and accounting for particle creation processes.

i) We have calculated numerically the produced baryon asymmetry for natural ranges of model parameters and for hundred different sets of the model parameters.

ii) The dependence of the produced baryon asymmetry on the model's parameters was explored. Namely, we have found the dependence B on m, α and λ_i for different sets of other parameters values.

19. It was shown that particles creation processes influence considerably the evolution of the scalar field and the generated baryon excess. We have proposed explicit account for the particle creation processes in the kinetic equations for the baryon charge carrying scalar field. It was found that particles creation leads to a considerable decrease of the field's amplitude, which reflects finally into strong damping of the baryon charge carried by the condensate.

i) We have studied particle creation processes semi-analytically and numerically. We have obtained self-consistently the frequency Ω and the rate Γ from the exact numerical analysis of the field's evolution. It was found that numerically calculated Ω may be quite different from the analytical estimation.

ii) The numerical analysis showed that B evolution and the final value of B after ϕ decay, numerically calculated with a precise account for particle creation processes, may be considerably different from those calculated semi-analytically for a wide range of model's parameters. The precise numerical account for particle creation points to stronger and earlier reduction (up to two orders of magnitude) of the B excess in comparison with the case of analytical account of particle creation processes.

Inhomogeneous SFC baryogenesis model, LSS and antimatter in the Universe

20. We explored a mechanism for producing baryon density perturbations during inflationary stage and studied the evolution of the baryon charge density distribution in the framework of the low temperature inhomogeneous SFC baryogenesis scenario.

i) We have proved numerically that this mechanism of production of baryon density perturbations may be important for the large scale structure formation of the Universe and particularly, may explain the existence of a characteristic scale of approximately $130h^{-1}$ Mpc (comoving size) in the distribution of the visible matter.

ii) The detailed numerical analysis showed that both the observed very large scale of the visible matter distribution in the Universe and the observed baryon asymmetry value could naturally appear as a result of the evolution of a complex scalar field condensate, formed at the inflationary stage.

21. We explored the possible generation of vast antimatter and matter structures during the early Universe evolution in inhomogeneous Scalar Field Condensate baryogenesis model.

i) The numerical analysis has shown that the model predicts vast antimatter domains, separated from the matter ones by baryonically empty voids. This is an interesting possibility as far as the observational data do not rule out the possibility of antimatter galaxies, antimatter galaxy, clusters and superclusters in the Universe.

ii) The model proposes an elegant mechanism for achieving a sufficient separation between regions occupied by baryons and those occupied by antibaryons, necessary to inhibit the contact of matter and antimatter regions with considerable density.

iii) Different possibilities for the characteristic scale of antimatter regions and their distance from the matter ones were studied, requiring an accordance with observational constraints from cosmic ray, gamma-ray and cosmic microwave background anisotropy data.

Processes of chiral tensor particles in the early Universe

22. We have studied the cosmological place and role of the chiral tensor particles. We have shown that the existence of the chiral tensor particles is allowed from cosmological considerations.

i) The dynamical cosmological effect, namely the speeding of the Friedmann expansion, due to the density increase caused by the introduction of the new chiral tensor particles, was evaluated.

ii) The characteristic interactions of the chiral tensor particles in the early Universe plasma and the corresponding period of their cosmological influence were determined.

iii) The strength of the ChT particles interactions was estimated on the basis of BBN constraints on additional particles. The interactions were estimated to be by two orders of magnitude weaker than the weak interactions. This result is in agreement with the experimental data and the theoretical indications.

List of publications

The results of this dissertation have been published in 51 papers: 25 in refereed international journals, 6 in refereed national journals, 20 in proceedings of international conferences and symposiums.

A. Refereed international and national journals

1. Kirilova D., Neutrinos from the Early Universe and physics beyond standard models, Open Physics, v.13, 2015, pp.22-33, IF:0.905

2. Kirilova D., Lepton Asymmetry and neutrino oscillations interplay, Hyperfine Interactions, v.215, Issue 1, 2013, pp.111-118 (DOI) 10.1007/s10751-013-0790-0, IF:0.21

3. Kirilova D., J.-M. Frere, Neutrino in the Early Universe, New Astronomy Reviews, v.56, issue 6, 2013, pp.169-180, IF:1.321

4. Kirilova D., BBN with Late Electron-Sterile Neutrino Oscillations - The Finest Leptometer, JCAP 1206, 2012, 007, IF:6.036

5. Kirilova D., On Lepton Asymmetry and BBN, Progress in Particle and Nuclear Physics 66, 2011, pp.260-265, IF:3.860

6. Kirilova D., Chizhov M., BBN Constraints on Neutrino and CNB, Progress in Particle and Nuclear Physics, v.64, Issue 2, 2010, pp. 375-378, IF:4.020

7. Chizhov M., Kirilova D., Speeding the Friedman expansion by chiral tensor particles, Int.J.Mod.Phys.A 24, 2009, pp.1643-1647, ISSN: 0217-751X, IF:0.98

8. Kirilova D., More General BBN Constraints on Neutrino Oscillations Parameters - Relaxed or Strengthened, IJMPD 16, 7, 2007, pp.1-14, IF:1.87

9. Kirilova D., Panayotova M., Relaxed Big Bang Nucleosynthesis constraints on neutrino oscillation parameters, JCAP 12, 2006, 014, IF: 6.7

10. Kirilova D., Neutrino oscillations and the early Universe, Central Eur. J. Phys.2, 2004, pp.467-491, IF: 0.381

11. Kirilova D., Neutrino Spectrum Distortion Due to Oscillations and its BBN Effect, Int.J.Mod.Phys. D13, 2004, pp.831-842, IF:1.5

12. Kirilova D., Baryogenesis Model predicting antimatter in the Universe, Nucl. Phys. Proc. Suppl. v.122, 2003, pp.404-408, IF:0.99

13. Kirilova D.,Overproduction of helium-4 in the presence of neutrino oscillations, Astropart. Phys. v.19, 2003, pp.409-417, IF:4.022

14. Kirilova D., Chizhov M., Neutrino oscillations in the early Universe, Nucl.Phys. B Proc. Suppl. 100, 2001, pp.360-362, IF:0.947

15. Kirilova D., Chizhov M., Cosmological nucleosynthesis and active-sterile neutrino oscillations with small mass differences: The resonant case, Nucl.Phys.B 591, 2000, pp.457-468, IF:4.225

16. Kirilova D., Chizhov M., Non-GUT Baryogenesis and Large Scale Structure of the Universe, MNRAS 314, pp.256-262, 2000, IF:4.685

17. Kirilova D., Chizhov M., Neutrino Degeneracy Effect on Neutrino Oscillations and Primordial Helium Yield, Nucl.Phys.B 534, pp.447-463, 1998, IF:3.322

18. Kirilova D., Chizhov M., Cosmological Nucleosynthesis and Active-Sterile Neutrino Oscillations with Small Mass Differences: The Nonresonant Case, Phys.Rev.D 58, pp.073004-073014, 1998, IF:3.558

19. Kirilova D., Chizhov M., Nonequilibrium Neutrino Oscillations and Primordial Production of He-4, Phys.Lett.B 393, 1997, pp.375-382, IF:3.581

20. Kirilova D., Chizhov M., Velchev T., Antisymmetric Tensor Particles in the

Early Universe, Compt. Rend. Bul. Acad. Sci., t.48, No 6, 1995, pp.25-28, IF: 0.198

21. Kirilova D., Baryon Density in alternative BBN Models, A&Astroph Tr., v.22, pp. 425-428, 2003

22. Kirilova D., Primordial He-4 Overproduction due to neutrino oscillations, A&Astroph Tr, v.22, pp.421-424, 2003

23. Kirilova D., Baryogenesis Model Suggesting Antigalaxies, A&Astroph Tr, 1998, v.15, pp. 211-217

24 Kirilova D., Chizhov M., Is There A Cosmological Evidence For Additional Particles,A&Astroph. Tr., 1998, v.15, pp.205-210

25. Chizhov M., Kirilova D., Generation of 128 Mpc Periodicity of the Universe in the Scalar Field Condensate Baryogenesis Scenario, A&Astroph. Tr., 1996, v.10, pp.69-75

26. Dolgov A., Kirilova D., Production of particles by a variable scalar field, Jadr. Phys. 51, p.273, 1990; Sov. J. Nucl. Phys. 51, p.172-177, 1990, IF: 0.2

27. Panayotova M., Kirilova D., The dependence of the baryon asymmetry generation on the couplings of the baryon charge carrying scalar field, BAJ 20, 2014, pp.45-50

28. Kirilova D., From Mateev's Baryogenesis Ideas to Contemporary Cosmological Constraints, Bulg. J. Phys. 38, 2011, pp.242-251

29. Kirilova D., Big Bang Nucleosynthesis: The best baryometer, speedometer and leptometer, BAJ 15, 2011, pp.3-17

30. Kirilova D., Neutrino in the Universe, BAJ 10, 2008, pp.1-9

31. Kirilova D., Panayotova M., The Role of Particle Creation Processes in the Scalar Condensate Baryogenesis model, Heron Press, Bulg.J.Phys. 34, s2, 2007, pp.330-335

B. Proceedings of international meetings

32. Kirilova D., Neutrinos and Physics Beyond Electroweak and Cosmological

Standard Models, invited review lecture in Theme Collection "Cosmology and Particle Physics Beyond Standard Models, Ten Years of the SEENET-MTP Network, edited by Luis lvarez-Gaum, Goran S. Djordjevic, Dejan Stojkovic, CERN-Proceedings-2014-001 ISBN 978-92-9083-398-7 pp.131-138, https://cds.cern.ch/

33. Kirilova D., Panayotova M., Inhomogeneous baryogenesis model and antimatter in the Universe, Proc. 8th Serbian-Bulgarian Astronomical Conference (VIII SBGAC), Leskovac, Serbia 8-12 May, Publ. Astron. Soc."Rudjer Boskovic " N11, 2013, pp.259-264

34. Kirilova D., On leptogenesis and lepton asymmetry effects in the early Universe, Proc. of the 45th Rencontres de Moriond, La Thuile, 2010, 2010 Cosmology, La Thuile, Aosta Valley, Italy, eds. E. Auge, J. Dumarchez, J.Tran Than Van, The GIOI Publishers, pp.363-365, SJR=0.1

35. Kirilova D., Neutrinos in Cosmology, invited review lecture Proceedings of the 6th SREAC Meeting "Astrophysics and Astrodynamics in Balkan Countries in the International Year of Astronomy", Belgrade, Serbia, 28-30 Sept. 2009, www.aob.bg.ac.yu/sreac, Publications of the Astronomical Observatory of Belgrade, 90, 2010 Eds: Istvan Vince and Tanyu Bonev, ISSN 0373-3742, pp.45-60

36. Kirilova D., Chizhov M., A Possible TeV Window on the Universe, Proceedings of XXIth Rencontres de Blois "Windows on the Universe", 21-26 June, 2009, in the Chateau de Blois, Loire Valley, France eds. L. Celnikier, J. Dumarchez and J. Tran Thanh Van, The Gioi Publishers, Vietnam GPXB 4 - 1000/XB-QLXB Series: Moriond Astrophysics Meeting, pp.627-628

37. Kirilova D., Non-equilibrium Neutrino In The Early Universe Plasma, AIP Conf. Proc., 1121, School and Workshop on Space Plasma Physics, 31.08-07.09, Sozopol, Bulgaria, ed.I. Zhelyazkov, 2009, pp.83-89, ISSN 0094-243X and http://sp.phys.uni-sofia.bg/Sozopol08 ISSN 1551-7616, SJR=0.148

38. Kirilova D., Generalized cosmological Constraints on Neutrino Oscillations -

Relaxed or Strengthened, Proc. 6th Intern. Symposium on Frontiers of Fundamental and Computational Physics, 26-29 September, Udine, Italy, Frontiers of Fundamental Physics, eds. B. Sidharth, F. Honsell, A. De Angelis, Kluwer Academic Publishers, 2006, pp. 55-59; DOI 10.1007/1-4020-4339-2-9

39. Kirilova D., Cosmological Constraints on Neutrino Oscillations, Proc. of Manev International Conference on Historical and Contemporary Aspects of Astronomy, Theoretical and Gravitational Physics, 20-22 May, 2004, Sofia, Prof. Manev's Legacy in Contemporary Astronomy, Theoretical and Gravitational Physics, eds. V. Gerdjikov, M. Tsvetkov, Haron Press Ltd., Sofia, 2005, pp.228-238

40. Kirilova D., Panayotova M., Cosmological constraints on neutrino oscillations for initially non-zero sterile state, presented at 4th Serbian-Bulgarian Astronomical Conference (IV SBGAC), 21-24 April 2004, Belgrade, Serbia, eds. M. Dimitrievich, V. Golev, L. Popovic and M. Tsvetkov, Publ. Astron. Soc. " Rudjer Boskovic " 5, 2005, pp.201-207

41. Kirilova D., Neutrino oscillations and the early Universe, invited review lecture, Proceedings of the XIII National Conference of Yugoslav Astronomers,17-20 Oct. 2002, Belgrade, Publ.Astron.Obs.Belgrade, No.75, 2003, pp.167-178

42. Kirilova D., Baryonic Content in Nonstandard BBN Models, to be published in Proc. of Int. Conference "Where's the Matter? Tracing Dark and Bright Matter with the New Generation of Large Scale Surveys", June 2001, Marseille, Treyer&Tresse Eds, Frontier Group, pp.273-275

43. Klecker B. et al. (20), Galactic Abundances: Report of Working Group 3, in proc. Joint SOHO-ACE Workshop "Solar and Galactic Composition", Bern, 6-9 March, 2001: AIP CP 598 "Solar and Galactic Composition" ed. Wimmer-Schweingruber R., American Institute of Physics, Melville, New York, 2001, pp.207-220

44. Busemann H., Altwegg K., Binns R., Chiappini C., Glockler G., P. Hoppe, D.

Kirilova, R. Leske, O.Manuel, R. Mewaldt, E. Mobius, S. Suess, R. Wieler, R. Wiens, R. Wimmer and N., Yanasak, Applications of Abundance Data and Requirements for Cosmochemical Modeling, in AIP Conf.Proc. 2001 of Joint SOHO-ACE Workshop "Solar and Galactic Composition", Bern, 6-9 March, 2001: CP598 "Solar and Galactic Composition" ed. Wimmer-Schweingruber R., American Institute of Physics 2001, pp. 357-379 and www.phim.unibe.ch/internal/nf01web/node76.html

45. Kirilova D., Primordially Produced Helium-4 in the presence of neutrino oscillations, Proc. Joint SOHO-ACE Workshop "Solar and Galactic Composition", Bern, 6-9 March, 2001, pp.405-410

46. Kirilova D., Chizhov M., Big Bang Nucleosynthesis and Cosmological Constraints on Neutrino Oscillations Parameters, invited review talk, Proceedings of the International Workshop "Hot Points in Astrophysics" JINR, Dubna, 22-26 August, 2000, pp.56-66

47. Kirilova D., Chizhov M., Lepton Asymmetry Effect on Neutrino Oscillations and Primordial Helium-4, in the International Conference CAPP 2000, Verbier, Switzerland, 17-28 July, 2000, Switzerland, published in "Cosmology and Particle Physics", AIP Conference Proceedings, Melville, New York, 2001, v.555, pp.433-436; eds. J. Garcia-Bellido, R. Durrer, and M. Shaposhnikov

48. Kirilova D., Chizhov M., Large Scale Structure and Baryogenesis, in Galaxy Clusters and the High-Redshift universe observed in X-rays, eds. J. Tran Thanh Van and Doris M. Neumann, Proc. of XXXVIth Rencontres de Moriond, XXI Moriond Astrophysics Meeting, Les Arcs, Savoie, France, March 10-17, 2001; e-proceedings on CD-ROM

49. Kirilova D., Chizhov M., Nonequilibrium Neutrino Oscillations and Primordial Helium Production, invited talk at the 17 International Conference on Neutrino Physics, NEUTRINO 96, Helsinki, 1996; Proc. of NEUTRINO 96, Helsinki, 1996, pp.478-484

50. Kirilova D., Big Bang Nucleosynthesis with Neutrino Oscillations, Fourth Advanced Research Workshop "GRAVITY, ASTROPHYSICS AND STRINGS AT THE BLACK SEA, June 10-16, 2008, Bulgaria,

http://tcpa.uni-sofia.bg/conf/GAS/gas2007.html

51. Kirilova D., Dolgov A., The Effect of Some Nonequilibrium Processes on the Primordial Nucleosynthesis, Proc. IUPAP Conference "Primordial Nucleosynthesis and the Evolution of Early Universe", Tokyo, Japan, 4-8 Sept. 1990, ed. K. Sato, J.Audouze, Kluwer Acad. Publishers, 1991, p.55-59.

BIBLIOGRAPHY

BIBLIOGRAPHY

Aad, G., and others (ATLAS Coll.) (2014a), *Phys.Rev.D*, *90*, 05,205.

Aad, G., and others (ATLAS Coll.) (2014b), *JHEP*, *09*, 037.

Abazajian, K., et al. (2012), A Wight Paper, *arXiv 1204.5379.*

Abdurashitov, J., and others (SAGE Coll.) (1996), *Phys.Rev.Lett.*, *77*, 4708.

Abe, K., et al. (2012), *Phys.Rev. Lett.*, *108*, 131,301.

Ade, P., and others (Planck Coll.) (2014), *Astron.Astrophys.*, *571*, A16.

Ade, P., and others (Planck Coll.) (2015), *arXiv:1502.01589.*

Adeva, B., et al. (1989), *Phys.Lett.B*, *231*, 509.

Adriani, O., and others (PAMELA Coll.) (2010), *Phys.Rev. Lett.*, *105*, 121,101.

Affleck, I., and M. Dine (1985), *Nucl. Phys.*, p. 361.

Alcaraz , J., and others (AMS Coll.) (1999), *Phys.Lett.*, p. 387.

Allison, W., and others (Soudan-2 Coll.) (1997), *Phys. Lett. B*, *391*, 491.

Arkani-Hamed, N., et al. (2000), *JHEP*, *0012*, 010.

Aseev, V., and others (Troitsk Collaboration) (2011), *Phys.Rev.D*, *84*, 112,003.

Athanassopoulos, C., and others (LSND Coll.) (1996), *Phys. Rev. Lett.*, *77*, 3082.

Aver, E., K. Olive, and E. Skillman (2010), *JCAP*, *05*, 003.

Bahcal, N. (1991), *Ap.J.*, *376*, 43.

Bahcall, J. (1989), *Neutrino Astrophysics*, Cambridge Univ.Press.

Bahcall, J., and M. Pinsonneault (1995), *Rev. Mod.Phys*, *67*, 781.

Barbieri, R., and A. Dolgov (1990), *Phys.Lett.B*, *237*, 440.

Barbieri, R., and A. Dolgov (1991), *Nucl.Phys.B*, *349*, 743.

Barger, V., et al. (1980), *Phys.Rev.D*, *22*, 2718.

Becker-Szendy, R., and others (IBM Coll.) (1995), *NPPS*, *38*.

Belotsky, K., et al. (2000), *Yad.Fiz.*, *63*, 290.

Bennett, C., et al. (2012), *arXiv:1212.5225v2*.

Berezhiani, Z., and R. Mohapatra (1995), *Phys.Rev.D*, *52*, 6607.

Berezhiani, Z., and A. Rossi (1995), *Phys.Rev.D*, *51*, 5229.

Berezinsky, V., et al. (1996), *Phys.Lett.B*, *365*, 185.

Blanchet, S., and P. Di Bari (2012), *New J.Phys.*, *14*, 125,012.

Boesgaard, A., and G. Steigman (1985), *Ann.Rev.Astr. Astophys.*, *23*, 319.

Brahmachari, B. (1999), *Phys.Lett.*, p. 243.

Broadhurst, T., R. Ellis, and T. Shanks (1988), *MNRAS*, *235*, 827.

Broadhurst, T., et al. (1990), *Nature*, *343*, 726.

Broadhurst, T., et al. (1995), in *Wide Field Spectroscopy and the Distant Universe*, vol. 178, edited by S. Maddox and A. Aragon-Salamanca.

Buchmuller, W., R. Peccei, and T. Yanagida (2005), *Ann.Rev.Nucl.Part.Sci.*, *55*, 311.

Bunch, T., and P. Davies (1978), *Proc. Roy. Soc.*, p. 117.

Busemann, H., et al. (2001), Applications of Abundance Data and Requirements for Cosmochemical Modeling , in *Proc. Joint SOHO-ACE Workshop "Solar and Galactic Composition", Bern, 6-9 March, 2001*, *American Institute of Physics Conference Series*, vol. 598, pp. 357–379.

Caldwel, D., and R. Mohapatra (1993), *Phys.Rev.D*, *48*, 3259.

Caneti, L., and M. Shaposhnikov (2010), *JCAP*, *1009*.

Canetti, L., M. Drewes, and M. Shaposhnikov (2012), *New J.Phys.*, *14*, 095,012.

Canetti, L., et al. (2013), *Phys.Rev.D*, *87*, 093,006.

Capozzi, F., et al. (2014), *Phys.Rev. D*, *89*, 093,018.

Carena, M., et al. (2013), *JHEP*, *1302*, 001.

Chardonnet, P., J. Orloff, and P. Salati (1997), *Phys.Lett. B*, *409*, 313.

Chechetkin, V., et al. (1982), *Phys. Lett. B*, *118*, 329.

Chizhov, M. (1993), *Mod. Phys. Lett. A*, *8*, 2753.

Chizhov, M. (1995), *Sov. J. Part. Nucl.*, *26*, 553.

Chizhov, M. (2004), *JETP Lett.*, *80*, 73.

Chizhov, M. (2005), *Phys. Part. Nucl. Lett.*, *2*, 193.

Chizhov, M. (2007), *Phys. Atom. Nucl.*, *70*, 123.

Chizhov, M. (2008), *arXiv:0705.3944arXiv:0709.2411*, *71*, 2096.

Chizhov, M. (2009), *Phys. Part. Nucl. Lett.*, *6*, 361.

Chizhov, M. (2011), *Phys. Part. Nucl.*, *42*, 93.

Chizhov, M., and A. Dolgov (1992), *Nucl.Phys.B*, *372*.

Chizhov, M., and G. Dvali (2011), *Phys.Lett.B*, *703*.

Chizhov, M., and D. Kirilova (2009), Speeding the Friedmann expansion by chiral tensor particles , *Int. J. Mod.Phys. A*, *24*, 1643–1647.

Chizhov, V., M. Bednyakov, and J. Budagov (2008), *Phys. Atom. Nucl.*, *71*, 2096.

Chun, E., A. Joshipura, and A. Smirnov (1996), *Phys.Rev.D*, *54*, 4654.

Cleveland, B., and others Homestake Coll. (1995), *Nucl. Phys. Proc. Suppl.*, *38*.

Cline, J. (1992), *Phys. Rev.Lett.*, *68*, 3137.

Coc, A., J.-P. Uzan, and E. Vangionio (2014), *arXiv:1403.6694v2*.

Cohen, A., et al. (1998), *Ap.J.*, *495*, 539.

Dar, A., and G. Shaviv (1996), *AP*, *468*, 933.

Davidson, S., E. Nardi, and Y. Nir (2008), *Phys.Rept.*, *466*, 105.

Di Bari, P., and R. Foot (2000), *PRD*, *61*, 105,012.

Dine, M., and A. Kusenko (2004), *Rev. Mod. Phys.*, *76*, 1.

Dine, M., L. Randall, and S. Thomas (1996), *Nucl.Phys.*, p. 291.

Dodelson, S., G. Gyuk, and M. Turner (1994), *Phys.Rev.D*, *49*, 5068.

Dolgov, A. (1981), *Sov.J.Nucl.Phys.*, *33*, 700.

Dolgov, A. (1992), *Phys. Rept.*, *222*, 309.

Dolgov, A. (2002), *Phys. Rept.*, *370*, 333.

Dolgov, A. (2011), *Phys.Atom.Nucl.*, *74*, 462.

Dolgov, A. (2014), *arXiv:1411.2280.*

Dolgov, A., and M. Fukugita (1992a), *Phys.Rev.D*, *46*, 5378.

Dolgov, A., and M. Fukugita (1992b), *Phys.Rev.D*, *46*, 5378.

Dolgov, A., and D. Kirilova (1988), *Int. J. Mod. Phys. A*, *3*, 267.

Dolgov, A., and D. Kirilova (1989), *Yad.Fiz.*, *50*, 1621–1629.

Dolgov, A., and D. Kirilova (1990), *Sov. J. Nucl. Phys.*, *51*, 172–177.

Dolgov, A., and D. Kirilova (1991), *J. Mosc. Phys. Soc.*, *1*, 217.

Dolgov, A., and J. Silk (1993), *Phys.Rev.D*, *47*, 4244.

Dolgov, A., and F. Villante (2004), *Nucl.Phys.B*, *679*, 261–298.

Dolgov, A., and Y. B. Zeldovich (1989), *Rev. Mod.Phys*, *53*, 1.

Dolgov, A., Z. Ya., and S. M. (1988), *Cosmology of the Early Universe.*

Dolgov, A., S. Hansten, and D. Semikoz (1997a), *Nucl.Phys.B*, *503*, 426–444.

Dolgov, A., H. S., and S. D. (1997b), *Nucl.Phys.B*, *503*, 426.

Dolgov, A., S. Hansen, S. Pastor, and D. Semikoz (2000), *Astropart.Phys.*, *14*, 79.

Dolgov, A., S. Hansen, S. Pastor, S. Petcov, and D. Semikoz (2002), *NPB*, *632*, 363.

Dolgov, A. D., Y. B. Zeldovich, and M. V. Sazhin (1991), *Basics of modern cosmology*, 1rd ed., 247 pp., Ed. Frontieres, Gif-sur-Yvette, France.

Donato, F., et al. (2001), *Ap.J.*, *563*, 172.

Drees, M. (1996), Recent Developments in Dark Matter Physics, in *12th DAE Symposium,Guwahati, Assam, India.*

Dvali, G., and A. Smirnov (1999), *Nucl.Phys.B*, *563*, 63.

Einasto, J., et al. (1994), *MNRAS*, *269*, 301.

Einasto, J., et al. (1997), *Nature*, *385*, 139.

Eisenstein, D., et al. (1998), *Ap.J.*, *494*, 1.

Enqvist, E., and A. Mazumdar (2003), *Phys.Rept.*, *380*, 99.

Enqvist, K., K. Kainulainen, and J. Maalampi (1990a), *Phys.Lett.B*, *249*, 531.

Enqvist, K., K. Kainulainen, and J. Maalampi (1990b), *Phys.Lett.B*, *244*, 186.

Enqvist, K., K. Kainulainen, and M. Thomson (1992), *Nucl.Phys.B*, *373*, 498.

Enqvist, K., H. Kurki-Suonio, and J. Valiviita (2000), *Phys.Rev.D*, *26*, 103,003.

Ettori, S., L. Guzzo, and M. Tarenghi (1995), *MNRAS*, *276*, 689.

Ettori, S., L. Guzzo, and M. Tarenghi (1997), *MNRAS*, *285*, 218.

Foot, R., and R. Volkas (1997), *Phys.Rev.D*, *55*, 5147.

Foot, R., M. Thomson, and R. Volkas (1996), *Phys.Rev.D*, *53*, R5349.

Frere, J.-M., T. Hambuye, and G. Vertonen (2009), *JHEP*, *0901*, 051.

Fukuda, Y., and others (Kamiokande Coll.) (1994), *Phys. Lett. B*, *335*, 237.

Fukuda, Y., and others (Kamiokande Coll.) (1996), *Phys.Rev.Lett.*, *77*, 1683.

Fukugita, M., and T. Yanagida (1986), *Phys.Lett. B*, *174*, 45.

Gamow, G. (1935), *Ohio Journal of Science*, *35*, 406.

Gamow, G. (1942), *Journal of the Washington Academy of Sciences*, *32*, 353.

Gamow, G. (1946), *Phys. Rev.*, *70*, 572.

Giusarma, E., et al. (2011), *Phys.Rev. D*, *83*, 115,023.

Glashow, S., and S. Weinberg (1977), *Phys.Rev.D*, *15*, 1958.

Gorbunov, D., and V. Rubakov (2011a), *Introduction to the theory of the early universe: Hot big bang theory*, 1st ed., 473 pp., Hackensack: World Scientific.

Gorbunov, D., and V. Rubakov (2011b), *Introduction to the theory of the early universe: Cosmological perturbations and inflationary theory*, 1st ed., 489 pp., World Scientific.

Hamann, J., et al. (2010), *Phys.Rev.Lett.*, *105*, 181,301.

Hampel, W., and others (GALLEX Coll.) (1996), *Phys.Lett.B*, *388*, 384.

Hannestad, S. (2010), *PPNP*, *65*, 185.

Hannestad, S., I. Tambora, and T. Tram (2012), *JCAP*, *1207*, 025.

Harris, R., and L. Stodolsky (1978), *Phys.Lett.B*, *78*, 313.

Hata, N., and P. Langacker (1995), *Phys.Rev.D*, *52*, 420.

Holanda, P., and A. Smirnov (2011), *Phys.Rev.D*, *83*, 113,011.

Iocco, F., et al. (2009), *Phys. Rept.*, *472*, 1–76.

Izotov, Y., and T. Thuan (2004), *Ap.J.*, *602*, 200–230.

Izotov, Y., and T. Thuan (2010), *Ap.J.*, *710*, L67.

Kappl, R., and M. Winkler (2014), *JCAP*, *1409*, 051.

Khlopov, M., and S. Petcov (1981), *Phys.Lett.B*, *99*, 117.

Khlopov, M., S. Rubin, and A. Sakharov (2000), *Phys. Rev.*, p. 083505.

Kirilova, D. (1988), Neutrino Oscillations and Primordial Nucleosynthesis, *JINR preprint E2-88-301*, pp. 1–14.

Kirilova, D. (1998a), Baryogenesis Model Suggesting Antigalaxies, *Astron. Astrop. Transaction*, *15*, 211–217.

Kirilova, D. (1998b), *AATr*, *15*, 211.

Kirilova, D. (2001a), Primordially Produced Helium-4 in the presence of neutrino oscillations , in *Proc. Joint SOHO-ACE Workshop "Solar and Galactic Composition", Bern, 6-9 March, 2001*, *American Institute of Physics Conference Series*, vol. 598, pp. 405–410.

Kirilova, D. (2001b), Baryonic Content in Nonstandard BBN Models, in *Proc. of Int. Conference "Where's the Matter? Tracing Dark and Bright Matter with the New Generation of Large Scale Surveys", June 2001, Marseille*, Frontier Group.

Kirilova, D. (2003a), Overproduction of helium-4 in the presence of neutrino oscillations , *Astropart. Phys.*, *19*, 409–417.

Kirilova, D. (2003b), Baryogenesis Model predicting Antimatter in the Universe, *Nucl.Phys.B Proc.Suppl.*, *122*, 404–408.

Kirilova, D. (2004a), Neutrino oscillations and the early Universe , *Central Eur. J. Phys.*, *2*, 467–491.

Kirilova, D. (2004b), Neutrino Spectrum Distorsion Due to Oscillations and its BBN Effect , *Int.J.Mod.Phys.D*, *13*, 831–842.

Kirilova, D. (2007), More General BBN Constraints on Neutrino Oscillations Parameters Relaxed or Strengthened , *Int.J.Mod.Phys.D*, *16*, 1–14.

Kirilova, D. (2009), Non-equilibrium Neutrino In The Early Universe Plasma , in *Proc. School and Workshop on Space Plasma Physics*, *AIP Conf. Proc.*, vol. 1121, edited by I. Zhelyazkov, pp. 83–89.

Kirilova, D. (2011a), Big Bang Nucleosynthesis: The best baryometer, speedometer and leptometer, *BAJ*, *15*, 3–17.

Kirilova, D. (2011b), From Mateev's Baryogenesis Ideas to Contemporary Cosmological Constraints, *Bulg. J. Phys.*, *38*, 242–251.

Kirilova, D. (2011c), On Lepton Asymmetry and BBN, *Prog.Part.Nucl.Phys.*, *66*, 260–265.

Kirilova, D. (2012), BBN with Late Electron-Sterile Neutrino Oscillations - The Finest Leptometer, *JCAP*, *06*, 007.

Kirilova, D. (2013), Lepton Asymmetry and neutrino oscillations interplay, *Hyperfine Interactions*, *215*, 111–118.

Kirilova, D. (2015), Neutrinos from the Early Universe and physics beyond standard models, *Open Phys.*, *13*, 22–33.

Kirilova, D., and M. Chizhov (1996a), Nonequilibrium Neutrino Oscillations and Primordial Helium Production, in *Proc. 17 International Conference on Neutrino Physics NEUTRINO 96 Int.*, pp. 478–484.

Kirilova, D., and M. Chizhov (1996b), *AATr*, *10*, 69.

Kirilova, D., and M. Chizhov (1997), Nonequilibrium Neutrino Oscillations and Primordial Production of He-4, *Phys.Lett.B*, *393*, 375–382.

Kirilova, D., and M. Chizhov (1998a), , *Astron. Astrop. Transaction*, *3*, 205.

Kirilova, D., and M. Chizhov (1998b), Neutrino Degeneracy Effect on Neutrino Oscillations and Primordial Helium Yield, *Nucl.Phys.B*, *534*, 447–463.

Kirilova, D., and M. Chizhov (1998c), Cosmological Nucleosynthesis and Active-Sterile Neutrino Oscillations with Small Mass Differences: The Nonresonant Case, *Phys.Rev.D*, *58*, 073,004–073,014.

Kirilova, D., and M. Chizhov (2000a), Neutrino Oscillations in the Early Universe , *Nucl.Phys.B*, *591*, 457–468.

Kirilova, D., and M. Chizhov (2000b), Non-GUT Baryogenesis and Large Scale Structure of the Universe, *MNRAS*, *314*, 256–262.

Kirilova, D., and M. Chizhov (2001a), Cosmological nucleosynthesis and active-sterile neutrino oscillations with small mass differences: The resonant case, *Nucl.Phys.B Proc.Suppl.*, *100*, 360–362.

Kirilova, D., and M. Chizhov (2001b), in *Verbier 2000, Cosmology and particle physics*, p. 433.

Kirilova, D., and M. Chizhov (2009), A Possible TeV Window on the Universe , in *Proceedings of XXIth Rencontres de Blois "Windows on the Universe"21-26 June, 2009, in the Chateau de Blois, Loire Valley, France*, edited by L. Celnikier, J. Dumarchez, and J. Tran Thanh Van, Moriond Astrophysics Meeting, The Gioi Publishers, Vietnam GPXB 4 - 1000/XB-QLXB.

Kirilova, D., and M. Chizhov (2010), BBN Constraints on Neutrino and CNB, *Prog.Part.Nucl.Phys.*, *64*, 375–378.

Kirilova, D., and J.-M. Frere (2012), Neutrinos in the early universe , *New Astron.Rev.*, *56*, 169–180.

Kirilova, D., and M. Panayotova (2006), Relaxed constraints on neutrino oscillation parameters , *JCAP*, *12*, 014.

Kirilova, D., and M. Panayotova (2007), The Account of Particle Creation Processes in the Scalar Condensate Baryogenesis model , *Bulg.J.Phys.*, *34*, 330–335.

Kirilova, D., and M. Panayotova (2013), Inhomogeneous baryogenesis model and antimatter in the Universe, in *Proc. 8th Serbian-Bulgarian Astronomical Conference (VIII SBGAC),Leskovac, Serbia 8-12 May*, *Publ. Astron.Soc."Rudjer Boskovic"*, vol. 11, pp. 259–264.

Kirilova, D., M. Chizhov, and T. Velchev (1995), Antisymmetric Tensor Particles in the Early Universe, *Comptes Rendus de l'Academie bulgare des Sciences*, *48*, 25.

Kirilova, D. P. (2001c), in *Proc. Int. Conf. Hot Points in Astrophysics*, p. 56.

Kirilova, D. P. (2006), Cosmological Constraints on Neutrino Oscillations - Relaxed or Strengthened , in *Proc. 6th Intern. Symposium on Frontiers of Fundamental and Computational Physics*, edited by B. Sidharth, F. Honsel, and A. De Angelis, Frontiers of Fundamental Physics, pp. 55–59.

Klecker, B., et al. (2001), Galactic Abundances: Report of Working Group 3 , in *Proc. Joint SOHO-ACE Workshop "Solar and Galactic Composition", Bern, 6-9 March, 2001*, *American Institute of Physics Conference Series*, vol. 598, pp. 207–220.

Kolb, E., and M. Turner (1990), *The Early Universe*, 3rd ed., 547 pp., Front.Phys., United States of America.

Komatsu, E., and others (WMAP) (2009), *Astrophys. J. Suppl*, *180*, 330.

Kopp, J., G. Maltoni, and T. Schwetz (2011), *Phys.Rev.Lett.*, *107*, 091,801.

Kostelecky, V., and S. Samuel (1995), *Phys.Rev. D*, *52*, 3184.

Krastev, P., and S. Petcov (1996), *Phys.Rev.D*, *53*, 1665.

Krauz, C., et al. (2005), *Eur.Phys.J.C*, *40*, 447.

Kuo, K., and J. Pantaleone (1989), *Rev.Mod.Phys.*, *61*, 937.

Kuo, T., and J. Panteleone (1989), *Rev.Mod.Phys.*, *61*, 937.

Kurki-Suonio, H., and E. Sihvola (2000), *Phys.Rev.Lett.*, *84*, 3756.

Kuzenko, A. (2009), *Phys. Rept.*, *481*, 1–28.

Kuzmin, V., V. Rubakov, and M. Shaposhnikov (1985a), *Phys. Lett. B*, *155*, 36.

Kuzmin, V., V. Rubakov, and M. Shaposhnikov (1985b), *Phys. Rev. Lett.*, *84*, 3756.

Langacker, P., S. Petcov, G. Steigman, and T. S. (1987), *Nucl.Phys.B*, *282*, 589.

Langacker, P., et al. (1983), *Phys.Lett.B*, *27*, 1228.

Langacker, P., et al. (1986), *Nucl.Phys.B*, *266*, 669.

Lausman, N., and C. Weert (1987), *Phys.Rev.*, *145*, 141.

Lesgourgues, J., and S. Pastor (2006), *Phys.Rep.*, *429*, 307.

Lesgourgues, J., and S. Pastor (2012), *Adv.High Energy Phys.*, *2012*, 608,515.

Li, T., and C. Yang (1956), *Phys.Rev.*, *104*, 254.

Liddle, A. R. (1998), *An introduction to modern cosmology*, 1rd ed., 129 pp., Wiley, Chichester, UK.

Linde, A. (1982), *PLB*, *116*, 335.

Linde, A. D., Y. B. Zeldovich, and M. V. Sazhin (1991), *Basics of modern cosmology*, 1rd ed., 247 pp., Ed. Frontieres, Gif-sur-Yvette, France.

Machado, P., et al. (2012), *JHEP*, *05*, 023.

Malaney, R., and G. Mathews (1985), *Ann.Rev.Astr. Astophys.*, *23*, 319.

Mangano, G., et al. (2005), *Nucl.Phys.B*, *729*, 221.

Mangano, G., et al. (2012), *PLB*, *708*, 1.

Manohar, A. (1987), *Phys.Lett.B*, *196*, 370.

Mayorov, A., et al. (2011), *JETP Lett.*, *93*, 628.

Mikheyev, S. P., and A. Y. Smirnov (1985), *Sov.J.Nucl.Phys.*, *42*, 913.

Mirizzi, A., et al. (2012), *Phys. Rev. D*, *86*, 053,009.

Morrissey, D., and M. Ramsey-Musolf (2012), *New J.Phys.*, *14*, 125,003.

Murayama, H., et al. (1993), *Phys.Rev.Lett.*, *70*, 1912.

Nakamura, T., and S. Petcov (2012), *Phys.Rev. D*, *86*, 010,001.

Nieves, J. (1989), *Phys.Rev.D*, *40*, 866.

Nötzold, D., and G. Raffelt (1998), *Nucl.Phys.B*, *307*, 924.

Olive, K., et al. (2014), *Chin. Phys. C*, *38*, 090,001.

Olive, K., G. Steigman, and T. Walker (2000), *Phys.Rept.*, *333*, 389.

Ormes, J., et al. (1997), *Ap.J.*, *482*, L187.

Pagel, B. (1997), *Nucleosynthesis and Chemical Evolution of Galaxies*, Cambridge Univ.Press.

Pal, P., and T. Pham (1989), *Phys.Rev.D*, *40*, 259.

Panayotova, M. (2011), *Bulg.J.Phys.*, *38*, 242.

Panayotova, M., and D. Kirilova (2012), *BAJ*, *20*, 45–50.

Panayotova, M., and D. Kirilova (2014), The dependence of the baryon asymmetry generation on the couplings of the baryon charge carrying scalar field, *BAJ*, *20*, 45–50.

Pastor, S., T. Pinto, and G. Raffelt (2009), *PRL*, *102*, 241,302.

Pettini, M., and R. Cooce (2012), *arXiv:1205.3785.*

Pettini, M., et al. (2008), *MNRAS*, *391*, 1499.

Pontecorvo, B. (1958a), *Sov. Phys. JETP*, *6*, 431.

Pontecorvo, B. (1958b), *Sov. Phys. JETP*, *7*, 172.

Pontecorvo, B. (1968), *Sov. Phys. JETP*, *26*, 984.

Primack, J., et al. (1995), *Phys.Rev.Lett.*, *74*, 2160.

Rana, N., and B. Mitra (1991), *Phys.Rev. D*, *44*, 393.

Reeves, H. (1972), *Phys.Rev. D*, *6*, 3363.

Rubakov, V., and M. Shaposhnikov (1996), *Usp. Fiz. Nauk*, *166*, 4931.

Rubakov, V., M. Sazhin, and . Verjaskin (1982), *Phys. Lett.*

Ruchayskiy, O., and A. Ivashko (2012), *JCAP*, *1210*, 014.

Sakharov, A. (1967), *JETP Lett.*, *5*, 24.

Sarkar, S. (1996), *Rep.Prog.Phys.*, *59*, 1493.

Sasaki, M., and others (BESS Collab.) (2008), *Adv. Space Res.*, *42*, 450.

Sasselov, D., and D. Goldwirth (1995), *Ap.J.*, *444*, L5.

Shi, X. (1996), *Phys.Rev.D*, *54*, 2753.

Shi, X., D. Schramm, and B. Fields (1993), *Phys.Rev.D*, *48*, 2563.

Shvartsman, V. (1969), *JETP Lett.*, *9*, 184.

Sigl, G., and G. Raffelt (1993), *Nucl.Phys.B*, *406*, 423.

Simha, and G. Steigman (2008), *JCAP*, *0808*, 011.

Starobinsky, A. (1982), *Phys. Lett.*, p. 175.

Stecker, F. (1985), *Nucl.Phys.B.*, *252*, 25.

Steigman, G. (1976), *Ann. Rev. Astr. Astrop.*, *14*, 339.

Steigman, G. (2008), *JCAP*, *0810*, 001.

Stodolsky, L. (1987), *Phys.Rev.D*, *36*, 2275.

Strumia, A., and F. Vissani (2010), *unpublished*, *3*, hep–ph/0606,054.

Terasawa, N., and K. Sato (1987), *Phys.Lett.B*, *185*, 412.

Vilenkin, A., and L. Ford (1982), *Phys.Rev.*, p. 1231.

von Ballmoos, P. (2014), *Hyperfine Int.*, *228*.

Wagoner, R., W. Fowler, and F. Hoyle (1967), *Astrophys. J.*, *148*, 3.

Weinberg, S. (1982), *Phys.Rev.Lett.*, *48*, 1303.

Weldon, H. (1982), *Phys.Rev.D*, *26*, 2789.

Wolfenstein, L. (1978), *Phys.Rev.D*, *17*, 2369.

Wright, E., et al. (1992), *Ap.J.*, *396*, L13.

Zeldovich, Y. B., and I. D. Novikov (1983), *Relativistic Astrophysics. Vol. 2. The Structure And Evolution Of The Universe*, 1rd ed., 718 pp., Chicago Univ., Chicago, USA.